Norwegian University
of Life Sciences

Master's Thesis 2021 60 ECTS
Faculty of Chemistry, Biotechnology, and Food Sciences

Synthesis Towards Two Sulphur-Containing Heterocyclic Fatty Acids

Åshild Moi Sørskår
Chemistry and Biotechnology

ACKNOWLEDGEMENTS

The work described herein was carried out at the Faculty of Chemistry, Biotechnology and Biotechnology (KBM) at the Norwegian University of Life Sciences.

I would like to express my sincerest gratitude towards my thesis advisors, Dr. Simen G. Antonsen and professor Yngve H. Stenstrøm for their expert advice and guidance throughout the course of my thesis. Through their availability and display of support, they have made this year rich in learning, even during the periods of strict government restrictions and Covid-19-related lockdowns that characterised the first semester and limited or prohibited on-campus activities.

In addition, I would like to thank Dorentina Osmani for her assistance and guidance in the initial stages of my thesis. I also appreciate the help of my fellow master student, Kristian Haugen, with whom I was able to explore one additional synthetic strategy.

Ås, December 2021

Åshild Sørskår

ABSTRACT

A total synthesis towards the methyl and ethyl esters of two sulphur-containing heterocyclic fatty acids that have been isolated from rapeseed oil, mustard oil, and garlic, was attempted. Since MS-EI analyses has been the sole method used for structure elucidation of these compounds, the aim of the synthesis was to obtain more extensive spectroscopic data of the fatty acids, and to confirm the proposed structures of the target molecules.

Altogether, five synthetic strategies were explored, where the key carbon-extending reactions used in the various synthetic pathways included lithiation-alkylation, oxidative cross-couplings, and olefination reactions. Of the five synthetic strategies explored herein, only one pathway afforded the complete carbon-skeleton common to both target molecules, which in this case was constituted by ethyl (*E*)-8-(5-hexylthiophen-2-yl)oct-2-enoate. However, the α,β-unsaturated ester could not be purified to a satisfactory degree. With time being at its limit, optimisation of some of the low-yielding reaction steps leading to this intermediate, as well as conducting the remaining hydrogenation steps, was left for future work.

SAMMENDRAG

Det ble forsøkt å utføre en totalsyntese av metyl- og etylesterne av to svovelinneholdende heterosykliske fettsyrer som er blitt isolert i små mengder fra rapsolje, sennepsolje og hvitløk. Formålet med totalsyntesen var å bidra til strukturoppklaring av disse fettsyrene, som kun er blitt strukturbestemt ved bruk av MS-EI tidligere.

Fem ulike syntesestrategier ble utprøvd, der alkylering ved bruk av organlitiumreagenser, oksidative krysskoblinger og olefineringsreaksjoner utgjorde de mest sentrale karbonforlengende reaksjonstypene i de ulike synteseveiene. Kun én av de fem forskjellige syntesestrategiene skulle vise seg å lede frem til det felles karbonskjelettet til målforbindelse, som i denne sammenheng ble utgjort av etyl (*E*)-8-(5-heksyltiofen-2-yl)okt-2-enoat. Dessverre lot det seg ikke gjøre å isolere denne α,β-umettede esteren med en slik grad av renhet at forbindelsen kunne omdannes videre til målforbindelsene. De gjenstående hydrogeneringstrinnene samt forbedring av enkelte lavtytende reaksjonstrinn ble dermed overlatt til fremtidig arbeid.

GRAPHICAL ABSTRACT

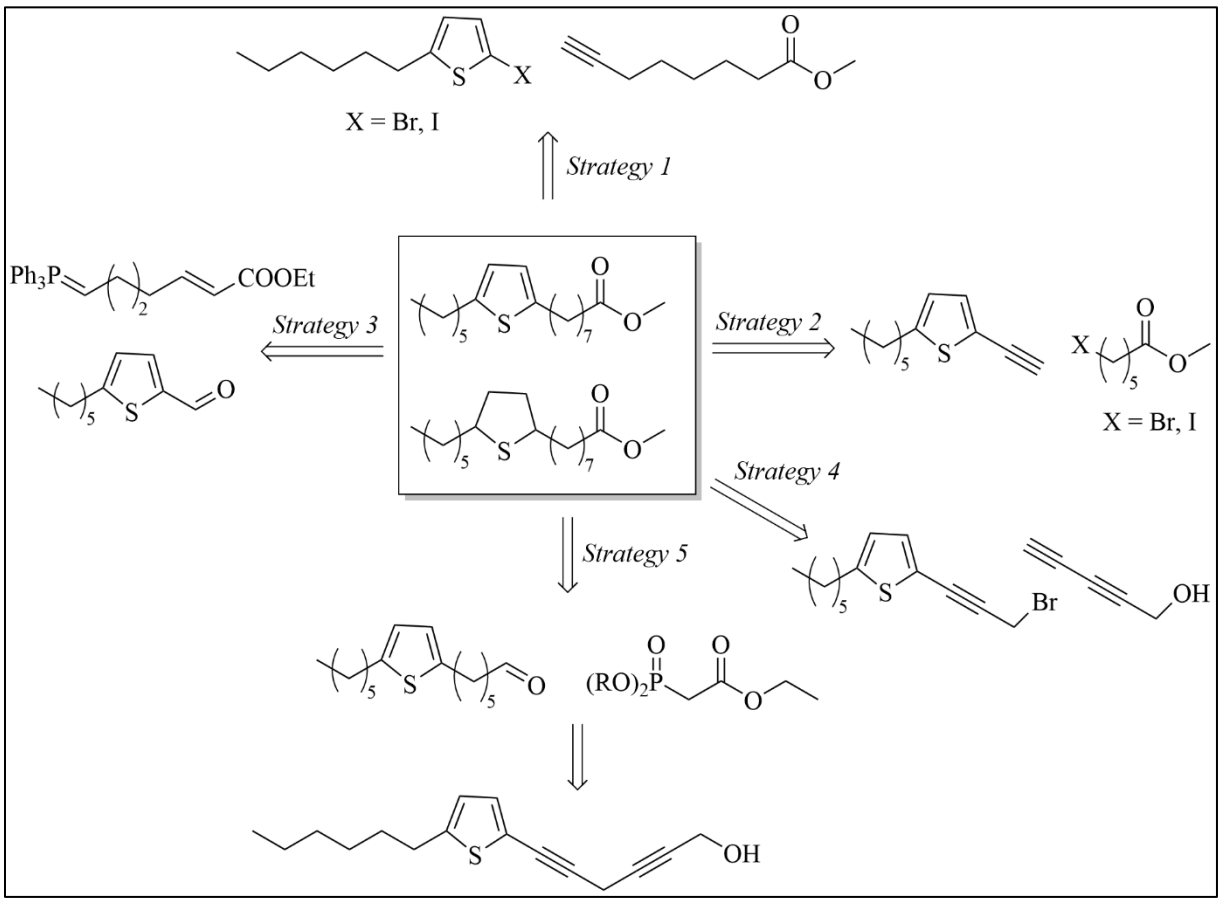

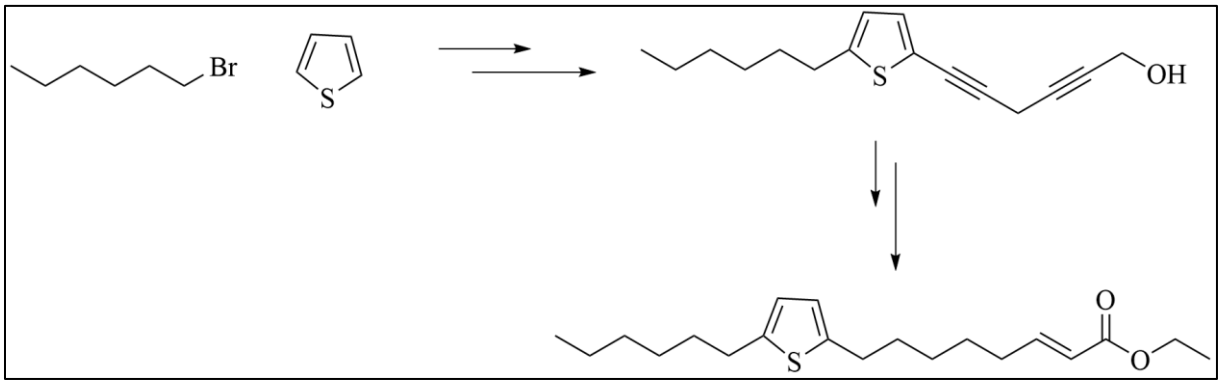

ABBREVIATIONS

5-LO	5-lipoxygenase
AA	Arachidonic Acid
BuLi	Butyllithium
Bu_4NBr	Tetrabutylammonium bromide
DHA	Docosahexaenoic Acid
DMF	Dimethylformamide
EPA	Eicosapentaenoic Acid
EtOAc	Ethyl acetate
FFA	Furan Fatty Acid
HWE	Horner-Wadsworth-Emmons
KAPA	Potassium Aminopropylamide
LO	Lipid Peroxyl Radical
LTA_4	Leukotriene A_4
LTB_4	Leukotriene B_4
LTC_4	Leukotriene C_4
LTD_4	Leukotriene D_4
MRSA	Methicillin-Resistant *Staphylococcus aureus*
NBS	*N*-Bromosuccinimide
NIS	*N*-Iodosuccinimide
PPARs	Peroxisome Proliferator Activated Receptors
PUFA	Polyunsaturated Fatty Acid
SHFA	Sulphur-Heterocyclic Fatty Acids
THF	Tetrahydrofuran
TMS	Trimethylsilyl
TTA	Tetradecylthioacetic Acid

CONTENTS

1. Introduction

1.1. Background

Mustard seed[1, 2], rapeseed[3 4, 5], and garlic[6, 7] oils have long traditions in Oceanic[8] and Asian[6, 7, 9-11] folk medicine as remedies for a variety of conditions, including colds[10], muscle pains[12], hypertension[13], oxidative stress[7, 13], and inflammation[6, 7, 13]. In addition, mustard and garlic are known as effective antimicrobial agents[7]. For this reason, mustard has long been used as a food preservative[3, 8, 9]. Many of the beneficial effects associated with mustard, rapeseed, and garlic have been linked to organo-sulphur compounds[6, 7, 14] (*figure 1.1*).

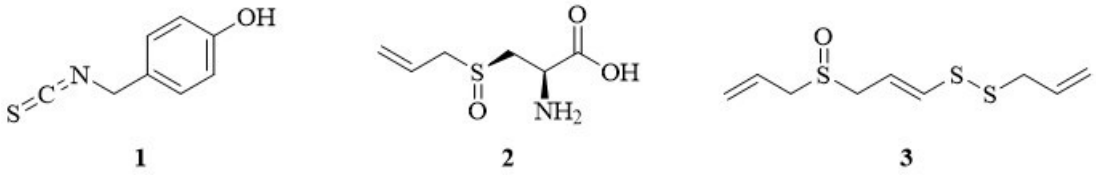

Figure 1.1: *Some organo-sulphur compounds found in mustard (**1**)[8] and garlic (**2-3**)[7].*

In 1988, a novel group of organo-sulphur compounds was discovered by Wijesundera and Ackman[15], who reported the probable occurrence of three sulphur-heterocyclic fatty acids (SHFAs) as minor components of unrefined rapeseed oil[15]. Based on mass spectrometric analyses, the authors tentatively suggested the structures **4-6** for the previously undocumented sulphur-containing fatty acids in rapeseed oil. Given their resemblance to oxygen-heterocyclic fatty acids, the authors conjectured that the SHFAs were likely to be native to the rape plant[15].

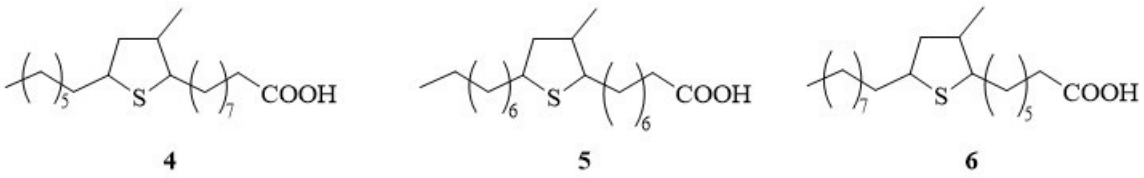

Figure 1.2: *Shows the proposed structures of the SHFAs **4-6.***

However, it is often assumed that alkyl-thiophenes, and sulphur-containing acids and esters arise from thermal and photochemical processing of unsaturated lipids in the presence of sulphur sources, in nature, or during analytical workup of organic samples[16-22]. Thus, when a similar finding was made in 2000, by a group of geologists who reported the occurrence of a series of thiophene-, thiolane-, and thiane-containing fatty acids in Spanish algal sediments (*figure 1.3*)[23], the incorporation of the heterocyclic moieties into the fatty acids were attributed to be the result of a geochemical preservation process of originally unsaturated fatty acids [23]. Like Wijesundera and Ackman[15], the researchers used MS as the sole mean of structure elucidation[23].

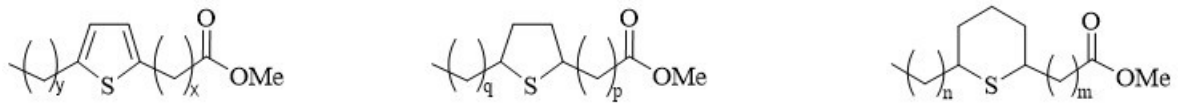

Figure 1.3: *Shows the general structure of the SHFAs found in Spanish sediments, where x=6-12, y=0-6, p=7,10,11,12, p=0,1,2,5, m= 7-9, and n=2-4.*

The existence of SHFAs as natural products was again reported in 2006, when Dembitsky *et al.*[24] reported the occurrence of three new SHFAs (**7-9**, *figure 1.4*) in garlic (*Allium sativum*)[24]. Encouraged by the findings of Wijesundera and Ackman[15], as well as the fact that bacteria of the genus *Streptomyces* are known to produce sulphur-containing carboxylic acids when grown in methionine-enriched environments[25, 26], the authors postulated that the SHFAs were naturally occurring in the garlic plant[24]. Again, MS was the only method used for structural determination of the SHFAs[24].

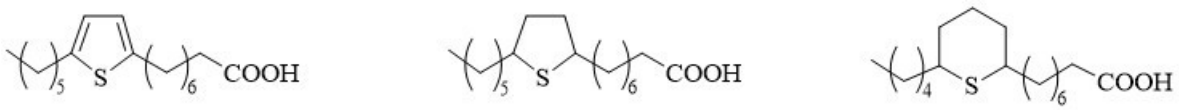

7 **8** **9**

Figure 1.4: *Shows the proposed structures of the SHFAs* ***7-9****.*

In 2017, Eibler *et al.*[27] reported the presence of a total of 21 SHFAs (*figure 1.5*) in unrefined oil samples from rape- and mustard seeds, both of which plants are members of the *Brassica* genus[27]. Their occurrence in samples of native mustard and rapeseed oil that had been prepared without the presence of external sulphur sources, suggests that SHFAs could be products of biosynthesis, and not some artefacts arising from chemothermal processing, as appears to be the case for the SHFAs found in algal sediments. While the three 3-methylated structures **4-6** were not among the structures proposed by Eibler *et al.*[27], MS analyses produced spectra corresponding to those obtained by Dembitsky *et al.*[24] for compound **8**, indicating some commonality between the SHFAs found in both garlic and species of the *Brassica* genus.

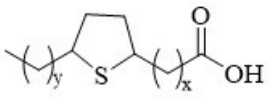

Figure 1.5: *Eibler et al.*[27] *reported the occurrence of 21 different tetrahydrothiophene-containing fatty acids, where x = 3-12 and y = 0-8*

Currently, little is known about the structural, chemical, and biological properties of these SHFAs. Although MS is a highly sensitive and versatile analytical tool, it has its limitations in that it cannot distinguish between fragments of the same molecular mass with different

structures. Similarly, it does not discriminate against optical or geometric isomers. Since all SHFAs have been elucidated by MS analyses exclusively, a more extensive characterisation of the SHFAs using complementary techniques such as NMR and IR, is expedient to confirm the proposed structures, assuming that these are, in fact, natural products.

1.2. Natural Products

Throughout history, natural products have been recognised for their therapeutical properties, having uses in the treatment of a wide range of illnesses[28-30]. Natural products are organic compounds that are produced by organisms in the primary or secondary metabolic pathways[31]. As such, natural products can be categorised as primary or secondary metabolites[31].

Primary metabolites, which category comprises carbohydrates, amino acids, lipids, and nucleic acids, are vital to the growth and development of all organisms and are widely distributed, with little or no structural variation, in all lifeforms[31]. In contrast, secondary metabolites are compounds that perform specialised functions and are produced only by a limited number of organisms, for example to provide them with a competitive advantage against competitors or predators. In medicinal natural product chemistry, it is generally the secondary metabolites that are of pharmacological value[31].

Before being put into pharmacological use, many secondary natural products are structurally modified to attain some desirable property. Molecules that share the same gross structural features but differ with respect to a functional group or an atom are called analogues.

For example, penicillin G[32] (**10**, *figure 1.6*) is an antibacterial compound produced by the fungus *Penicillium chrysogenum (P.chrysogenum),* that antagonises gram positive bacteria[32-34]. Since it decomposes under acidic conditions, **10** is normally administered by intramuscular or intravenous injection[33, 35]. However, ampicillin (**11**, *figure 1.6*), an analogue of the natural product **10** in which an additional amine group is inserted between the amide bond and the phenyl group tolerates the acidic environment of the gut and is therefore suitable for oral intake[33, 36]. Furthermore, the insertion of the amine group allows **11** to permeate the cell walls of some gram-negative bacteria, thus broadening the spectrum of bacteria the analogue inhibits[33, 34, 36].

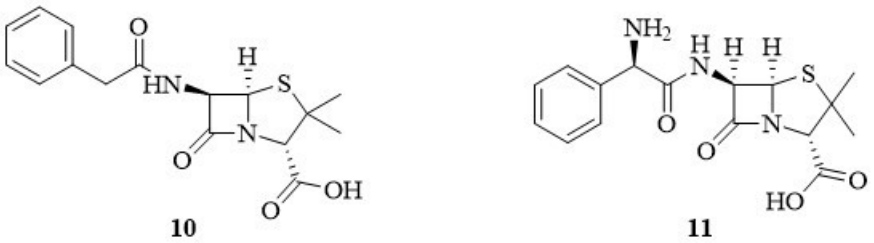

10 11

Figure 1.6.: *Shows the structures of penicillin G (**10**) and its structural analogue, ampicillin (**11**).*

Hence, small structural modifications to a molecule might significantly alter the bioactivity of a compound.

1.2.1. Fatty Acids

In terms of their structure, SHFAs constitute a peculiar group of fatty acids. Generally, fatty acids are characterised as monocarboxylic acids with a linear, aliphatic hydrocarbon chain constituted by 4-28 carbon atoms, where the hydrocarbon chains can be saturated, monounsaturated, or polyunsaturated[37]; *i.e.,* they may contain zero, one, or several carbon-carbon double bonds. Fatty acids are normally considered to be primary metabolites, and are widely distributed in substances such as waxes, plant- and animal fats, where they occur as triacylglycerol esters, and function as water repellents, thermal insulation and energy storages[38, 39]. Since fatty acids constitute parts of phospholipids, which make up cellular membranes[38], they also function as permeability barriers in the cell[39]. Furthermore, via their incorporation in diacylglycerols, fatty acids are important secondary messengers and facilitators of intracellular signalling[38].

Not all fatty acids needed to sustain normal biological functions can be biosynthesised in human metabolic pathways. Thus, dietary intake of certain ω-3 and ω-6 polyunsaturated fatty acids (PUFAs)[40, 41], *i.e.,* fatty acids that are unsaturated from the third and sixth carbon counted from the non-carboxyl end, is usually required to sustain normal growth and development. Particularly, intake of α-linolenic acid (**12**) is considered essential as it can be further metabolised to eicosapentaenoic acid (EPA, **13**) and docosahexaenoic acid (DHA, **14**) (*figure 1.7)*[38, 40, 41], both of which are associated with numerous health benefits.

Supplementation of EPA and DHA in the diet has been linked to improved cardiovascular health[40, 42, 43], as well as hypolipidemic[44-46], anti-inflammatory[40, 44], and anticancer[40] effects. As such, fatty acids constitute a group of compounds capable of stimulating several health-promoting effects.

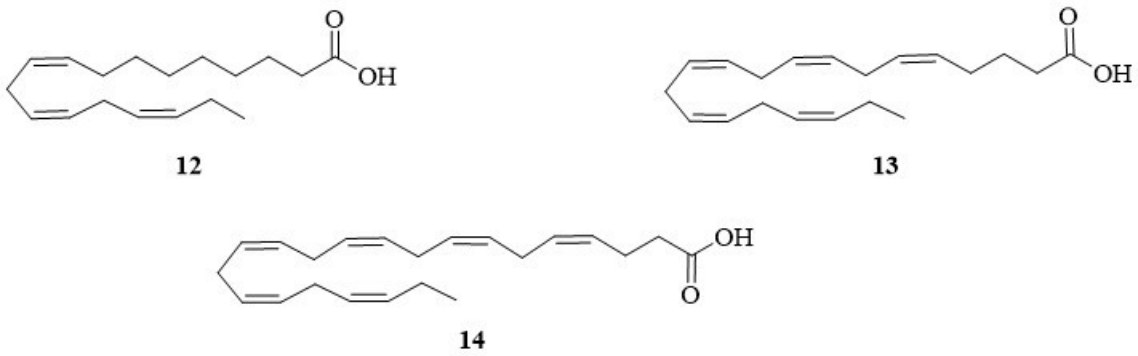

Figure 1.7.: *Shows the structures of α-linoleic acid (**12**) EPA (**13**) and DHA (**14**).*

1.2.1.1. Furan Fatty Acids

Furan fatty acids (FFAs) are structurally analogous to SHFAs in that they have a heterocycle embedded in the hydrocarbon chain, only with oxygen constituting the heteroatom in place of sulphur. Compared to SHFAs, FFAs are more widely distributed in nature, and are found in both aquatic and earthbound lifeforms, with fish being particularly rich sources of FFAs[47]. Although non-methylated FFAs have been detected[48], FFAs usually contain methyl groups at the 3-position or the 3,4-positions of the furan ring (*figure 1.8)*[49].

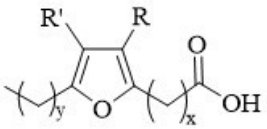

Figure 1.8: *Shows the general structure of an FFA, where x = 8, 10, or 12, y = 2, 4, or 6, R = H or CH_3, and R = H or CH_3.*[48, 49].

Similar to EPA and DHA, intake of FFAs has been linked to a reduced risk of cardiovascular disease[47], as well as hypolipidemic[50], and anti-inflammatory[51] effects. Additionally, antioxidant[49, 52-55], and antimicrobial activities[56] of FFAs have been reported.

In one study[51], the ethyl ester of an FFA (**15a**, *figure 1.9*) was found to have a more potent anti-inflammatory effect than the corresponding EPA ethyl ester[51]. Another FFA (**16**, *figure 1.9*) proved capable of inhibiting the growth and development of methicillin-resistant *Staphylococcus aureus* (MRSA)[56], the occurrence of which is becoming an increasingly worrisome public health problem, making this a very interesting finding. The free fatty acid of the former (**15b)** was examined for its antioxidative effect on brain cells, producing results which indicated its effectiveness in counteracting the onset of Alzheimer's disease[53].

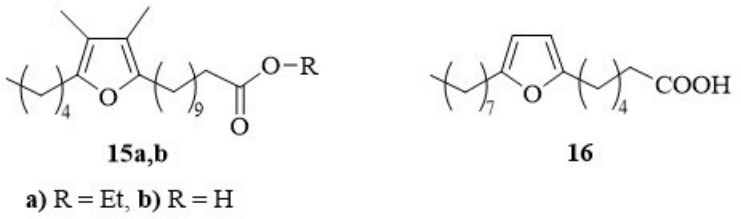

Figure 1.9: *Shows the structures of FFAs shown to have anti-inflammatory (**15a**), anti-Alzheimer (**15b**), and antimicrobial (**16**) effects.*

The potent radical scavenging ability of FFAs has been ascribed to the furan ring, which is capable of neutralising two lipid peroxyl radicals (LO) via their addition to the 2,5-positions[47] (*scheme 1.1.*).

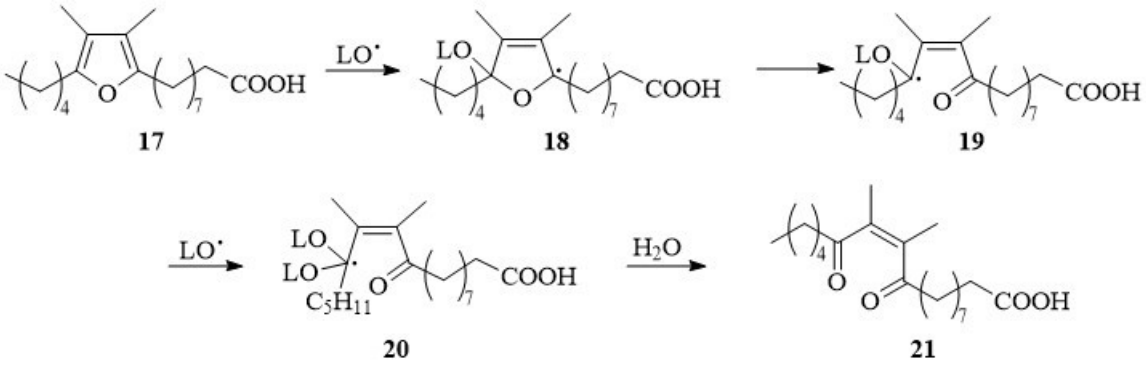

Scheme 1.1.: *Shows the mechanism by which FFAs neutralise LOs*

Addition of the first radical at the 2- or 5-position results in the opening of the furan ring and generates a mesomeric radical to which a second LO may add, yielding a diacetal structure[47]. 3,4-methylated FFAs have been shown to exhibit higher antioxidant activity than tocopherols (vitamin E)[49]. Thus, the incorporation of 3,4-methylated FFAs into phospholipids has been viewed as especially important for the stability of fatty acids in food and biological systems[54].

While the biological effects of SHFAs may not be identical to FFAs, it is conceivable that they might show similar activities. This is exemplified by one study in which the hypolipidemic effects of synthetic fatty acid analogues that had furan- and thiophene-moieties embedded in their structures (**22, 23**, *figure 1.10*) were examined; in this study, the thiophene and furan fatty acid analogues were found to have comparable antihyperlipidemic effects[57]. Biological assaying of SHFAs may therefore produce interesting results, if FFAs are indicative of their potential biological activities. Furthermore, the natural abundance of FFAs makes it conceivable that SHFAs are also naturally occuring[15].

22 23

Figure 1.10: *Shows the structures of the furan- and thiophene-containing fatty acid analogues found to have comparable hypolipidemic effects*[57].

1.2.1.2. 5-Lipoxygenase and LTA4 Hydrolase Inhibitors

Although little is known about the biological effects of SHFAs, a compelling analogy can be drawn from three studies in which compounds designed to inhibit production of pro-inflammatory leukotrienes were synthesised. Leukotrienes are a group of compounds that are generated by the action of 5-lipoxygenase (5-LO) in the metabolism of the ω-6 PUFA arachidonic acid (AA, **24**) as part of the inflammatory response of white blood cells[58]. In particular, leukotriene B_4 (LTB_4, **25**), which is formed from leukotriene A_4 (LTA_4, **26**) (*figure 1.11.*), has been identified as a significant mediator of inflammatory conditions such as psoriasis, ulcerative colitis, and rheumatoid arthritis[59].

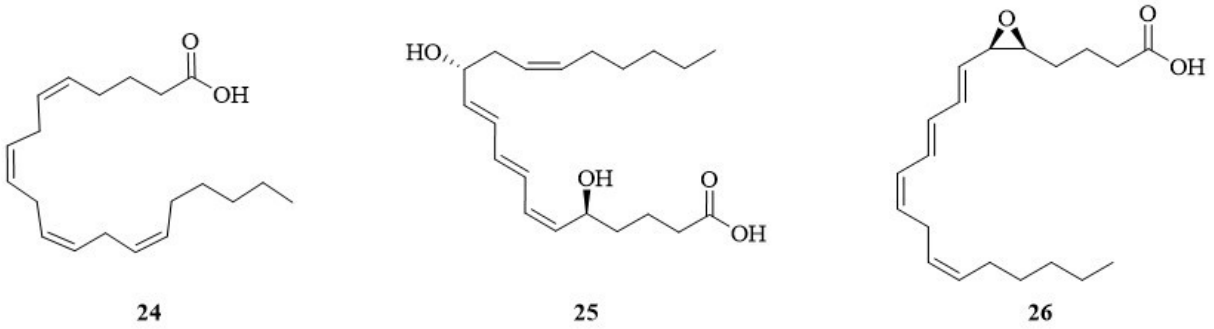

24 25 26

Figure 1.11: *Shows the structures of AA (**24**), and two leukotrienes, LTB_4 (**25**), and LTA_4 (**26**).*

As such, impeding on 5-LO action was the target in one study, in which Corey *et al*[60] reported a 5-LO inhibitory effect of the sulphur-containing fatty acid analogues **27-29** (*figure 1.12*).

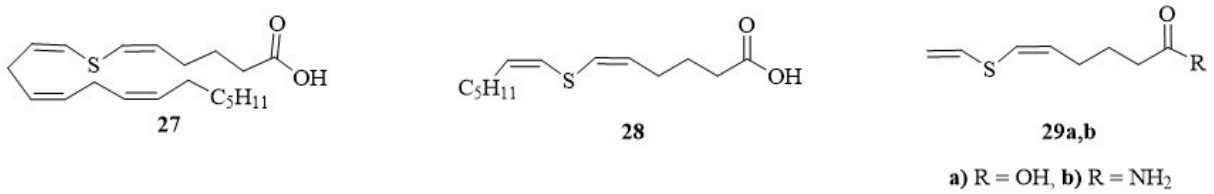

27 28 29a,b

a) R = OH, **b)** R = NH_2

Figure 1.12.: *Shows the sulphur-containing fatty analogues **27-29a,b** with 5-LO inhibitory effects.*

The authors found that the enzyme was completely deactivated when incubated with the irreversible inhibitors under aerobic conditions over time[60].

A similar finding was obtained later, when Hanko *et al*[61] investigated the 5-LO inhibitory effects of a series of sulphur-containing fatty acid analogues, all mimicking the proposed

transition-state intermediate **30** (*figure 1.13*). The authors hypothesised that substituting the negative charge with a non-ionised electronegative atom would create a stable intermediate, which again would inhibit 5-LO activity. Of all the analogues that were investigated, the most potent inhibitory effect was exhibited by **31**, which bore most structural resemblance to **30**[61]. Shortening the carbon chain length or altering the functionality of the carbon chain by replacing a double bond with a single or a triple bond significantly reduced the potency of the inhibitors[61]. By comparing the inhibitory action of sulphur-containing analogues to that of corresponding non-sulphur-containing analogues, the authors concluded that the sulphur moiety was essential to obtain optimal inhibitory effect[61].

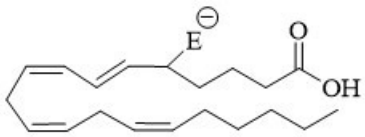

30

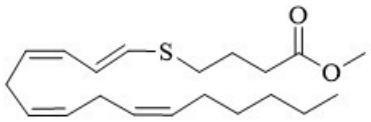

31

Figure 1.13: *Shows the proposed transition state intermediate (**30**) and the most potent 5-LO inhibitor (**31**) of the structures investigated by Hanko et al*[61]

In a later study[59], compounds that specifically targeted inhibition of LTA_4 hydrolase, an enzyme that catalyses the formation of LTB_4 from LTA_4 were designed. Of the numerous compounds that were analysed, the two thiophene-containing fatty acid analogues **32** and **33** (*figure 1.14*) exhibited the most potent inhibitory effects, with the fractions of *in vitro* inhibition being 84% and 90% respectively[59]. An important structural feature of these compounds appeared to be the lengths of the carboxylic-chain substituents on the thiophene, which corresponded exactly to the distance between the carboxyl group and the triene moieties of LTA_4[59]. Of the two thiophene fatty acids, only **33** was metabolically stable, exhibiting a 40% inhibitory effect on LTB_4 bioproduction when administered orally to rats[59].

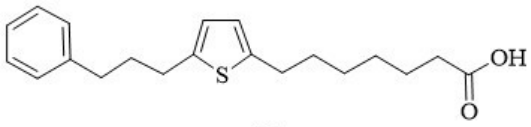

32

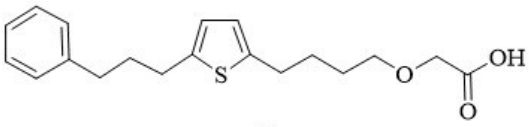

33

Figure 1.14: *Shows the structure of the two most potent LTA_4 hydrolase inhibitors.*

While the hypothesised therapeutical effects of these enzyme inhibitors were not confirmed in this study, the finding is still noteworthy given the structural resemblance of **32** to, for example **7**, which was one of the structures elucidated by Dembitsky *et al*[24].

1.2.1.3. TETRADECYLTHIOACETIC ACID

Tetradecylthioacetic acid (TTA, **34**, *figure 1.15*) constitutes another fascinating case study relating to sulphur-containing fatty acid analogues. TTA is a saturated 3-thia-substituted fatty acid reported to induce hypolipidemia[62-65], as well as various immunomodulatory responses, such as anti-oxidative[66, 67], cardioprotective[63, 67], and anti-inflammatory[64, 68, 69] actions. Furthermore, TTA has been reported to exhibit anti-proliferative effects on malignant cells[70-72].

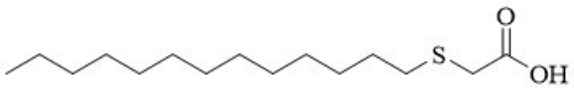

34

Figure 1.15: *Shows the structure of TTA (**50**).*

An interesting biochemical effect of the inclusion of a heteroatom, such as sulphur or oxygen, at the β-position is that it prevents compounds from being β-oxidised[62, 63, 65, 73-76]. Instead, TTA is initially catabolised via ω-oxidation[62, 74, 77], which is otherwise a minor pathway for biological degradation of fatty acids[38]. The slow metabolic degradation of the 3-heterosubstituted fatty analogues appears to enhance the biological impact these compounds may have[66, 76].

Many of the beneficial effects of TTA have been linked to its interactions with peroxisome proliferator activated receptors (PPARs), for which TTA is a potent ligand[62, 66, 67, 73, 78]. PPARs are a group of nuclear receptors responsible for regulating fatty acid metabolic processes[38], including those relating to insulin sensitisation[79]. Furthermore, PPARs are involved in regulatory aspects of inflammatory responses, cell cycle control, apoptosis, atherosclerosis, and[79], by stimulating proliferation of cells, carcinogenesis[80]. Thus, ligand-binding of TTA to the PPARα-receptor has been suggested to stimulate hypolipidemia through induction of fatty acid oxidation[62], and may also explain the observed anti-inflammatory and stenosis-reducing effects of TTA post-surgey[68] However, some studies indicate that the beneficial effects of TTA are not due to PPAR-activation alone[71, 81], and so the total therapeutic mechanisms of TTA remain elusive. Nevertheless, this demonstrates the impact the inclusion of a heteroatom into fatty acids may have.

1.3. ORGANO-SULPHUR COMPOUNDS IN GARLIC, MUSTARD, AND RAPESEED

Many of the therapeutical properties of garlic, mustard and rapeseeds are attributed to their organo-sulphur contents, the occurrence of which is well-documented[7, 9, 10, 82-86]. Notably, garlic *oil* has been shown to alleviate oxidative stress and inflammation, and to prevent

hyperglycaemia, which is causative of diabetes[87]. In addition, garlic oil has also been linked to various immunomodulatory effects such as suppressing allergic responses by impeding on the release of β-hexosaminidase, which stimulates histamine response[88]. Furthermore, garlic oil has been shown to inhibit proliferation of malignant cells[89]. To this end, allicin (**35**), diallyl sulphide (**36**), diallyl disulphide (**37**), and diallyl trisulphide (**38**), are some of the organo-sulphur species that have been identified as important biologically active components of garlic oil (*figure 1.16)*[7].

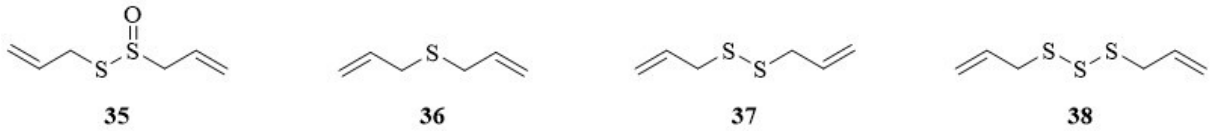

Figure 1.16: *Shows the structures* ***35-38****.*

In the *Brassica* species, sulphur-containing components such as isothiocyanates are believed to originate from hydrolysis of glucosinolates[84, 86, 90, 91] (*scheme 1.2)*

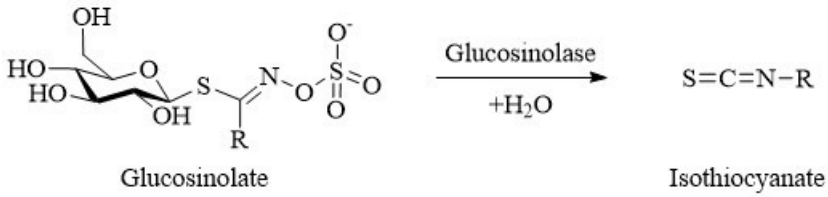

Scheme 1.2.: *Shows the enzymatic hydrolysis of a glucosinolate[86], where R = arbitrary side chain.*

Isothiocyanates have been of particular pharmaceutical interest as they are capable of stimulating anti-inflammatory and antioxidative responses[90], as well as inhibiting microbial growth[92]. In this context, allyl isothiocyanate (**39**, *figure 1.17*), which is found in both mustard and rapeseeds[85, 93], constitutes an interesting example, as it has exhibited anticancer[93, 94], neuroprotective[86, 95], insecticidal[96], antiparasitic[86], cardioprotective[86], and antidiabetic properties[86, 95], in addition to antimicrobial activities[86] and anti-inflammatory[95] effects.

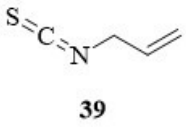

Figure 1.17: *Shows the structures of allyl isothiocyanate (39)*

Apart from exhibiting pharmacological activities, isothiocyanates also play a role as flavouring agents[97-99]. In rapeseed oil, a widely used cooking oil, attention has therefore been aimed at the impact these sulphur-containing compounds have on the quality of the canola oil as a food product. Sulphur-containing compounds in rapeseed oil have been categorised as volatile,

thermolabile, and non-volatile[15, 84, 100]. The volatile compounds, mainly isothiocyanates, thiocyanates, and sulphates, have been linked to inhibitory effects on hydrogenation catalysts[91, 101] and disagreeable odours, which, interestingly, resemble garlic[102]. Since hydrogenation is an effective way of increasing the shelf-life of canola oil, by preventing oxidation and resulting off-flavours of the oil[103], the former can be viewed as problematic. However, volatile sulphur compounds have been found to constitute only a small part of the total sulphur content of canola oil[85]. Indeed, the discovery of SHFAs was brought about by the realisation that a significant part of sulphur-containing compounds in rapeseed oil is constituted by these non-volatile compounds, which may also inhibit hydrogenation[15]. Thus, a proper characterisation of SHFAs can also be of industrial interest.

1.4. Chemical Background

1.4.1. Structure Elucidation

The structures of all the SHFAs described in literature to have occurred in plants[15, 24, 27] have been elucidated by the use of MS with an electron ionization (EI) source at 70eV. The advantage of this technique is that it generates spectra that are reproducible across most or all mass spectrometers[104]. Once a chemical structure has been confirmed, a comparison with formerly obtained MS spectra therefore provides a means of identifying the compound. A limitation of structure determination by the sole use of MS is that the mass spectra do not provide exact information about how the fragments that constitute the compound were originally connected, sometimes making interpretation complicated[105].

The challenge of structure determination by MS is illustrated by the discussion of Eibler *et al.*[27] in their structure elucidation of **40**. Based on the fragmentation pattern, four structures (**40-43**), all corresponding to the same molecular mass and formula, could appear plausible (*figure 1.18)*.

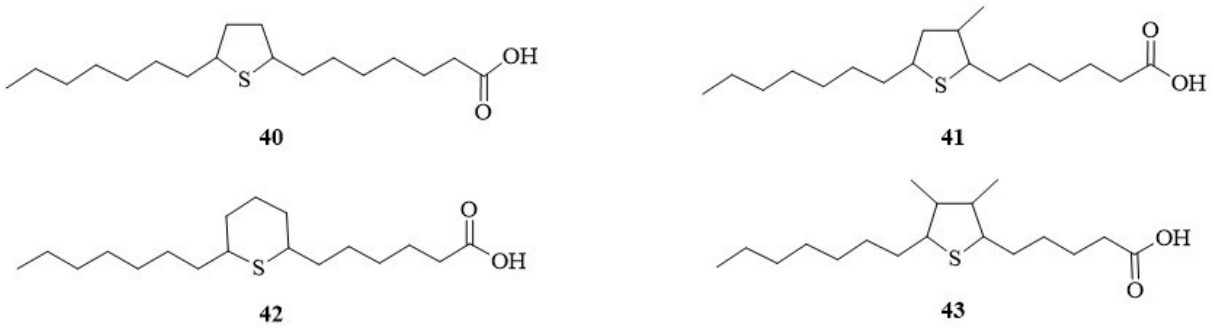

Figure 1.18: *Shows the structures* ***40-43.***

Assuming that SHFAs are biosynthesised from commonly occurring fatty acids, the authors eliminated **41** as a possibility since its biosynthesis would most likely have required a

methylated C_{17}-precursor, which is a highly unconventional fatty acid structure[27]. Notably, **41** would correspond to the structures proposed by Wijesundera and Ackman[15], and be highly analogous to most of the reported structures of FFAs. By reference to Dembitsky *et al*[24], **42** was also ruled out by Eibler *et al.*[27], as the spectrum showed a base peak at *m/z* 229, which reportedly is uncharacteristic for the thiane-containing fatty acids[24]. Since the fragmentation pattern seemed to correspond to **40** to a higher degree, **43** was also ruled out as a possibility, leading them to conclude that **40** was the most probable structure corresponding to this spectrum[27].

While the arguments provided for this structure are well-considered, their discussion exemplifies how structure determination by MS is not necessarily a straightforward task. Thus, MS is seldom the sole method of structure elucidation for molecules smaller than 2000 Da[105]. Instead, MS analyses are routinely and advantageously coupled to complementary techniques such as NMR, IR, and X-ray crystallography when the structures of smaller, novel molecules are to be determined[105].

Another limitation of EI-MS is that it cannot be used to assign stereochemistry to optically active molecules. All the SHFAs with a saturated heterocycle contain at least two chiral centra, which, in theory, could give rise to 2^2=4 stereoisomers (*figure 1.19*). As evidenced by optical rotation measurements performed on samples containing mixed fractions of SHFAs, the naturally occurring SHFAs are likely to be enantiomerically pure[27].

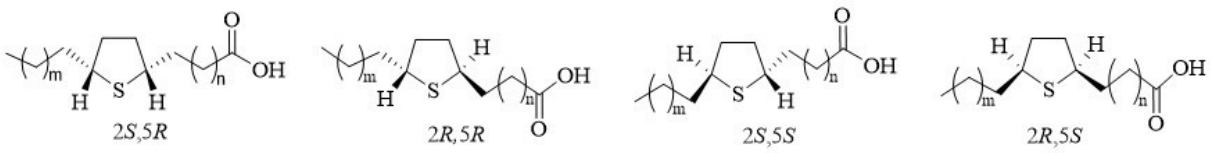

Figure 1.19: *SHFAs with saturated five-membered rings may give rise to four different stereoisomers.*

However, since the structures have only been investigated by MS, no information is currently available about the absolute configurations of SHFAs found in samples of mustard seed, rapeseed, and garlic oil.

1.4.1.1. Total Synthesis As a Means of Structure Elucidation

The above section illustrates how structure determination of previously undocumented natural products can be challenging. Even when complementary spectroscopic techniques are used, structure elucidation may be complicated[106, 107]. Indeed, in a review[106] covering challenges relating to modern structure elucidation, it was estimated that over 300 structural revisions, some of which included gross reassignments of the originally suggested structures, were undertaken only in the 14 year period from 1990-2004[106]. The misassigned structures ranged

from simpler chemical structures such as the coumarin **45**, to more complex molecules such as the marine antineoplastic agent bryostatin 3 (**47**) (*table 1.1.*)[106]. Another interesting example includes the structural revision of (-)-mucosin (**49**), an eicosanoid with an unusual bicyclic core isolated from the Mediterranean sponge *Reniera mucosa*[108, 109].

Table 1.1.: *Shows the misassigned and the reassigned structures of two compounds.*

Misassigned Structure	Revised Structure
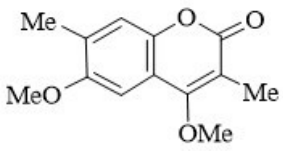 **44**	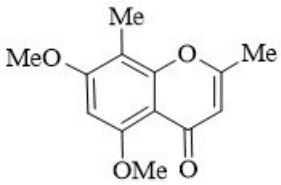 **45**
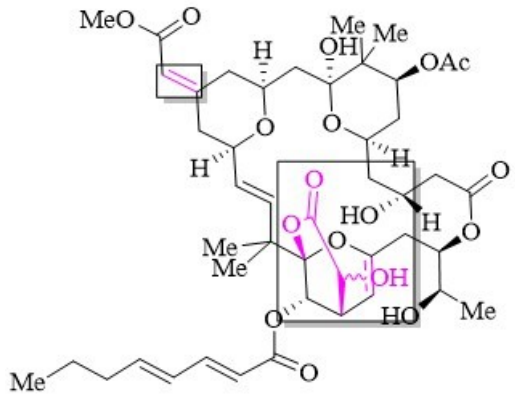 **46**	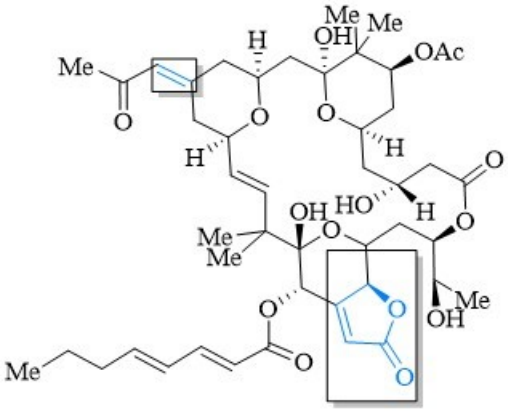 **47**
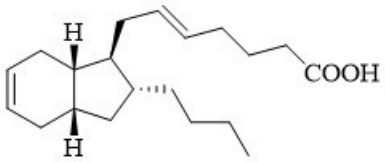 **48**	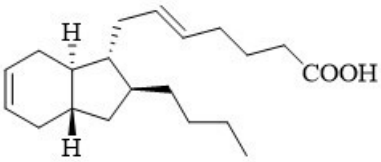 **49**

Originally, the coumarin structure had been determined by the combined uses of UV, IR, MS, and NMR[110]. However, a total synthesis of the originally suggested structure **44**[111] revealed discrepancies between the spectral data of the synthetically produced **44** and those reported in literature for the natural product[111]. Spectra consistent with those obtained for the natural product were generated only when the structure and the total synthesis strategy was revised to **45**[111].

Similarly, the structure of **47** was originally elucidated by combining spectroscopic techniques including NMR, UV, and MS[112], reassigned by extensive 2D NMR analyses[113, 114], and confirmed by total synthesis[115].

When a total synthesis of **48**, which was the structure that had originally been proposed for (-)-mucosin, was performed, spectral analyses of **48** proved that the stereochemistry of the natural product had been misassigned[108]. Aided by density functional theory calculations, the structure was reassigned to **49**, of which a new total synthesis was performed[109]. The spectra that **49** generated agreed with those obtained of the natural product[109].

As these examples demonstrate, there may be challenges related to the interpretation of spectral data, and total synthesis is sometimes the best way to confirm a structure. Indeed, as the coumarin and (-)-mucosin examples illustrate, total synthesis can be key to discovering that a structure has been misassigned in the first place. Given the lacking spectroscopic documentation that exist for SHFAs, a total synthesis could be an appropriate way of attaining more extensive characterisation, and to confirm the structures of these peculiar natural products.

1.4.2. The Alkyne Zipper Reaction

The alkyne zipper reaction is a process in which a linear, internal alkyne is isomerised to a terminal alkyne (*scheme 1.3*).

Scheme 1.3: *The alkyne zipper reaction involves the isomerisation of an internal to a terminal alkyne.*

The alkyne zipper reaction is usually performed using potassium 1,3-diaminopropanide (KAPA) as a catalyst, which has the advantage that it can act as a simultaneous proton donor and acceptor[116, 117]. The isomerisation proceeds via a rapid proton exchange between the alkyne and the diamine catalyst (*scheme 1.4*)[117, 118].

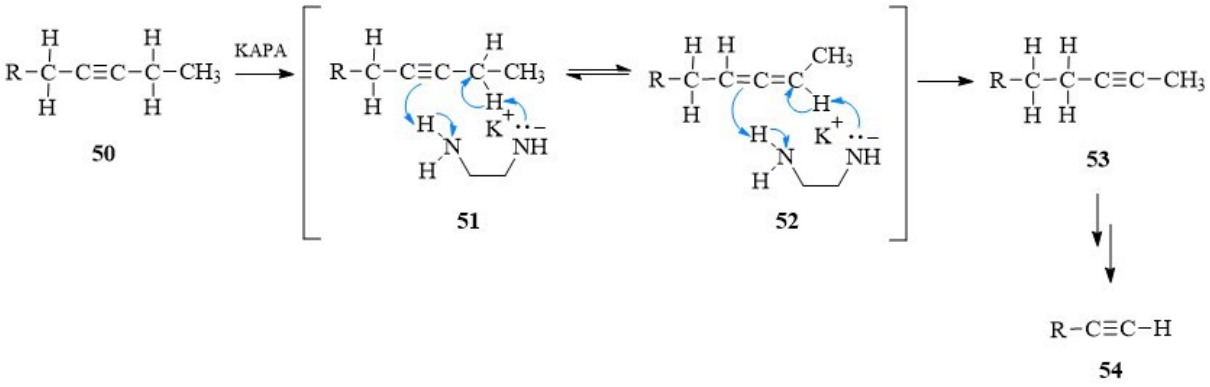

Scheme 1.4: *Mechanism of KAPA-catalysis[117].*

A contributing factor to the efficiency of the reaction is the favourable geometry formed between the diamine catalyst and the alkyne[118]. The 1,3-proton transfers in alkyne-allene

systems are, to varying degrees, of both inter- and intramolecular nature[119], as mediated by the base catalyst[118].

Since the alkyne zipper reaction involves the formation of a product that is less thermodynamically stable than the starting material, it is termed a "contra-thermodynamic" process[116, 117]. Particularly, the terminal alkyne is significantly less thermodynamically stable species than the internal alk-2-yne[120, 121]. Instead of being governed by thermodynamics, the internal-to-terminal alkyne isomerisation may therefore be viewed as a kinetically controlled process in which the formation of the alk-2-yne-carbanion constitutes the rate-determining step[120]. Upon deprotonation, the alk-2-yne tautomerizes between the two carbanionic species shown in *scheme 1.5* below[120].

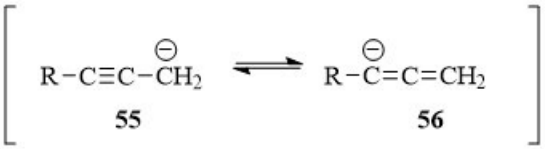

Scheme 1.5: *Shows the two electronic tautomeric states of the alk-2-yne cation.*

Of the two tautomeric forms, **55** constitutes the more stable species[120], as the greater *s*-character of the carbon on which the negative charge rests in **55** contributes to lowering the energy of the carbanion[120]. Consequently, **55** is also the predominant tautomeric from, and a terminal alkyne is therefore more susceptible to be formed upon re-protonation[120]. Since it commences in the formation of the carbanion, production of the alk-1-yne is generally favoured if the catalyst is in molar excess[120].

Currently, the alkyne zipper reaction is not widely applied in synthetic reactions. However, it has been predicted to have a greater impact in the years to come[122], and provides an interesting means of obtaining acetylene functionalisation.

1.4.3. Transition Metal Catalysed Reactions

1.4.3.1. Oxidative Cross-Coupling

Reactions that lead to the formation of new carbon bonds are fundamental to organic synthesis. One way of achieving such transformations is through oxidative cross-coupling, in which a transition metal is used to catalyse the carbon-extension. A series of name-reactions, such as the Sonogashira[123, 124], Negishi[125, 126], and Suzuki-Miyaura[127, 128] couplings, fall into this category.

In the oxidative cross-coupling between an organic nucleophile and electrophile, the mechanistic cycle (*scheme 1.6*) is initiated by the oxidative addition of the metal catalyst (M) to the organic electrophile (R_1-X)[129-131]. The resulting species (R_1-M-X) then undergoes trans-metalation with the organic nucleophile (R_2M_1) to form a R_1-M-R_2 intermediate[129-131]. The cycle terminates in cross-coupling of the organic substrates and the concomitant reductive elimination and regeneration of the metal catalyst[129-131]

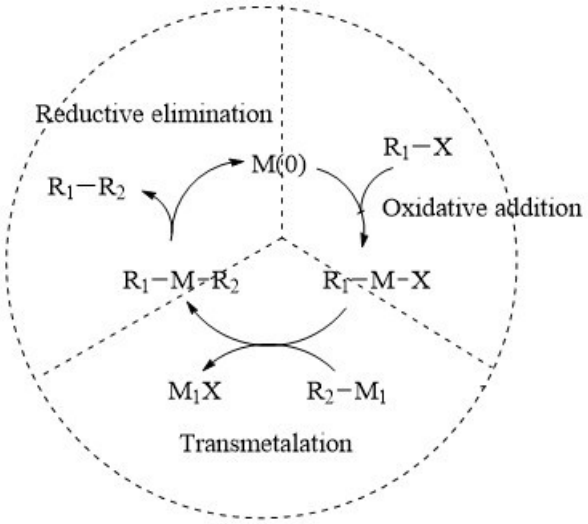

Scheme 1.6.: *Outlines a general mechanism for oxidative cross-coupling*

Coupling of two electrophiles or two nucleophiles can be achieved in an analogous manner. The former requires an extra reductant to compensate for the electron-deficiency of the two substrates, while the latter requires an additional oxidant for the opposite reason[129, 130, 132-134].

While the steps of oxidative addition and reductive elimination are general to all oxidative cross-coupling reactions, the trans-metalation step differs in each reaction, since it relies on different organometallic species and reaction conditions[135, 136].

The Sonogashira reaction traditionally involves the palladium-catalysed coupling of a vinyl or aryl halide to a terminal alkyne, where copper(I)iodide usually is present as a co-catalyst, along with an amine base as a solvent and activator (*scheme 1.7*)[137-139].

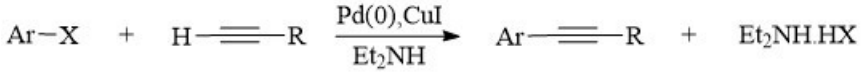

Scheme 1.7: *The Sonogashira coupling involves a terminal alkyne and an aryl or vinyl halide.*

Since it depends on the combined actions of two metal catalysts, a comprehensive understanding of the reaction mechanism has not yet been formed[137, 139]. As such, it is generally accepted that the reaction proceeds via two separate catalytic cycles – one involving the

oxidative addition of the palladium(0) catalyst to the aryl or vinyl halide, and the other the association of the copper co-catalyst with the alkyne to form the active alkynyl copper intermediate (*scheme 1.8*)[137-139].

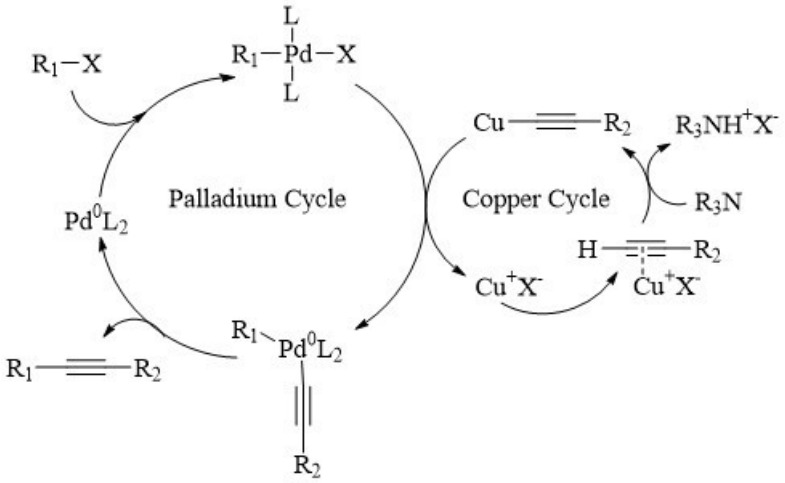

Scheme 1.8.: *The Sonogashira reaction proceeds via two separate cycles*[137]

The oxidative insertion of the palladium(0) catalyst into the vinyl or aryl halide is by some considered to be the rate-limiting step[137, 139-141]. However, evidence suggesting that the trans-metalation is rate-limiting has also been provided[142, 143]. Although the reaction sequence of the copper cycle is poorly understood, it is believed that the alkyne associates with the copper salt in coordination with the base to form the alkynyl copper intermediate[137-139]. The two cycles meet in the subsequent trans-metalation step, in which both substrates are coordinated to the palladium(II) catalyst before they eventually undergo cross-coupling and reductive elimination of the palladium(0) catalyst[137, 138].

The Sonogashira reaction is one of the most common ways of coupling alkynes to obtain arylacetylenes or enyne structures[141, 144-146]. The reaction exhibits high functional group tolerance and can generally be run under mild conditions in a reaction setup that is technically undemanding[137, 144, 145, 147]. However, the Sonogashira coupling is limited by the tendency of terminal alkynes to undergo homocoupling in the presence of copper and oxygen, which usually requires that the often-expensive acetylene reagent is added in excess[137, 146, 148, 149].

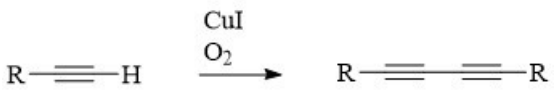

Scheme 1.9: *Terminal alkynes may undergo homocoupling in the presence of copper and air.*

For oxidative cross-couplings that do not involve acetylenes, the Suzuki cross-coupling reaction has the most far-reaching applications in both industry and academia[145, 150-152]. In the Suzuki

coupling reaction, organoboronic acids or esters constitute the active nucleophile that may undergo cross-coupling with an organic halide or pseudohalide (*scheme 1.10*). As such, the weakly nucleophilic organoboron compound requires activation by an appropriate base to participate in the trans-metalation step[135].

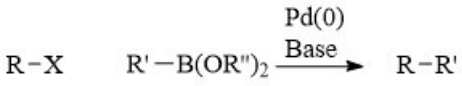

Scheme 1.10: *General outline of a Suzuki reaction, where X = Cl, Br, I, R and R' = (alkyl), vinyl or aryl, and R'' = H or alkyl substituent.*

The Negishi reaction resembles the Suzuki cross-coupling reaction except that organozinc species typically constitute the nucleophile that may undergo Pd- or Ni-catalysed cross-coupling to an organic halide or triflate (*scheme 1.11*)[153]. Unlike the organoboron species used in the Suzuki reaction, the organozinc compounds do not require activation of an additional base, owing to their greater intrinsic reactivity[154].

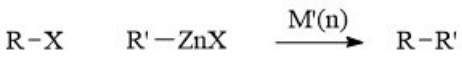

Scheme 1.11: *General outline of a Negishi reaction, where X = Cl, Br, I, R and R' = (alkyl), vinyl, aryl, or alkynyl and M = Pd, Ni, n = 0, II*

Oxidative cross-coupling reactions involving sp^3-hybridised species have historically been limited by the slow oxidative addition of transition metal into the alkyl halide, and the tendency of alkyl halides to undergo β-hydride elimination during the catalytic process[155-158]. Thus, these types of catalytic transformations have typically featured two unsaturated species[125]. However, as oxidative cross-coupling reactions have been developed to suit a broader substrate scope, examples of Sonogashira-[159-163], Suzuki-[164, 165], and Negishi[166-169]-type cross-couplings involving sp^3-hybridised species have emerged in literature, with one interesting example of the latter, featuring the oxidative cross-coupling of two sp^3-hybridised species, being depicted in *scheme 1.12* below[170].

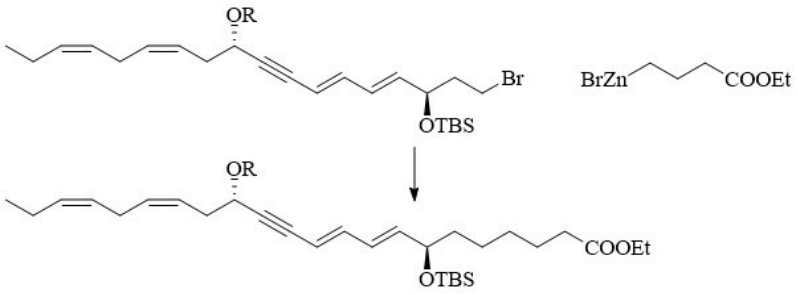

Scheme 1.12: *Literature example of an sp^3-to-sp^3 Negishi type cross-coupling[170].*

1.4.3.2. Transition Metal-Catalysed Reduction

Reduction of alkenes and alkynes is often achieved by a transition metal catalysed process, with the most common hydrogenation catalysts being palladium and platinum[138]. As outlined in *scheme 1.13.* below, hydrogenation takes place on the surface of the metallic catalyst, which is usually distributed on an inert support, such as charcoal[138]. The catalytic process is initiated as hydrogen adsorbs to the surface of the metal catalyst, causing breakage of the H-H bonds[138]. The hydrogen atoms are then made available for metal-mediated attachment to the organic substrate[138]. Subsequently, the unsaturated hydrocarbon is bonded to the metal, and hydrogen is transferred from the metal to the alkene[138].

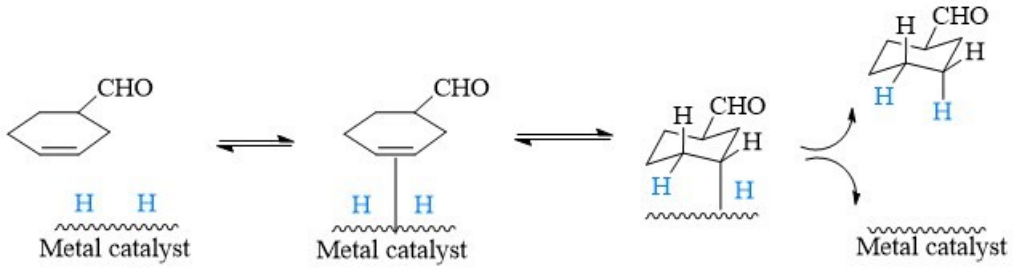

Scheme 1.13.: *Shows the transition metal-catalysed hydrogenation of an alkene*[138]

Alkynes undergo transition metal-mediated hydrogenation by an analogous mechanism, in which the corresponding alkane is usually afforded[138]. As indicated by the intact aldehyde group in *scheme 1.13*, reduction of carbon-carbon bonds is usually favoured over reduction of carbonyl groups under these conditions[138].

1.4.3.3. Metallic Catalyst Poisoning Effect of Sulphur

Although use of transition metal catalysis can be highly advantageous in cross-coupling and redox reactions, there are some limitations to applying transition metal catalysis to thiophene compounds, owing to the chemical properties of the heteroatom.

Sulphur has a high affinity for chemisorption to transition metal catalysts[171-173]. Thus, sulphur-containing compounds exhibit severe poisoning effects on metallic catalysts, as bonding of sulphur to the catalysts will make the metallic catalysts unavailable for binding to their substrates[171-173]. Even when present in trace amounts only, sulphur will inhibit the catalytic effect of the transition metals, making it suitably termed a transition metal-catalyst poison[171]. The poisoning effect is linked to the valence electron configuration of the catalyst poison, where inhibition is exhibited only if the toxic element possesses an unfilled valence orbital that can participate in the formation of chemosorptive bonds with the metal catalyst, thereby impeding on the access of the reactant to the catalyst active site[171-173].

In thiophene, the sulphur atom possesses one lone pair that participates in the aromatic sextet. Meanwhile, it retains another lone pair that is available for bonding to other elements, as illustrated in *scheme 1.14.* below.

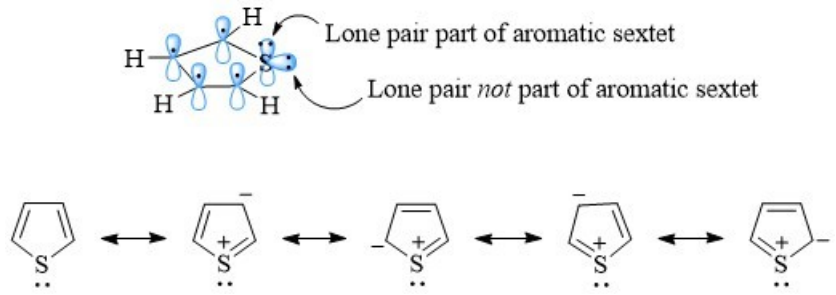

Scheme 1.14: *The sulphur in thiophene contains a lone pair that does not participate in the aromatic system*[174].

Due to the strength of the chemisorptive bond formed between sulphur and transition metal-catalysts, catalytic hydrogenation of thiophene compounds is highly ineffective, as the exchange between the thiophenes adsorbed to the metallic catalyst and the thiophenes in the free phase will occur very slowly[171]. For catalytic hydrogenation of thiophenes to occur at a significant scale, the metal catalyst would therefore need to be present in equal or excess molar amounts to the thiophene compound[175]. Alternatively, metal-catalysed reduction of thiophenes has been reported to occur under harsh conditions, such as elevated temperatures and pressures[175, 176]. However, in these instances, the hydrogenated product was only obtained in moderate yields, often along with the de-sulphurisation products[176]. Thus, alternative approaches need to be taken when thiophene compounds are to be reduced.

1.4.4. Ionic Hydrogenation

A route to hydrogenation that is compatible with sulphur-containing compounds, is reduction by ionic hydrogenation. Ionic hydrogenation is a reduction method in which hydrogen is introduced to an electron-deficient carbon centre by the combined actions of a proton donor (acid) and a hydride donor (*scheme 1.15*)[177, 178].

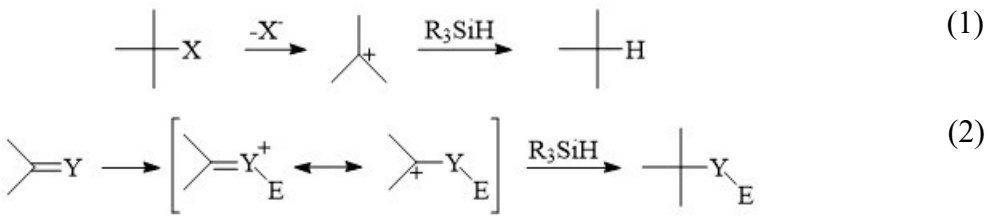

Scheme 1.15: *General outline of ionic hydrogenations of saturated (1) and unsaturated carbon centres, where R_3SiH constitutes the hydride donor*

The method depends on the formation of a carbenium ion, and the relative stability of the carbocationic species formed[177, 179]. The carbon centre must be sufficiently electron-deficient to effectuate hydride transfer from the donor molecule[177]. Thus, if the positive charge of the cationic species can be appreciably stabilised within the molecule structure, the carbenium ion will be incapable of abstracting a hydride ion from the donor molecule[177]. Meanwhile, if the intermediate carbocation is too unstable, ionic hydrogenation will not occur. For example, the dioxelium ion (**57**) is too stable to accept a hydride ion, whereas the secondary cyclohexylium cation (**58**) is too unstable to undergo this transfer[177]. Compared to the secondary cation (**58**), the tertiary carbocation (**59**) possesses the appropriate stability that allows it to undergo ionic hydrogenation[177].

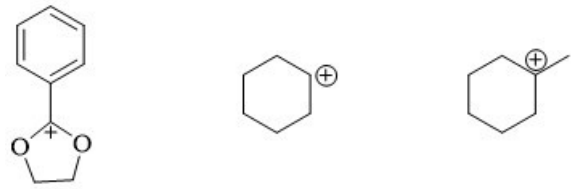

Figure 1.20: *Carbenium intermediates that are too stable (**57**), too unstable (**58**), or appropriately stable (**59**) to undergo ionic hydrogenation*[177]

The most commonly used hydride donors are organosilanes, which, compared to metal hydride alternatives such as germanes and stannanes, generally exhibit less reactivity toward the acid, allowing for a broader range of applications[177, 179]. The hydridic nature of silanes lies in the polarity of the Si-H bond, in which the lesser electronegativity of silicon leaves the hydrogen with a partial negative charge ($R_3Si^{\delta+}$-$H^{\delta-}$)[177, 180]. As such, silanes do not spontaneously transfer hydride ions when dispersed in solution with an unsaturated hydrocarbon[177, 180]. Hydrogenation occurs when the silane is activated, usually by transition metals or a Brønsted/Lewis acid[177, 180, 181]. Furthermore, as delineated in *figure 1.21.* below, the hydride-donating ability of the silane is influenced by the substituents of the silicon, where triethylsilane generally displays the greatest donating power, while diphenylsilane constitutes the weakest hydride donor[176, 179].

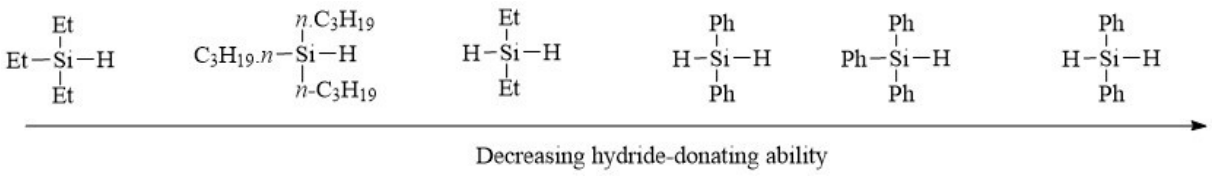

Figure 1.21.: *Order of decreasing hydride-donating ability of silanes*[176].

Triethylsilane (Et_3SiH) is most frequently chosen as the hydride donor, in conjunction with trifluoroacetic acid (CF_3CO_2H) as the proton donor[176-180, 182]. The CF_3CO_2H/Et_3SiH-hydrogenating pair is capable of reducing thiophenes[175, 179]. Like in electrophilic substitutions to thiophenes, hydrogenation of thiophenes is favoured at the α-positions[175, 179]. The ionic hydrogenation process of thiophenes to tetrahydrothiophenes is therefore initiated by the addition of a proton to the 2-position, which results in the formation of a thiophenium ion (**61**)[175]. A hydride ion is then donated from the silane to the 3-position of the thiophene, generating the 2,3-dihydrothiophene intermediate (**62**)[175]. Subsequent rapid hydrogenation of the intermediate affords the tetrahydrothiophene **64** as the product[175] (*scheme 1.15.*). The alternative route, in which the hydride is added to the 5-position of the intermediate instead of the 3-position is unlikely to occur, as the dihydrothiophene **65** is not observed as a product[175].

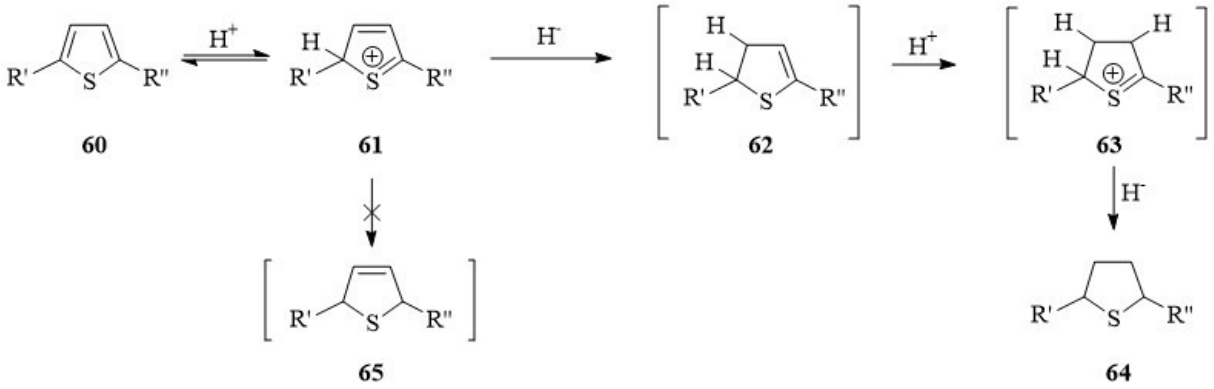

Scheme 1.15: *Mechanism of ionic hydrogenation of thiophenes[176].*

The presence of alkyl substituents at the α-positions significantly enhances the rate of hydrogenation of thiophenes when compared to unsubstituted thiophenes[175, 179]. Oppositely, thiophenes with strong electron-withdrawing substituents, such as halogens, carboxy or ester groups in conjugation to the aromatic system are largely deactivated for hydrogenation by this method[179].

Since carbonylic compounds are only moderately activated for ionic hydrogenation by CF_3CO_2H, ionic hydrogenation can be used to selectively reduce carbon double bonds in the presence of carbonyl compounds[179]. Indeed, this preferentiality is also seen in α,β-unsaturated ketones, where the alkene bond is selectively reduced over the carbonyl group (*scheme 1.16*), affording the corresponding saturated ketones in high yields[179]. Similarly, reduction of thiophenes can be achieved without affecting an ester group[175].

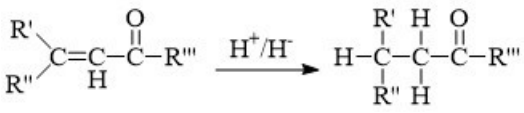

Scheme 1.16*: α,β-unsaturated ketones are reduced to the corresponding ketones when the hydrogenating pair is present in amounts that allow for reduction of one double bond only[179].*

Compared to corresponding alkenes, alkynes are less susceptible to hydrogenation by organosilicon compounds[177], and studies concerning ionic hydrogenation of alkynes are limited[178, 182, 183]. As such, alkynes in conjugation with electron-rich aryl groups have been reported to be completely hydrogenated in modest yields using the CF_3CO_2H/Et_3SiH-hydrogenating pair[177 184], with improvements in yield being reported when stronger acid conditions were employed[177, 185]. However, alkyne reduction by this hydrogenation pair is slow, largely causing the Et_3SiH to decompose before significant hydrogenation is effectuated[183]. To this end, the tungsten hydride ($Cp(CO)_3WH$) in conjunction with CF_3CO_2H has proven to be a more effective hydride donor in the reduction of alkynes, capable of reducing the triple bond via the initial formation of divinyltriflate intermediates (*scheme 1.17*)[183]. Nevertheless, ionic hydrogenation of alkynes is a slow process[183].

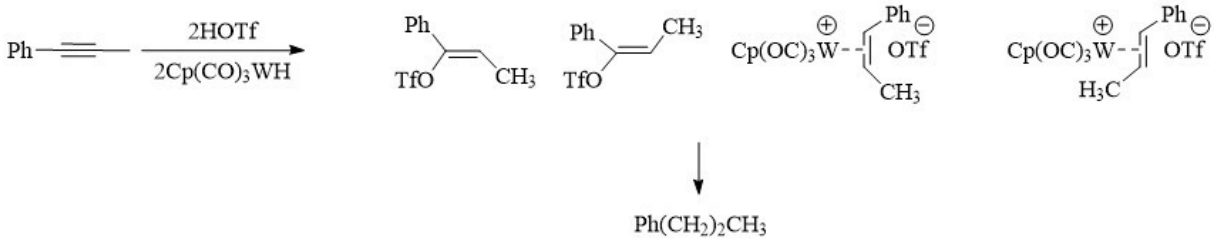

Scheme 1.17.: *Shows the reduction of an alkyne via divinyl triflate intermediates.*

1.4.5. Olefination Reactions

Olefination reactions are reactions that lead to the formation of new carbon-carbon double bonds. One of the earliest reported reactions in this category is the Wittig reaction[186], which involves the reaction of an aldehyde or a ketone with a phosphonium ylide to afford an alkene (*scheme 1.18*)[187-189].

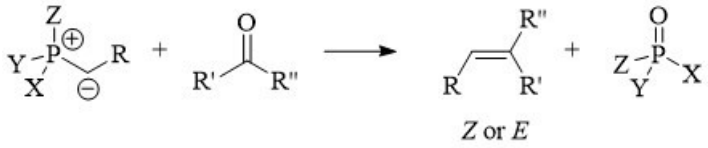

Scheme 1.18: *Outline of the Wittig reaction, where X, Y, Z = alkyl, aryl, or alkoxy substituents.*

The mechanistic details of the reaction has been a topic of discussion throughout the years[188-190], however, the modern interpretation appears to be that the reaction is initiated by nucleophilic attack of the negatively charged ylide carbon on the carbonyl centre, resulting in a four-membered cyclic intermediate (*scheme 1.19*)[138, 189-191].

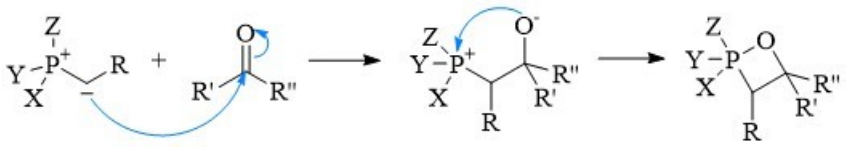

Scheme 1.19: *The Wittig reaction is initiated by the formation of the oxaphosphetane intermediate*[138].

Lacking intrinsic stability, the oxaphosphetane intermediate then collapses, in a process that generates the olefin along with the phosphine oxide (*scheme 1.20*)[138].

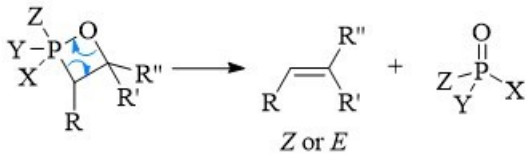

Scheme 1.20: *The alkene is generated from the collapse of the oxaphosphetane intermediate*[138]

One drawback of the Wittig reaction is that the neutral phosphonium oxide by-product is often difficult to separate from the alkene product[192]. This challenge is largely overcome in the Horner-Wadsworth-Emmons (HWE)[193, 194] olefination reaction, which may be viewed as a modified version of the Wittig reaction[195, 196]. In the HWE olefination, phosphonate ions are used in place of the phosphonium ylide (*scheme 1.21*), which generates the easy-to-remove phosphorus acid salts, along with the target alkene[191, 192].

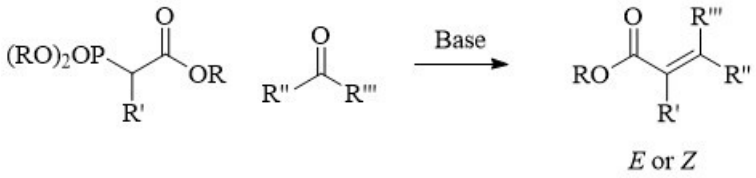

Scheme 1.21: *Outlines the HWE olefination.*

Both olefination reactions provide the advantages that the phosphorous reagents are easy to prepare, offer high reactivity, and tolerate a wide set of conditions and substrate scope[189, 197]. Furthermore, both the Wittig and the HWE reaction can be tuned to be highly stereoselective by managing the reaction conditions and the properties of the phosphorus-containing nucleophiles[188, 191, 196, 198].

For example, in the Wittig reaction, use of non-stabilised ylides, *i.e.*, ylides that carry alkyl substituents on the ylidic carbon provide a high degree of (*Z*)-stereoselectivity, whereas stabilised ylides – those containing aryl, vinyl, halo, or alkoxy substituents on the ylidic carbon – predominantly furnish the (*E*)-stereoisomer[188, 191].

Similarly, the HWE olefination preferentially leads to the formation of (*E*)-isomers when traditional reactions conditions and di-alkylated phosphonate species are employed. As such,

the reaction can be made highly (*Z*)-selective under the appropriate conditions when phosphonates such as bis(trifluoroethyl)phosphonoacetates, or diphenylphosphonoacetates, that carry highly electrophilic or bulky substituents on the phosphorus atom, are employed[191, 196, 198].

Apart from providing a means of obtaining a high yield of geometrically pure stereoisomers, these olefination reactions also serve a role as carbon-carbon extending reactions, further adding to their usefulness to organic synthetic reactions.

1.4.6. Substitution Reactions

1.4.6.1. The Finkelstein Reaction

The Finkelstein reaction is a halide exchange reaction in which one halogen group is substituted by another (eq.1)[199].

$$RX + X' \rightleftharpoons RX' + X^- \qquad (1)$$

The reaction typically involves the exchange of a chloro- or a bromo group with a fluoro or an iodo group via an S_N2 mechanism. The preparation of iodides by this method usually achieved by the use of NaI in acetone. This produces the alkyl iodide along with sodium chloride or bromide[199] (*scheme 1.22)*.

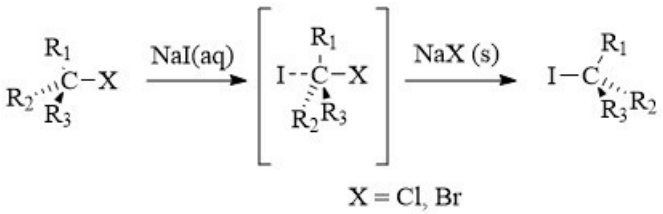

Scheme 1.22: *The Finkelstein reaction proceeds via an S_N2 mechanism.*

Since both salts are insoluble in this medium, the equilibrium is shifted in favour of product formation, as reagents for the reverse reactions are made unavailable[199]. Thus, iodides can be readily obtained from the parenting alkyl chlorides or bromides.

1.4.6.2. The Appel Reaction

One way of converting primary and secondary alcohols into the corresponding organic halide is through the Appel reaction, in which the hydroxyl group is substituted by a halogen by the combined actions of triphenylphosphines and halogenomethanes[200]. The reaction is initiated by attack of the phosphine on the halogen attached to the halogenomethane, resulting in a S_N2-type displacement of the halogen to the phosphine centre (*scheme 1.23*)[200]. The anionic species that arises from de-halogenation of the halogenomethane then proceeds to deprotonate the

hydroxyl group, thus activating the alcohol as a stronger nucleophile[200]. Subsequent nucleophilic attack of the alkoxy species on the positive phosphine centre displaces the halogen once again to the solution[200]. The carbon centre attached to the triphenylphosphine is then subjected to nucleophilic attack by the displaced halide anion, leading to the elimination of the triphenylphosphine oxide, and the generation of a halogenated product[200].

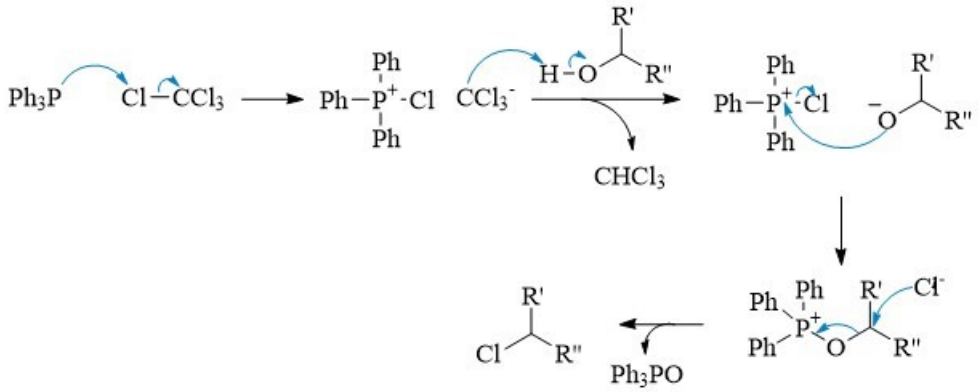

Scheme 1.23: *The Appel reaction*[200]

While the reaction traditionally features a carbon tetrachloride[200, 201], it has been modified to include the production of bromides and iodides[202-204], making it a synthetically useful reaction that may activate primary and secondary alcohols for further modifications.

1.5. Synthetic Strategies

Since **8** has been reported to occur in both *Allium* and *Brassica*[24, 27], a total synthesis and subsequent structure determination of this compound is of particular interest. With **7**, which has been isolated from garlic[24], differing from **8** only with respect to the unsaturation of the heterocycle, a total synthesis of this molecule should be achievable through a similar synthetic route. Insofar as no data exist that could be used to confirm the absolute stereochemistry of the optically active SHFA **8**, an asymmetric synthetic approach is not targeted initially. Furthermore, since only the methyl esters of the SHFAs have been isolated thus far, a synthetic approach should be taken towards the fatty acid methyl esters **65** and **66** (*figure 1.22*).

65 **66**

Figure 1.22: *The structures of the target molecules.*

1.5.1. Former Syntheses of SHFAs

Currently, the only recorded synthesis approach leading to a naturally occurring SHFA appears to be one reported for **8**, which is described in a patent[205]. This synthetic strategy involved

irradiating 9,12-octadienoic (**67**) and elemental sulphur with ultrasonic waves to afford a mixture of **8** and its corresponding dihydrothiophene analogue (**68**) in yields of 56% and 39%, respectively[205] (*scheme 1.24*).

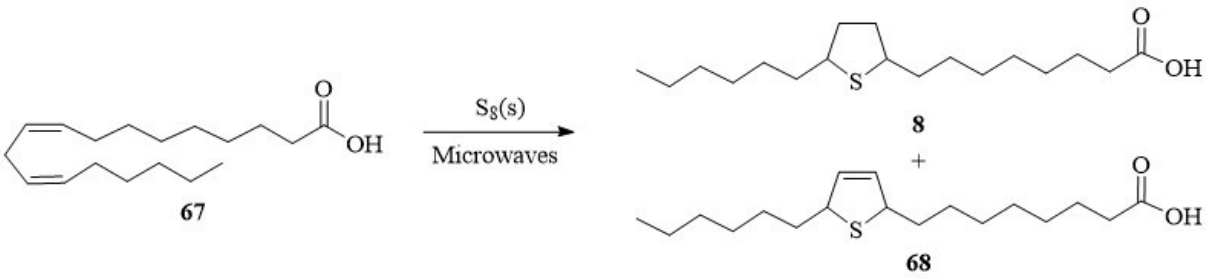

Scheme 1.24: *Outlines the synthesis process described in the patent[205].*

In addition, total synthesis of polyunsaturated analogues have been achieved by Flock *et al.*[206] (**61-62**) and by Yasser *et al*[207] (**63a,b**) (*figure 1.23*).

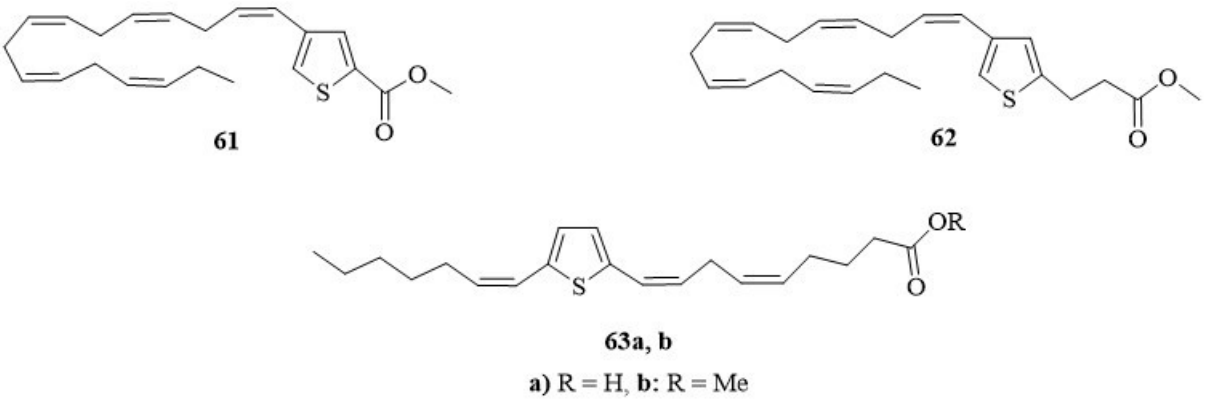

Figure 1.23: *Shows the structures of polyunsaturated analogues obtained by total synthesis.*

Yet, there does not seem to be any records of a total, piecewise, synthesis of the natural products reported to occur in *Allium* and *Brassica*.

1.5.2. STRATEGY 1

One retrosynthetic analysis is presented in *scheme 1.25* below and involves a convergent approach towards the target molecules.

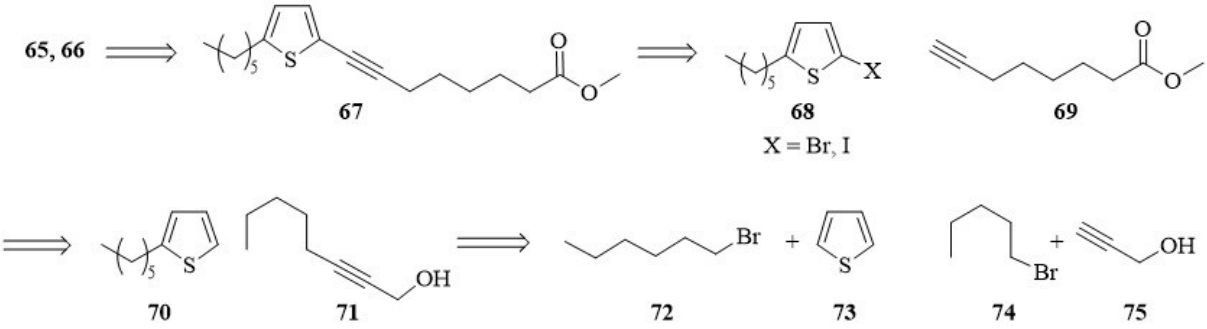

Scheme 1.25.: *Retrosynthesis, Strategy 1*

The pivotal step of this synthetic approach is the formation and subsequent reduction of the intermediate **67**, which in turn hinges on the successful cross-coupling of alkyne ester **69** to the alkyl thiophene **68**. Synthesis of the key intermediate **67** can be accomplished via a Sonogashira cross-coupling procedure between **68** and **69**. The coupling partner **69** can be synthesised from **74** and **75** and isomerised via the alkyne zipper reaction to achieve the acetylene functionalisation that the cross-coupling requires.

Considering the poisoning effect of sulphur on metal catalysts, and the relatively low thermodynamic reactivity of alkynes[208], the cross-coupling step might impose one of the greatest challenges of this synthetic route. The toxic effect of thiophene on metal catalysts might also make catalytic hydrogenation an unsuited method for reduction of the alkyne. Since the alkyne is unlikely to be compatible with ionic hydrogenation to any large degree, finding a method that selectively reduces the triple bond to an alkane without affecting the ester moiety is also a key step.

1.5.3. STRATEGY 2

A linear synthetic strategy (*scheme 1.26*) can also be envisioned for the syntheses of **65** and **66**.

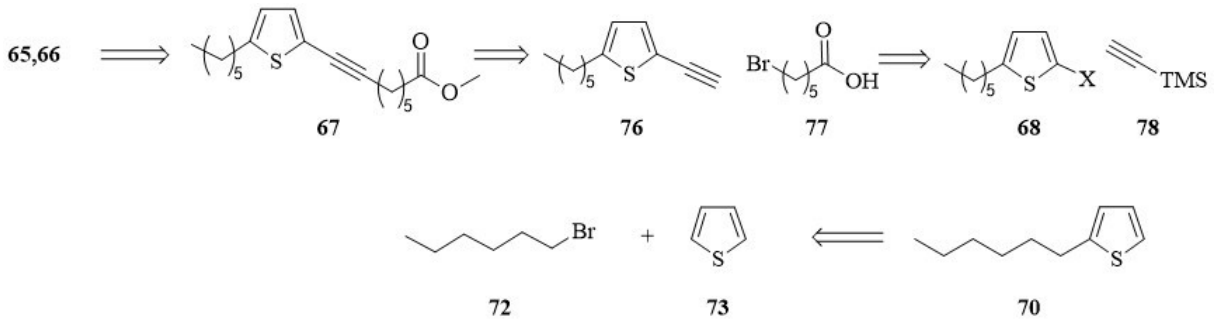

Scheme 1.26.: *Retrosynthesis, Strategy 2.*

In this case, the two cross-coupling steps leading to **67** are also the most crucial since they furnish the final carbon skeleton. Given the relative reluctance of sp^3-hybridised species to participate in oxidative cross-coupling, the sp-to-sp^3 cross-coupling between **76** and **77** might constitute the greatest challenge of this synthetic approach, especially when considering the potentially inhibitory effect of the thiophene on transition metals.

1.5.4. STRATEGY 3

Both the strategies outlined above rely heavily on acetylene functionalisation and palladium-catalysed cross-couplings, in which scenarios the poisoning effect of thiophene, and appropriate activation of the alkyne might be limiting to the successes of the carbon-extending reactions. Another limiting factor in these strategies might be selective hydrogenation of the alkyne to the

corresponding alkane. Thus, a strategy that is less dependent on these factors can also be envisioned (*scheme 1.27*)

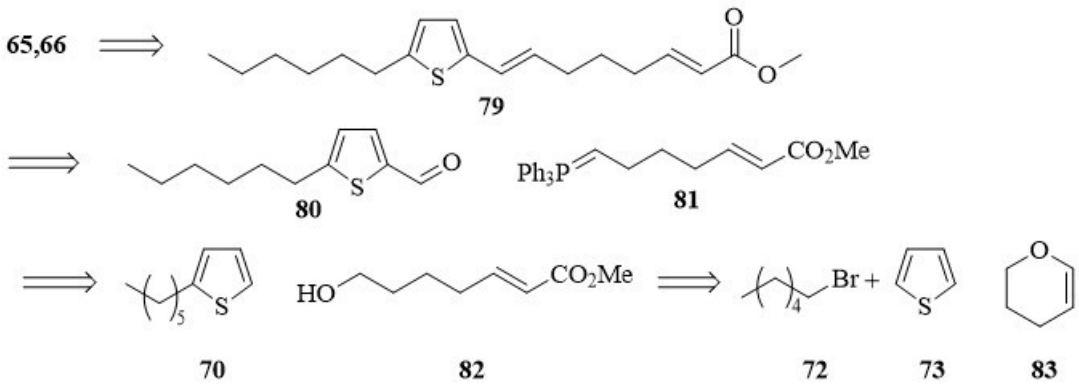

Scheme 1.27: *Retrosynthesis, Strategy 3*

In this reaction scheme, carbon-carbon extension can be accomplished via an olefination reaction between the thiophene aldehyde **80** and the triphenylphosphine ester **81**, to furnish the thiophene-diene ester **79**. The α,β-unsaturated ester **82** can be obtained by oxidative ring-opening of 3,4-dihydrofuran (**83**), and subsequent HWE olefination of the resulting ω-hydroxy carboxylic acid to afford the ester. Subsequent conversion of the ω-hydroxyl group into the Wittig reagent should prepare it for the final olefination reaction that furnishes the 18-carbon skeleton. Methods involving the selective reduction of alkenes are highly developed and should therefore be applicable to **79** as well. Indeed, it is conceivable that the synthesis of **66** can be achieved in one concerted hydrogenation step from **79** using ionic hydrogenation.

1.5.5. STRATEGY 4

A third convergent strategy is presented in *scheme 1.28* below.

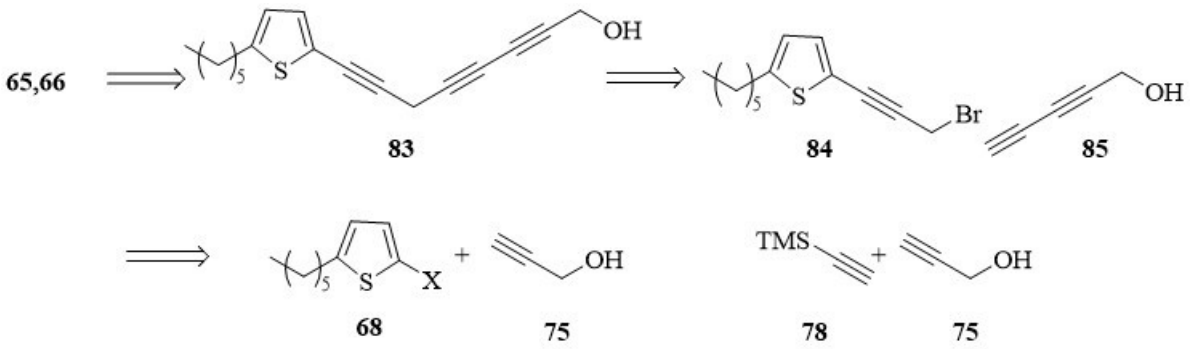

Scheme 1.28: *Retrosynthesis. Strategy 4*

This strategy is founded on acetylene functionality, which is the key to obtaining the triyne intermediate **83**. The thiophene triyne can be furnished from coupling of the thiophene alkyne **84** and the 1,3-diynol **85**. The former can be afforded from a Sonogashira coupling of **75** to **68**,

whereas **85** can be formed from an oxidative coupling of **75** to **78**, followed by cleavage of the TMS group to afford **85**. Subsequent redox and esterification reactions should furnish the target molecules **65** and **66.**

1.5.6. STRATEGY 5

A retrosynthetic strategy that encompasses elements from both *Strategy 3* and *4* is presented in *scheme 1.29.* below, and involves a linear approach towards the target molecules **65** and **66**.

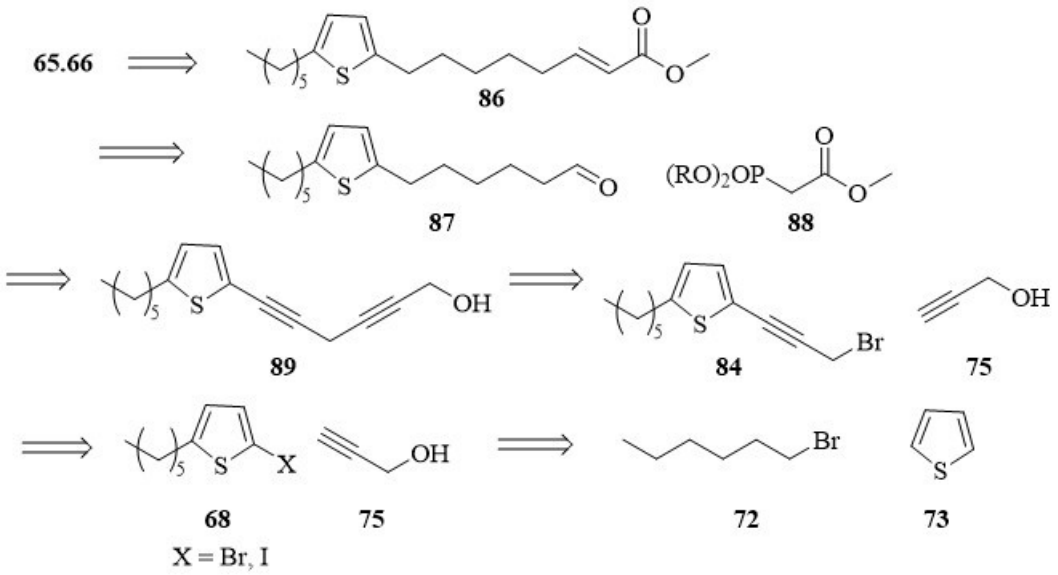

Scheme 1.29: *Retrosynthesis, Strategy 5*

Instead of going via the triyne, the six-carbon substituent that will eventually furnish the ester substituent is obtained by two subsequent couplings of propargyl alcohol – firstly to thiophene, and subsequently to the propargylbromide thiophene. As such, preparation of the diyne, and its subsequent hydrogenation are likely to be the most critical steps of this synthetic strategy. If the intermediate **89** is obtained, the resulting alcohol might be converted into an aldehyde in preparation for olefination.

In principle, this could be done either by proceeding directly to the diynic aldehyde **90** (*path A*, *scheme 1.30*), or by reducing the diyne prior to oxidation of the alcohol, to afford the alkanol **91** (*path B*, *scheme 1.30*).

On the one hand, *path A* would be a more step-efficient approach, considering that the α,β-unsaturated ester **86** eventually produced would also need reduction. Synthetising a propargylic aldehyde might also be advantageous in that the high electron density could provide a more reactive species, which in turn could produce a higher yield in the olefination step. However, the enhanced reactivity of the propargylic aldehyde might also produce conjugate additions,

alkyne-to-allene isomerisations, or other undesired side-reactions. Thus, path B will afford an intermediate species with a more predictable behaviour and reactivity, which is also beneficial.

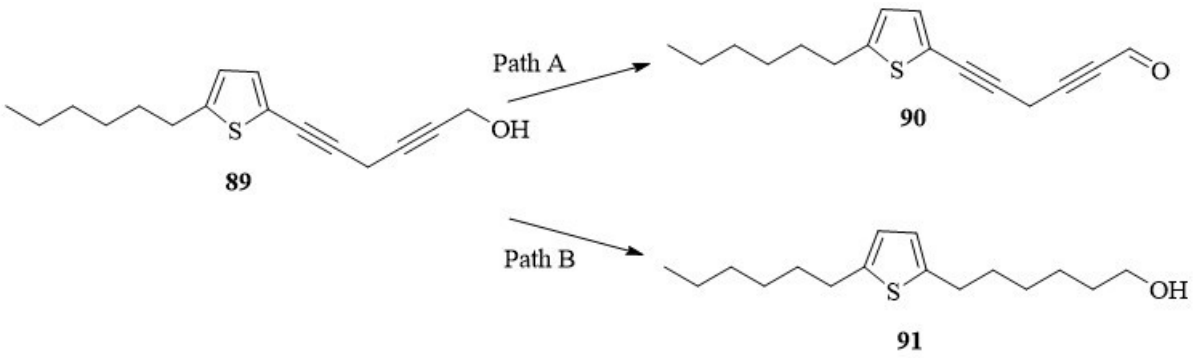

Scheme 1.30: *Path A and B.*

Having decided on a pathway. subsequent reduction of the olefin and the thiophene will then afford the target molecules **65** and **66**.

1.6. AIM OF THE ASSIGNMENT

The aim of the assignment is to perform a total synthesis of the methyl esters of the SHFAs **7** and **8**. Since the absolute configuration of **66** is unknown, an asymmetric synthesis approach is beyond the scope of this assignment. If total synthesis is achieved, the compounds will be subjected to MS-EI analysis for a comparison with the spectra obtained from the natural products. Thus, confirming the gross structures of these SHFAs is also a target of this thesis.

Given the potential pharmacological properties of **65** and **66**, preparation of the SHFAs for biological assaying might also be an interesting secondary goal. However, biological testing will not be in focus of this thesis. Hence, the main objective is to achieve total synthesis of **65** and **66**, thereby contributing to structure elucidation of the SHFAs found to occur in garlic-, rapeseed-, and mustard oil.

2. Results and Discussion

2.1. Synthesis and Halogenation of 2-hexylthiophene

The alkylated thiophene common to all the synthetic pathways was synthesised by coupling 1-bromohexane (**72**) to thiophene (**73**) (*scheme 2.1.*), according to a literature procedure[209]. Due to a Covid-19-related lockdown, the reaction was left stirring for two weeks when attempted the first time, affording **70** in a 55% yield. Evidence for the successful reaction was provided by the spectral data, which were in agreement with those reported in literature[209, 210].

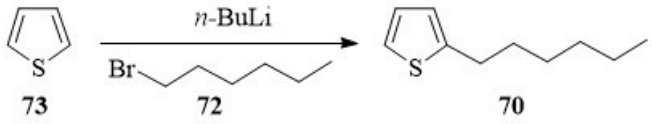

Scheme 2.1.: *Alkylation of thiophene*

A new attempt at the reaction afforded **70** in a 58% yield, which was only a moderate improvement to the original attempt. Hence, it appeared that the reaction yield was not significantly affected by the extended period of time in which it was allowed to run in the first attempt.

Since THF was used as the only solvent, it is conceivable that the *n*-BuLi was poorly disaggregated under the given reaction conditions. Furthermore, it could be that the *n*-BuLi exhibited some degree of interaction with the THF solvent in addition to interacting with the thiophene. Thus, the reaction was attempted a third time, this time adding a small amount of HMPA in the hope that this would improve dissociation of the *n*-BuLi aggregates, and thereby the yield. However, the improvement was only moderate, and the compound was afforded in a 60% yield. This slight improvement did not justify the additional purification step required for the removal of HMPA, which had been distilled along with the target compound **70**.

It is conceivable that adding a greater molar excess of the organolithium reagent could help improve the yield, as this would ensure a more complete deprotonation of the thiophenes in solution. Alternatively, a more reactive organolithium reagent such as *s*ec-BuLi or *tert*-BuLi might be employed for the same purpose. However, the former could also have led to poly-substitution if already-substituted thiophenes were lithiated in place of the intended unsubstituted thiophene molecules. Furthermore, considering the relative quanta of the target compound that was nevertheless obtained, the low cost of the cross-coupling reagents, and the hazard of handling organolithium reagents, testing these hypotheses did not appear worthwhile.

Subsequent to its synthesis, **70** was brominated according to a literature procedure[211]. This afforded **68a** in an 84% yield (*scheme 2.2.*). Spectral data corresponded to those reported in literature[211].

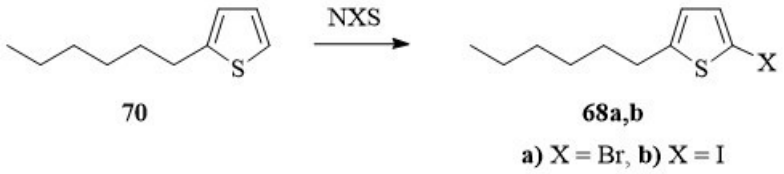

Scheme 2.2.: *Halogenation of **70**.*

Iodination was also attempted according to a different literature procedure[212]. Following the original procedure, **70**, and NIS, which was used as the iodinating agent, were added in exact equimolar amounts (1:1). Judging from the ^{1}H NMR spectrum of the crude product, this reaction afforded the mono-iodinated target molecule in a 3:1 mixture together with the unreacted starting material. Since the iodinated **68b**, and **70.** proved impossible to separate by flash column chromatography, the reaction was attempted again, this time adding a slight excess of NIS, in a ratio of 1.1 equivalents of NIS to 1 equivalent of **70**. This produced the mono-iodinated product exclusively in a 96% yield. Spectral data were in agreement with those reported in literature[212].

2.2. Strategy 1: Synthesis of 2-octyn-1-ol and 7-octyn-1-ol

In the first step towards the eight-carbon carboxylic substituent envisioned for *Strategy 1*, 2-octyn-1-ol (**71**) was synthesised by coupling 1-bromopentane (**74**) to propargyl alcohol (**75**) (*scheme 2.3.*) in an 82% yield.

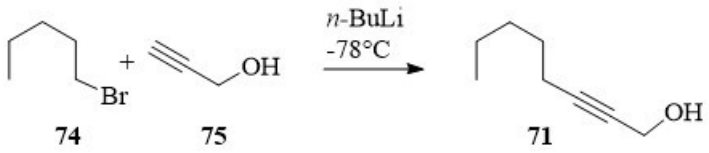

Scheme 2.3.: *Synthesis of **71**.*

Indicative of the successful reaction was the NMR spectra of the purified compound, which were in agreement with literature data[213, 214].

The alkynol **70** was isomerised to 7-octyn-1-ol (**92**) via the alkyne zipper reaction (*scheme 2.4.*) in a 70% yield by following a literature procedure[215]. A comparison of ^{1}H and ^{13}C NMR data with literature values[213, 214] confirmed the success of the reaction.

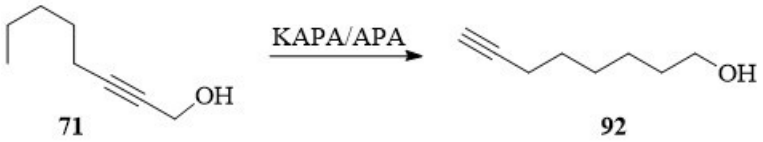

71 92

Scheme 2.4.: *Isomerisation of* ***71.***

The isomerisation reaction was originally performed using KH/1,3-diaminopropane as a catalyst. When the potassium hydride was not washed prior to running the reaction, the mineral oil co-eluted along with the alkynol, and had to be removed mechanically by a Pasteur pipette. Thus, washing of the salt proved advantageous to the purification process.

When addition of the diamine to the washed hydride was attempted at room temperature, this resulted in a vigorous reaction that left the fume hood covered in a diamjne foam. At a later stage, this was circumvented by cooling the reaction flask to 0°C before adding the solvent.

To test if a less hazardous procedure could be developed, the alkyne zipper was also attempted using sodium hydride in conjunction with 1,3-diaminopropane instead of potassium hydride. Sodium hydride provides the advantage of being less pyrophoric in reaction with air than potassium hydride. Furthermore, NaH has a much more uniform distribution of crystals than KH in mineral oil, which makes it easier to weigh out the intended amounts accurately. However, it appeared that the diamine solvent was poorly activated by this hydride, as isomerisation did not occur. This, perhaps, reflects the relative reactivities of the hydrides.

A literature search found that a NaH-based zipper reaction had been performed in conjunction with 1,2-diaminoethane instead of 1,3-diaminopropane[216]. Therefore, the alkyne zipper reaction was attempted again using the NaH/1,2-diaminoethane pair at a slightly elevated temperature. This time, the reaction went to completion, affording the isomerised alkynol in a 43% yield.

One explanation for the success in this case could be that NaH was more effectively solvated in 1,2-diaminoethane owing to the smaller alkyl moiety of the solvent. However, the yield was significantly lower than that obtained when KH was used. An attempt at improving the yield by treating the aqueous phase with HCl to a neutral and acidic pH before phase extraction was performed. This was to ensure that the alkynol was protonated, so that it remained in the organic phase upon subsequent workup. In this way, the alkynol was afforded in a 50% yield. The modest improvement in yield did not justify the amounts of HCl required to neutralise the strongly basic diamine solution.

Thus, even though this latter procedure allows for the use of a slightly less hazardous reagent, it comes at the expense of atom efficiency, which must be taken into consideration when choosing between the two catalyst pairs.

2.3. Strategy 1: Oxidation and Methylation of 92

The next step in *Strategy 1* involved oxidation of the alkynol **92**, which was achieved according to a modified literature procedure[216]. This afforded the alkynolic acid **93** in a 75% yield.

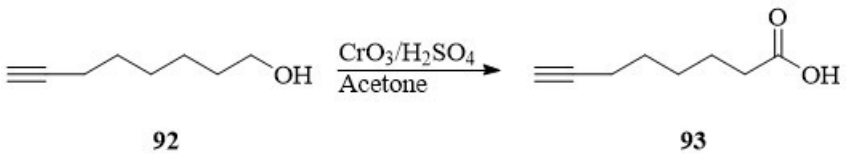

92 **93**

Scheme 2.5: *Oxidation of* ***92.***

The acid was then esterified according to a different literature procedure[217], affording the methyl ester **69** in a 90% yield. In both cases, spectral data were in agreement with literature values[216, 217].

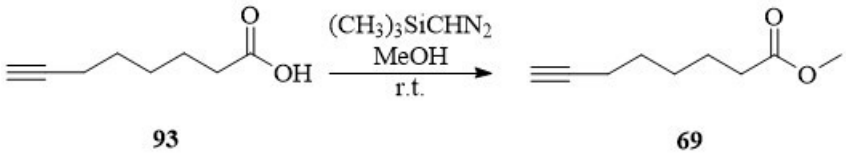

93 **69**

Scheme 2.6: *Esterification of* ***93****.*

2.4. Strategy 1: Alternative Synthesis Attempt of 7-Octynyoic Acid and Methyl 7-Octynoate

Despite the relative success of the alkyne zipper reaction, it was decided to attempt an alternative synthesis strategy for the eight-carbon carboxylic substituent, involving the eventual production of **93** from the coupling of ethynyltrimethylsilane (**78**) to 6-bromohexanoic acid (**77**) to produce **94**. The advantage of this approach was that it could potentially reduce the synthetic pathway by a step, and that acetylene functionalisation could be obtained without using pyrophoric hydrides. The cross-coupling was executed by following a literature procedure[218].

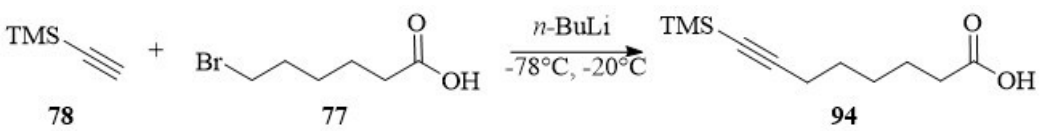

78 **77** **94**

Scheme 2.7: *Synthesis of* ***94****.*

The major product of this reaction appeared to result from nucleophilic attack on the carbonyl, and the target cross-coupling product was afforded in a 11% yield only, as indicated by a comparison with literature data[218, 219].

Before this strategy was abandoned, transition-metal catalysed coupling of the methyl ester of **77** to **78** was attempted. A rationale for this approach is that nucleophilic attack of the carbonyl would not occur in the absence of a strong organolithium base, so that the transition metal catalysis could, to a greater extent, facilitate the desired C_{sp}-to-C_{sp3} cross-coupling. Using the methyl ester seemed especially appropriate, considering that the methylated SHFAs were the targets of the synthesis.

Firstly, the methyl ester **95** was afforded from the commercial grade carboxylic acid **77** in an 86% yield by following a literature procedure[220].

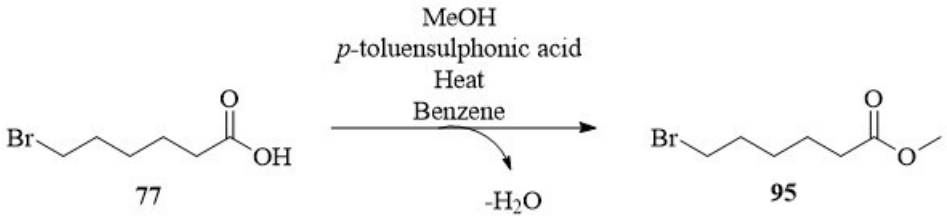

Scheme 2.8: *Synthesis of the methyl ester* ***95.***

Palladium-catalysed cross-coupling of **95** to **78** was then attempted, however, no cross-coupling product was obtained in this case.

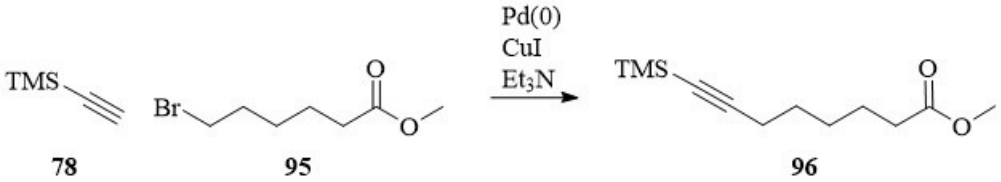

Scheme 2.9: *Attempted synthesis of* ***96****.*

On the one hand, the use of **78** and **95** to obtain the eight-carbon substituent is a marginally more step-efficient approach than going via the alkynols **71** and **92** to obtain the same molecule. This approach is also advantageous in that the hazard of employing potassium hydride is avoided. Furthermore, use of the toxic chromium(VII) is avoided, which provides both environmental benefits and reduced health risk.

However, since organolithium reagents seem to mainly target the carbonyl centre, efficient cross-coupling requires the use of precious transition metals. Although the transition metals are

used in catalytic amounts only, their application may also have negative environmental impacts. In addition to this, **77** and **78** are significantly more expensive than **74** and **75**. Thus, even when considering the cost of the additional solvents used as a reaction medium and for purification in the five-step synthesis of the eight-carbon chain, the original strategy is more economically feasible. Moreover, the synthesis of **92** does not require the removal of a protecting group, arguably making it more atom efficient than the synthesis of **96**. Thus, further attempts at synthesising the acetylene ester substituent through this synthetic route was not performed.

2.5. Strategy 1: Sonogashira Cross-coupling

An attempt at connecting **92** and **68a** by a Sonogoshira cross-coupling reaction was performed. The literature procedure[221] was conducted at room temperature, using triethylamine as the only solvent, and bis(triphenylphosphine)palladium(II) dichloride as the palladium salt, with both reagents being present in the reaction mixture initially.

A rationale for this approach is that the triphenylphosphines could conceivably act as chelating agents, sequestering the toxic effect of sulphur on the palladium catalyst. Nevertheless, the intended cross-coupling proved unsuccessful. Instead, the diyne **98** was isolated as the major product of the reaction (*scheme 2.10*). Thus, it appears that the competing homocoupling reaction was favoured under these conditions.

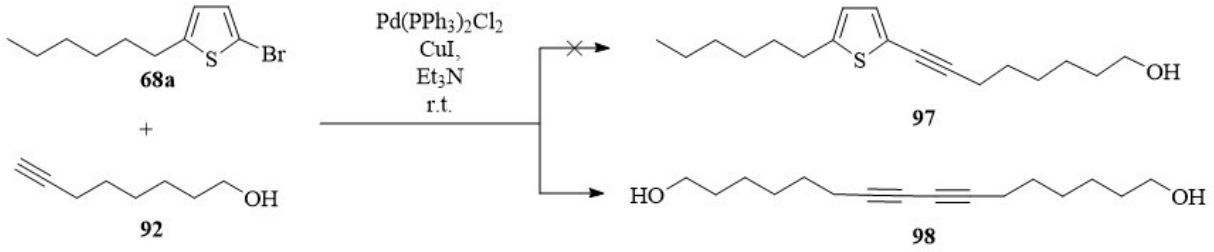

Scheme 2.10.: *The attempted coupling of **90** and **68a** afforded the homocoupling product **96** as the major product.*

In the referenced procedure[221], the thiophene did not contain an alkyl substituent. Given the reported success of the otherwise analogous procedure, one explanation could therefore be that the added hexyl substituent made it so that **68a.** was not properly solvated in triethylamine. Thus, the reactants may not have come into satisfactory contact with each other. Another explanation could be that the room temperature in the laboratory was too low to overcome the kinetic barrier of this heterocoupling reaction. In addition, it is possible that the reaction conditions were not sufficiently anaerobic, which could further facilitate alkyne dimerization.

A new attempt at a Sonogashira cross-coupling was therefore attempted, this time between **69** and **68b** by following a different literature procedure[222]. Relative to the former procedure, modifications in the new procedure included raising the temperature to 90°C, and slowly adding the alkynol to the reaction mixture. Given that slow addition of the alkyne has been reported to be a way of overcoming the issue of homocoupling[146, 148, 223], the latter seemed especially appropriate.

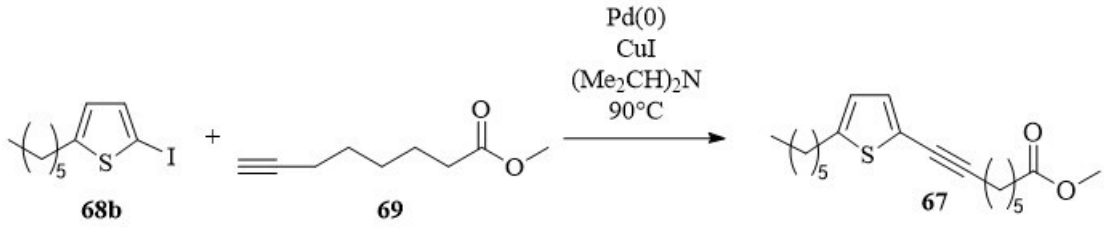

Scheme 2.11: *Attempted Sonogashira cross-coupling*

However, the reaction conditions seemed to predominantly result in cleavage of the iodide group instead of cross-coupling. To test if the more stable bromide could facilitate cross-coupling, coupling of **68a** to **69** was attempted by following the same procedure. While it appeared that the brominated species tolerated the reaction conditions, the attempt did not result in cross-coupling.

As a final modification to the procedure, the reaction was attempted a final time adding THF as a co-solvent, to rule out that poor solubility had been an error source. No cross-coupling product was afforded with this modification either.

Having ruled out solubility, temperature, and presence of air as possible error sources, it appeared that the failure of the acetylenic ester to undergo cross-coupling was due to insufficient activation of the cross-coupling partners.

Before abandoning this approach entirely, a third literature procedure[207] that involved a highly analogous reaction system was therefore attempted. In the new procedure, piperidine was used as the base, and was added in catalytic amounts only. Given the high similarity of the reaction system, the hope was that this base would somehow enhance the interaction of the copper cocatalyst with the acetylene. However, this did not result in cross coupling either. Thus, with all efforts being fruitless, no further attempts at Sonogashira couplings in *Strategy 1* were undertaken.

2.6. Strategy 2: Attempted Synthesis of **67**

Instead of synthesising the skeleton of the eight-carbon carboxylic substituent prior to attachment to **68**, the synthetic strategy was revised to involve a linear synthesis sequence. Starting from **68**, the next in this sequence concerned coupling **78** to **68a**, thus producing the first building block of the carboxylic substituent (*scheme 2.12*).

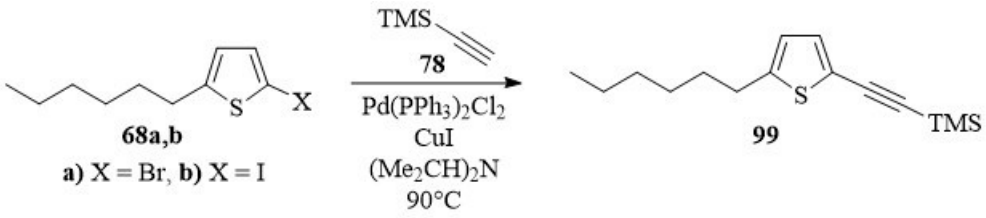

Scheme 2.12.: *Shows the Sonogashira coupling between **68a,b** and **78**.*

The Sonogashira coupling of **68a** and **78** was attempted by following the procedure referred to above[222]. Although it failed in the coupling of the alkyne ester **69**, the ^{1}H NMR analysis of the crude product indicated that the cross-coupling in this case was successful, as peaks corresponding to the literature data for **99** were produced[224, 225]. Furthermore, no dimerization products could be detected in the spectrum, or in any fractions eluted from the silica gel flash chromatography. However, the spectrum of the crude oil also revealed that some **68a** remained in the crude mixture. After an initial purification attempt, the starting material appeared to remain in a significant amount, and the compound was still not satisfactorily purified after two subsequent attempts at purification by silica gel flash chromatography.

To test if the more reactive iodo group would promote a more complete reaction, the same procedure was attempted using the iodinated thiophene **68b** This afforded the cross-coupling product **97** in an 82% yield, which was a significant improvement to the 58% yield reported in the original procedure[222]. The improved yield is most likely a reflection of the enhanced reactivity of the iodo group. As such, it is interesting to note that the iodo group was tolerated in this case, when it had been cleaved off in the attempted cross-coupling in *Strategy 1*.

A rationale for this could be that the palladium-activated **68b** accepted a proton in place of the intended acetylenic cross-coupling partner **69** in *Strategy 1*. As such, the contrasting outcomes of the two reactions could be a reflection of the relative acidities and reactivities of the two alkynes. The high electropositivity of silicon relative to carbon should grant a higher electron density to the **78** when compared to the mostly aliphatic **69**. Thus, **78** should also possess higher nucleophilicity, and improved ability to undergo cross-coupling. This, in turn, might explain

why the cross-coupling product was generated in a high yield this instance, when the same cross-coupling procedure failed in *Strategy 1*.

After having successfully obtained **99** the next step was removal of the TMS protecting group (*scheme 2.13*). This afforded **76** in a 49% yield, as seen by the disappearance of the TMS peak in the NMR spectra, and the characteristic absorption of a terminal alkyne in the IR spectrum.

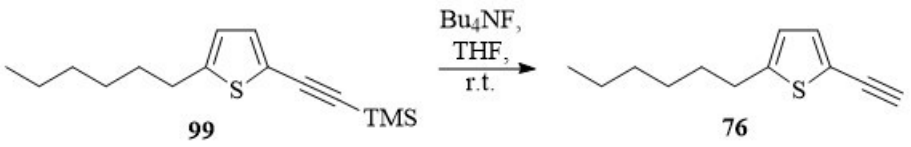

Scheme 2.13: *Deprotection of* ***99****.*

Coupling of the methyl ester **100** to **76** was attempted using a nickel-catalysed Sonogashira-type coupling procedure found in literature[163]. The iodinated ester **100** had been prepared from **95** via a Finkelstein reaction in an 83% yield.

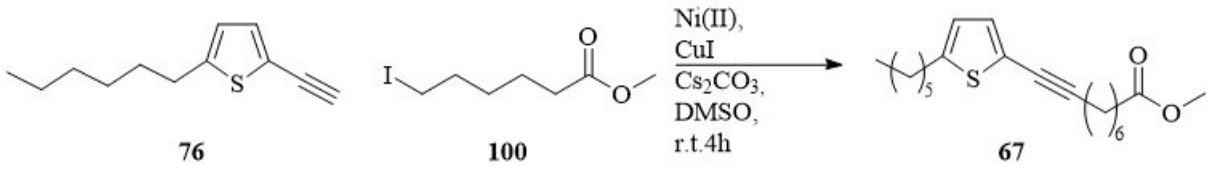

Scheme 2.14: *Attempted sp-to-sp*^{3}*-Sonogashira coupling.*

The cross-coupling attempt proved unsuccessful, which could be a combinatory effect of the poisoning effect of the thiophene on the metal catalyst, and the low intrinsic reactivity of aliphatic sp^3-hydridised carbons towards oxidative cross-couplings. As such, no further attempts at finalising this strategy were pursued.

2.7. Attempt at Cobalt-catalysed Reductive Cross-coupling

To test if the 18-carbon backbone could be prepared without going via unsaturated substituents to the thiophene, a strategy involving the direct cobalt-catalysed cross-coupling of methyl 8-bromooctanoate (**101a**) to **68** was attempted (*scheme 2.15*). This approach presented the advantage of being significantly more step-efficient than the former strategies. Indeed, this would circumvent the challenge of reducing an unsaturated substituent in addition to the thiophene. The reason why transition-metal catalysis was chosen over organometal-facilitated cross-coupling, which had been used to introduce the hexyl substituent, was the fear that the strongly basic environment would only target a nucleophilic attack of the ester carbonyl.

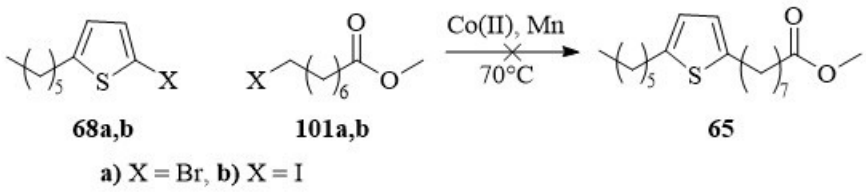

Scheme 2.15: *Attempted reductive cross-coupling.*

Methyl 8-bromooctanoate (**101a**) was prepared from 8-bromooctanoic acid (**102**) in a 97% yield, according to the previously referenced procedure[220]. The bromo group was then substituted for an iodo group by means of a Finkelstein reaction, affording **101b** in a 75% yield (*scheme 2.16*).

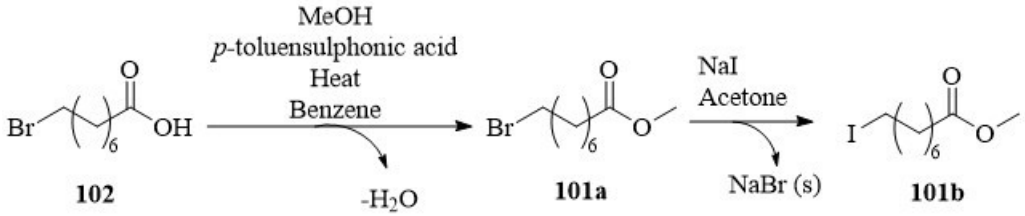

Scheme 2.16: *Synthesis of methyl 7-iodooctanoate*

The methyl ester **101b** and the alkyl-thiophene **68b** were then subjected to reductive cross-coupling according to a literature procedure[226]. However, the attempt did not result in any cross-coupling product.

Since the original procedure involved an unsubstituted bromothiophene, an attempt at coupling **101b** to 2-bromothiophene (**103a**) was performed (*scheme 2.17*). The latter had been prepared in a 64% yield by following a procedure[227]. The attempt was intended as a positive control, to test if the initial failure of the reaction arose from poor solubility of the reagents. However, this did result in cross coupling either.

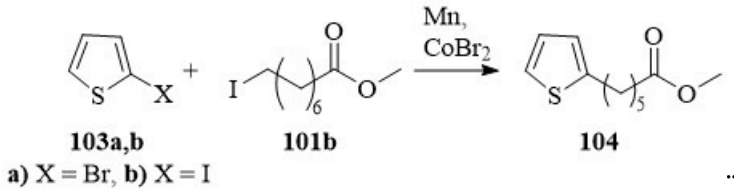

Scheme 2.17*: Positive control*

As a final positive control, the same cross-coupling procedure was attempted using 2-iodothiophene (**103b**) instead of **103b,** to test if the more reactive iodo group would produce the desired outcome. The former had been prepared in a 68% yield by following a literature

procedure[228]. With this final adjustment being unsuccessful as well, this strategy was abandoned.

2.8. Strategy 3: Synthesis of Ethyl (*E*)-7-(triphenyl-λ5 phosphaneylidene)hept-2-enoate

The third envisioned strategy was pursued in collaboration with another master student. The first step involved the oxidative ring-opening of 3,4-dihydropyran, and subsequent HWE olefination of the resulting carboxylic acid, to afford the ω-hydroxylated α,β-unsaturated ester **82**. This was done as a one-pot synthesis, according to a literature procedure (*scheme 2.18*)[229]. Due to an unavailability methyl diethylphosphonoacetate, the ethyl ester was synthesised instead of the methyl ester, using the corresponding ethyl HWE-reagent (**106**).

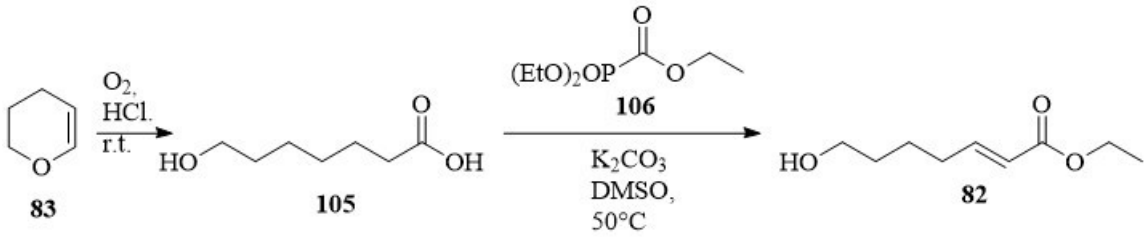

Scheme 2.18: *One-pot synthesis of ethyl (E)-7-hydroxyhept-2-enoate (**82**).*

This afforded the (*E*)-isomer in a 70% yield, as was evidenced by the ^{1}H NMR spectrum, which gave rise to two alkene peaks at δ6.95 and 5.82, with coupling constants J = 15.7.

Subsequently, the hydroxyl group was substituted by iodine by means of an Appel-type reaction, by following a procedure found in literature (*scheme 2.19*)[230].

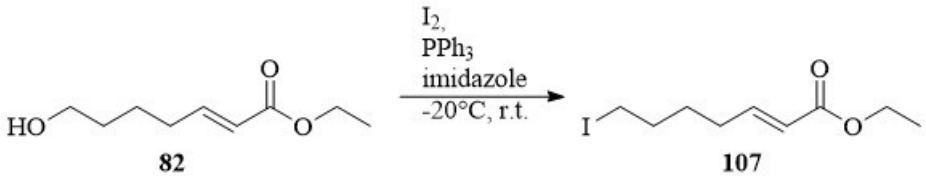

Scheme 2.19: *Appel substitution of **82** to afford **107**.*

This afforded the substitution product **107** in an 62% yield, as indicated by an upfield shift of the protons adjacent to the substitution site, from δ 3.65 to δ 3.19. Similarly, in the ^{13}C NMR spectrum, the carbon at which the substitution had taken place was now observed at around δ33, where it had previously been observed at δ 62.67. The iodo group was then substituted by a triphenylphosphine group by following the same literature procedure[230], affording the Wittig reagent **81** in a 63% yield (*scheme 2.20*).

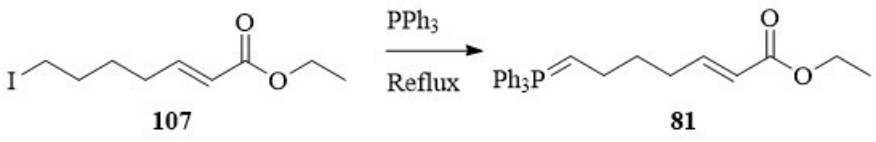

Scheme 2.20: *Conversion of **107** into the Wittig reagent **81**.*

In this case, the successful substitution was evidenced by the appearance of 15 protons in the aromatic range of the ^{1}H NMR spectrum, which corresponded to the three phenyl groups attached to the phosphorus. In addition, the peak at δ 3.19 that had corresponded to the protons neighbouring the iodine group was gone, and instead, a new peak at δ 3.58, corresponding to a single proton was now observed. Thus, it was apparent that the phosphine ester was successfully synthetised.

2.9. Strategy 3: Attempted Synthesis of **79**

In the next step of *Strategy 3*, 5-hexylthiophene-2-carbaldehyde (**80**) was synthesised in a 54% yield according to a literature procedure (*scheme 2.21*)[231]. The ^{1}H NMR spectral data were in agreement with those reported in the literature procedure[231].

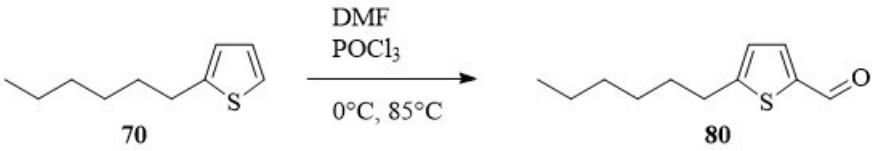

Scheme 2.21: *Synthesis of the thiophene-aldehyde*

Olefination was then attempted according to a different literature procedure (*scheme 2.22*)[232]. However, no olefin was produced in this reaction.

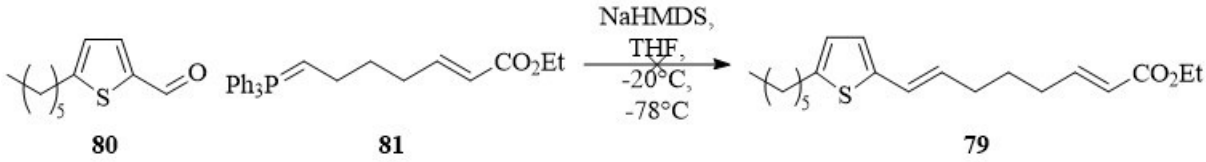

Scheme 2.22: *Attempted Wittig reaction*

A reason for the failure of this reaction could be that the combination of the thiophene unit and the three phenyl groups of the Wittig reagent gave too much steric hindrance for the two reaction centres to come together. To this end, it was contemplated whether the use of less bulky substituents on the phosphorus could help overcome any perceived steric hindrances. However, since time was coming short, no further attempts at achieving this last olefination step were conducted.

2.10. Strategy 4 and 5: Synthesis of 2-(3-bromopropynyl)-5-hexylthiophene

By following a literature procedure[207], 3-(5-hexylthiophene)-prop-2-yn-1-ol (**108**) was afforded by means of a Sonogashira cross-coupling between **68b** and **75**, in a 90% yield.

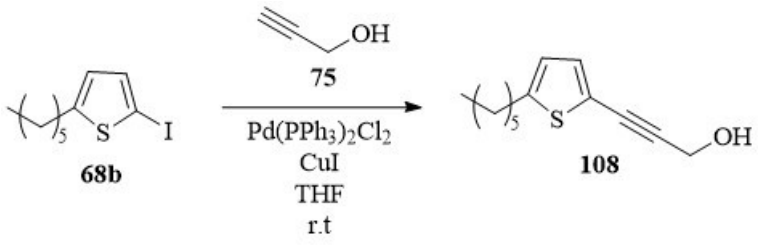

Scheme 2.23: *Synthesis of 3-(5-hexylthiophen-2-yl)prop-2-yn-1-ol (**108**).*

Excellent yields were afforded even when the reaction was upscaled from a milligram scale to a gram scale.

Spectral analyses were indicative of the successful cross-coupling, where the downfield shift of one aromatic carbon from δ 69.46, corresponding to the iodinated carbon in the starting material, to δ 119.70 in the ^{13}C NMR spectrum of the product, provided the most compelling evidence for an altered carbon skeleton.

With the cross-coupling being successful, **108** was then converted into the corresponding brominated species (**84**) by means of an Appel substitution. This afforded the propargylbromide **84** in a 74% yield (*scheme 2.24*).

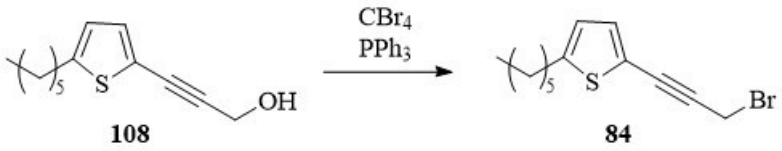

Scheme 2.24: *Appel substitution of **106**.*

In the ^{1}H NMR spectrum, the successful conversion was evidenced by the upfield shift of the propargylic protons from δ 4.49 to δ 4.19. Similarly, a new peak was observed in the alkane range of the ^{13}C NMR spectrum, while the C-O peak at δ51.96 could no longer be detected. More significantly, a clear shift in the alkyne peaks, from δ 90.46 and 79.78 to δ 87.24 and 80.67, as well as a fractional shift of the four peaks in the aromatic range of about 0.3ppm for each peak, indicated a change in the electronic environment of the π-conjugated system. Thus, the common intermediate of strategy 4 and 5 was successfully synthesised.

2.11. Strategy 4: Attempted Diyne Synthesis

An attempted synthesis of the diyne **109** was performed by following a literature procedure[233], in which copper(I) iodide and molecular oxygen acted as catalysts (*scheme 2.25*). The outcome of the reaction could not be satisfactorily assessed from the NMR spectra of the crude residue, and purification was therefore attempted. Even when a gradient eluent system was used, no diyne could be detected in the eluted fractions.

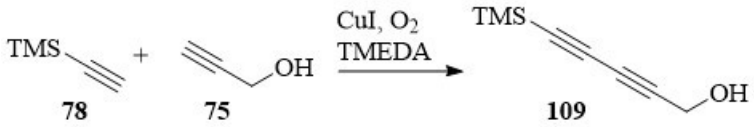

Scheme 2.25: *Attempt at diyne synthesis.*

Since the reaction outlined in *scheme 2.25* relied on molecular oxygen as an oxidant, it is possible that the failure arose from insufficient aerobic conditions. However, instead of attempting the same procedure under a richer oxygen supply, it was decided to follow a second procedure[234] that did not require an external oxidant.

The new procedure involved coupling of the iodinated acetylene **110** to **75** (*scheme 2.26*).

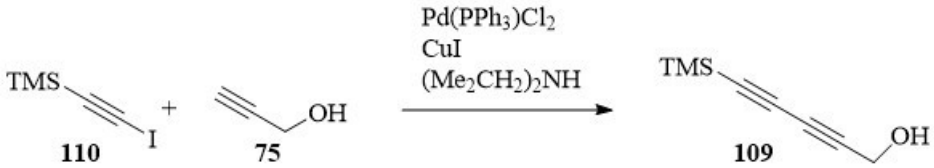

Scheme 2.26: *New attempt at synthesising **109**.*

Thus, **110** had to be procured before the reaction could be attempted. This was initially attempted by treating TMS-acetylene with *n*-hexyllithium, and then introducing a solution of molecular iodine in ether to the reaction solution (*scheme 2.27*).

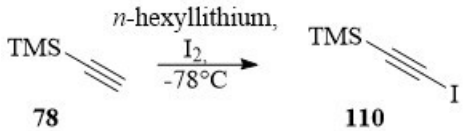

Scheme 2.27: *Attempted synthesis of **110**.*

Although NMR analyses of the crude oil seemed to indicate that the target compound had been produced, **110** was not isolated after purification by silica gel flash chromatography. Since the iodinated product had been detected in the crude oil, it is possible that exposure to UV light caused dissociation of the alkyne-iodine bond such that the product could not be isolated.

Alternatively, it is possible that the yield had not been very high to begin with, and that modifications to the procedure, such as longer reaction time after addition of *n*-hexyllithium and I_2 could promote a better result.

However, since the procedure did not appear to be optimal, a different strategy was attempted[235], using NIS as the iodinating agent (*scheme 2.28*).

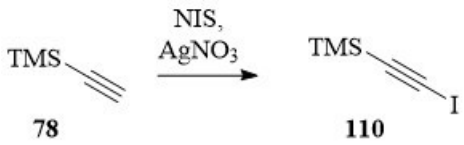

Scheme 2.28: *Synthesis of* ***110.***

This afforded the target compound as a semi-crystalline compound in a 40% yield.

The **110** fraction was used in the cross-coupling procedure outlined in *scheme 2.26*. While the ^{13}C NMR spectrum of the crystalline crude residue could indicate that a diynic species had been produced, it could not be isolated in any significant amount upon purification. As such, this strategy did not appear to be optimal, and thus, it was not pursued further.

2.12. STRATEGY 5: SYNTHESIS OF THE DIYNE **89**

Having obtained **84**, the next step in the fifth synthetic strategy involved coupling of the propargylic bromide to **75** (*scheme 2.29*).

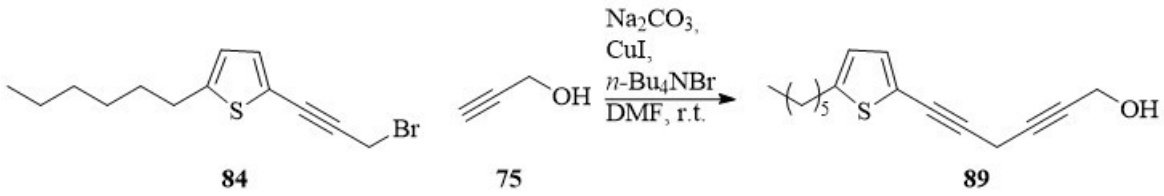

Scheme 2.29: *Synthesis of the diyne* ***89****.*

This afforded the diyne **89** in an 85% yield, as witnessed by the appearance of four peaks in the alkyne range in the ^{13}C NMR spectrum, none of which overlapped with the alkyne peaks of the starting material. Furthermore, a slight shift of the four peaks in the aromatic range indicated a change in the π-conjugated system.

2.13. STRATEGY 5: REDOX

Having successfully obtained **89**, it was decided to follow *path B* outlined in the retrosynthetic analysis, as time was becoming short. Despite the possibility that the thiophene could interfere with the reaction, catalytic hydrogenation of the diyne was therefore attempted based on a

literature procedure[236]. The hydrogenation proved surprisingly facile, affording the target alkanol **91** in a 46% yield, along with the completely hydrogenated **111** in a 25% yield relative to the starting material, when stirred under hydrogen for 24 hours (*scheme 2.30*).

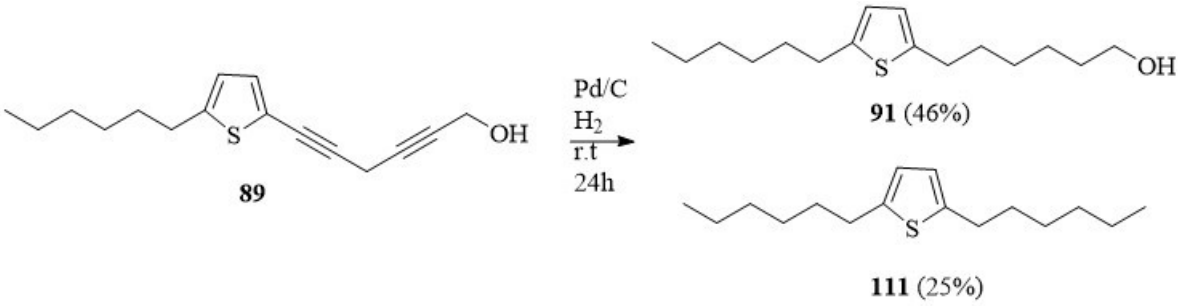

Scheme 2.30: *Hydrogenation of the diyne* ***89****.*

In both cases, the reduction was evidenced in the ^{1}H NMR spectrum by the disappearance of the dublet at δ 4.29, corresponding to the two propargyl protons, and the singlet at δ 3.45, belonging to the protons of the -CH_2 group in-between the two alkynes. In addition, the ^{1}H NMR spectrum produced a single peak in the aromatic range, indicative of a symmetrical, disubstituted thiophene. The main difference between the ^{1}H NMR spectra of the two reduction products was that the spectrum belonging to the still-hydroxylated **91** showed a peak at around δ 3.60, corresponding to the two protons adjacent to the hydroxyl group, whereas the spectrum of **111** showed peaks corresponding to C-H-shifts only.

In the ^{13}C NMR spectrum, no alkyne shifts could be detected, further indicating that the reduction had been successful. Moreover, only two peaks were seen in the aromatic range in both respective spectra, which was suggestive of a symmetric thiophene. However, in the ^{13}C NMR spectrum of the target molecule **91**, the two aromatic carbons nearly overlapped, being separated by a few ppms only. In contrast, the ^{13}C NMR spectrum of the completely hydrogenated **111** produced two distinctive peaks at δ143.12 and 123.09. In addition to the significant difference of the aromatic carbons, the ^{13}C NMR spectrum of **111** produced no peak outside the alkane range. By contrast, the spectrum of **91** showed a peak at δ63.15, corresponding to the C-O bonded carbon.

The two different outcomes were confirmed by IR spectroscopy, in which **111** produced no hydroxyl peak, whereas **91** gave rise to the characteristic broad absorption at 3300cm^{-1},

The two hydrogenated compounds were readily separated by column flash chromatography, where the completely hydrogenated product eluted in a *n*-hexane eluent, whereas the alkanol

eluted only when a more polar gradient was used. However, with this undesired side reaction constituting a significant loss of yield, the hydrogenation procedure was not optimal.

To test if a shorter reaction time would prevent over-reduction, the procedure was attempted again, this time shortening the reaction time to 12 hours. This produced a mixture of the target molecule and partially hydrogenated products that could not be separated by silica gel flash chromatography. Thus, it appears that the optimal reaction time is somewhere between 12 and 24 hours. However, with time being limited, no further attempts at fine-tuning the reaction conditions were done.

In the next step of the synthetic strategy, the alkanol **91** was oxidised to the corresponding aldehyde in a 91% yield based on a literature procedure (*scheme 2.31*)[217].

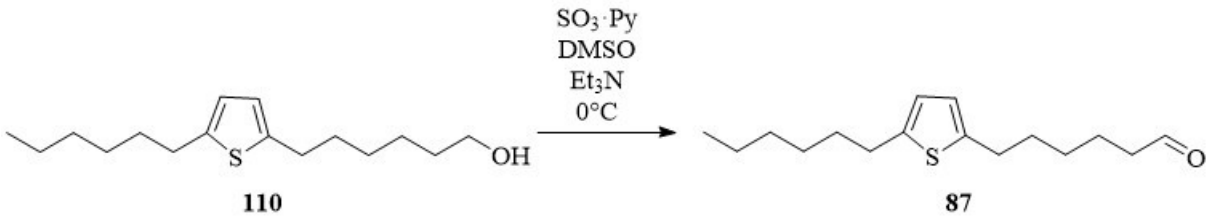

110 **87**

Scheme 2.31: *Oxidation of **91**.*

The successful oxidation was confirmed by the appearance of an aldehyde proton at δ 9.78 in the ^{1}H NMR spectrum, as well as an aldehyde peak at δ 202.8 in the ^{13}C NMR spectrum. The IR spectrum gave no characteristic hydroxyl absorption, indicating that all the alcohol was converted into the aldehyde, and that the oxidation had not proceeded to the corresponding carboxylic acid. Thus, the diyne **89** had successfully been converted into the intended olefination partner.

2.14. STRATEGY 5: OLEFINATION

In the last carbon-extending reaction of *Strategy 5*, the thiophene aldehyde **87** was subjected to olefination according to a literature procedure[237], using ethyl diethylphosphonoacetate (**106**) to obtain the α,β-unsaturated ethyl ester **86** (*scheme 2.32*).

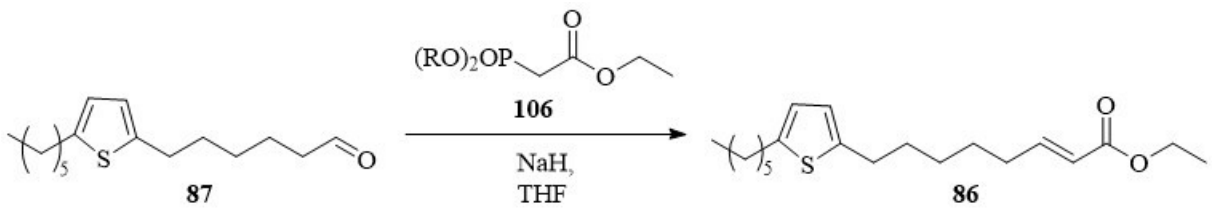

87 **86**

Scheme 2.32: *Olefination.*

The appearance of two peaks at δ 6.95 and 5.81 with coupling constants J = 15.6 Hz and J = 15.7 Hz, respectively, seemed to indicate that the *(E)*-alkene had been successfully synthetised.

However, it also appeared that a co-eluting impurity had been isolated in the purification process, in a 1:1 ratio with the target product, as the integrals of the alkene protons could not be adjusted to a higher value than 0.5 without producing a mismatch with the remaining peaks. Furthermore, two peaks with an integral value of 1, occurring at δ 4.19 and 2.19, that could not be accounted for based on the structure, were also observed, even after a second attempt at purifying the compound over silica gel flash chromatography.

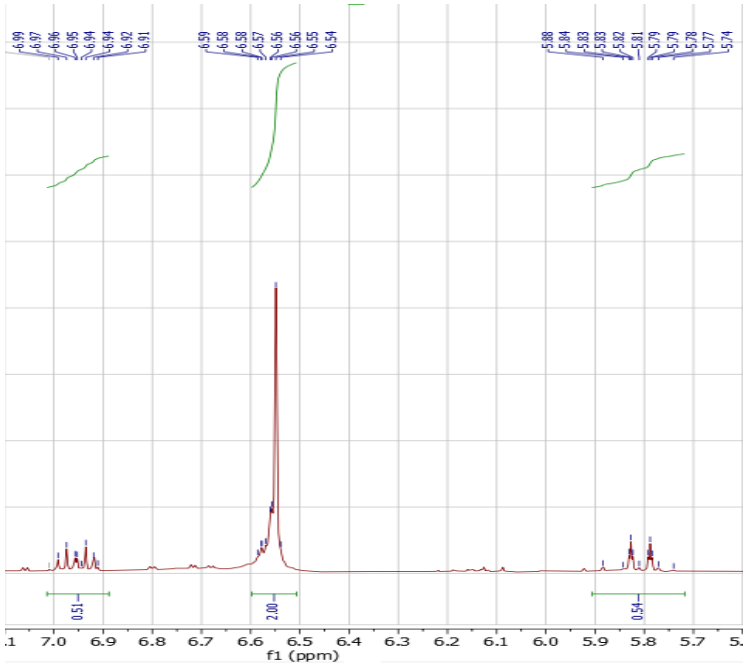

Figure 2.1: *The appearance of two peaks, corresponding well to an α,β-unsaturated ester indicated that the olefination had been partially successful.*

It was suspected that the observed impurities arose from unreacted HWE reagent, as the two impurities seemed to correspond to the spectrum obtained for this reagent. Thus, it was attempted to wash the residue using 2M NaOH, in the hope that the HWE reagent would be deprotonated, and thereby water-soluble. However, this did not produce a cleaner spectrum.

Overall, it appeared that the carbon skeleton of the target molecule had been successfully synthetised, although it could not be isolated with satisfactory purity. With the impurity constituting such a significant amount of the isolated residue, it appeared counterproductive to attempt reduction of the double bond, as the stoichiometric amounts of the reducing reagent could not be strictly controlled. This, in turn, could lead to over-reduction, where the ester moiety was targeted in the process, or under-reduction, where only a fraction of the already-

mixed compound was reduced. At this stage, there was no time left to run a new series of reactions to try to produce a different outcome. Hence, achieving the complete synthesis of the target molecules was left for future work.

3. Conclusion and Future Perspectives

Altogether, two linear, and three convergent synthetic strategies were attempted, whereof only *Strategy 5* came near completion, being limited only by the high impurity of the α,β-unsaturated intermediate isolated in the last carbon-extending step.

While optimising the last reaction steps of *Strategy 5* should be of primary focus in any future work, it would be interesting to test if one of the convergent strategies could be brought to completion, in order to devise a strategy that is less highly impacted by any low-yielding steps. To this end, revisiting *Strategy 1* is appealing, as the ester substituent can be built from cheap, readily available precursors, in a straightforward, high-yielding series of reactions. In contrast, *Strategy 4* uses reagents that are significantly more expensive and, with the synthesis of the diyne intermediate proving demanding, involves a more challenging set of reactions.

The success of *Strategy 1* was limited by the relative inertness of the respective coupling partners towards oxidative cross-coupling. To this end, it would be interesting to test if a Negishi- or Suzuki-type protocol (*scheme 3.1.*) could promote the final cross-coupling step. A rationale for this is that the introduction of an organozinc or organoboron group would increase the nucleophilicity of the acetylenic cross-coupling partner **69**, something which perhaps could compensate for its reluctance to undergo cross-coupling in a Sonogashira setting. Thus, if this strategy is revisited, an alternative means of activating the acetylene should be explored.

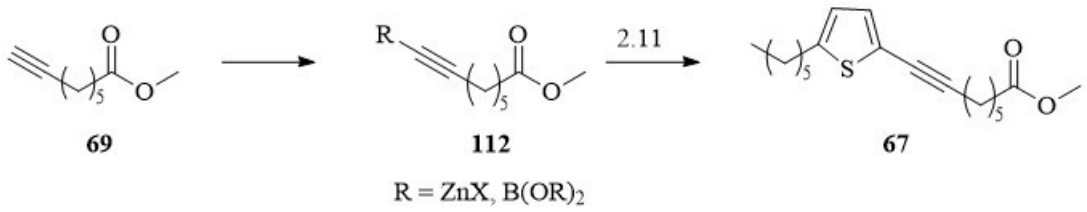

Scheme 3.1: *Conversion into an organozinc or organoboron species might appropriately activate the alkyne ester* ***69*** *for cross-coupling.*

What concerns *Strategy 3*, this is strategy already being developed by another master student.

As for *Strategy 5,* all reactions leading up to the reduction of the diyne produced good to excellent yields. Although, compared to the rest of the reaction yields, the output of the initial alkylation of thiophene was on the lower side. However, since relatively large quanta were nevertheless obtained, one lower-yielding step this early in the synthetic process can be tolerated. Furthermore, both thiophene and 1-bromohexane are relatively inexpensive and readily available reagents. Thus, any attempts at improving the atom-efficiency of this step may

be viewed as an environmentally directed effort rather than an economically motivated endeavour.

By contrast, optimising the conditions for the hydrogenation of the diyne **89** is more critical, as this intermediate can only be obtained over a series of steps. In this instance, a significant production of by-products corresponds to an inefficient use of time, atomic, and economic resources, to a much greater extent.

Future attempts at increasing the yield of the hydrogenation step will most likely be a matter of finding the appropriate relationship between catalyst loading and reaction time; since finding the appropriate time window between 12 to 24 hours when using the catalyst loading employed herein, or trying to control the amount of hydrogen present in the reaction flask, will be highly impractical, the two more feasible alternatives will be to either upscale the catalyst-to-diyne ratio, and run the reaction for a shorter time period, or to lower the catalyst loading, and let the reaction run for an even longer period.

The drawback of the former is that using a higher catalyst loading in this step will be more expensive, and less environmentally friendly. In terms of the latter, the poisoning effect of the thiophene on the metal catalyst should not be underestimated, and herein probably lies a fine line between efficient catalysis, and partial inhibition.

When attempting the olefination reaction again, the stoichiometric equivalents should be carefully controlled such that any remaining HWE reagent can be easily removed upon phase extraction during the workup of the reaction. Alternatively, since the attempted procedure did not appear to be optimal, finding a different procedure for this step might also be a viable option.

While optimising these reaction steps should be at the foremost focus of any future work, trying to reduce the number of steps of the synthetic pathway could also be of interest eventually. To this end, it would be interesting to test if the diynic aldehyde **90** could participate in olefination, without producing any undesired side-reactions. In this case, tuning the hydrogenation method to selectively reduce the alkyne and alkene bonds over the ester moiety would be essential.

Another possible way of reducing the steps of the synthetic route is to couple the commercially prepared propargylbromide **113** directly to **68b** (*scheme 3.2.*).

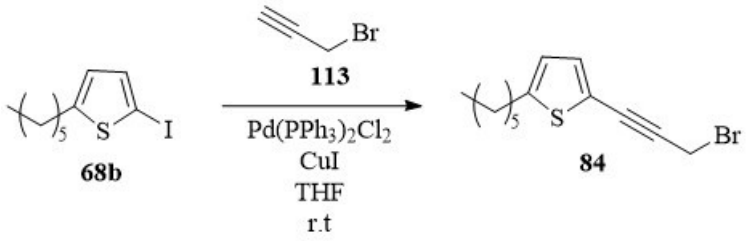

Scheme 3.2: *By direct coupling* ***113*** *to* ***68b*** *the synthetic route could potentially be reduced by one step.*

Even though this reagent is more expensive than both propargyl alcohol and tetrabromomethane, the added expense of two purification steps, as well as the requirement for buying two reagents in place of one might justify this cost.

Overall, despite the fact that the **86** could not be purified to a satisfactory degree, it appears likely that *Strategy 5* can be turned into a highly efficient synthetic pathway by fine-tuning the reactions discussed herein.

In addition to optimising the mentioned reactions, future work will need to include finding the appropriate redox conditions that may furnish the target molecules **65** and **66**. Obtaining **65**, can be done using *L*-Selectride®, or other reactions setups that selectively targets the double bonds over the ester moiety. In terms of synthetising **66**, this can be achieved by ionic hydrogenation, either by going directly from the α,β-unsaturated ester **86**, or from **65**. Having developed the appropriate reaction series, obtaining the methyl esters will most likely be as simple as substituting the ethyl Horner reagent with the corresponding methyl Horner reagent. Alternatively, the structures may be re-esterified to the corresponding methyl esters prior to MS analysis, for a comparison with the literature spectra.

Thus, herein is reported a promising synthetic pathway towards the target molecules **65** and **66** Although neither a total synthesis or structure confirmation, which were the main goals of this thesis, were achieved, the general tools needed to realise a total synthesis, and to confirm the proposed structures of the target SHFAs, have been developed.

4. Experimental Procedures

4.1. General Remarks

All reactions were carried out under a nitrogen atmosphere unless otherwise stated.

Thin Layer Chromatography (TLC) was performed on Merck TLC silica gel 60 F_{254} sheets. UV or permanganate were used to monitor TLC unless otherwise stated.

Flash column chromatography was performed using Merck Silica Gel 60 (0.040-0.063µm) as the stationary phase.

NMR spectra were recorded on a Bruker Ascend 400 instrument at 25°C, at 400 MHz (^{1}H NMR) or 100 MHz (^{13}C NMR). CD_3Cl was used as a solvent unless otherwise stated, and the reference peak was calibrated to 7.26ppm (^{1}H NMR) and 77.16 (^{13}C NMR).

IR spectra were recorded on an Agilent Technologies 5500 Series FTIR instrument.

UV spectra were recorded on a Biochrom Libra S32 computer.

4.2. SYNTHESIS OF 2-OCTYN-1-OL (**71**)

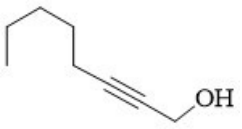

Figure 4.1: *2-octyn-1-ol (71)*

To a stirred solution of THF (150mL) and HMPA (42 mL) under nitrogen, propargyl alcohol (5.83mL, 5.61g, 100mmol) was added. The mixture was cooled to -78°C before *n*-BuLi (80mL, 2.5M in *n*-hexane, 200mmol) was added dropwise. The resulting solution was heated to -30°C and stirred for 1h before 1-bromopentane (24.4g, 20mL, 161mmol) was added dropwise. The orange suspension was stirred at room temperature overnight, and the reaction was quenched by the addition of water (100mL). The aqueous phase was extracted using small amounts of ethyl acetate (5x50mL), and the combined organic phases were washed with brine (100mL), dried over anhydrous sodium sulphate, and concentrated under reduced pressure. The crude oil was purified using a silica gel plug (*n*-hexane:EtOAc 5:1), affording the alkynol **71** as a yellow oil.

Yield: 82% (10.3g)

R_f = 0.22 (Permanganate)

^{1}HNMR (400MHz, $CDCl_3$): δ (ppm) 4.24-4.23 (s, *J* = 2.08 Hz, 2H), 2.22-2.17 (tq, *J* = 2.25 Hz, 2H), 1.67-1.38 (m, *J* = 5.58 Hz, 2H), 1.37-1.26 (m, *J* = 2.83 Hz, 4H), 0.87 (td, *J* = 3.11 Hz, 3H)

^{13}C NMR (100MHz, CDCl3): δ (ppm) 86.6, 78.2, 51.4, 31.0, 28.3, 22.2, 18.7, 13.9

IR: 3300, 2920.9, 2853.6, 2200, 1461.0, 1377.1, 1136.6, 1013.5 cm^{-1}

4.3. SYNTHESIS OF 7-OCTYN-1-OL (**92**)

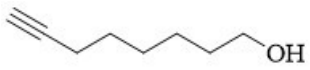

Figure 4.2: *7-octyn-1-ol (92)*

Method 1:

Potassium hydride (35% suspension in mineral oil, 10.5g, 91.7mmol) was weighed in a threeneck flask, and washed with diethyl ether (3x50mL). 1,3-diaminopropane (100mL) was added dropwise to the washed salt at 0°C. The white suspension was stirred at room temperature for 1 hour, affording a foaming pale-yellow solution before 2-octyn-1-ol (**71**) (3.33g, 26.4mmol) was added dropwise. The resulting brown mixture was stirred at room temperature overnight, and then quenched by the slow addition of crushed ice. The aqueous phase was extracted with ethyl acetate (3x100mL), and the combined organic layers were washed with HCl (1M, 50mL) and brine (50mL), dried over anhydrous sodium sulphate, and concentrated under reduced pressure. The resiude was purified using silica gel flash chromatography (*n*-hexane/EtOAc 5:1), affording the alkynol as a yellow oil.

Yield: 70%

Method 2:

Sodium hydride (2g, 49.7mmol, 60% dispersion in mineral oil) was weighed out in a three-neck round bottom flask, and washed with pentane (3x30mL). Ethylenediamine (50mL) was then added dropwise to the flask, and the temperature was gradually raised to 50°C and stirred at this temperature for 1hour. 2-octyn-1-ol (**71**) (1.5g, 11.9 mmol) was added dropwise to the resulting purple suspension, and the reaction mixture was stirred overnight. The reaction was quenched by slow addition of water, and the aqueous phase was extracted three times with small amounts of ethyl acetate. The combined organic layers were washed with HCl (1M), and brine, dried over anhydrous sodium sulphate, and concentrated under reduced pressure. The residue was purified by silica gel flash chromatography (*n*-hexane:EtOAc 5:1).

Yield: 43%

R_f: 0.13 (permanganate)

^{1}H NMR (400 MHz, $CDCl_3$): δ (ppm) 3.65 (td, J = 6.6, 2.5 Hz, 2H), 2.19 (td, J = 7.0, 2.7 Hz, 2H), 1.94 (t, J = 2.7 Hz, 1H), 1.58 – 1.32 (m, 9H).

^{13}C NMR (100MHz, $CDCl_3$): δ (ppm) 84.7, 68.3, 63.0, 32.7, 28.6, 28.5, 25.3, 18.4

IR: 3295.6, 2932.1, 2859.4, 2115.4, 1461.0, 1052.7 cm^{-1}

4.4. SYNTHESIS OF 7-OCTYNOIC ACID (**93**)

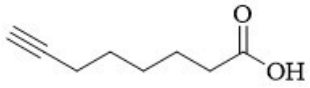

Figure 4.3: *7-octynoic acid (**93**)*

To an ice cold, stirred solution of CrO_3 (3.5g, 35mmol) in water (50mL), concentrated sulphuric acid (11.2mL) was added. A solution of 7-octyn-1-ol (**92**) (3.3g, 26.1mmol) in acetone (15mL) was then added dropwise to the solution, and the reaction mixture was stirred at room temperature overnight. The solution was diluted in EtOAc (50mL), and the aqueous phase was extracted with small amounts of EtOAc. The combined organic phases were washed with brine, filtered over Celite, dried over anhydrous sodium sulphate, and concentrated under reduced pressure. The crude oil was purified by silica gel flash chromatography (*n*-hexane:EtOAc 5:1), affording the acid as a pale yellow oil.

Yield = 75%

^{1}H NMR (400 MHz, $CDCl_3$): δ (ppm) 10.86 (s, 1H), 2.37 (td, *J* = 7.5, 1.4 Hz, 2H), 2.20 (tdd, *J* = 7.0, 2.7, 1.4 Hz, 2H), 1.94 (td, *J* = 2.7, 0.9 Hz, 1H), 1.66 (pd, *J* = 7.4, 1.5 Hz, 2H), 1.60 – 1.30 (m, 4H).

^{13}C NMR (101 MHz, $CDCl_3$): δ (ppm) 179.92, 84.27, 68.40, 33.81, 28.10, 28.05, 27.70, 24.14, 23.68, 18.23, 18.12.

IR: 3295.5, 3027.2, 2937.7, 2674.3, 2115.4, 1707.1, 1410.7, 1276.4, 1226.1, 1089.5, 940.8, 733.9 cm^{-1}

4.5. SYNTHESIS OF METHYL 7-OCTYNOATE (**69**)

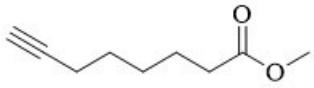

Figure 4.4: *Methyl 7-octynoate (**69**).*

To a stirred, ice-cold solution of 7-octynoic acid (**93**) (1g, 7.13mmol) and MeOH (16.4mL) in diethyl ether (25mL), $TMSCHN_2$ (4mL, 2.0M in hexane, 4.3mmol) was added. The reaction mixture was stirred overnight, then concentrated under reduced pressure. The crude product was purified by silica gel flash chromatography (*n*-hex:EtOAc 7:3), affording the title product as a clear oil.

Yield: 90% (6.48mmol, 1g)

R_f: 0.63 (Permanganate)

^{1}H NMR (400 MHz, $CDCl_3$): δ (ppm) 3.67 (d, *J* = 1.6 Hz, 3H), 2.35 – 2.30 (m, 2H), 2.20 (dt, *J* = 7.1, 3.5 Hz, 2H), 1.94 (t, *J* = 2.6 Hz, 1H), 1.68 – 1.61 (m, 2H), 1.55 (dd, *J* = 8.5, 6.9 Hz, 2H), 1.47 – 1.41 (m, 2H).

^{13}C NMR (100 MHz, $CDCl_3$): δ (ppm) 174.24, 84.47, 68.46, 68.40, 51.63, 34.06, 28.32, 28.21, 24.56, 18.37.

4.6. Esterification Procedure With Azeotropic Removal of Water

To a solution of the bromocarboxylic acid (22.6mmol) in benzene (20mL) at room temperature, methanol (4.3mL, 3.33mmol, 45mmol) and *p*-toluenesulphonic acid (0.22g, 1.16mmol) were added. Subsequently, the reaction mixture was heated at reflux for 2 days with azeotropic removal of water. The crude content was then concentrated under reduced pressure, and purified by silica gel flash chromatography (*n*-hexane:EtOAc 7:3)

4.6.1. Methyl 6-bromohexanoate (**95**)

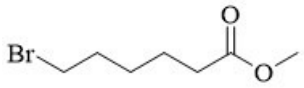

Figure 4.5: *Methyl 6-bromohexanoate (**95**).*

Yield: 85%

^{1}H NMR (400 MHz, $CDCl_3$): δ (ppm) 3.67 (s, 3H), 3.41 (t, *J* = 6.8 Hz, 2H), 2.33 (t, *J* = 7.4 Hz, 2H), 1.88 (p, *J* = 6.9 Hz, 2H), 1.69 – 1.63 (m, 2H), 1.52 – 1.44 (m, 2H).

^{13}C NMR (100 MHz, $CDCl_3$): δ (ppm) 173.83, 51.39, 33.63, 33.27, 32.18, 27.46, 23.87

IR: 2948.8, 2864.9, 1735.1, 1433.0, 1365.9, 1253.9, 1198.1, 1002.3, 884.9, 733.9 cm^{-1}

4.6.2. Methyl 8-bromooctanoate (**101a**)

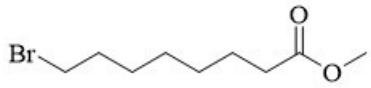

Figure 4.6: *Methyl 8-bromooctanoate (**101a**)*

Yield: 97%

^{1}H NMR (400 MHz, $CDCl_3$): δ (ppm) 3.56 (s, 3H), 3.29 (t, *J* = 6.8 Hz, 2H), 2.20 (t, *J* = 7.5 Hz, 2H), 1.74 (p, *J* = 6.9 Hz, 2H), 1.57 – 1.49 (m, 2H), 1.37 – 1.28 (m, 2H), 1.22 (p, *J* = 3.6 Hz, 4H).

^{13}C NMR (100 MHz, $CDCl_3$): δ (ppm) 174.38, 51.62, 34.13, 34.01, 32.82, 29.04, 29.00, 28.51, 28.08, 24.93.

4.7. Finkelstein Reaction, General Procedure

To a solution of the alkyl bromide (8.96mmol) in acetone (10mL), NaI (2.68g, 17.92mmol) was added. The solution was stirred under a nitrogen atmosphere overnight, and the solvent was removed under reduced pressure. The residue was suspended in dichloromethane, and inorganic salts were removed by filtration. The compound was concentrated under reduced pressure, affording the product as a yellow oil.

4.7.1. Ethyl 6-iodohexanoate

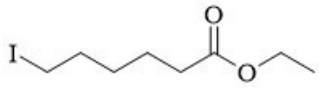

Figure 4.7: *Ethyl 6-iodohexanoate*

Yield: 83%

^{1}H NMR (400 MHz, $CDCl_3$): δ (ppm) 4.13 (q, *J* = 7.1 Hz, 2H), 3.18 (t, *J* = 7.0 Hz, 2H), 2.31 (t, *J* = 7.4 Hz, 2H), 1.84 (dt, *J* = 14.6, 7.1 Hz, 2H), 1.65 (dt, *J* = 15.3, 7.5 Hz, 2H), 1.51 – 1.37 (m, 2H), 1.25 (t, *J* = 7.1 Hz, 3H).

^{13}C NMR (101 MHz, $CDCl_3$): δ (ppm) 173.94, 60.77, 34.54, 33.57, 30.41, 24.32, 14.71, 7.02.

4.7.2. Methyl 8-iodooctanoate (**101b**)

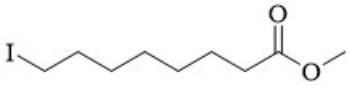

Figure 4.8: *Methyl 8-iodooctanoate (**101b**)*

Yield: 75%

^{1}H NMR (400 MHz, $CDCl_3$): δ (ppm) 3.66 (s, 3H), 3.18 (t, *J* = 7.0 Hz, 2H), 2.30 (t, *J* = 7.5 Hz, 2H), 1.81 (p, *J* = 7.0 Hz, 2H), 1.63 (dd, *J* = 11.4, 6.0 Hz, 2H), 1.43 – 1.35 (m, 2H), 1.32 (dt, *J* = 8.1, 3.8 Hz, 4H).

^{13}C NMR (100 MHz, $CDCl_3$): δ (ppm) 174.33, 51.62, 34.14, 33.55, 30.42, 29.03, 28.30, 24.95, 7.24

4.8. SYNTHESIS OF ETHYL (*E*)-7-HYDROXYHEPT-2-ENOATE (**82**)

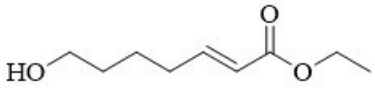

Figure 4.9: *Ethyl (E)-7-hydroxyhept-2-enoate (**82**)*

To a stirred solution of 3,4-dihydropyran (8.4g, 100mmol) in water (50mL), HCl (1M, 0.9mL) was added. The reaction was stirred for 3hours at room temperature under open air, before potassium carbonate (15.2g, 110mmol), ethyl diethylphosphonoacetate (21.8mL, 22.4g, 110mmol) and DMSO (32mL) were added. Subsequently, the reaction flask was sealed and stirred overnight under a nitrogen atmosphere at 50°C. The reaction mixture was extracted three times using small amounts of EtOAc, and the combined organic layers were dried over anhydrous sodium sulphate and concentrated under reduced pressure. The crude residue was purified over silica gel flash chromatography () affording the title product as an oil.

Yield: 70%

^{1}H NMR (400 MHz, $CDCl_3$): δ (ppm) 6.95 (dtd, *J* = 15.7, 7.0, 1.2 Hz, 1H), 5.82 (dq, *J* = 15.7, 1.4 Hz, 1H), 4.23 – 4.06 (m, 3H), 3.65 (q, *J* = 5.5 Hz, 2H), 2.24 (qd, *J* = 7.0, 1.5 Hz, 2H), 1.62 – 1.50 (m, 4H), 1.28 (td, *J* = 7.1, 1.2 Hz, 3H).

^{13}C NMR (100 MHz, $CDCl_3$): δ (ppm) 166.84, 148.94, 121.74, 62.67, 60.33, 32.22, 31.99, 24.37, 14.40.

4.9. SYNTHESIS OF ETHYL (*E*)-7-IODOHEPT-2-ENOATE (**107**)

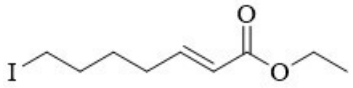

Figure 4.10: *Ethyl (E)-7-iodohept-2-enoate (**107**)*

Triphenylphosphine (5.134g, 19.61mmol) and imidazole (1.326g, 19.47mmol) were added to a stirred solution of ethyl (*E)*-7-hydroxyhept-2-enoate (**82**) (2.165g, 12.57mmol) in anhydrous dichloromethane (130mL). The resulting mixture was stirred at -20°C for 15minutes before iodine (4.95g, 19.52mmol) was added in one portion. The reaction was stirred for additional 15 minutes at this temperature, and then for 35 minutes at room temperature. Subsequently, the reaction was quenched by addition of a saturated solution sodium thiosulphate (15mL). The aqueous phase was extracted three times using small portions of dichloromethane, dried over anhydrous sodium sulphate, and concentrated under reduced pressure. The crude residue was purified over silica gel flash chromatography (8% EtOAc in *n*-hexane), affording the title product as a pale-yellow oil.

Yield: 62%

R_f: 0.4

^{1}H NMR (400 MHz, $CDCl_3$): δ 6.93 (dt, *J* = 15.6, 7.0 Hz, 1H), 5.83 (dt, *J* = 15.7, 1.6 Hz, 1H), 4.18 (q, *J* = 7.1 Hz, 2H), 3.19 (t, *J* = 6.9 Hz, 2H), 2.23 (qd, *J* = 7.2, 1.6 Hz, 2H), 1.85 (p, *J* = 7.0 Hz, 2H), 1.59 (tt, *J* = 9.6, 6.3 Hz, 2H), 1.29 (t, *J* = 7.2 Hz, 3H).

^{13}C NMR (101 MHz, $CDCl_3$) δ (ppm) 166.55, 148.11, 121.92, 60.24, 32.74, 31.01, 28.87, 14.28, 6.15.

4.10. Synthesis of Ethyl (*E*)-7-(triphenyl-λ5-phosphaneylidene)hept-2-enoate (**82**)

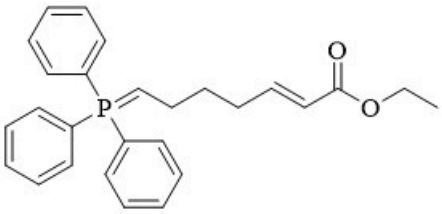

Figure 4.11: *Ethyl (E)-7-(triphenyl-λ5-phosphaneylidene)hept-2-enoate (**82**)*

To a solution of ethyl (*E*)-7-iodohept-2-enoate (**107**) (1g, 3.56mmol) in anhydrous acetonitrile (40mL), triphenylphosphine (4.25g, 16.2mmol) was added in one portion, and the resulting mixture was heated under reflux overnight. The solution was concentrated under reduced pressure, and the crude residue was purified over silica gel flash chromatography using a gradient eluent system, starting with dichloromethane to elute the remaining triphenylphosphine, followed by an eluent gradient with 5% MeOH in dichloromethane. This afforded the title compound as a clear oil.

Yield: 63%

R_f: 0.59

^{1}H NMR (400 MHz, DMSO): δ (ppm) 7.95 – 7.68 (m, 15H), 5.75 (s, 3H), 4.09 (q, *J* = 7.1 Hz, 2H), 3.58 (s, 1H), 2.24 (q, *J* = 6.9 Hz, 2H), 1.60 (tt, *J* = 16.6, 7.6 Hz, 4H), 1.20 (t, *J* = 7.1 Hz, 3H).

^{13}C NMR (100 MHz, DMSO): δ (ppm) 165.32, 148.32, 134.71, 133.42, 133.32, 130.08, 129.95, 121.33, 118.68, 117.83, 59.51, 54.70, 29.86, 13.96.

4.11. SYNTHESIS OF 2-HEXYLTHIOPHENE (**70**)

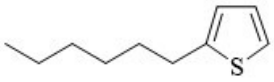

Figure 4.12: *2-hexylthiophene (**70**)*

To a stirred solution of thiophene (6.6mL, 7g, 80mmol) in dry THF (50mL) at -78°C, *n*-BuLi (33.3mL, 2.5M in hexanes, 83.2mmol) was added dropwise. The resulting mixture was stirred for 1 hour at this temperature, before 1-bromohexane (15.1 g, 90.0 mmol was added slowly to the solution. The reaction solution was stirred at room temperature overnight, and then quenched by the addition of cold water. The aqueous phase was extracted with ether (3x50mL), and the combined organic phases were washed with water, then dried over anhydrous magnesium sulphate, and concentrated under reduced pressure. The fraction was purified by distillation under vacuum, which afforded the title product as a colourless oil.

B.p. (1mBar): 70°C

Yield: 58%

^{1}H NMR: δ (ppm) 7.10 (dd, *J* = 2.56 Hz, 1H), 6.92 (dd, *J* = 2.82 Hz, 1H), 6.78 (dd, *J* = 3.32 Hz, 1H), 2.84-2.80 (t, *J* = 7.66 Hz, 2H), 1.72-1.66 (p, *J* = 7.37 Hz, 2H), 1.41-1.27 (m, *J* = 4.95 Hz, 6H), 0.91-0.87 (m, *J* = 6.70 Hz, 3H)

^{13}C NMR: δ (ppm) 145.9, 126.63, 123.58, 122.71, 31.78, 31.59, 29.94, 28.82, 22.59, 14.09

IR: 2926.5, 2853.8, 1455.4, 851.3 cm^{-1}

4.12. SYNTHESIS OF 2-BROMO-5-HEXYLTHIOPHENE (68A)

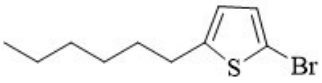

Figure 4.13: *2-bromo-5-hexylthiophene (**68a**)*

To a two-neck flask containing glacial acetic acid (70mL) 2-hexylthiophene (**70**) (7.7g, 45.8mmol) was added, and the solution was stirred for 10min. NBS (8.38g, 47.1mmol) was then added slowly to the solution. The reaction mixture was stirred overnight, and then quenched by the addition of NaOH (2M, 70mL). The aqueous phase was extracted with diethyl ether (3x100mL), and the combined organic layers were washed with brine until pH = 7. Subsequently, the organic layer was dried over anhydrous magnesium sulphate and concentrated under reduced pressure. The crude oil was purified by silica gel flash chromatography (*n*-hexane), affording the title compound as a colourless liquid.

R_f: 0.55

^{1}H NMR (δ): 6.84 (d, *J* = 3.64 Hz, 1H), 6.52 (dd, *J* = 3.64 Hz 1H), 2.75-2.71 (m, *J* = 7.62 Hz, 2H), 1.67-1.58 (m, *J* = 7.60, 2H), 1.38-1.22 (m, *J* = 4.69 Hz, 6H), 0.92-0.83 (m, *J* = 6.86, 3H)

^{13}C NMR: δ 147.66, 129.37, 124.33, 108.54, 31.51, 31.42, 30.33, 28.65, 22.55, 14.06

IR: 2926.5, 2853.8, 1444.2, 1047.1, 963.2, 789.8 cm^{-1}

4.13. SYNTHESIS OF 2-IODO-5-HEXYLTHIOPHENE (**68B**)

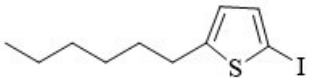

Figure 4.14: *2-iodo-5-hexylthiophene (**68b**)*

To a stirred, ice-cold solution of 2-hexylthiophene (1.2g, 7.4mmol) in a 1:1 mixture of dichloromethane (20mL) and glacial acetic acid (20mL), NIS (1.8g, 8,14mmol) was added slowly. The reaction mixture was stirred at room temperature overnight before the solution was neutralised by addition of a saturated solution of $NaHCO_3$. The aqueous phase was extracted with dichloromethane (3x30mL), and the combined organic layers were washed with brine (3x20mL), dried over anhydrous magnesium sulphate, and concentrated under reduced pressure. The crude oil was purified by column flash chromatography (*n*-hexane), affording the title product as a colourless liquid.

Yield: 96%

R_f: 0.54 (UV)

^{1}H NMR (400 MHz, CD_2Cl_2) δ 7.04 (d, J = 3.6 Hz, 1H), 6.50 – 6.44 (m, 1H), 2.83 – 2.70 (m, 2H), 1.63 (p, J = 7.5 Hz, 2H), 1.41 – 1.24 (m, 6H), 0.94 – 0.83 (m, 3H).

^{1}HNMR: 7.02 (1H), 6.45 (1H), 2.79-2.72(2H), 1.65-1.52(2H), 1.37- (6H), (3H)
^{13}CNMR: 152.56, 136.89, 126.13, 69.65, 31.85, 31.84, 39.59, 29.0, 22.89, 14.4
IR: 2926.5, 2853.8, 1433.0, 1214.9, 1041.5, 940.8, 733.9 cm^{-1}

4.14. SYNTHESIS OF 2-IODOTHIOPHENE (**103B**)

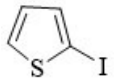

Figure 4.15: *2-iodothiophene (**103b**)*

To a stirred solution of thiophene (1.023g, 1mL, 12.1mmol) in anhydrous ether (20mL) at -78°C, *n*-HeLi (2.3M in hexane, 5.3mL, 12.19mmol) was added dropwise. The mixture was left stirring at room temperature for 1 hour, before a solution of iodine (3.07g, 12.1mmol) in anhydrous ether (40mL) was added slowly at 0°C. The flask was covered in aluminium foil, and the reaction was stirred for 1 hour at room temperature. After 1 hour, the reaction was quenched by pouring the reaction into ice water, and the aqueous layer was extracted with diethyl ether (3x30mL). The combined organic phases were washed with saturated aqueous sodium metabisulfite (30mL) and then brine (30mL). dried over anhydrous Na_2SO_4 and concentrated under reduced pressure. The crude oil was purified using silica gel flash chromatography (*n*-pentane), affording the product as a colourless oil .

Yield: 68%

^{1}H NMR (400 MHz, MeOD): δ (ppm) 7.39 (dq, *J* = 5.5, 1.2 Hz, 1H), 7.17 (dq, *J* = 3.7, 1.2 Hz, 1H), 6.73 (ddd, *J* = 6.6, 3.0, 1.3 Hz, 1H).

^{13}C NMR (100 MHz, MeOD): δ (ppm) 136.75, 131.35, 128.59, 72.63

4.15. SYNTHESIS OF 2-BROMOTHIOPHENE (**103A**)

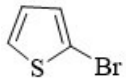

Figure 4.16: *2-bromothiophene (**103a**)*

To a stirred solution of NBS (6.54g, 36mmol) in chloroform (10mL) and glacial acetic acid (10mL), thiophene (3g, 2.87mL, 36mmol) was added. The resulting solution stirred at 80°C for 45 minutes, and the reaction was quenched by the addition of water (20mL). The solution was washed with KOH (1.6M, 20mL) and water (20mL), before the organic layer was dried over anhydrous sodium sulphate and concentrated under reduced pressure. The residue was distilled under vacuum.

Yield: 64%

^{1}H NMR (400 MHz, MeOD): δ 7.27 (dt, *J* = 5.6, 1.2 Hz, 1H), 6.99 (dt, *J* = 3.7, 1.1 Hz, 1H), 6.87 – 6.77 (m, 1H).

^{13}C NMR (100 MHz, MeOD): δ (ppm) 129.74, 127.47, 127.08, 111.33.

4.16. SYNTHESIS OF 2-(5-HEXYLTHIOPHEN-2-YL)-ETHYNYL TRIMETHYLSILANE (**99**)

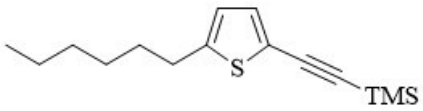

Figure 4.17: *2-(5-hexylthiophen-2-yl)ethynyl trimethylsilane (**99**)*

To a stirred solution of 2-iodo-5-hexylthiophene (**68b**) (1.83g, 7.4mmol, 1eq.) in diisopropylamine (16mL) under nitrogen at room temperature, $Pd(PPh_3)_2Cl_2$ (0.120g, 0.171 mmol, 0.02 eq.) and CuI (0.085g, 0.446 mmol, 0.06eq.) were added in one portion. The temperature was then raised to 90°C, and when the temperature was stable, ethynyltrimethylsilane (1.07mL, 0.757g, 7.4mmol, 1eq.) was added dropwise to the reaction mixture. The solution was stirred at 90°C overnight, after which time it was allowed to reach room temperature, The solvent was removed under reduced pressure, and the crude was purified by silica gel flash column chromatography (*n*-hexane).

Yield: 82%

R_f: 0.6 (UV)

^{1}H NMR: δ (ppm) 7.04 (*J* 3.60, 1H) 6.60 (*J* = 3.60, 1H) 2.77-2.75 (*J* = 8.04,15.08, 2H), 1.63 (*J* =14.84, 2H), 1.35-1.26 (*J* = 1.72, 13.16, 3.60, 2.44, 6H), 0.89-0.86 (*J* = 6.80, 3H), 0.27-0.26 (9H)

^{13}C NMR (100 MHz, $CDCl_3$): δ (ppm)148.55, 132.84, 124.11, 120.54, 77.48, 76.84, 31.67, 31.65, 30.31, 28.79, 22.70, 14.21, 0.07

IR: 2954.4, 2853.8, 2143.4, 2070.7, 1581.7, 1455.4, 1248.4, 1164.5, 1063.9, 834.5, 756.2cm^{-1}

4.17. SYNTHESIS OF 2-ETHYNYL-5-HEXYLTHIOPHENE (76)

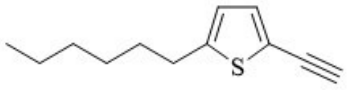

Figure 4.18: *2-ethynyl-5-hexylthiophene (76)*

To stirred solution of 2-(5-hexylthiophene)-2-yl)-ethynyl-trimethylsilane (**99**) (3.1g, 11.6mmol) in THF (30mL) at room temperature, Bu_4NF (1.0M in THF, 4mL, 4.00mmol) was added. The reaction mixture was stirred overnight, filtered, and concentrated under reduced pressure. The crude was purified by silica gel flash column chromatography (*n*-hexane), affording the product as a colourless oil.

Yield: 49%

R_f: 0.30

^{1}H NMR (400 MHz, $CDCl_3$): δ (ppm) 7.09 (d, *J* = 3.6 Hz, 1H), 6.63 (d, *J* = 3.6 Hz, 1H), 3.29 (s, 1H), 2.78 (q, *J* = 7.5 Hz, 3H), 1.68 – 1.63 (m, 2H), 1.31 (qd, *J* = 7.4, 4.9 Hz, 6H), 0.90 (d, *J* = 6.1 Hz, 3H).

^{13}C NMR (101 MHz, $CDCl_3$): δ (ppm) 149.08, 133.58, 126.25, 124.41, 119.63, 80.82, 77.95, 31.97, 31.96, 30.60, 29.15, 23.01, 14.52.

IR: 3306.8, 2926.5, 2853.8, 2104.2, 1461.0, 1226.1, 1142.2 1030.3, 801.0 cm^{-1}

4.18. SYNTHESIS OF 5-HEXYLTHIOPHENE-2-CARBALDEHYDE (**80**)

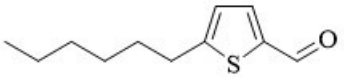

Figure 4.19: *5-hexytlhiophene-2-carbaldehyde (**80**)*

To a stirred solution of 2-hexylthiophene (**70**) (1.00g, 5.95mmol) in 1,2-dichloroethane (20mL), anhydrous dimethylformamide (0.46mL, 5.95mmol) was added dropwise. The mixture was cooled to 0°C before phosphoryl oxychloride (2.54, 5.95mmol) was added slowly. The reaction mixture was stirred at this temperature for 20 minutes, before being heated to 85°C, and stirred at this temperature overnight. After cooling the solution to room temperature, the reaction was quenched by addition of water (30mL), and the aqueous phase was extracted three times using small amounts of dichloromethane. The combined organic layers were washed with water, dried over anhydrous magnesium sulphate and concentrated under reduced pressure. The crude oil was purified over silica gel flash column chromatography (*n*-hexane/EtOAc 3:1), affording the title product as a pale-yellow oil.

Yield: 54%

R_f: 0.82

^{1}H NMR (400 MHz, CDCl3): δ (ppm) 9.82 (s, 1H), 7.61 (d, *J* = 3.8 Hz, 1H), 6.90 (dd, *J* = 3.8, 1.0 Hz, 1H), 2.91 – 2.78 (m, 2H), 1.70 (h, *J* = 6.8 Hz, 2H), 1.36 – 1.25 (m, 6H), 0.89 (td, *J* = 6.2, 3.7 Hz, 4H).

^{13}C NMR (101 MHz, $CDCl_3$) δ (ppm) 182.80, 157.95, 141.74, 137.16, 125.96, 122.83, 31.59, 31.38, 30.98, 28.82, 22.65, 14.17.

4.19. SYNTHESIS OF 3-(5-HEXYLTHIOPHEN-2-YL)-PROP-2-YN-1-OL (**108**)

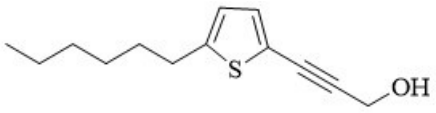

Figure 4.20: *3-(5-hexylthiophen-2-yl)prop-2-yn-1-ol (**108**)*

To a stirred solution of $Pd(Ph_3)_2Cl_2$ (297mg, mmol) and CuI (164mg, mmol) in THF (14mL), piperidine (2.52mL, mmol) and 2-iodo-5-hexylthiophene (**68b**) (2.8g, 1.68mL, 9.5mmol) were added. The reaction flask was de-aerated, then flushed under nitrogen before propargyl alcohol (1.44g, 148mL, mmol) was added, causing the temperature in the reaction flask to increase significantly. The reaction mixture was stirred for 3 hours at room temperature (ca. 21°C), before the residue was suspended in EtOAc (30mL) and filtered over Celite using EtOAc as an eluent. The resulting organic phase was washed with a saturated solution of ammonium chloride and dried over anhydrous magnesium sulphate. The solvent was removed under reduced pressure, and the resulting crude product was purified by silica gel flash chromatography (*n*-hexane:EtOAc 9:1), affording the title product as a yellow oil.

Yield: 90% (1.9g)

R_f: 0.1 (UV)

^{1}H NMR (400MHz, $CDCl_3$): δ (ppm) 7.03 (d, *J* = 3.56 Hz, 1H), 6.63 (d, *J* = 3.60 Hz, 1H), 4.49 (s, 2H), 2.77-2.74 (t, *J* = 7.58 Hz, 2H), 1.66-1.60 (p, *J* = 7.36 Hz, 3H), 1.36-1.26 (m, *J* =7.12 Hz, d, *J* = 3.52 Hz, 6H), 0.89-0.86 (m, *J* = 6,74 Hz, 3H)

^{13}C NMR (100MHz, $CDCl_3$): δ (ppm) 148.74, 132.64, 124.20, 119.70, 90.46, 79.78, 51.96, 31.65, 31.63, 30.30, 28.83, 22.69, 14.20

IR: 3299.6, 2924.9, 2852.2, 2220.3, 1638.1, 1465.4, 1191.4, 1012.5, 906.2, 800.0, 727.3, 195 cm^{-1},

UV: λ_{max} = 246.8, 276.8, 306.6 nm, ε = 526 $M^{-1}cm^{-1}$

4.20. SYNTHESIS OF 2-(3-BROMOPROP-1-YN-1-YL)-5-HEXYLTHIOPHENE (**84**)

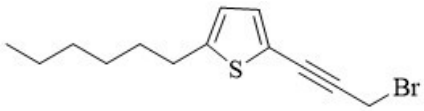

Figure 4.21: *2-(3-bromoprop-1-yn-1-yl)-5-hexylthiophene (**84**)*

To a stirred, ice-cold solution of 3-(5-hexyl)-thiophene-2-yl-prop-2-yn-1-ol (**108**) (1.9g, 8.5mmol) and CBr_4 (3.11g, 9.4mmol) in dichloromethane (60mL), PPh_3 (2.72g, 10.34mmol) was added. The resulting mixture was stirred for 3 hours at room temperature (ca. 21°C), and then concentrated under reduced pressure. The concentrate was suspended in *n*-pentane (200mL) and stirred vigorously using a laboratory spoon. The resulting precipitate was filtered off, and the organic phase was concentrated *in vacuo* and purified over silica gel flash column chromatography (*n*-hex:EtOAc 9:1),

Yield: 74% (1.78g)

R_f: 0.65

^{1}H NMR: 7.06 (d, *J* 3.60,1H), 6.64 (d, *J* 3.60, 1H), 4.19 (s, 2H), 2.77-2.75 (m, *J* 7.56, 2H), 1.68-1-61 (p, *J* 7.56, 2H), 1.38-1.35 (m, *J* 3.64, 2H), 1.31-1.26 (m, *J* 14.30, 5H), 0.90-0.87 (m, *J* 13.68, 3H)

^{13}C NMR: 149.13, 132.97, 124.01, 119.01, 87.24, 80.87, 31.33, 31.32, 30.02, 28.50, 22.37, 15.51, 13.88

IR: 2924.9, 2852.2, 2220.3, 1756.2, 1644.4, 1465.4, 1197.0, 1049.4, 929.6, 800.0 cm^{-1}

UV: λ_{MAX} = 236.9, 271.6 nm, ε = 564 $M^{-1}cm^{-1}$

4.21. SYNTHESIS OF 6-(5-HEXYLTHIOPHEN-2-YL)HEXA-2,5-DIYN-1-OL (**89**)

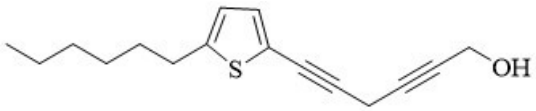

Figure 4.22: *6-(5-hexylthiophen-2-yl)hexa-2,5-diyn-1-ol (**89**)*

To a stirred mixture of Na_2CO_3 (0.994g, 9.38mmol), CuI (1.19g, 6.24mmol), and *n*-Bu_4NBr (0.497g, 1.54mmol) in DMF (30mL) at -20°C, propargyl alcohol (0.37mL, 0.36g, 6.35mmol) was added, followed by addition of 2-(3-bromoprop-1-yn-1-yl)-5-hexylthiophene (**84**) (1.78g, 6.24mmol). The reaction solution was stirred overnight, and diluted in diethyl ether (15mL), causing a white precipitate to form. The resulting suspension was filtered over a short silica plug, and the filtrate was suspended in water (30mL). The aqueous phase was extracted with small amounts of diethyl ether, and the combined organic layers were washed with a saturated solution of ammonium chloride, dried over anhydrous magnesium sulphate, and concentrated under reduced pressure. The crude residue was purified by silica gel flash chromatography (*n*-hexane:EtOAc 5:1), affording the title product as an liquid crystalline substance.

Yield: 85% (1.38g)

^{1}H NMR: δ (ppm) 6.99 (d, *J* = 3.60 1H), 6.60 (d, *J* = 3.56 1H), 4.30-4.27 (dt, *J* = 4.24, *J* = 2.12 2H), 3.45 (s, *J* = 2.10, 2H), 2.77-2.73 (m, *J* = 7.56, 2H), 1.66-1.60 (m, *J* = 14.44, 2H), 1.37-1.24 (m, *J* = 18.24, 3.6, 7H), 0.91-0.86 (td, 3H)

^{13}C NMR: δ (ppm) 147.96, 132.08, 124.02, 120.22, 86.21, 79.82, 79.09, 74.89, 51.45, 31.66, 31.64, 30.27, 28.82, 22.69, 14.20, 11.01

IR: 3333.1, 2930.5, 2862.2, 2287.4, 2225.9, 1733.8, 1655.6, 1538.1,1464.6, 1308.9, 1197.0, 1129,9, 916.4, 800.0 cm^{-1}

UV: λ_{MAX} = 236.9, 271.6 nm, ε_{MAX} = 1508 $M^{-1}cm^{-1}$

4.22. SYNTHESIS OF 6-(5-HEXYLTHIOPHEN-2-YL)HEXAN-1-OL (**91**)

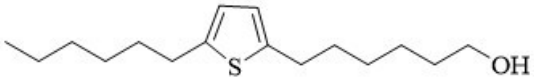

Figure 4.23: *6-(6-hexylthiophen-2-yl)hexan-1-ol (**91**)*

A solution of 6-(5-hexyltiophen-2-yl)hexa-2,5-diyn-1-ol (**89**) (630mg, 2.4mmol) and Pd/C (10%, 398mg) in anhydrous methanol (52mL) was flushed under nitrogen before the inert atmosphere was replaced by a H_2 atmosphere by sparging the reaction mixture under a H_2 balloon. The reaction was stirred under a H_2 atmosphere overnight, then filtered, and concentrated under reduced pressure. The crude residue was purified by silica gel flash column chromatography using a gradient eluent system to separate the over-reduced product **111** (*n*-hexane, R_f = 0.42) from the target compound **91** (*n*-hexane:EtOAc 5:1, $R_{f(\text{hexane})}$ = 0, $R_{f(n\text{-hexane:EtOAc 5:1})}$ = 0.08)

Yield: 46%

R_f: 0.075

^{1}H NMR (400 MHz, $CDCl_3$): δ (ppm) 6.55 (s, 2H), 3.64 (t, *J* = 6.6 Hz, 1H), 2.74 (td, *J* = 7.7, 4.7 Hz, 4H), 1.62 (ddt, *J* = 23.6, 13.4, 5.1 Hz, 6H), 1.46 – 1.20 (m, 12H), 0.91 – 0.86 (m, 3H).

^{13}C NMR (100MHz, $CDCl_3$): δ (ppm) 123.50, 63.15, 32.83. 31.83, 31.74, 30.32, 30.21, 28.98, 25.63, 22.73, 14.23

IR: 3355.5, 3064.7, 2930.5, 2852.2, 1722.7, 1644.6, 1560.5, 1459.8, 1376.0, 1191.4, 1129.9, 1051.6, 794.4, 727.3 cm^{-1}

4.23. SYNTHESIS OF 6-(5-HEXYLTHIOPHEN-2-YL)HEXANAL (**87**)

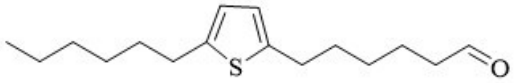

Figure 4.24: *6-(5-hexylthiophen-2-yl)hexanal (**87**)*

To a solution of 6-(5-hexylthiophen-2-yl)hexan-1-ol (**91**) (0.260g, 0.97mmol) and DMSO (1.1mL, 15.5mmol) in anhydrous dichlormethane (0.3mL) at 0°C, triethylamine (0.77mL, 5.53mmol) and SO3·Py (52mg, 3.25mmol) were added. The reaction was stirred for 2 hours, and quenched by addition of brine. The aqueous phase was extracted with hexane three times, and the combined organic layers were dried over anhydrous magnesium sulphate and concentrated under reduced pressure. The crude oil was purified over silica gel flash chromatography (*n*-hexane:EtOAc 5:1)

Yield: 91% (235mg)

R_f: 0.09

^{1}H NMR (400 MHz, $CDCl_3$) δ (ppm) 9.78 (m, 1H), 6.48 (s, 2H), 2.74 – 2.64 (m, 4H), 1.58 (ddt, *J* = 15.2, 11.5, 6.5 Hz, 6H), 1.34 – 1.23 (m, 8H), 0.82 (d, *J* = 6.5 Hz, 3H).

^{13}C NMR (100 MHz) δ (ppm) 202.80, 123.63, 123.46, 31.82, 31.73, 31.53, 30.31, 30.04, 28.97, 28.70, 22.72, 21.95, 14.22

4.24. SYNTHESIS OF ETHYL (E)-8-(5-HEXYLTHIOPHEN-2-YL)OCT-2-ENOATE (**86**)

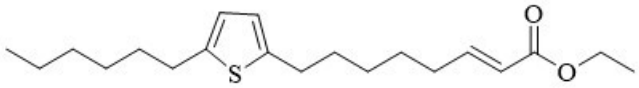

Figure 4.25: Ethyl (E)-8-(5-hexylthiophen-2-yl)oct-2-enoate (86)

Sodium hydride (0.046g, mmol, 60% suspension in mineral oil) was washed three times using n-hexane, and suspended in THF (0.3mL). To the resulting suspension, ethyl diethylphosphonoacetate (0.25mL, 282mg, 1.26mmol) was added dropwise at room temperature. The mixture was stirred for 1 hour, before a solution of the 6-(5-hexylthiophen-2-yl)hexanal (**87**) (235mg, 0.882mmol) in THF (0.3mL) was added. The reaction was stirred overnight and quenched by addition of a saturated solution of ammonium chloride. The aqueous phase was extracted three times using n-hexane, and the combined organic layers were dried over anhydrous sodium sulphate and concentrated under reduced pressure. The crude residue was purified over silica gel flash column chromatography (n-hexane:EtOAc).

5. REFERENCES

1. Marc, E. B.; Nelly, A.; Annick, D.-D.; Frederic, D., Plants used as remedies antirheumatic and antineuralgic in the traditional medicine of Lebanon. *Journal of Ethnopharmacology* **2008,** *120* (3), 315-334.
2. Yang, R.; Zhou, Q.; Wen, C.; Hu, J.; Li, H.; Zhao, M.; Zhao, H., Mustard seed (Sinapis Alba Linn) attenuates imiquimod-induced psoriasiform inflammation of BALB/c mice. *The Journal of Dermatology* **2013,** *40* (7), 543-552.
3. Rahman, M.; Browne, J. J.; Van Crugten, J.; Hasan, M. F.; Liu, L.; Barkla, B. J., In Silico, Molecular Docking and In Vitro Antimicrobial Activity of the Major Rapeseed Seed Storage Proteins. *Frontiers in Pharmacology* **2020,** *11* (1340).
4. Saeidnia, S.; Gohari, A., Importance of Brassica napus as a medicinal food plant. *Journal of medicinal plant research* **2012,** *6*, 2700-2703.
5. Ujjal Kumar, N.; lt; sup; gt; lt; sup; gt; Hoy-Taek, K.; lt; sup; gt; lt; sup; gt; Khadiza, K.; lt; sup; gt; lt; sup; gt; Jong-In, P.; lt; sup; gt; lt; sup; gt; Kwon-Kyoo, K.; lt; sup; gt; lt; sup; gt; and Ill-Sup, N.; lt; sup; gt; lt; sup; gt, Modification of Fatty Acid Profiles of Rapeseed (<italic>Brassica napus</italic> L.) Oil for Using as Food, Industrial Feed-Stock and Biodiesel. *Plant Breed. Biotech.* **2016,** *4* (2), 123-134.
6. Jahandideh, M.; Kharazi, P.; Jafariazar, Z.; Fahimi*, S., Preparation of a Topical Product from Allium sativum Retrieved from Iranian Traditional Medicine. *Research Journal of Pharmacognosy* **2019,** *6* (4), 3-6.
7. Faris, A., Garlic and its Active Compounds: A Novel Strategy to Fight Diseases Through Modulating Biological Activities. *Pharmacognosy Journal* **2020,** *12* (6).
8. Rahman, M.; Khatun, A.; Liu, L.; Barkla, B. J., Brassicaceae Mustards: Traditional and Agronomic Uses in Australia and New Zealand. *Molecules* **2018,** *23* (1), 231.
9. Adeli Milani, M.; Ghobadi Dana, M.; Ghanbarzadeh, B.; Alizadeh, A.; Ghasemi Afshar, P., Comparison of the Chemical Compositions and Antibacterial Activities of Two Iranian Mustard Essential Oils and Use of these Oils in Turkey Meats as Preservatives. *Applied Food Biotechnology* **2019,** *6* (4), 225-236.
10. Liu, L.; Liu, T.; Li, G.; Wang, Q.; Ng, T., Isolation and determination of p-hydroxybenzoylcholine in traditional Chinese medicine Semen sinapis Albae. *Analytical and Bioanalytical Chemistry* **2003,** *376* (6), 854-858.
11. Seki, T.; Hosono, T.; Ozaki-Masuzawa, Y., Chemistry of Sulfur-Containing Compounds Derived from Garlic and Their Functions. In *Chemistry of Korean Foods and Beverages*, American Chemical Society: 2019; Vol. 1303, pp 43-55.
12. Khan, S. A.; Shahid, S.; Jameel, M.; Ahmad, A., In vitro antibacterial, antifungal and GC-MS analysis of seeds of Mustard Brown. *Int j pharm Chem* **2016,** *6* (4), 107-15.
13. Lin, F.; Huang, X.; Xing, F.; Xu, L.; Zhang, W.; Chen, Z.; Ke, X.; Song, Y.; Zeng, Z., Semen Brassicae reduces thoracic aortic remodeling, inflammation, and oxidative damage in spontaneously hypertensive rats. *Biomedicine & Pharmacotherapy* **2020,** *129*, 110400.
14. Venkatesh, Y. P., Chapter 14 - Immunomodulatory Attributes of Aged Garlic Extract and Its Components. In *Immunology*, Hayat, M. A., Ed. Academic Press: 2018; pp 203-224.
15. Wijesundera, R. C.; Ackman, R. G., Evidence for the probable presence of sulfur-containing fatty acids as minor constituents in canola oil. *Journal of the American Oil Chemists' Society* **1988,** *65* (6), 959-963.
16. Saiz-Jimenez, C., The origin of alkylbenzenes and thiophenes in pyrolysates of geochemical samples. *Organic Geochemistry* **1995,** *23* (1), 81-85.
17. Friedman, B.; Brophy, P.; Brune, W. H.; Farmer, D. K., Anthropogenic Sulfur Perturbations on Biogenic Oxidation: SO2 Additions Impact Gas-Phase OH Oxidation Products of α- and β-Pinene. *Environmental Science & Technology* **2016,** *50* (3), 1269-1279.
18. Surratt, J. D.; Lewandowski, M.; Offenberg, J. H.; Jaoui, M.; Kleindienst, T. E.; Edney, E. O.; Seinfeld, J. H., Effect of Acidity on Secondary Organic Aerosol Formation from Isoprene. *Environmental Science & Technology* **2007,** *41* (15), 5363-5369.
19. Liggio, J.; Li, S.-M., Organosulfate formation during the uptake of pinonaldehyde on acidic sulfate aerosols. *Geophysical Research Letters* **2006,** *33* (13).

20. Iinuma, Y.; Müller, C.; Böge, O.; Gnauk, T.; Herrmann, H., The formation of organic sulfate esters in the limonene ozonolysis secondary organic aerosol (SOA) under acidic conditions. *Atmospheric Environment* **2007,** *41* (27), 5571-5583.
21. Stone, E. A.; Yang, L.; Yu, L. E.; Rupakheti, M., Characterization of organosulfates in atmospheric aerosols at Four Asian locations. *Atmospheric Environment* **2012,** *47*, 323-329.
22. Sinninghe Damste, J. S.; De Leeuw, J. W., Analysis, structure and geochemical significance of organically-bound sulphur in the geosphere: State of the art and future research. *Organic Geochemistry* **1990,** *16* (4), 1077-1101.
23. Russell, M.; Hartgers, W. A.; Grimalt, J. O., Identification and geochemical significance of sulphurized fatty acids in sedimentary organic matter from the Lorca Basin, SE Spain. *Geochimica et Cosmochimica Acta* **2000,** *64* (21), 3711-3723.
24. Dembitsky, V. M.; Abu-Lafi, S.; Hanuš, L. O., Occurrence of Sulfur-Containing Fatty Acids in Allium sativum. *Natural Product Communications* **2007,** *2* (7), 1934578X0700200713.
25. Surette, R.; Vining, L. C., Formation of 3-methylthioacrylic acid from methionine by Streptomyces lincolnensis. Isolation of a peroxidase. *J Antibiot (Tokyo)* **1976,** *29* (6), 646-52.
26. Šturdiková, M.; Proksa, B.; Rosenberg, M.; Fuska, J., Production of 3-methylthioacrylic acid by Streptomyces kasugaensis. *Letters in Applied Microbiology* **1994,** *18* (3), 165-167.
27. Eibler, D.; Hammerschick, T.; Buck, L.; Vetter, W., Up to 21 Different Sulfur-Heterocyclic Fatty Acids in Rapeseed and Mustard Oil. *Journal of the American Oil Chemists' Society* **2017,** *94* (7), 893-903.
28. Newman, D. J.; Cragg, G. M.; Snader, K. M., The influence of natural products upon drug discovery. *Natural Product Reports* **2000,** *17* (3), 215-234.
29. Butler, M. S., The role of natural product chemistry in drug discovery. *J Nat Prod* **2004,** *67* (12), 2141-53.
30. Baker, D. D.; Chu, M.; Oza, U.; Rajgarhia, V., The value of natural products to future pharmaceutical discovery. *Nat Prod Rep* **2007,** *24* (6), 1225-44.
31. Secondary Metabolism: The Building Blocks and Construction Mechanisms. In *Medicinal Natural Products*, 2009; pp 7-38.
32. Fleming, A., On the Antibacterial Action of Cultures of a Penicillium, with Special Reference to Their Use in the Isolation of B. influenzae. *Reviews of Infectious Diseases* **1980,** *2* (1), 129-139.
33. Peptides, Proteins, and Other Amino Acid Derivatives. In *Medicinal Natural Products*, 2009; pp 421-484.
34. Vardanyan, R. S.; Hruby, V. J., 32 - Antibiotics. In *Synthesis of Essential Drugs*, Vardanyan, R. S.; Hruby, V. J., Eds. Elsevier: Amsterdam, 2006; pp 425-498.
35. Castle, S. S., Penicillin G. In *xPharm: The Comprehensive Pharmacology Reference*, Enna, S. J.; Bylund, D. B., Eds. Elsevier: New York, 2007; pp 1-6.
36. ACRED, P.; BROWN, D. M.; TURNER, D. H.; WILSON, M. J., PHARMACOLOGY AND CHEMOTHERAPY OF AMPICILLIN—A NEW BROAD-SPECTRUM PENICILLIN. *British Journal of Pharmacology and Chemotherapy* **1962,** *18* (2), 356-369.
37. Moss, G. P.; Smith, P. A. S.; Tavernier, D., Glossary of class names of organic compounds and reactivity intermediates based on structure (IUPAC Recommendations 1995). *Pure and Applied Chemistry* **1995,** *67* (8-9), 1307-1375.
38. Nelson, D. L.; Cox, M. M.; Lehninger, A. L., *Lehninger principles of biochemistry*. 2019.
39. Sadava, D.; Hillis, D.; Heller, C.; Berenbaum, M., *Life: The Science of Biology*. 10 ed.; Sinauer: U.S.A., 2014; Vol. 1, p 426.
40. Simopoulos, A. P., Omega-3 fatty acids in health and disease and in growth and development. *The American Journal of Clinical Nutrition* **1991,** *54* (3), 438-463.
41. Devarshi, P. P.; Grant, R. W.; Ikonte, C. J.; Hazels Mitmesser, S., Maternal Omega-3 Nutrition, Placental Transfer and Fetal Brain Development in Gestational Diabetes and Preeclampsia. *Nutrients* **2019,** *11* (5), 1107.
42. Ruxton, C. H.; Reed, S. C.; Simpson, M. J.; Millington, K. J., The health benefits of omega-3 polyunsaturated fatty acids: a review of the evidence. *J Hum Nutr Diet* **2004,** *17* (5), 449-59.
43. Mozaffarian, D.; Wu, J. H., Omega-3 fatty acids and cardiovascular disease: effects on risk factors, molecular pathways, and clinical events. *J Am Coll Cardiol* **2011,** *58* (20), 2047-67.

44. Méndez, L.; Dasilva, G.; Taltavull, N.; Romeu, M.; Medina, I., Marine Lipids on Cardiovascular Diseases and Other Chronic Diseases Induced by Diet: An Insight Provided by Proteomics and Lipidomics. *Marine Drugs* **2017,** *15* (8), 258.
45. Backes, J.; Anzalone, D.; Hilleman, D.; Catini, J., The clinical relevance of omega-3 fatty acids in the management of hypertriglyceridemia. *Lipids in Health and Disease* **2016,** *15* (1), 118.
46. Roth, E. M., ω-3 carboxylic acids for hypertriglyceridemia. *Expert Opinion on Pharmacotherapy* **2015,** *16* (1), 123-133.
47. Spiteller, G., Furan fatty acids: Occurrence, synthesis, and reactions. Are furan fatty acids responsible for the cardioprotective effects of a fish diet? *Lipids* **2005,** *40* (8), 755-771.
48. Vetter, W.; Ulms, K.; Wendlinger, C.; van Rijn, J., Novel non-methylated furan fatty acids in fish from a zero discharge aquaculture system. *NFS Journal* **2016,** *2*, 8-14.
49. Masuchi Buscato, M. H.; Müller, F.; Vetter, W.; Weiss, J.; Salminen, H., Furan fatty acids in enriched ω-3 fish oil: Oxidation kinetics with and without added monomethyl furan fatty acid as potential natural antioxidant. *Food Chemistry* **2020,** *327*, 127087.
50. Lauvai, J.; Becker, A.-K.; Lehnert, K.; Schumacher, M.; Hieronimus, B.; Vetter, W.; Graeve, L., The Furan Fatty Acid 9M5 Acts as a Partial Ligand to Peroxisome Proliferator-Activated Receptor gamma and Enhances Adipogenesis in 3T3-L1 Preadipocytes. *Lipids* **2019,** *54* (5), 277-288.
51. Wakimoto, T.; Kondo, H.; Nii, H.; Kimura, K.; Egami, Y.; Oka, Y.; Yoshida, M.; Kida, E.; Ye, Y.; Akahoshi, S.; Asakawa, T.; Matsumura, K.; Ishida, H.; Nukaya, H.; Tsuji, K.; Kan, T.; Abe, I., Furan fatty acid as an anti-inflammatory component from the green-lipped mussel <em>Perna canaliculus</em&gt. *Proceedings of the National Academy of Sciences* **2011,** *108* (42), 17533.
52. Ishii, K.; Okajima, H.; Okada, Y.; Watanabe, H., Effects of Phosphatidylcholines Containing Furan Fatty Acid on Oxidation in Multilamellar Liposomes. *CHEMICAL & PHARMACEUTICAL BULLETIN* **1989,** *37* (5), 1396-1398.
53. Teixeira, A.; Cox, R. C.; Egmond, M. R., Furan fatty acids efficiently rescue brain cells from cell death induced by oxidative stress. *Food & Function* **2013,** *4* (8), 1209-1215.
54. Vetter, W.; Wendlinger, C., Furan fatty acids – valuable minor fatty acids in food. *Lipid Technology* **2013,** *25* (1), 7-10.
55. Lemke, R. A. S.; Peterson, A. C.; Ziegelhoffer, E. C.; Westphall, M. S.; Tjellström, H.; Coon, J. J.; Donohue, T. J., Synthesis and scavenging role of furan fatty acids. *Proceedings of the National Academy of Sciences* **2014,** *111* (33), E3450.
56. Dasagrandhi, C.; Ellamar, J. B.; Kim, Y. S.; Kim, H.-R., Antimicrobial activity of a novel furan fatty acid, 7,10-epoxyoctadeca-7,9-dienoic acid against methicillin-resistant Staphylococcus aureus. *Food Science and Biotechnology* **2016,** *25* (6), 1671-1675.
57. Parker, R. A.; Kariya, T.; Grisar, J. M.; Petrow, V., 5-(Tetradecyloxy)-2-furancarboxylic acid and related hypolipidemic fatty acid-like alkyloxyarylcarboxylic acids. *Journal of Medicinal Chemistry* **1977,** *20* (6), 781-791.
58. Smith, W. L.; Murphy, R. C., Chapter 9 - The Eicosanoids: Cyclooxygenase, Lipoxygenase and Epoxygenase Pathways. In *Biochemistry of Lipids, Lipoproteins and Membranes (Sixth Edition)*, Ridgway, N. D.; McLeod, R. S., Eds. Elsevier: Boston, 2016; pp 259-296.
59. Labaudiniere, R.; Hilboll, G.; Leon-Lomeli, A.; Lautenschlaeger, H. H.; Parnham, M.; Kuhl, P.; Dereu, N., .omega.-[(.omega.-Arylalkyl)aryl]alkanoic acids: a new class of specific LTA4 hydrolase inhibitors. *Journal of Medicinal Chemistry* **1992,** *35* (17), 3156-3169.
60. Corey, E. J.; Cashman, J. R.; Eckrich, T. M.; Corey, D. R., A new class of irreversible inhibitors of leukotriene biosynthesis. *Journal of the American Chemical Society* **1985,** *107* (3), 713-715.
61. Hanko, R.; Hammond, M. D.; Fruchtmann, R.; Pfitzner, J.; Place, G. A., Design, synthesis, and 5-lipoxygenase-inhibiting properties of 1-thio-substituted butadienes. *Journal of Medicinal Chemistry* **1990,** *33* (4), 1163-1170.
62. Bremer, J., The biochemistry of hypo- and hyperlipidemic fatty acid derivatives: metabolism and metabolic effects. *Progress in Lipid Research* **2001,** *40* (4), 231-268.
63. Øie, E.; Berge, R. K.; Ueland, T.; Dahl, C. P.; Edvardsen, T.; Beitnes, J. O.; Bohov, P.; Aukrust, P.; Yndestad, A., Tetradecylthioacetic acid increases fat metabolism and improves cardiac function in experimental heart failure. *Lipids* **2013,** *48* (2), 139-54.
64. Fredriksen, J.; Ueland, T.; Dyrøy, E.; Halvorsen, B.; Melby, K.; Melbye, L.; Skalhegg, B. S.; Bohov, P.; Skorve, J.; Berge, R. K.; Aukrust, P.; Frøland, S. S., Lipid-lowering and anti-

inflammatory effects of tetradecylthioacetic acid in HIV-infected patients on highly active antiretroviral therapy. *Eur J Clin Invest* **2004,** *34* (10), 709-15.
65. Asiedu, D. K.; Demoz, A.; Skorve, J.; Grav, H. J.; Berge, R. K., Acute modulation of rat hepatic lipid metabolism by sulphur-substituted fatty acid analogues. *Biochemical Pharmacology* **1995,** *49* (7), 1013-1022.
66. Berge, R. K.; Skorve, J.; Tronstad, K. J.; Berge, K.; Gudbrandsen, O. A.; Grav, H., Metabolic effects of thia fatty acids. *Current Opinion in Lipidology* **2002,** *13* (3), 295-304.
67. Khalid, A. M.; Hafstad, A. D.; Larsen, T. S.; Severson, D. L.; Boardman, N.; Hagve, M.; Berge, R. K.; Aasum, E., Cardioprotective effect of the PPAR ligand tetradecylthioacetic acid in type 2 diabetic mice. *Am J Physiol Heart Circ Physiol* **2011,** *300* (6), H2116-22.
68. Kuiper, K. K. J.; Muna, Z. A.; Erga, K. S.; Dyrøy, E.; Svendsen, E.; Berge, R. K.; Nordrehaug, J. E., Tetradecylthioacetic acid reduces stenosis development after balloon angioplasty injury of rabbit iliac arteries. *Atherosclerosis* **2001,** *158* (2), 269-275.
69. Aukrust, P.; Wergedahl, H.; Müller, F.; Ueland, T.; Dyrøy, E.; Damås, J. K.; Frøland, S. S.; Berge, R. K., Immunomodulating effects of 3-thia fatty acids in activated peripheral blood mononuclear cells. *Eur J Clin Invest* **2003,** *33* (5), 426-33.
70. Tronstad, K. J.; Bruserud, O.; Berge, K.; Berge, R., Antiproliferative effects of a non-β-oxidizable fatty acid, tetradecylthioacetic acid, in native human acute myelogenous leukemia blast cultures. *Leukemia : official journal of the Leukemia Society of America, Leukemia Research Fund, U.K* **2002,** *16*, 2292-301.
71. Berge, K.; Tronstad, K. J.; Flindt, E. N.; Rasmussen, T. H.; Madsen, L.; Kristiansen, K.; Berge, R. K., Tetradecylthioacetic acid inhibits growth of rat glioma cells ex vivo and in vivo via PPAR-dependent and PPAR-independent pathways. *Carcinogenesis* **2001,** *22* (11), 1747-1755.
72. Abdi-Dezfuli, F.; Frøyland, L.; Thorsen, T.; Aakvaag, A.; Berge, R. K., Eicosapentaenoic acid and sulphur substituted fatty acid analogues inhibit the proliferation of human breast cancer cells in culture. *Breast Cancer Res Treat* **1997,** *45* (3), 229-39.
73. Lundåsen, T.; Pedrelli, M.; Bjørndal, B.; Rozell, B.; Kuiper, R. V.; Burri, L.; Pavanello, C.; Turri, M.; Skorve, J.; Berge, R. K.; Alexson, S. E. H.; Tillander, V., The PPAR pan-agonist tetradecylthioacetic acid promotes redistribution of plasma cholesterol towards large HDL. *PLoS One* **2020,** *15* (3), e0229322.
74. Arge, R.; Dessen, J. E.; Østbye, T. K.; Ruyter, B.; Thomassen, M. S.; Rørvik, K. A., Effects of tetradecylthioacetic acid (TTA) treatment on lipid metabolism in salmon hearts-in vitro and in vivo studies. *Fish Physiol Biochem* **2018,** *44* (2), 703-716.
75. Pangopoulos, M. K.; Nolsøe, J. M. N.; Antonsen, S. G.; Colas, R. A.; Dalli, J.; Aursnes, M.; Stenstrøm, Y.; Hansen, T. V., Enzymatic studies with 3-oxa n-3 DPA. *Bioorganic Chemistry* **2020,** *96*, 103653.
76. Hamberg, M.; Chechetkin, I. R.; Grechkin, A. N.; de León, I. P.; Castresana, C.; Bannenberg, G., Synthesis of 3-oxalinolenic acid and β-oxidation-resistant 3-oxa-oxylipins. *Lipids* **2006,** *41* (5), 499-506.
77. Larsen, L. N.; Granlund, L.; Holmeide, A. K.; Skattebøl, L.; Nebb, H. I.; Bremer, J., Sulfur-substituted and alpha-methylated fatty acids as peroxisome proliferator-activated receptor activators. *Lipids* **2005,** *40* (1), 49-57.
78. Hafstad, A. D.; Khalid, A. M.; Hagve, M.; Lund, T.; Larsen, T. S.; Severson, D. L.; Clarke, K.; Berge, R. K.; Aasum, E., Cardiac peroxisome proliferator-activated receptor-α activation causes increased fatty acid oxidation, reducing efficiency and post-ischaemic functional loss. *Cardiovascular Research* **2009,** *83* (3), 519-526.
79. Auwerx, J., PPARgamma, the ultimate thrifty gene. *Diabetologia* **1999,** *42* (9), 1033-49.
80. Demetri, G. D.; Fletcher, C. D.; Mueller, E.; Sarraf, P.; Naujoks, R.; Campbell, N.; Spiegelman, B. M.; Singer, S., Induction of solid tumor differentiation by the peroxisome proliferator-activated receptor-gamma ligand troglitazone in patients with liposarcoma. *Proc Natl Acad Sci U S A* **1999,** *96* (7), 3951-3956.
81. Røst, T. H.; Haugan Moi, L. L.; Berge, K.; Staels, B.; Mellgren, G.; Berge, R. K., A pan-PPAR ligand induces hepatic fatty acid oxidation in PPARalpha-/- mice possibly through PGC-1 mediated PPARdelta coactivation. *Biochim Biophys Acta* **2009,** *1791* (11), 1076-83.

82. Schepetkin, I. A.; Kirpotina, L. N.; Khlebnikov, A. I.; Balasubramanian, N.; Quinn, M. T., Neutrophil Immunomodulatory Activity of Natural Organosulfur Compounds. *Molecules* **2019,** *24* (9), 1809.
83. Shahidi, F.; Ambigaipalan, P.; Chandrasekara, A., Recent Advances in Phytochemicals in Fruits and Vegetables. In *Fruit and Vegetable Phytochemicals*, 2017; pp 1323-1356.
84. Abraham, V.; deMan, J. M., Determination of total sulfur in canola oil. *Journal of the American Oil Chemists' Society* **1987,** *64* (3), 384-387.
85. Abraham, V.; Deman, J. M., Determination of volatile sulfur compounds in canola oil. *Journal of the American Oil Chemists Society* **1985,** *62* (6), 1025-1028.
86. Williams, J. R.; Rayburn, J. R.; Cline, G. R.; Sauterer, R.; Friedman, M., Effect of allyl isothiocyanate on developmental toxicity in exposed Xenopus laevis embryos. *Toxicology Reports* **2015,** *2*, 222-227.
87. Liu, C.-T.; Hsu, T.-W.; Chen, K.-M.; Tan, Y.-P.; Lii, C.-K.; Sheen, L.-Y., The Antidiabetic Effect of Garlic Oil is Associated with Ameliorated Oxidative Stress but Not Ameliorated Level of Pro-inflammatory Cytokines in Skeletal Muscle of Streptozotocin-induced Diabetic Rats. *J Tradit Complement Med* **2012,** *2* (2), 135-144.
88. Kyo, E.; Uda, N.; Kasuga, S.; Itakura, Y., Immunomodulatory Effects of Aged Garlic Extract. *The Journal of Nutrition* **2001,** *131* (3), 1075S-1079S.
89. Lau, B. H. S.; Tadi, P. P.; Tosk, J. M., Allium sativum (Garlic) and cancer prevention. *Nutrition Research* **1990,** *10* (8), 937-948.
90. Miękus, N.; Marszałek, K.; Podlacha, M.; Iqbal, A.; Puchalski, C.; Świergiel, A. H., Health Benefits of Plant-Derived Sulfur Compounds, Glucosinolates, and Organosulfur Compounds. *Molecules* **2020,** *25* (17), 3804.
91. Rutkowski, A.; Gwiazda, S.; Krygier, K., Sulfur compounds affecting processing of rapeseed. *Journal of the American Oil Chemists' Society* **1982,** *59* (1), 7-11.
92. Peng, C.; Zhao, S.-Q.; Zhang, J.; Huang, G.-Y.; Chen, L.-Y.; Zhao, F.-Y., Chemical composition, antimicrobial property and microencapsulation of Mustard (Sinapis alba) seed essential oil by complex coacervation. *Food Chemistry* **2014,** *165*, 560-568.
93. Bhattacharya, A.; Li, Y.; Shi, Y.; Zhang, Y., Enhanced inhibition of urinary bladder cancer growth and muscle invasion by allyl isothiocyanate and celecoxib in combination. *Carcinogenesis* **2013,** *34* (11), 2593-2599.
94. Núñez-Iglesias, M. J.; Novío, S.; García, C.; Pérez-Muñuzuri, E.; Soengas, P.; Cartea, E.; Velasco, P.; Freire-Garabal, M., Glucosinolate-Degradation Products as Co-Adjuvant Therapy on Prostate Cancer in Vitro. *International Journal of Molecular Sciences* **2019,** *20* (20), 4977.
95. Fimognari, C.; Turrini, E.; Ferruzzi, L.; Lenzi, M.; Hrelia, P., Natural isothiocyanates: Genotoxic potential versus chemoprevention. *Mutation Research/Reviews in Mutation Research* **2012,** *750* (2), 107-131.
96. Ranger, C. M.; Reding, M. E.; Oliver, J. B.; Moyseenko, J. J.; Youssef, N.; Krause, C. R., Acute Toxicity of Plant Essential Oils to Scarab Larvae (Coleoptera: Scarabaeidae) and Their Analysis by Gas Chromatography-Mass Spectrometry. *Journal of Economic Entomology* **2013,** *106* (1), 159-167.
97. Dhingra, O. D.; Costa, M. L. N.; Silva Jr, G. J., Potential of Allyl Isothiocyanate to Control Rhizoctonia solani Seedling Damping Off and Seedling Blight in Transplant Production. *Journal of Phytopathology* **2004,** *152* (6), 352-357.
98. Kasamaki, A.; Takahashi, H.; Tsumura, N.; Niwa, J.; Fujita, T.; Urasawa, S., Genotoxicity of flavoring agents. *Mutation Research Letters* **1982,** *105* (6), 387-392.
99. Additives, E. P. o. F.; Food, N. S. a. t., Scientific Opinion on the safety of allyl isothiocyanate for the proposed uses as a food additive. *EFSA Journal* **2010,** *8* (12), 1943.
100. Devinat, G.; Biasini, S.; Naudet, M., *Rev. Ft. Corps Gras* **1980,** *27*.
101. de Man, J. M.; Pogorzelska, E.; de Man, L., Effect of the presence of sulfur during the hydrogenation of canola oil. *Journal of the American Oil Chemists' Society* **1983,** *60* (3), 558-562.
102. Moser, H. A.; Evans, C.; Mustakas, G.; Cowan, J., Flavor and oxidative stability of some linolenate-containing oils. *Journal of the American Oil Chemists' Society* **1965,** *42* (9), 811-813.
103. Coenen, J. W., Hydrogenation of edible oils. *Journal of the American Oil Chemists' Society* **1976,** *53* (6), 382-389.

104. De Hoffmann, E.; Stroobant, V., *Mass Spectrometry : Principles and Applications*. Wiley: Somerset, 2013.
105. Kind, T.; Fiehn, O., Advances in structure elucidation of small molecules using mass spectrometry. *Bioanalytical Reviews* **2010,** *2* (1), 23-60.
106. Nicolaou, K. C.; Snyder, S. A., Chasing Molecules That Were Never There: Misassigned Natural Products and the Role of Chemical Synthesis in Modern Structure Elucidation. *Angewandte Chemie International Edition* **2005,** *44* (7), 1012-1044.
107. Amagata, T., 2.18 - Missasigned Structures: Case Examples from the Past Decade. In *Comprehensive Natural Products II*, Liu, H.-W.; Mander, L., Eds. Elsevier: Oxford, 2010; pp 581-621.
108. Gallantree-Smith, H. C.; Antonsen, S. G.; Görbitz, C. H.; Hansen, T. V.; Nolsøe, J. M. J.; Stenstrøm, Y. H., Total synthesis based on the originally claimed structure of mucosin. *Organic & Biomolecular Chemistry* **2016,** *14* (36), 8433-8437.
109. Nolsøe, J. M. J.; Antonsen, S.; Görbitz, C. H.; Hansen, T. V.; Nesman, J. I.; Røhr, Å. K.; Stenstrøm, Y. H., Total Synthesis of (−)-Mucosin and Revision of Structure. *The Journal of Organic Chemistry* **2018,** *83* (24), 15066-15076.
110. Al-Tel, T. H.; Abu Zarga, M. H.; Sabri, S. S.; Feroz, M.; Fatima, N.; Shah, Z.; Atta ur, R., Phenolics from Colchicum decaisnei. *Phytochemistry* **1991,** *30* (9), 3081-3085.
111. Kalinin, A. V.; Snieckus, V., 4,6-Dimethoxy-3,7-dimethylcoumarin from Colchicum decaisnei. Total synthesis by carbamoyl Baker-venkataraman rearrangement and structural revision to isoeugenetin methyl ether. *Tetrahedron Letters* **1998,** *39* (28), 4999-5002.
112. Pettit, G. R.; Herald, C. L.; Kamano, Y., Antineoplastic agents. 93. Structure of the Bugula neritina (marine bryozoa) antineoplastic component bryostatin 3. *The Journal of Organic Chemistry* **1983,** *48* (26), 5354-5356.
113. Schaufelberger, D. E.; Chmurny, G. N.; Beutler, J. A.; Koleck, M. P.; Alvarado, A. B.; Schaufelberger, B. W.; Muschik, G. M., Revised structure of bryostatin 3 and isolation of the bryostatin 3 26-ketone from Bugula neritina. *The Journal of Organic Chemistry* **1991,** *56* (8), 2895-2900.
114. Chmurny, G. N.; Koleck, M. P.; Hilton, B. D., Bryostatins revisited: a new bryostatin 3 and the use of NMR to determine stereochemistry in the C-20-C-23 area. *The Journal of Organic Chemistry* **1992,** *57* (19), 5260-5264.
115. Ohmori, K.; Ogawa, Y.; Obitsu, T.; Ishikawa, Y.; Nishiyama, S.; Yamamura, S., Total Synthesis of Bryostatin 3. *Angewandte Chemie International Edition* **2000,** *39* (13), 2290-2294.
116. Brown, C. A.; Yamashita, A., Saline hydrides and superbases in organic reactions. IX. Acetylene zipper. Exceptionally facile contrathermodynamic multipositional isomeriazation of alkynes with potassium 3-aminopropylamide. *Journal of the American Chemical Society* **1975,** *97* (4), 891-892.
117. The Alkyne Zipper Reaction in Asymmetric Synthesis. In *Modern Alkyne Chemistry*, 2014; pp 365-394.
118. Wotiz, J. H.; Barelski, P. M.; Koster, D. F., Mechanism of the base-catalyzed prototropic propargylic rearrangement in vicinal diamines. *The Journal of Organic Chemistry* **1973,** *38* (3), 489-493.
119. Cram, D. J.; Willey, F.; Fischer, H. P.; Scott, D. A., Base-Catalyzed Intramolecular 1,3- and 1,5-Proton Transfers. *Journal of the American Chemical Society* **1964,** *86* (23), 5370-5371.
120. Carr, M. D.; Gan, L. H.; Reid, I., Acetylene–allene isomerisations. Part I. Base catalysis by potassium t-butoxide in t-butyl alcohol. *Journal of the Chemical Society, Perkin Transactions 2* **1973,** (5), 668-672.
121. Benson, S. W.; Cruickshank, F. R.; Golden, D. M.; Haugen, G. R.; O'Neal, H. E.; Rodgers, A. S.; Shaw, R.; Walsh, R., Additivity rules for the estimation of thermochemical properties. *Chemical Reviews* **1969,** *69* (3), 279-324.
122. Introduction. In *Modern Alkyne Chemistry*, 2014; pp 1-8.
123. Sonogashira, K., Cross-Coupling Reactions to sp Carbon Atoms. In *Metal-Catalyzed Cross-Coupling Reactions*, 1998; pp 203-229.
124. Sonogashira, K.; Tohda, Y.; Hagihara, N., A convenient synthesis of acetylenes: catalytic substitutions of acetylenic hydrogen with bromoalkenes, iodoarenes and bromopyridines. *Tetrahedron Letters* **1975,** *16* (50), 4467-4470.

125. Negishi, E.-I.; Liu, F., Palladium- or Nickel-Catalyzed Cross-Coupling with Organometals Containing Zinc, Magnesium, Aluminum, and Zirconium. In *Metal-Catalyzed Cross-Coupling Reactions*, 1998; pp 1-47.
126. Baba, S.; Negishi, E., A novel stereospecific alkenyl-alkenyl cross-coupling by a palladium- or nickel-catalyzed reaction of alkenylalanes with alkenyl halides. *Journal of the American Chemical Society* **1976,** *98* (21), 6729-6731.
127. Miyaura, N.; Suzuki, A., Stereoselective synthesis of arylated (E)-alkenes by the reaction of alk-1-enylboranes with aryl halides in the presence of palladium catalyst. *Journal of the Chemical Society, Chemical Communications* **1979,** (19), 866-867.
128. Miyaura, N.; Yamada, K.; Suzuki, A., A new stereospecific cross-coupling by the palladium-catalyzed reaction of 1-alkenylboranes with 1-alkenyl or 1-alkynyl halides. *Tetrahedron Letters* **1979,** *20* (36), 3437-3440.
129. Shi, W.; Liu, C.; Lei, A., Transition-metal catalyzed oxidative cross-coupling reactions to form C–C bonds involving organometallic reagents as nucleophiles. *Chemical Society Reviews* **2011,** *40* (5), 2761-2776.
130. Liu, C., Introduction. In *Transition Metal Catalyzed Oxidative Cross-Coupling Reactions*, Lei, A., Ed. Springer Berlin Heidelberg: Berlin, Heidelberg, 2019; pp 1-10.
131. Oxidative Coupling – Bonding between Two Nucleophiles. In *Oxidative Cross-Coupling Reactions*, 2016; pp 1-5.
132. Knappke, C. E. I.; Grupe, S.; Gärtner, D.; Corpet, M.; Gosmini, C.; Jacobi von Wangelin, A., Reductive Cross-Coupling Reactions between Two Electrophiles. *Chemistry – A European Journal* **2014,** *20* (23), 6828-6842.
133. Liu, C.; Zhang, H.; Shi, W.; Lei, A., Bond Formations between Two Nucleophiles: Transition Metal Catalyzed Oxidative Cross-Coupling Reactions. *Chemical Reviews* **2011,** *111* (3), 1780-1824.
134. Amatore, M.; Gosmini, C., Direct Method for Carbon–Carbon Bond Formation: The Functional Group Tolerant Cobalt-Catalyzed Alkylation of Aryl Halides. *Chemistry – A European Journal* **2010,** *16* (20), 5848-5852.
135. Suzuki, A., Cross-Coupling Reactions of Organoboron Compounds with Organic Halides. In *Metal-Catalyzed Cross-Coupling Reactions*, 1998; pp 48-97.
136. Matos, K.; Soderquist, J. A., Alkylboranes in the Suzuki−Miyaura Coupling: Stereochemical and Mechanistic Studies. *The Journal of Organic Chemistry* **1998,** *63* (3), 461-470.
137. Chinchilla, R.; Nájera, C., Recent advances in Sonogashira reactions. *Chemical Society Reviews* **2011,** *40* (10), 5084-5121.
138. Clayden, J.; Greeves, N.; Warren, S. G., Organic chemistry. **2012**.
139. Schaub, T. A.; Kivala, M., Cross-Coupling Reactions to sp Carbon Atoms. In *Metal-Catalyzed Cross-Coupling Reactions and More*, 2014; pp 665-762.
140. Gottardo, C.; Kraft, T. M.; Hossain, M. S.; Zawada, P. V.; Muchall, H. M., Linear free-energy correlation analysis of the electronic effects of the substituents in the Sonogashira coupling reaction. *Canadian Journal of Chemistry* **2008,** *86* (5), 410-415.
141. an der Heiden, M. R.; Plenio, H.; Immel, S.; Burello, E.; Rothenberg, G.; Hoefsloot, H. C. J., Insights into Sonogashira Cross-Coupling by High-Throughput Kinetics and Descriptor Modeling. *Chemistry – A European Journal* **2008,** *14* (9), 2857-2866.
142. He, C.; Ke, J.; Xu, H.; Lei, A., Synergistic Catalysis in the Sonogashira Coupling Reaction: Quantitative Kinetic Investigation of Transmetalation. *Angewandte Chemie International Edition* **2013,** *52* (5), 1527-1530.
143. Echavarren, A. M.; Homs, A., Mechanistic Aspects of Metal-Catalyzed C,C- and C,X-Bond Forming Reactions. In *Metal-Catalyzed Cross-Coupling Reactions and More*, 2014; pp 1-64.
144. Wang, X.; Song, Y.; Qu, J.; Luo, Y., Mechanistic Insights into the Copper-Cocatalyzed Sonogashira Cross-Coupling Reaction: Key Role of an Anion. *Organometallics* **2017,** *36* (5), 1042-1048.
145. Monfette, S.; Brown, A. R.; Dubé, P.; Ide, N. D.; Lewis, C. A.; Piper, J. L.; Shekhar, S.; Yu, S., Selected Catalytic Reactions. In *Practical Synthetic Organic Chemistry*, 2020; pp 269-375.
146. Chinchilla, R.; Nájera, C., The Sonogashira Reaction: A Booming Methodology in Synthetic Organic Chemistry. *Chemical Reviews* **2007,** *107* (3), 874-922.

147. Plenio, H., Catalysts for the Sonogashira Coupling—The Crownless Again Shall Be King. *Angewandte Chemie International Edition* **2008,** *47* (37), 6954-6956.
148. Thorand, S.; Krause, N., Improved Procedures for the Palladium-Catalyzed Coupling of Terminal Alkynes with Aryl Bromides (Sonogashira Coupling). *The Journal of Organic Chemistry* **1998,** *63* (23), 8551-8553.
149. Mohajer, F.; Heravi, M. M.; Zadsirjan, V.; Poormohammad, N., Copper-free Sonogashira cross-coupling reactions: an overview. *RSC Advances* **2021,** *11* (12), 6885-6925.
150. Carrow, B. P.; Hartwig, J. F., Distinguishing Between Pathways for Transmetalation in Suzuki−Miyaura Reactions. *Journal of the American Chemical Society* **2011,** *133* (7), 2116-2119.
151. Thomas, A. A.; Denmark, S. E., Pre-transmetalation intermediates in the Suzuki-Miyaura reaction revealed: The missing link. *Science* **2016,** *352* (6283), 329-332.
152. Fyfe, J. W. B.; Watson, A. J. B., Strategies towards Chemoselective Suzuki–Miyaura Cross-Coupling. *Synlett* **2015,** *26* (09), 1139-1144.
153. Diner, C.; Organ, M. G., The Negishi Cross-Coupling Reaction. In *Organic Reactions*, pp 1-62.
154. K?rti, L. s. C. B., *Strategic applications of named reactions in organic synthesis : background and detailed mechanisms*. Elsevier Academic: Burlington, MA, 2005.
155. Kambe, N.; Iwasaki, T.; Terao, J., Pd-catalyzed cross-coupling reactions of alkyl halides. *Chemical Society Reviews* **2011,** *40* (10), 4937-4947.
156. Campeau, L.-C.; Hazari, N., Cross-Coupling and Related Reactions: Connecting Past Success to the Development of New Reactions for the Future. *Organometallics* **2019,** *38* (1), 3-35.
157. Chass, G. A.; Kantchev, E. A. B.; Fang, D.-C., The fine balance between one cross-coupling and two β-hydride elimination pathways: a DFT mechanistic study of Ni(π-allyl)2-catalyzed cross-coupling of alkyl halides and alkyl Grignard reagents. *Chemical Communications* **2010,** *46* (16), 2727-2729.
158. Jana, R.; Pathak, T. P.; Sigman, M. S., Advances in Transition Metal (Pd,Ni,Fe)-Catalyzed Cross-Coupling Reactions Using Alkyl-organometallics as Reaction Partners. *Chemical Reviews* **2011,** *111* (3), 1417-1492.
159. Zhang, Z.-H.; Dong, X.-Y.; Du, X.-Y.; Gu, Q.-S.; Li, Z.-L.; Liu, X.-Y., Copper-catalyzed enantioselective Sonogashira-type oxidative cross-coupling of unactivated C(sp3)−H bonds with alkynes. *Nature Communications* **2019,** *10* (1), 5689.
160. Dong, X.-Y.; Zhang, Y.-F.; Ma, C.-L.; Gu, Q.-S.; Wang, F.-L.; Li, Z.-L.; Jiang, S.-P.; Liu, X.-Y., A general asymmetric copper-catalysed Sonogashira C(sp3)–C(sp) coupling. *Nature Chemistry* **2019,** *11* (12), 1158-1166.
161. Sun, F.-N.; Yang, W.-C.; Chen, X.-B.; Sun, Y.-L.; Cao, J.; Xu, Z.; Xu, L.-W., Enantioselective palladium/copper-catalyzed C–C σ-bond activation synergized with Sonogashira-type C(sp3)–C(sp) cross-coupling alkynylation. *Chemical Science* **2019,** *10* (32), 7579-7583.
162. Eckhardt, M.; Fu, G. C., The First Applications of Carbene Ligands in Cross-Couplings of Alkyl Electrophiles: Sonogashira Reactions of Unactivated Alkyl Bromides and Iodides. *Journal of the American Chemical Society* **2003,** *125* (45), 13642-13643.
163. Fan, Q.; Sun, H.; Xie, S.; Dong, Y.; Li, X.; Fuhr, O.; Fenske, D., Nickel-Catalyzed Sonogashira Coupling Reactions of Nonactivated Alkyl Chlorides under Mild Conditions. *Organometallics* **2021,** *40* (14), 2240-2245.
164. Ludwig, J. R.; Simmons, E. M.; Wisniewski, S. R.; Chirik, P. J., Cobalt-Catalyzed C(sp2)–C(sp3) Suzuki–Miyaura Cross Coupling. *Organic Letters* **2021,** *23* (3), 625-630.
165. Netherton, M. R.; Dai, C.; Neuschütz, K.; Fu, G. C., Room-Temperature Alkyl−Alkyl Suzuki Cross-Coupling of Alkyl Bromides that Possess β Hydrogens. *Journal of the American Chemical Society* **2001,** *123* (41), 10099-10100.
166. Palao, E.; López, E.; Torres-Moya, I.; de la Hoz, A.; Díaz-Ortiz, Á.; Alcázar, J., Formation of quaternary carbons through cobalt-catalyzed C(sp3)–C(sp3) Negishi cross-coupling. *Chemical Communications* **2020,** *56* (59), 8210-8213.
167. Wollnitzke, P.; Essig, S.; Gölz, J. P.; von Schwarzenberg, K.; Menche, D., Total Synthesis of Ajudazol A by a Modular Oxazole Diversification Strategy. *Organic Letters* **2020,** *22* (16), 6344-6348.
168. Mason, J. D.; Terwilliger, D. W.; Pote, A. R.; Myers, A. G., Practical Gram-Scale Synthesis of Iboxamycin, a Potent Antibiotic Candidate. *Journal of the American Chemical Society* **2021,** *143* (29), 11019-11025.

169. Thaler, T.; Haag, B.; Gavryushin, A.; Schober, K.; Hartmann, E.; Gschwind, R. M.; Zipse, H.; Mayer, P.; Knochel, P., Highly diastereoselective Csp3–Csp2 Negishi cross-coupling with 1,2-, 1,3- and 1,4-substituted cycloalkylzinc compounds. *Nature Chemistry* **2010,** *2* (2), 125-130.
170. Tungen, J. E.; Aursnes, M.; Dalli, J.; Arnardottir, H.; Serhan, C. N.; Hansen, T. V., Total Synthesis of the Anti-inflammatory and Pro-resolving Lipid Mediator MaR1n−3 DPA Utilizing an sp3–sp3 Negishi Cross-Coupling Reaction. *Chemistry – A European Journal* **2014,** *20* (45), 14537-14537.
171. Maxted, E. B., The Poisoning of Metallic Catalysts. In *Advances in Catalysis*, Frankenburg, W. G.; Komarewsky, V. I.; Rideal, E. K.; Emmett, P. H.; Taylor, H. S., Eds. Academic Press: 1951; Vol. 3, pp 129-178.
172. Barbier, J.; Lamy-Pitara, E.; Marecot, P.; Boitiaux, J. P.; Cosyns, J.; Verna, F., Role of Sulfur in Catalytic Hydrogenation Reactions. In *Advances in Catalysis*, Eley, D. D.; Pines, H.; Weisz, P. B., Eds. Academic Press: 1990; Vol. 37, pp 279-318.
173. Dunleavy, J., Final Analysis: Sulfur as a Catalyst Poison. *Platinum Metals Review - PLATIN MET REV* **2006,** *50*, 110-110.
174. *Thiophenes*. Springer: 2016; Vol. 39, p 298.
175. Kursanov, D. N.; Parnes, Z. N.; Bolestova, G. I.; Belen'kii, L. I., Ionic hydrogenation of thiophenes. *Tetrahedron* **1975,** *31* (4), 311-315.
176. Yuzhi, l.; Dong, Z.; Wang, P.; Zhou, H.-B., Thiophene Oxidation and Reduction Chemistry. 2014; pp 227-293.
177. L. Larson, G.; L. Fry, J., Ionic and Organometallic-Catalyzed Organosilane Reductions. In *Organic Reactions*, pp 1-737.
178. Bullock, R. M., Ionic Hydrogenations. In *The Handbook of Homogeneous Hydrogenation*, 2006; pp 153-197.
179. Kursanov, D. N.; Parnes, Z. N.; Loim, N. M., Applications of Ionic Hydrogenation to Organic Synthesis. *Synthesis* **1974,** *1974* (09), 633-651.
180. Nagai, Y., HYDROSILANES AS REDUCING AGENTS. A REVIEW. *Organic Preparations and Procedures International* **1980,** *12* (1-2), 13-48.
181. Rendler, S.; Oestreich, M., Diverse Modes of Silane Activation for the Hydrosilylation of Carbonyl Compounds. In *Modern Reduction Methods*, 2008; pp 183-207.
182. Liu, T.; Wang, X.; Yin, D., Recent progress towards ionic hydrogenation: Lewis acid catalyzed hydrogenation using organosilanes as donors of hydride ions. *RSC Advances* **2015,** *5* (92), 75794-75805.
183. Luan, L.; Song, J.-S.; Bullock, R. M., Ionic Hydrogenation of Alkynes by HOTf and Cp(CO)3WH. *The Journal of Organic Chemistry* **1995,** *60* (22), 7170-7176.
184. Zdanovich, V. I.; Kudryavtsev, R. V.; Kursanov, D. N. Bull. Acad. Sci., USSR, Div. Chem. Sci.: 1970.
185. Kursanov, D. N.; Parnes, Z. N.; Lyakhovetskii, Y. I.; Bolestova, G. I. Bull. Acad. Sci. USSR, Div. Chem. Sci. : 1984.
186. Wittig, G.; Haag, W., Über Triphenyl-phosphinmethylene als olefinbildende Reagenzien (II. Mitteil.1)). *Chemische Berichte* **1955,** *88* (11), 1654-1666.
187. Rocha, D. H. A.; Pinto, D. C. G. A.; Silva, A. M. S., Applications of the Wittig Reaction on the Synthesis of Natural and Natural-Analogue Heterocyclic Compounds. *European Journal of Organic Chemistry* **2018,** *2018* (20-21), 2443-2457.
188. Maryanoff, B. E.; Reitz, A. B., The Wittig olefination reaction and modifications involving phosphoryl-stabilized carbanions. Stereochemistry, mechanism, and selected synthetic aspects. *Chemical Reviews* **1989,** *89* (4), 863-927.
189. Byrne, P. A.; Gilheany, D. G., The modern interpretation of the Wittig reaction mechanism. *Chemical Society Reviews* **2013,** *42* (16), 6670-6696.
190. Vedejs, E.; Marth, C. F., Mechanism of Wittig reaction: evidence against betaine intermediates. *Journal of the American Chemical Society* **1990,** *112* (10), 3905-3909.
191. Gu, Y.; Tian, S.-K., Olefination Reactions of Phosphorus-Stabilized Carbon Nucleophiles. In *Stereoselective Alkene Synthesis*, Wang, J., Ed. Springer Berlin Heidelberg: Berlin, Heidelberg, 2012; pp 197-238.
192. Mikołajczyk, M.; Midura, W. H.; Mohamed Ewas, A. M.; Perlikowska, W.; Mikina, M.; Jankowiak, A., Horner Olefination Reaction in Organic Sulfur Chemistry and Synthesis of Natural and

Bioactive Products. *Phosphorus, Sulfur, and Silicon and the Related Elements* **2008,** *183* (2-3), 313-325.
193. Horner, L.; Hoffmann, H.; Wippel, H. G., Phosphororganische Verbindungen, XII. Phosphinoxyde als Olefinierungsreagenzien. *Chemische Berichte* **1958,** *91* (1), 61-63.
194. Wadsworth, W. S.; Emmons, W. D., The Utility of Phosphonate Carbanions in Olefin Synthesis. *Journal of the American Chemical Society* **1961,** *83* (7), 1733-1738.
195. Kobayashi, K.; Tanaka, K.; Kogen, H., Recent topics of the natural product synthesis by Horner–Wadsworth–Emmons reaction. *Tetrahedron Letters* **2018,** *59* (7), 568-582.
196. A. Bisceglia, J.; R. Orelli, L., Recent Applications of the Horner-Wadsworth-Emmons Reaction to the Synthesis of Natural Products. *Current Organic Chemistry* **2012,** *16* (19), 2206-2230.
197. A. Bisceglia, J.; R. Orelli, L., Recent Progress in the Horner-Wadsworth-Emmons Reaction. *Current Organic Chemistry* **2015,** *19* (9), 744-775.
198. Roman, D.; Sauer, M.; Beemelmanns, C., Applications of the Horner–Wadsworth–Emmons Olefination in Modern Natural Product Synthesis. *Synthesis* **2021,** *53* (16), 2713-2739.
199. Smith, M.; March, J., *March's advanced organic chemistry : reactions, mechanisms, and structure*. John Wiley & Sons: Hoboken, N.J., 2007.
200. Appel Reaction. In *Comprehensive Organic Name Reactions and Reagents*, pp 95-99.
201. Appel, R., Tertiary Phosphane/Tetrachloromethane, a Versatile Reagent for Chlorination, Dehydration, and P□N Linkage. *Angewandte Chemie International Edition in English* **1975,** *14* (12), 801-811.
202. Chavan, S. P.; Kawale, S. A.; Patil, N. B.; Kalbhor, D. B., Application of allylic amine formation from aziridine-2-ol under Appel reaction condition: Synthesis of N-(tert-butoxycarbonyl)-D-vinyl glycine methyl ester. *Tetrahedron Letters* **2021,** *73*, 153119.
203. Kalkeren, H. A. v.; Delft, F. L. v.; Rutjes, F. P. J. T., Catalytic Appel reactions. *Pure and Applied Chemistry* **2012,** *85* (4), 817-828.
204. Eljo, J.; Carle, M. S.; Murphy, G. K., Hypervalent Iodine-Based Activation of Triphenylphosphine for the Functionalization of Alcohols. *Synlett* **2017,** *28* (20), 2871-2875.
205. Vital'evich, R. I.; Rakhimovna, A. V.; Valiulovna, K. R.; Ljabibovich, S. G.; Maratovich, A. A.; Aleksandrovich, P. E. Process for simultaneous preparation of 8-(5-hexylthiophan-2-yl)caprylic acid and 8-(5-hexyl-3,4-dehydrothiophan-2-yl)caprylic acid by ultrasound-mediated heterocyclization of linoleic acid with sulfur. 2007.
206. Flock, S.; Kristin Holmeide, A.; Skattebøl, L., Syntheses of Some Sulfur-Containing Polyunsaturated Fatty Acids as Potential Lipoxygenase Inhibitors. *Synthetic Communications* **2007,** *37* (22), 4005-4015.
207. Mohamed, Y.; Solum, E., An efficient stereoselective synthesis of a sulfur-bridged analogue of bosseopentaenoic acid as a potential antioxidant agent. *Arkivoc* **2017,** *2017*, 10-19.
208. Haley, M. M., Modern Alkyne Chemistry. Catalytic and Atom-Economic Transformations. Edited by Barry M. Trost and Chao-Jun Li. *Angewandte Chemie International Edition* **2015,** *54* (29), 8332-8332.
209. Kuo, C.-Y.; Huang, Y.-C.; Hsiow, C.-Y.; Yang, Y.-W.; Huang, C.-I.; Rwei, S.-P.; Wang, H.-L.; Wang, L., Effect of Side-Chain Architecture on the Optical and Crystalline Properties of Two-Dimensional Polythiophenes. *Macromolecules* **2013,** *46* (15), 5985-5997.
210. Belletête, M.; Blouin, N.; Boudreault, P.-L. T.; Leclerc, M.; Durocher, G., Optical and Photophysical Properties of Indolocarbazole Derivatives. *The Journal of Physical Chemistry A* **2006,** *110* (51), 13696-13704.
211. Kuo, C.-Y.; Liu, Y.; Yarotski, D.; Li, H.; Xu, P.; Yen, H.-J.; Tretiak, S.; Wang, H.-L., Synthesis, electrochemistry, STM investigation of oligothiophene self-assemblies with superior structural order and electronic properties. *Chemical Physics* **2016,** *481*, 191-197.
212. He, C.; He, Q.; Zhang, S.; Tan, X.; Gao, H.; Cheng, X., Ionic Bent Shape Ternary Facial Amphiphiles. *Chinese Journal of Chemistry* **2013,** *31* (6), 839-844.
213. Poleschner, H.; Heydenreich, M., 13C NMR chemical shifts of unbranched alk-2-yn-1-ols, ω-alkyn-1-ols and 'internal' alkyn-1-ols. *Magnetic Resonance in Chemistry* **1995,** *33* (11), 917-921.
214. Yang, Y.; Zimmt, M. B., Shape-Directed Patterning and Surface Reaction of Tetra-diacetylene Monolayers: Formation of Linear and Two-Dimensional Grid Polydiacetylene Alternating Copolymers. *Langmuir* **2015,** *31* (45), 12408-12416.

215. Reddy, C. R.; Jithender, E.; Prasad, K. R., Total Syntheses of the Proposed Structure for Ieodoglucomides A and B. *The Journal of Organic Chemistry* **2013,** *78* (9), 4251-4260.
216. Reyes, S.; Huigens Iii, R. W.; Su, Z.; Simon, M. L.; Melander, C., Synthesis and biological activity of 2-aminoimidazole triazoles accessed by Suzuki–Miyaura cross-coupling. *Organic & Biomolecular Chemistry* **2011,** *9* (8), 3041-3049.
217. Ogawa, N.; Amano, T.; Kobayashi, Y., Synthesis of Optically Active Maresin 2 and Maresin 2n-3 DPA. *Synlett* **2021,** *32* (03), 295-298.
218. Ye, B.; Jiang, P.; Zhang, T.; Ding, Y.; Sun, Y.; Hao, X.; Li, L.; Wang, L.; Chen, Y., Total Synthesis of the Highly N-Methylated Peptide Jahanyne. *The Journal of Organic Chemistry* **2018,** *83* (12), 6741-6747.
219. Yang, P.-Y.; Liu, K.; Ngai, M. H.; Lear, M. J.; Wenk, M. R.; Yao, S. Q., Activity-Based Proteome Profiling of Potential Cellular Targets of Orlistat − An FDA-Approved Drug with Anti-Tumor Activities. *Journal of the American Chemical Society* **2010,** *132* (2), 656-666.
220. Perlikowska, W.; Mikołajczyk, M., A Short Synthesis of Enantiomeric Phytoprostanes B1 Type I. *Synthesis* **2009,** *2009* (16), 2715-2718.
221. Herron, A. N.; Liu, D.; Xia, G.; Yu, J.-Q., δ-C-H Mono- and Dihalogenation of Alcohols. *Journal of the American Chemical Society* **2020,** *142* (6), 2766-2770.
222. Shaik, B.; Park, J. H.; An, T. K.; Noh, Y. R.; Yoon, S. B.; Park, C. E.; Yoon, Y. J.; Kim, Y.-H.; Lee, S.-G., Small asymmetric anthracene–thiophene compounds as organic thin-film transistors. *Tetrahedron* **2013,** *69* (38), 8191-8198.
223. Jie, X.; Shang, Y.; Hu, P.; Su, W., Palladium-Catalyzed Oxidative Cross-Coupling between Heterocycles and Terminal Alkynes with Low Catalyst Loading. *Angewandte Chemie International Edition* **2013,** *52* (13), 3630-3633.
224. Rondeau-Gagné, S.; Curutchet, C.; Grenier, F.; Scholes, G. D.; Morin, J.-F., Synthesis, characterization and DFT calculations of new ethynyl-bridged C60 derivatives. *Tetrahedron* **2010,** *66* (23), 4230-4242.
225. Jones, L.; Pask, C. M.; Kazlauciunas, A.; Gulcur, M.; Lin, L., Synthesis and Characterisation of Fused Heterocyclic Molecular Rods: A Combined Experimental and Theoretical Study on Diethynyl Dithienothiophenyl Derivatives. *ChemistrySelect* **2017,** *2* (21), 5958-5964.
226. Cai, D.-J.; Lin, P.-H.; Liu, C.-Y., Cobalt-Catalyzed Reductive Alkylation of Heteroaryl Bromides: One-Pot Access to Alkylthiophenes, -furans, -selenophenes, and -pyrroles. *European Journal of Organic Chemistry* **2015,** *2015* (24), 5448-5452.
227. Sund, P.; Pettersson, F.; Österbacka, R.; Wilén, C.-E., Conductivity, interaction and solubility of hetero-bifunctional end-capped β,β'-dihexylsubstituted sexithiophenes. *Journal of Applied Polymer Science* **2018,** *135* (43), 46830.
228. Takahashi, K.; Tarutani, S., Efficient Synthesis of 2-Iodo and 2-Dicyanomethyl Derivatives of Thiophene, Selenophene, Tellurophene, and Thieno[3,2-b]thiophene. *Heterocycles* **1996,** *43* (9), 1927 - 1935.
229. Nieto, C. T.; Salgado, M. M.; Domínguez, S. H.; Díez, D.; Garrido, N. M., Rapid access with diversity to enantiopure flexible PNA monomers following asymmetric orthogonal strategies. *Tetrahedron: Asymmetry* **2014,** *25* (13), 1046-1060.
230. Aursnes, M.; Tungen, J. E.; Vik, A.; Dalli, J.; Hansen, T. V., Stereoselective synthesis of protectin D1: a potent anti-inflammatory and proresolving lipid mediator. *Organic & Biomolecular Chemistry* **2014,** *12* (3), 432-437.
231. Long, J.; Liu, X.; Guo, H.; Zhao, B.; Tan, S., Effect of conjugated side groups on the photovoltaic performances of triphenylamine-based dyes sensitized solar cells. *Dyes and Pigments* **2016,** *124*, 222-231.
232. Tan, C. K.; Zhou, L.; Yeung, Y.-Y., Aminothiocarbamate-Catalyzed Asymmetric Bromolactonization of 1,2-Disubstituted Olefinic Acids. *Organic Letters* **2011,** *13* (10), 2738-2741.
233. Khomane, N. B.; Meshram, H. M.; Rode, H. B., Studies towards the synthesis of trocheliophorolides. *Tetrahedron Letters* **2018,** *59* (22), 2157-2160.
234. Ng, P. S.; Bates, R. W., Synthesis of hydroxylated pyrrolidines by allenic cyclisation. *Tetrahedron* **2016,** *72* (41), 6356-6362.

235. Amatore, C.; Blart, E.; Genet, J. P.; Jutand, A.; Lemaire-Audoire, S.; Savignac, M., New synthetic applications of water-soluble acetate Pd/TPPTS catalyst generated in Situ. evidence for a true Pd(0) species intermediate. *The Journal of Organic Chemistry* **1995,** *60* (21), 6829-6839.
236. Saito, Y.; Matsumoto, K.; Bag, S. S.; Ogasawara, S.; Fujimoto, K.; Hanawa, K.; Saito, I., C8-alkynyl- and alkylamino substituted 2′-deoxyguanosines: a universal linker for nucleic acids modification. *Tetrahedron* **2008,** *64* (16), 3578-3588.
237. Banerjee, S.; Nayek, A.; Sinha, S.; Bhaumik, T.; Ghosh, S., Alkoxy group facilitated ring closing metathesis (RCM) of acyclic 1,6-dienes: Facile synthesis of non-racemic highly substituted cyclopentenols. *Journal of Molecular Catalysis A: Chemical* **2006,** *254* (1), 85-92.

APPENDIX

A.1. 2-OCTYN-1-OL (**71**) SPECTRAL DATA

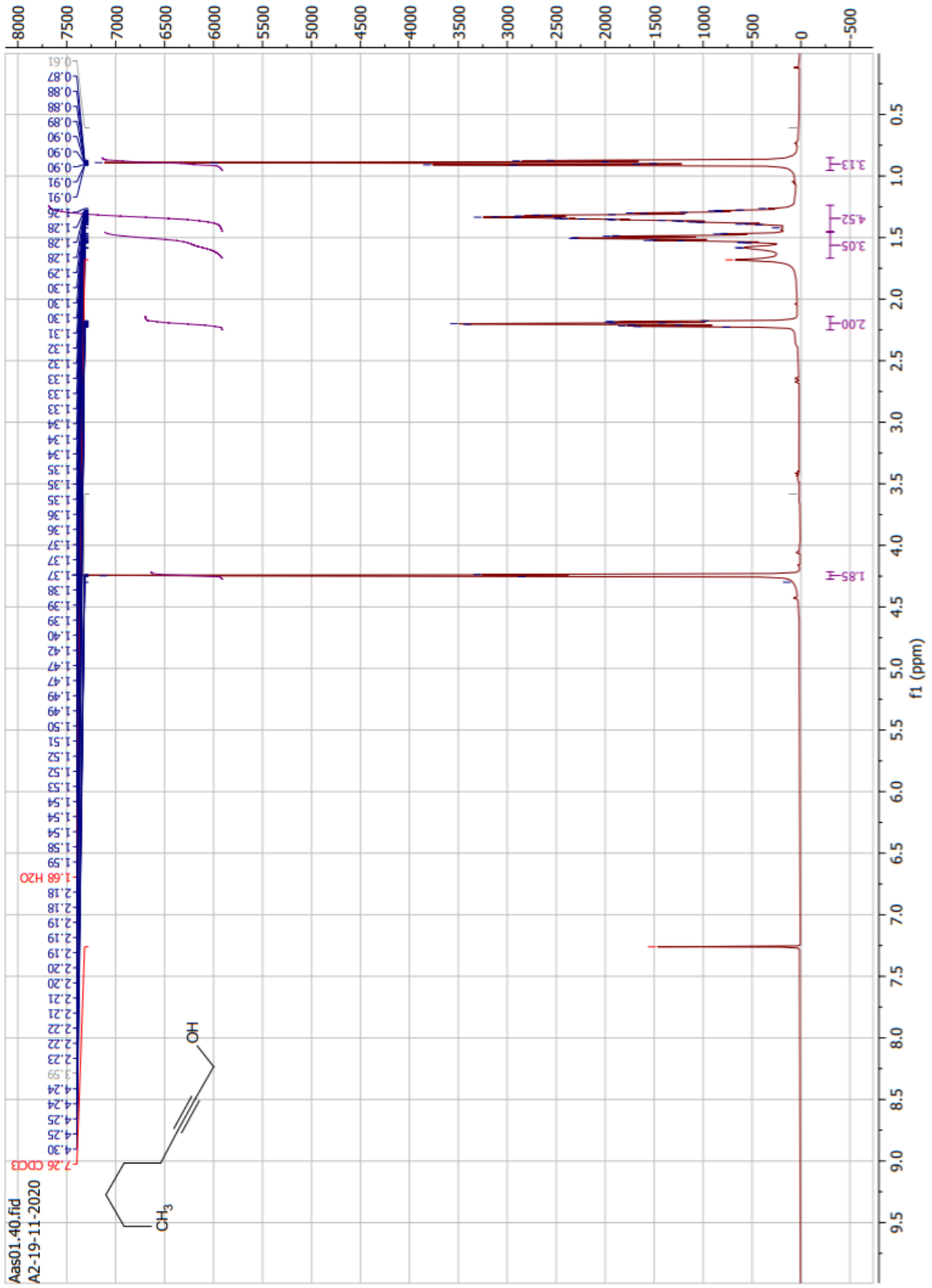

Figure A.1: *^{1}H NMR (400MHz, $CDCl_3$) spectrum of 2-octyn-1-ol (**71**)*

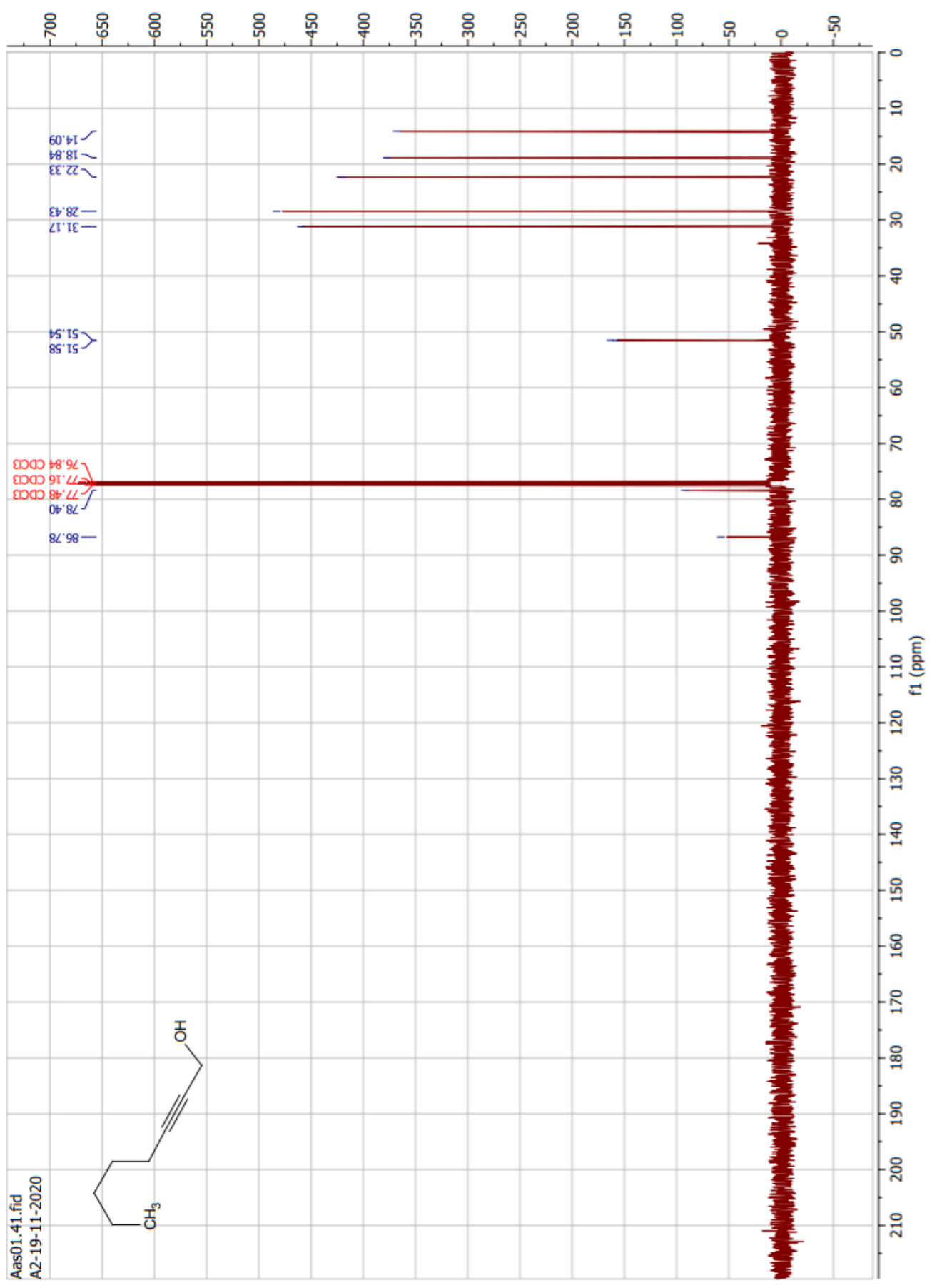

Figure A.2: *^{13}C NMR (100MHz, $CDCl_3$) spectrum of 2-octyn-1-ol (**71**)*

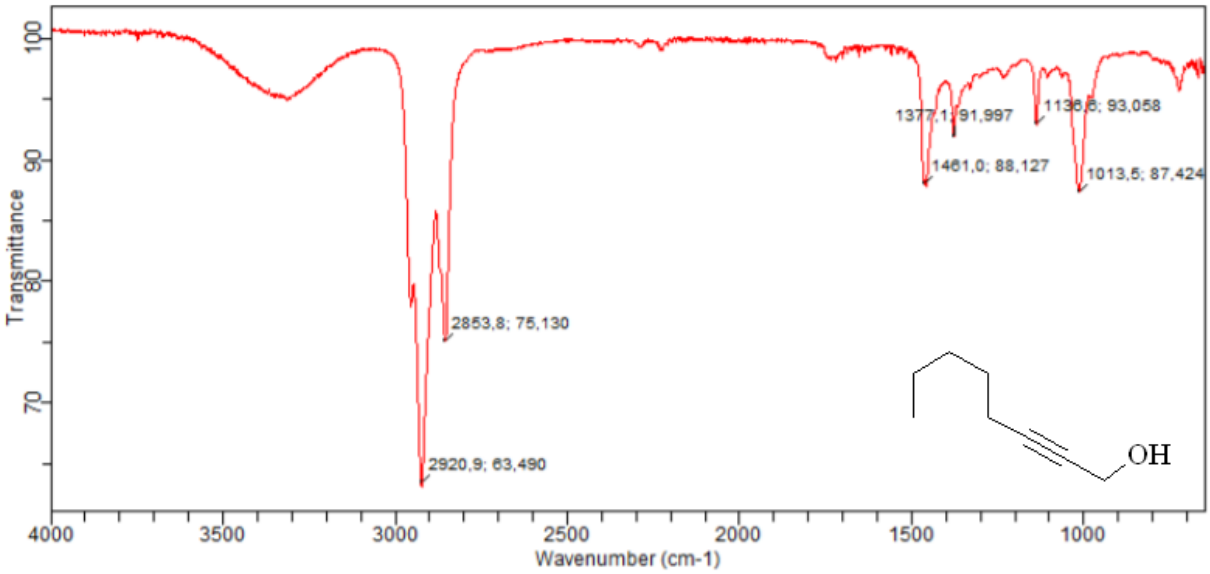

Figure A.3: *IR spectrum of 2-octyn-1-ol (**71**)*

A.2. 7-OCTYN-1-OL SPECTRAL DATA (**92**)

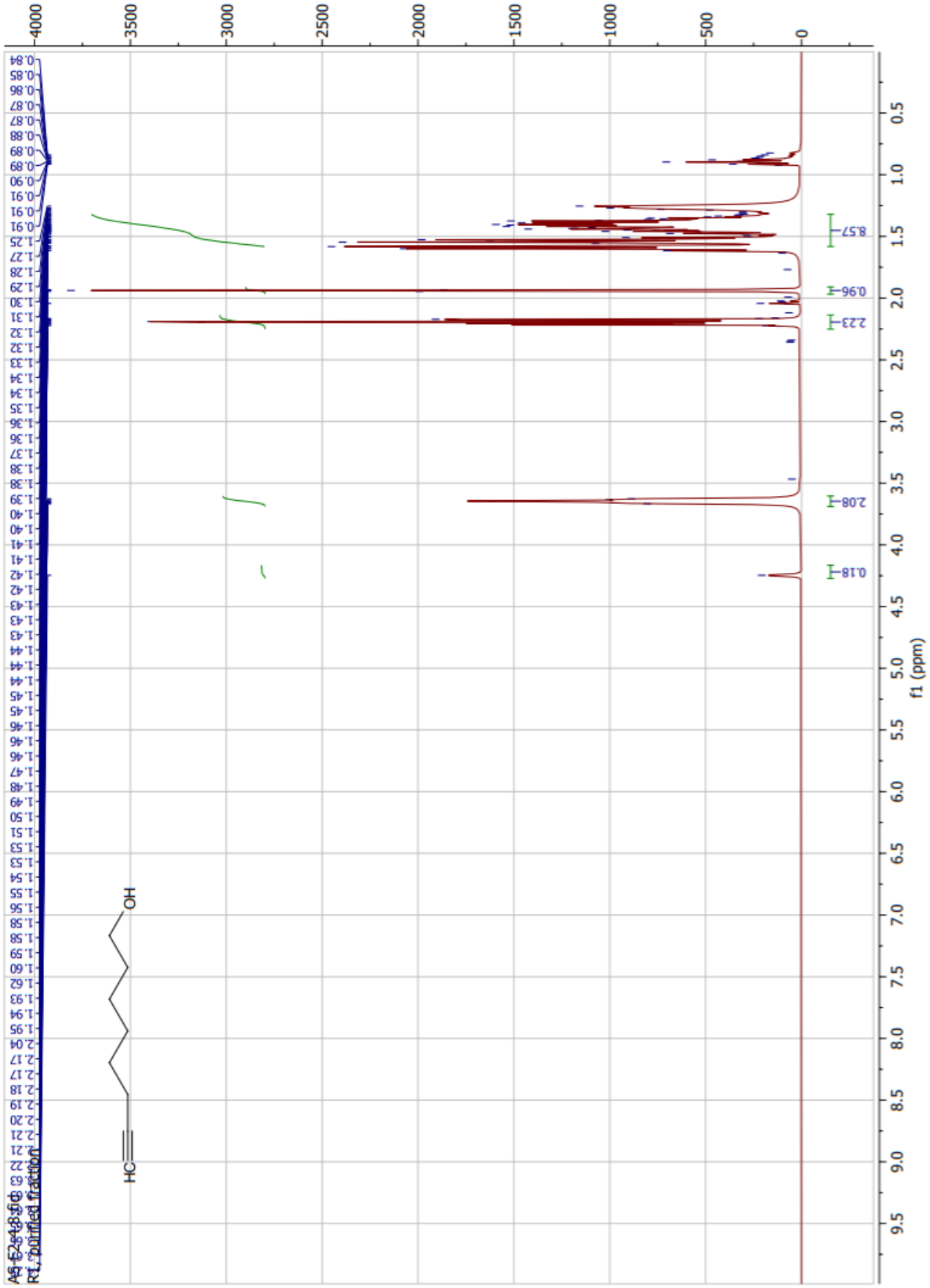

Figure A.4: *^{1}H NMR (400MHz, $CDCl_3$) spectrum of 7-octyn-1-ol (**92**)*

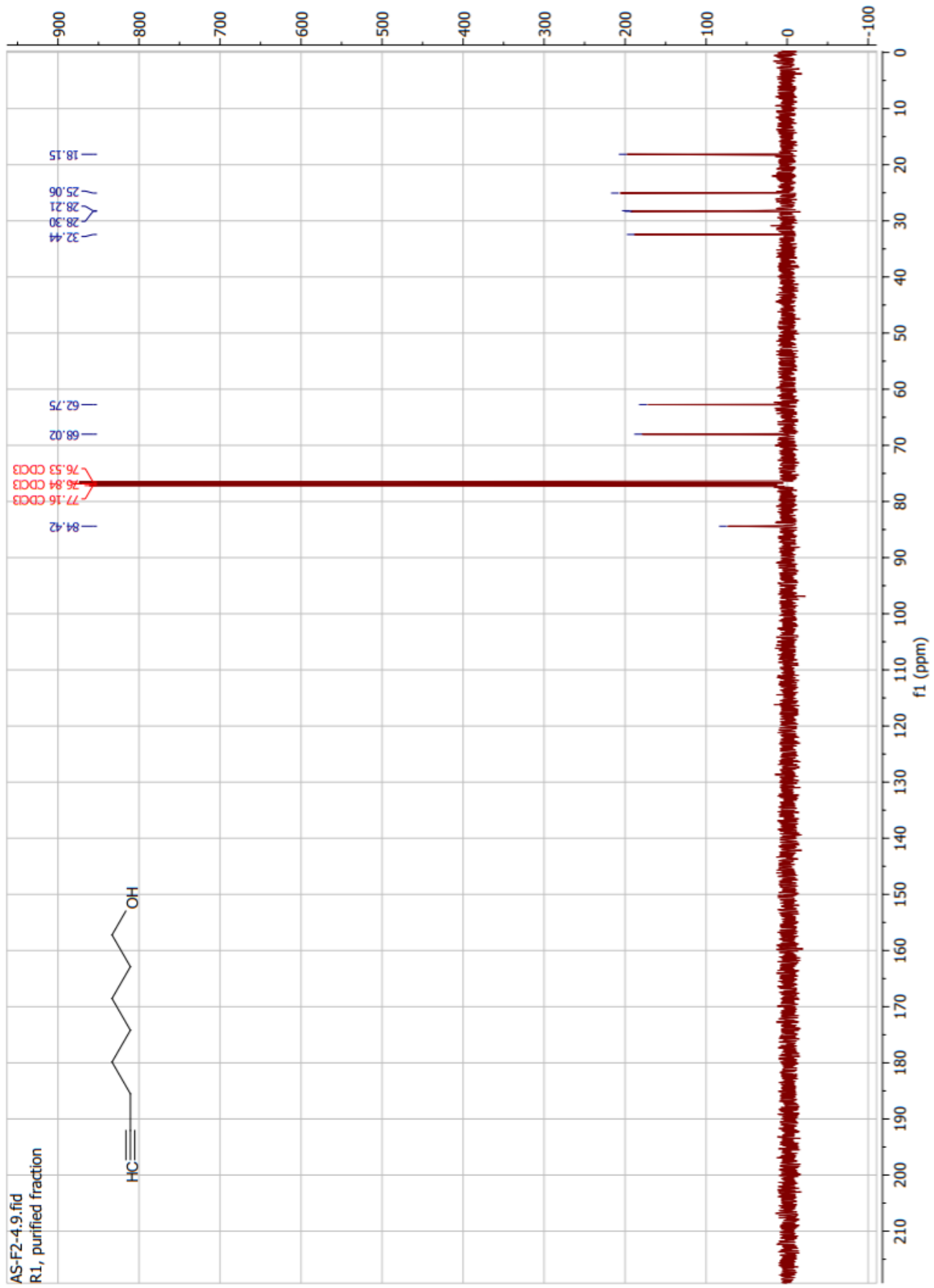

Figure A.5: *^{13}C NMR (100MHz, $CDCl_3$) spectrum of 7-octyn-1-ol (**92**).*

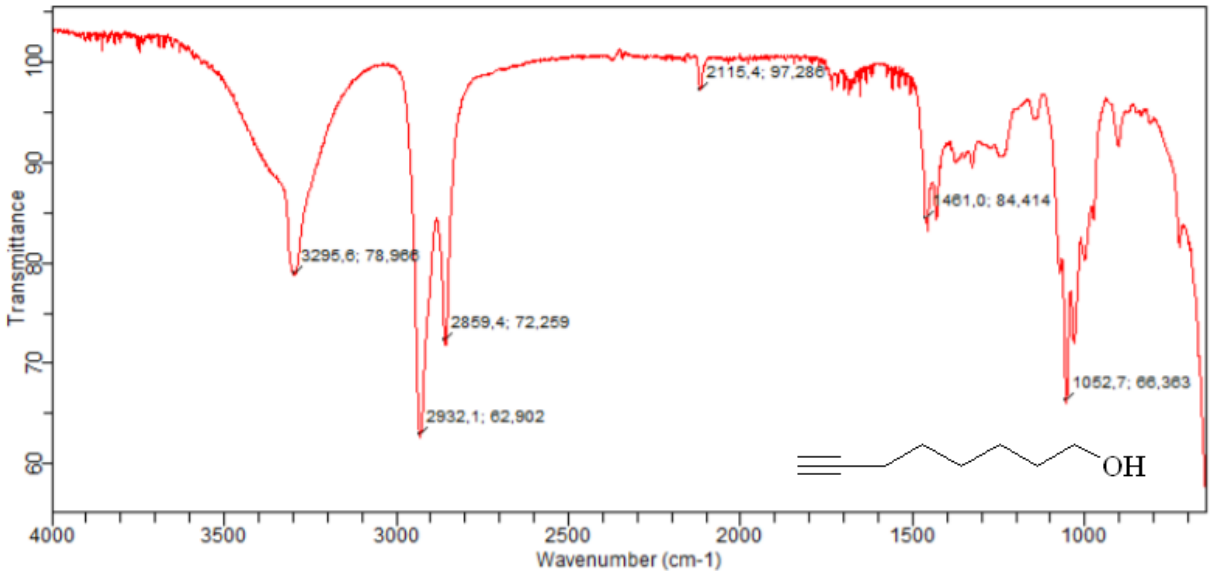

Figure A.7.: *IR spectrum of 7-octyn-1-ol (**92**)*

A.3. 7-OCTYNOIC ACID SPECTRAL DATA (**93**)

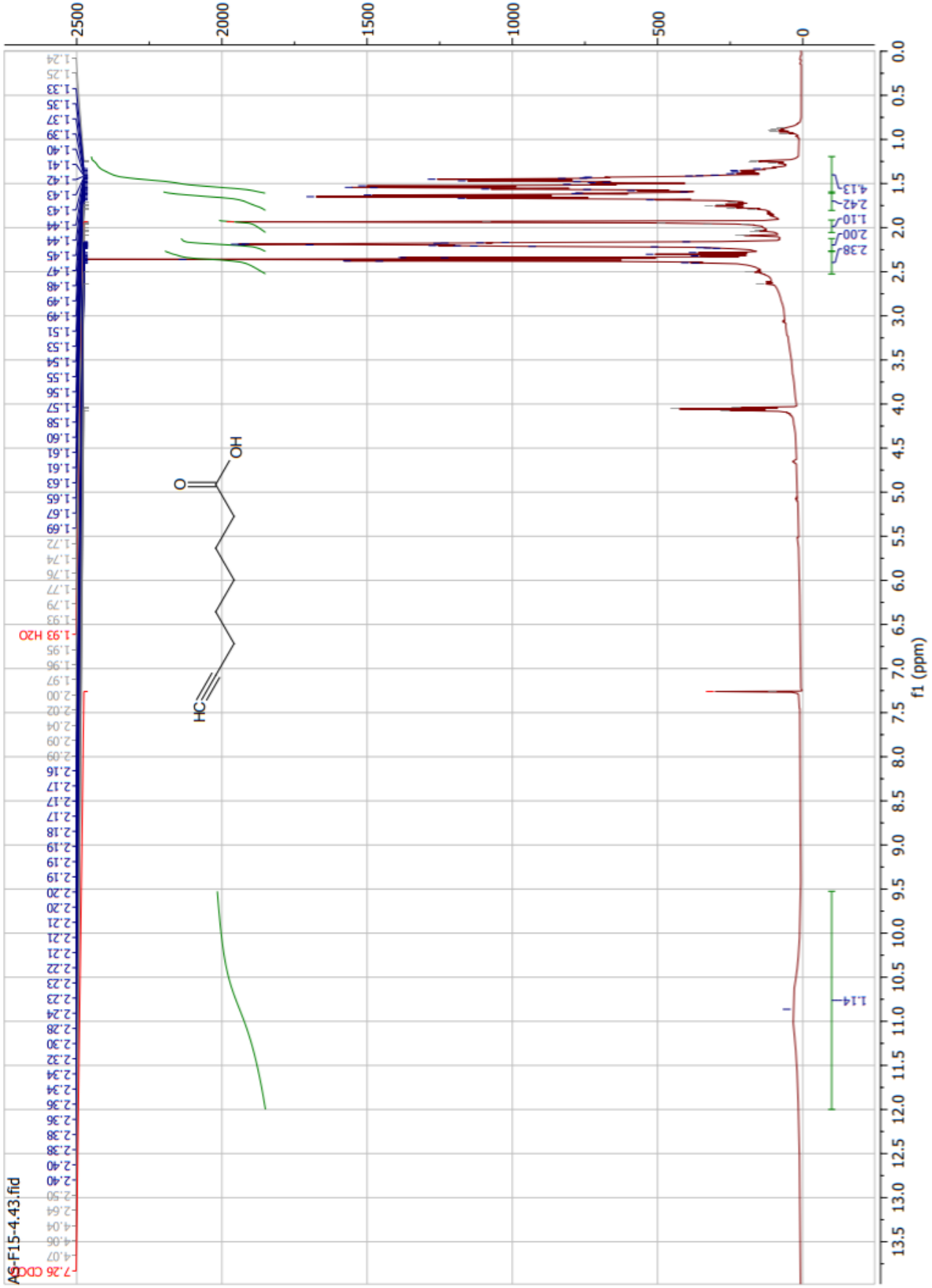

Figure A.8: *^{1}H NMR (400MHz, $CDCl_3$) spectrum of 7-octynoic acid (**93**)*

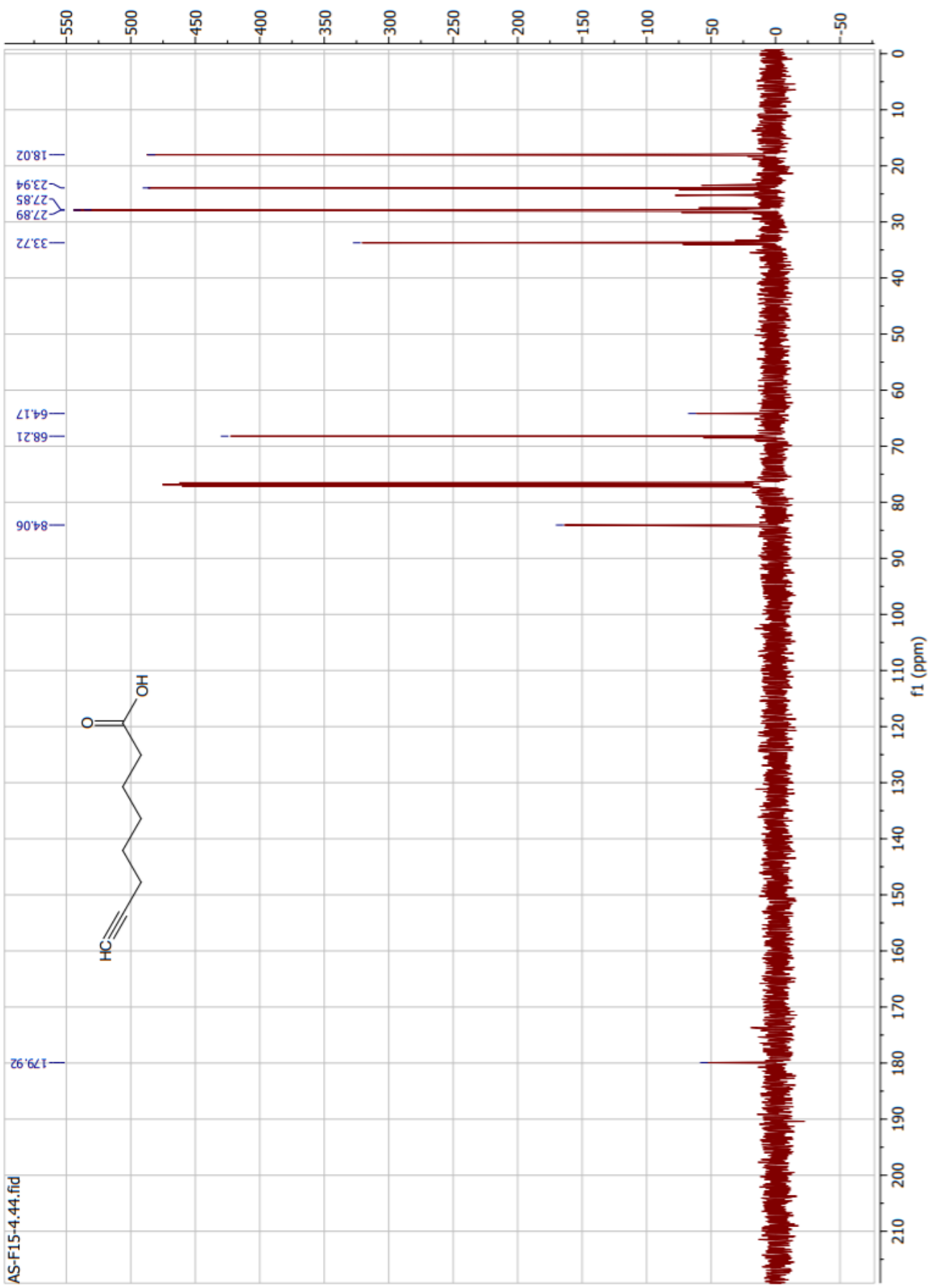

Figure A.9: *^{13}C NMR (100MHz, $CGCl_3$) spectrum of 7-octynoic acid (**93**)*

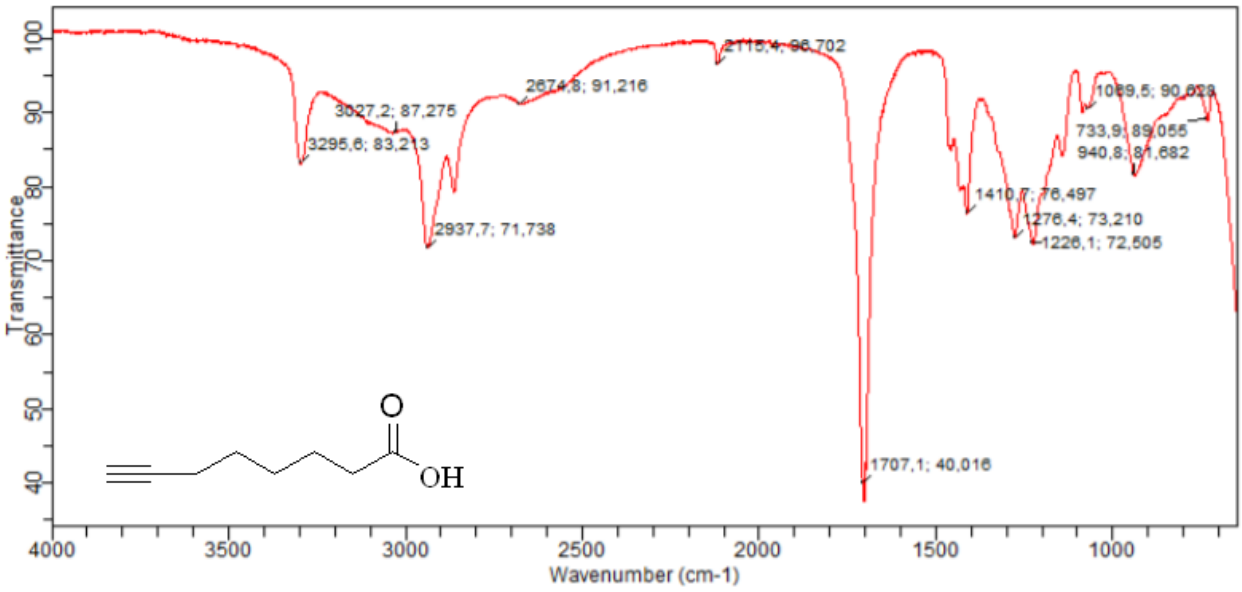

Figure A.10: *IR spectrum of 7-octynoic acid (**93**)*

A.4. METHYL 7-OCTYNOATE (**69**) SPECTRAL DATA

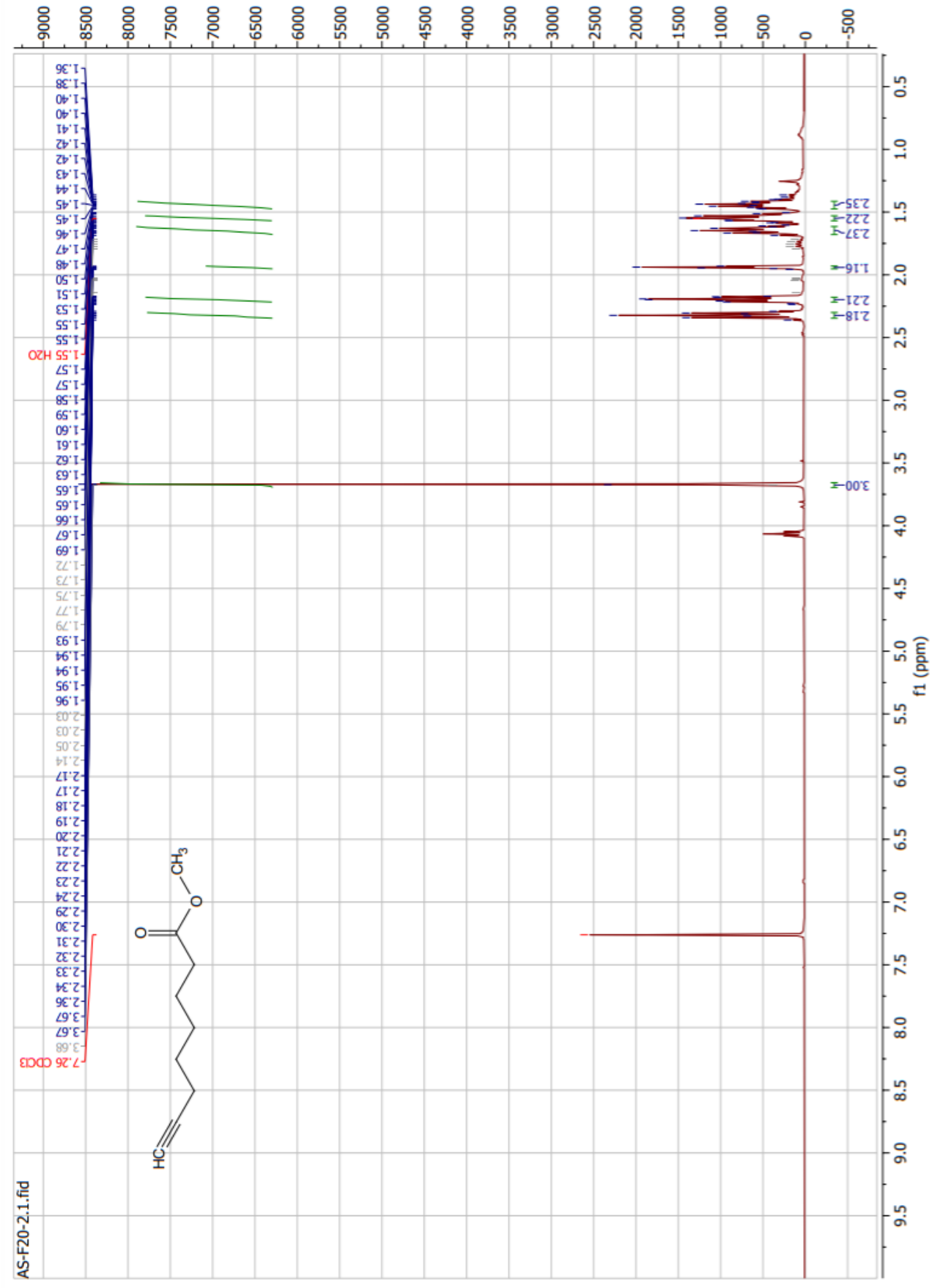

Figure A.11: *^{1}H NMR (400MHz, $CDCl_3$) spectrum of methyl 7-octynoate (**69**)*

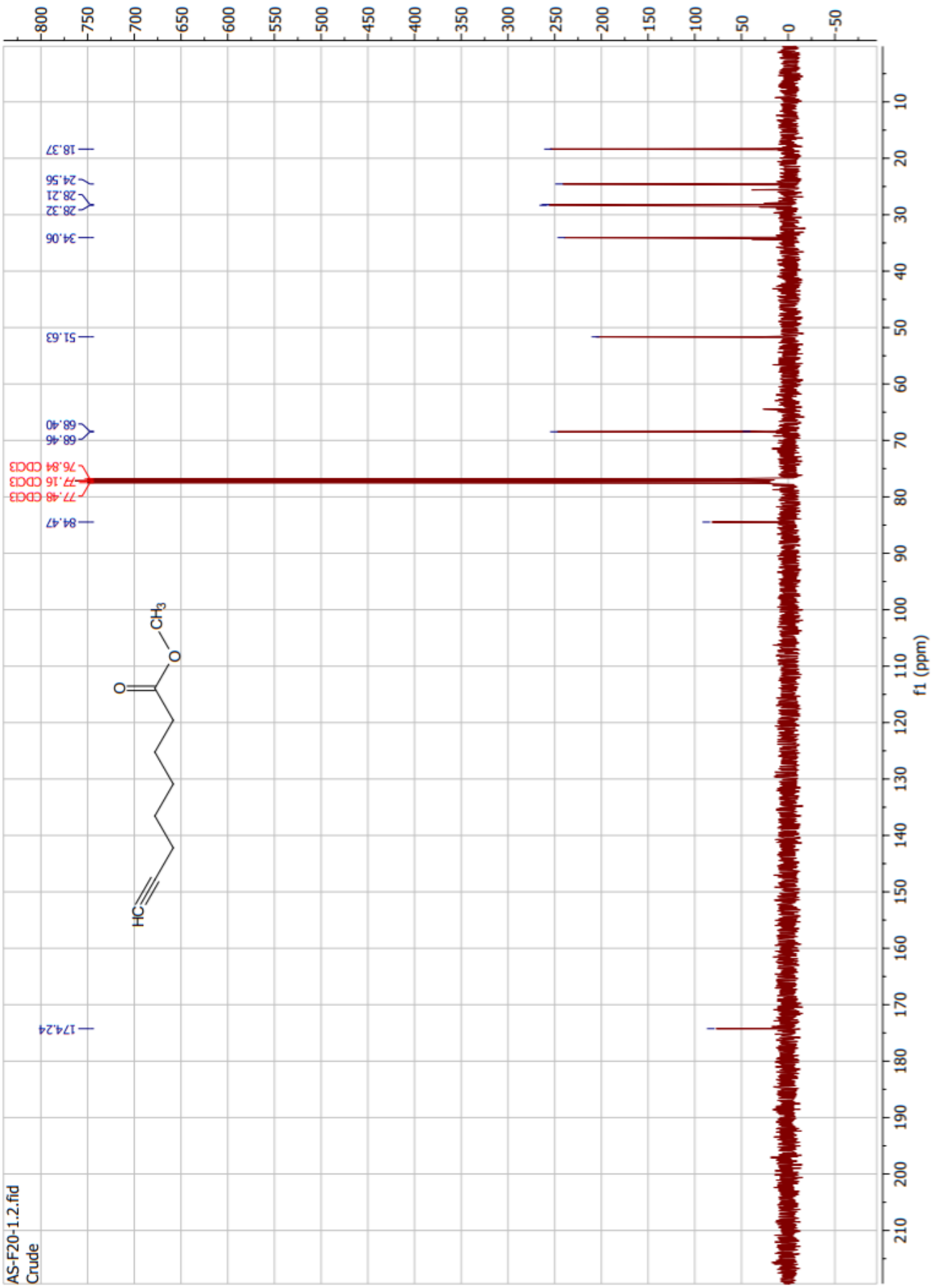

Figure A.12: *^{13}C NMR (100MHz, $CDCl_3$) spectrum of methyl 7-octynoate (**69**)*

A.5. METHYL 6-BROMOHEXANOATE SPECTRAL DATA

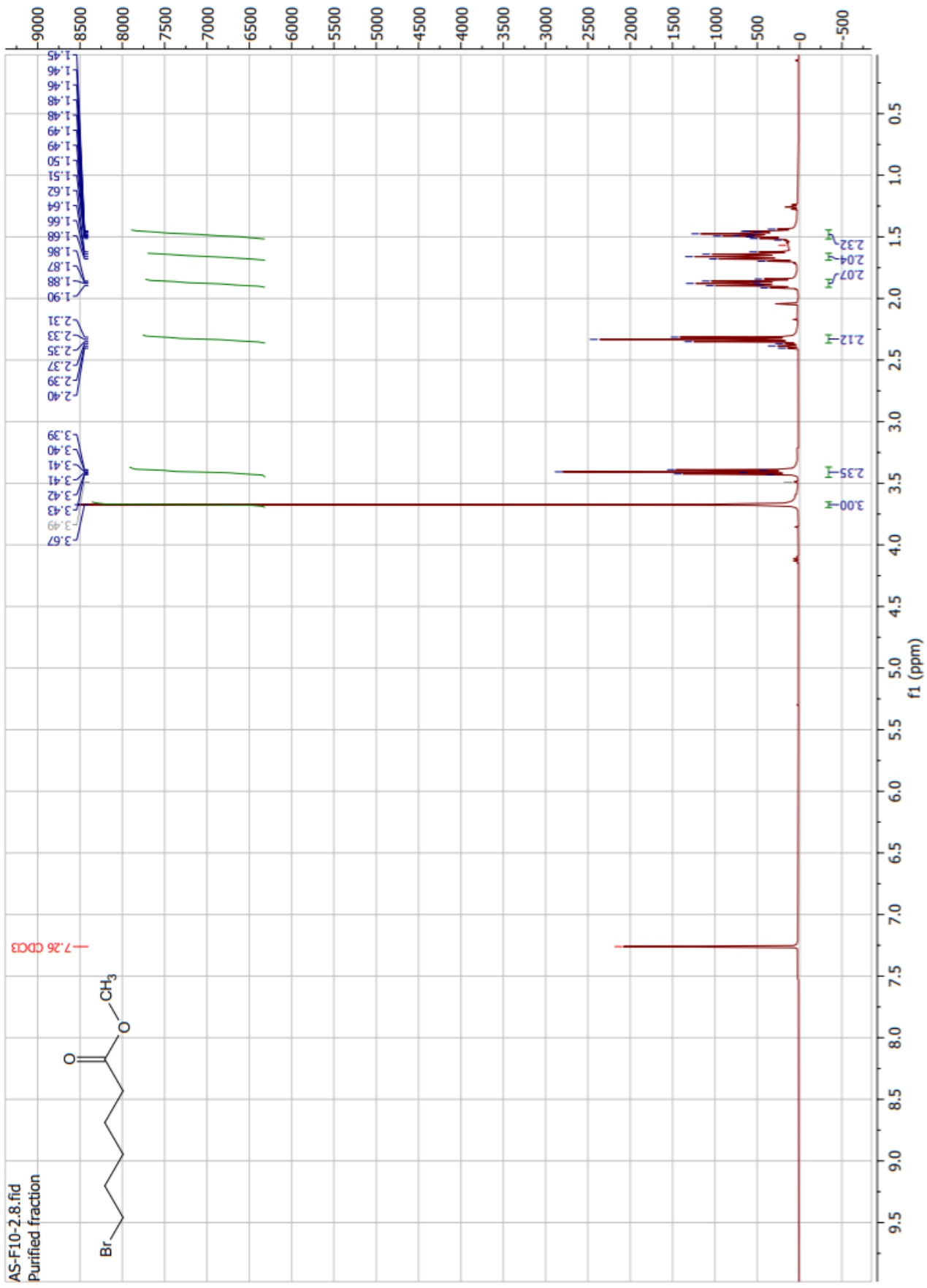

Figure A.13: *^{1}H NMR (400MHz, $CDCl_3$) spectrum of methyl 6-bromohexanoate (**95**)*

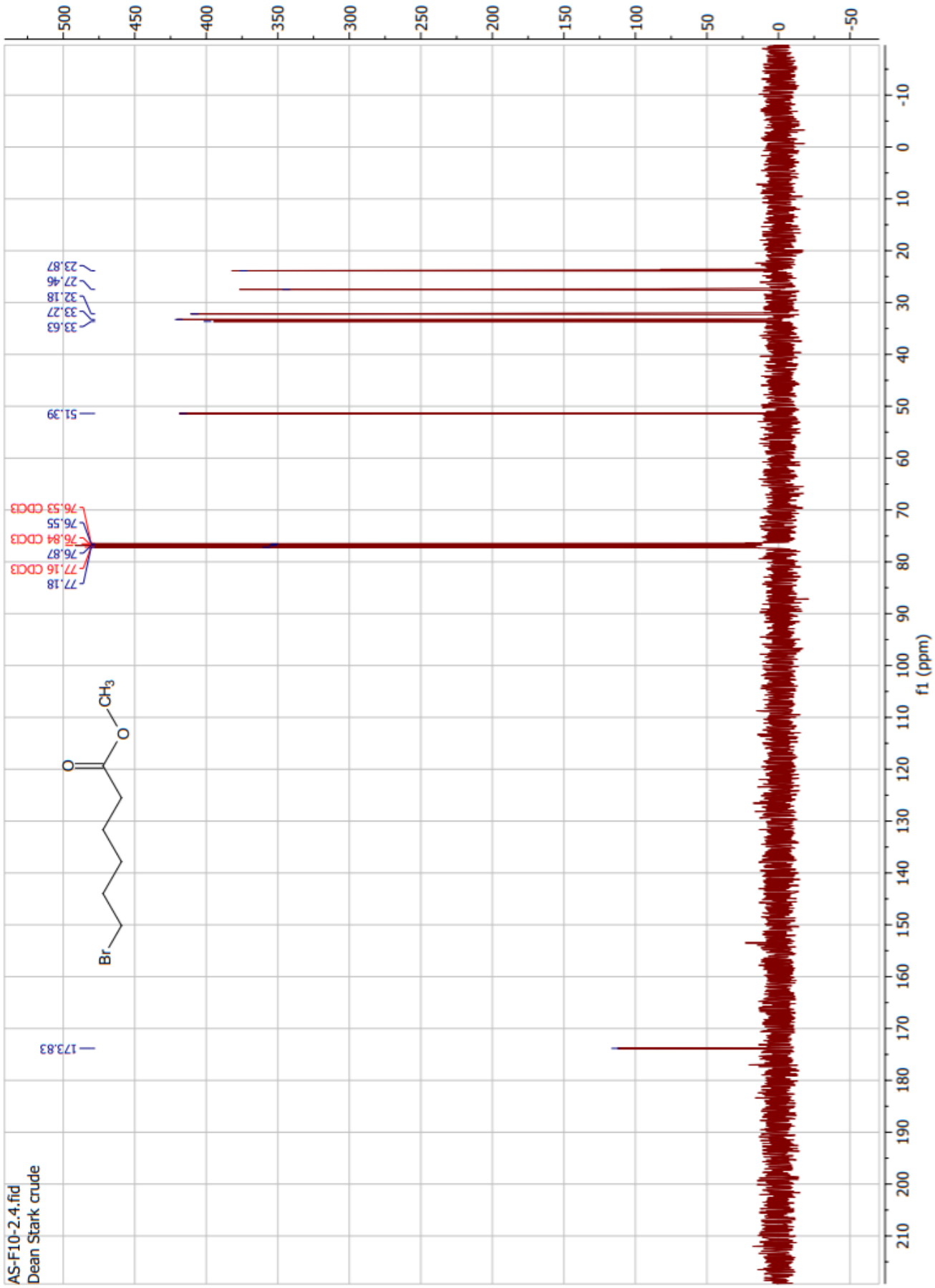

Figure A.14: *^{13}C NMR (100MHz, $CDCl_3$) spectrum of methyl 6-bromohexanoate (**95**)*

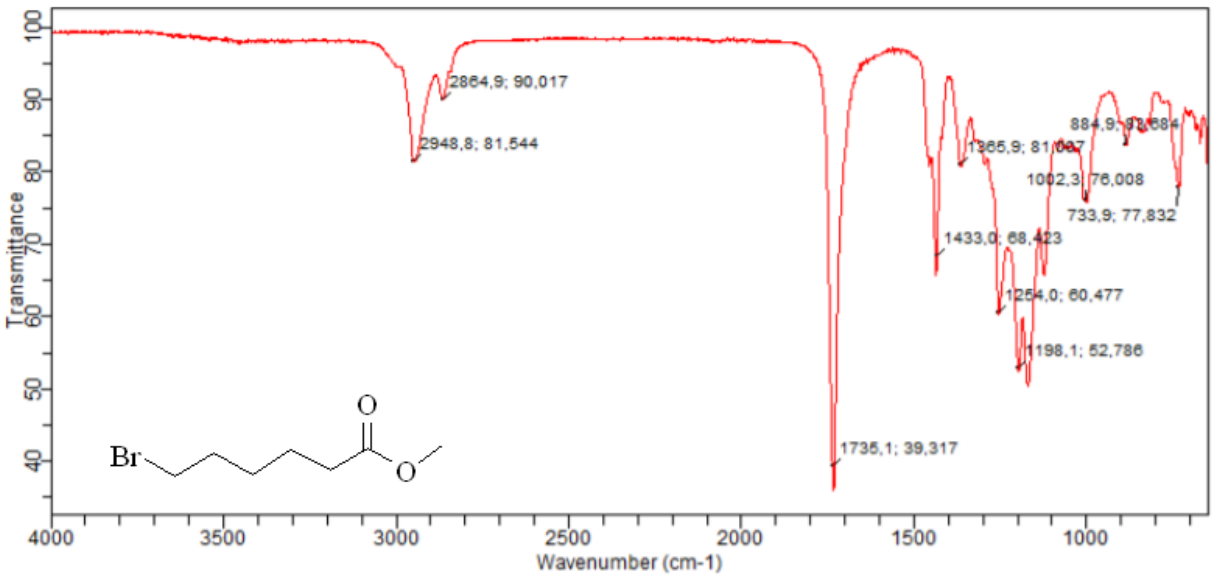

Figure A.15: *IR spectrum of methyl 6-bromohexanoate (95)*

A.6. METHYL 8-BROMOOCTANOATE (**101A**) SPECTRAL DATA

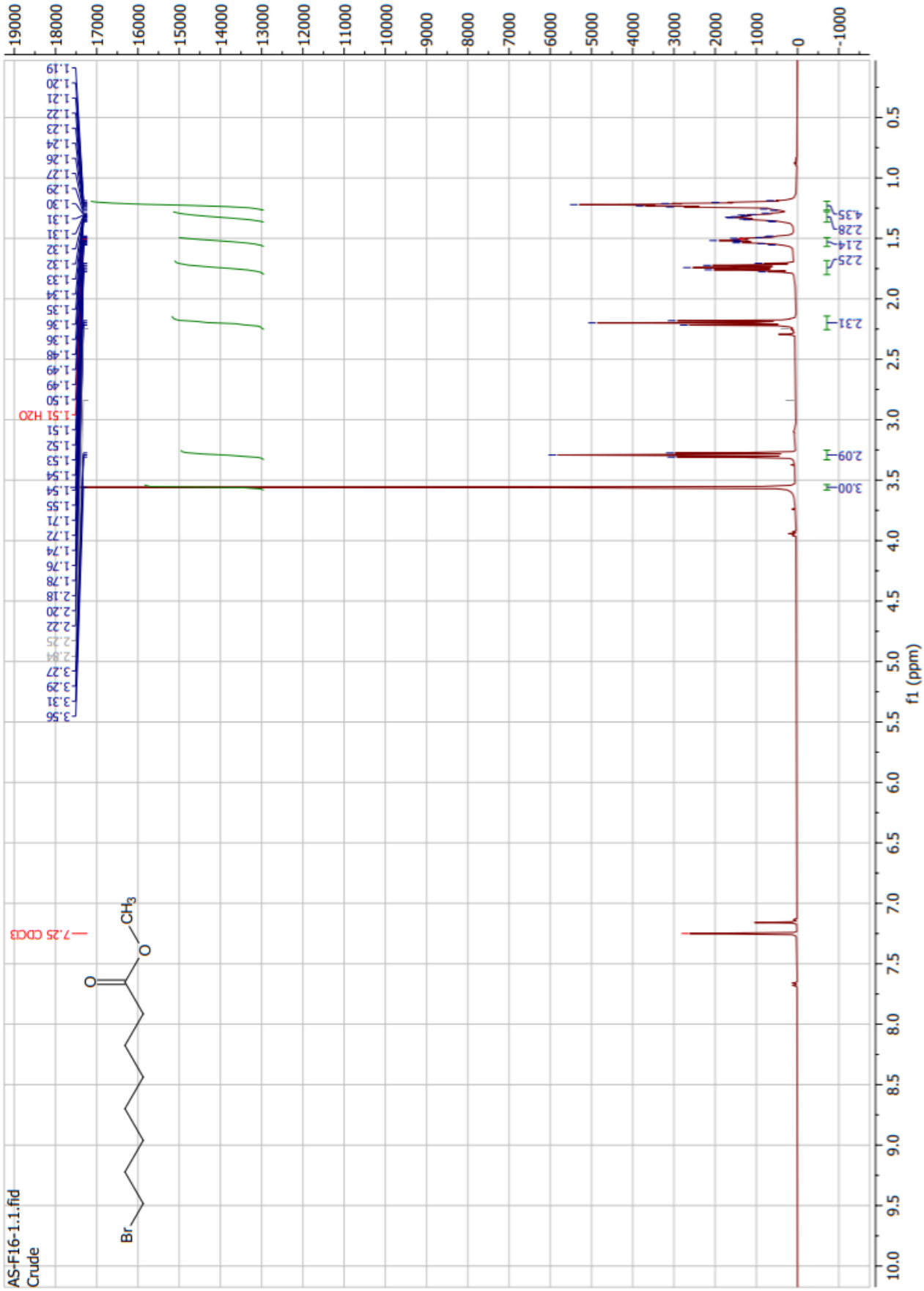

Figure A.16: *^{1}H NMR (400MHz, $CDCl_3$) spectrum of methyl 8-bromooctanoate (**101a**)*

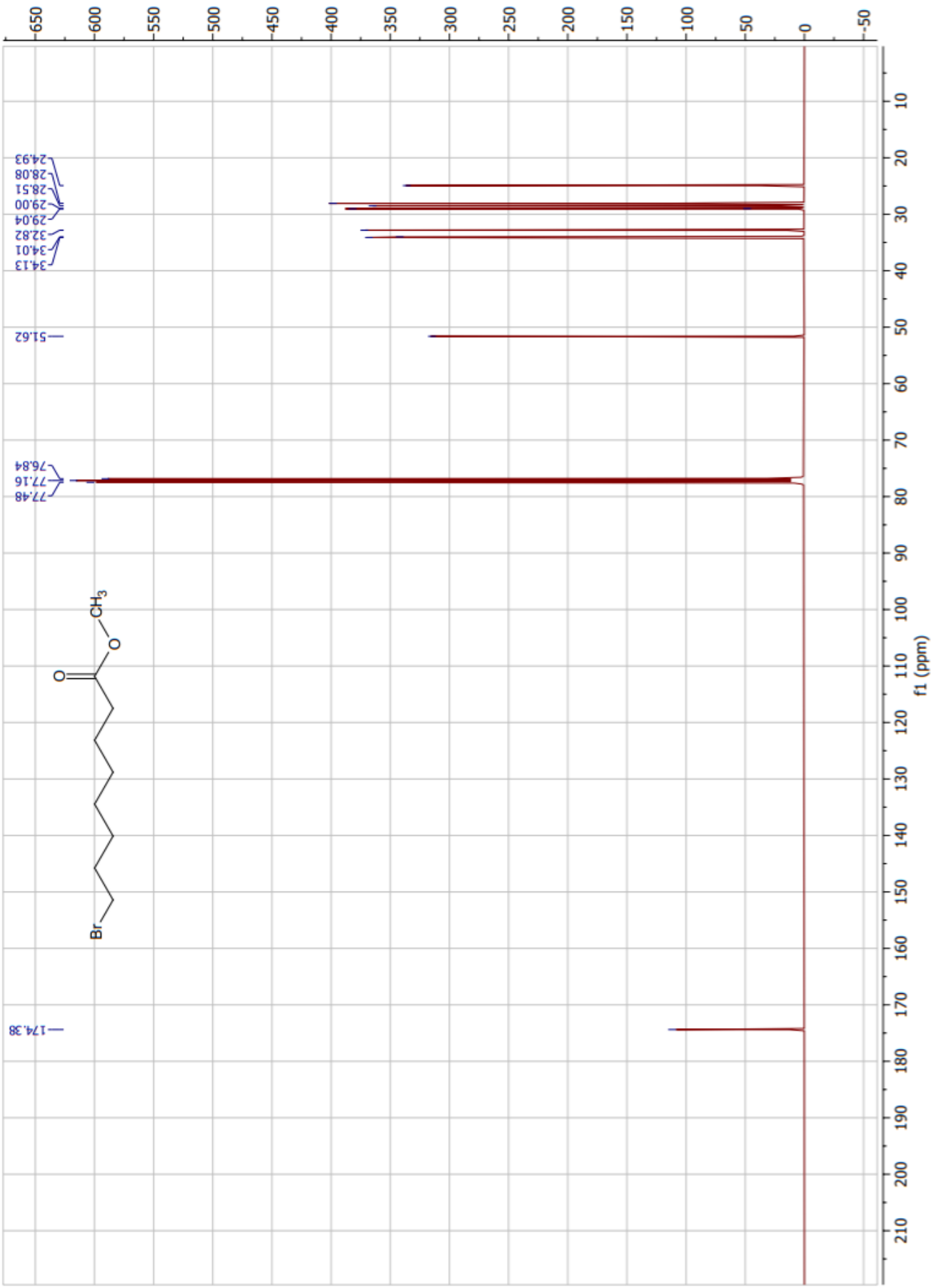

Figure A.17: *^{13}C NMR (100MHz, $CDCl_3$) spectrum of methyl 8-bromooctanoate (**101a**).*

A.7. ETHYL 6-IODOHEXANOATE SPECTRAL DATA

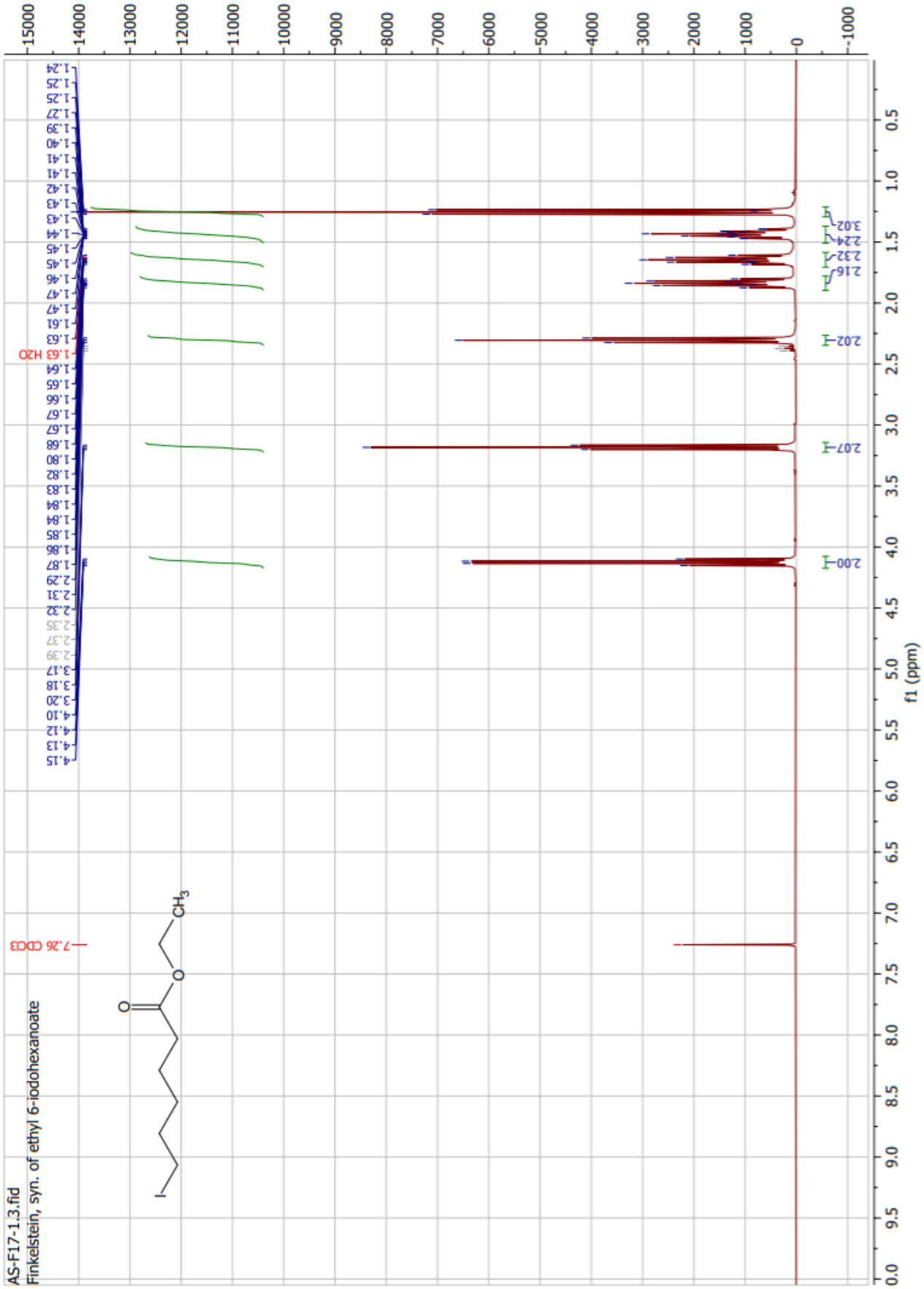

Figure A.18: *^{1}H NMR (400MHz, $CDCl_3$) spectrum of ethyl 6-bromohexanoate*

Figure A.19: *^{13}C NMR (100MHz, $CDCl_3$) spectrum of ethyl 6-iodohexanoate*

A.8. METHYL 8-IODOOCTANOATE (**101B**) SPECTRAL DATA

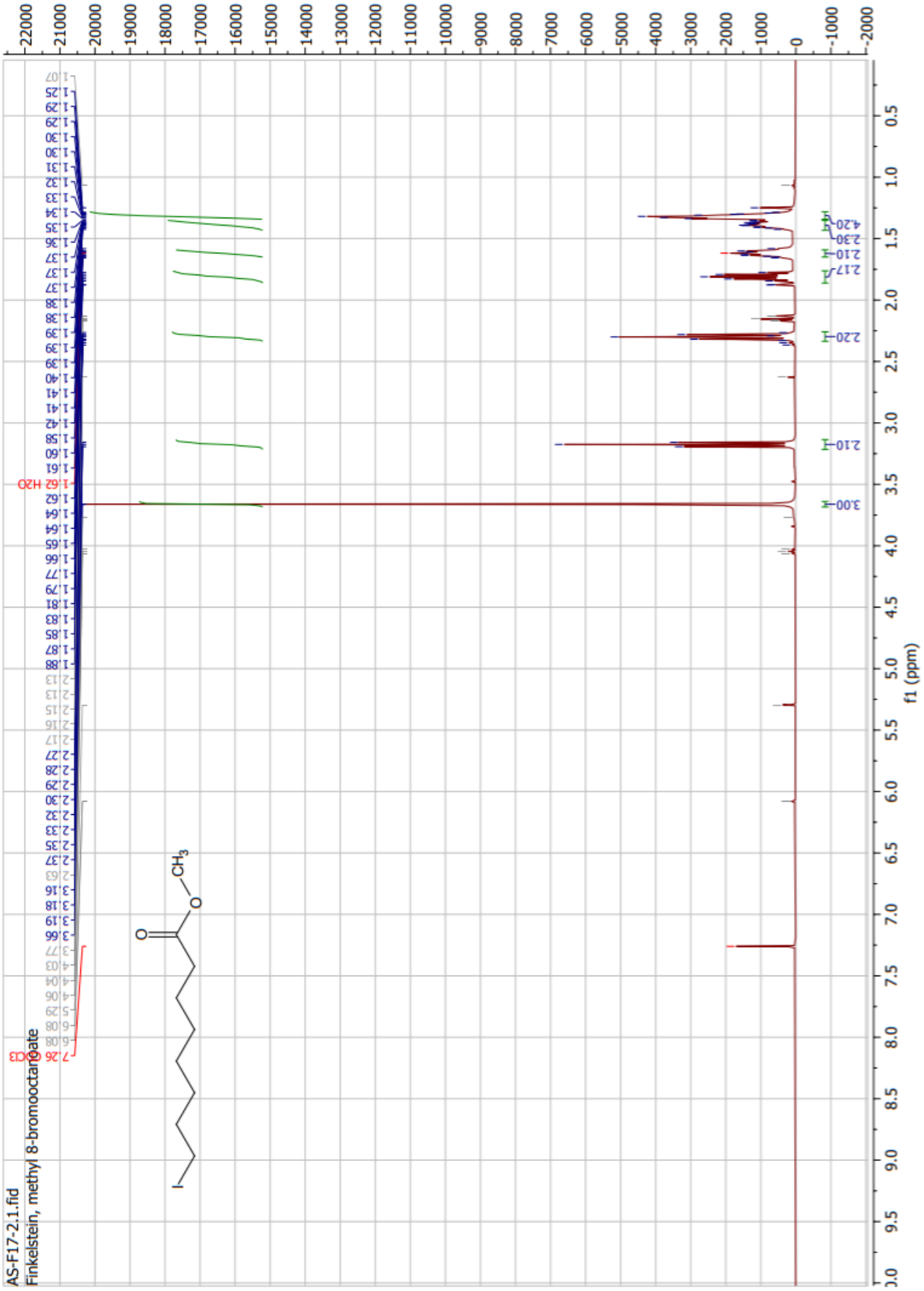

Figure A.20: *^{1}H NMR (400MHz, $CDCl_3$) spectrum of methyl 8-iodooctanoate (**101b**)*

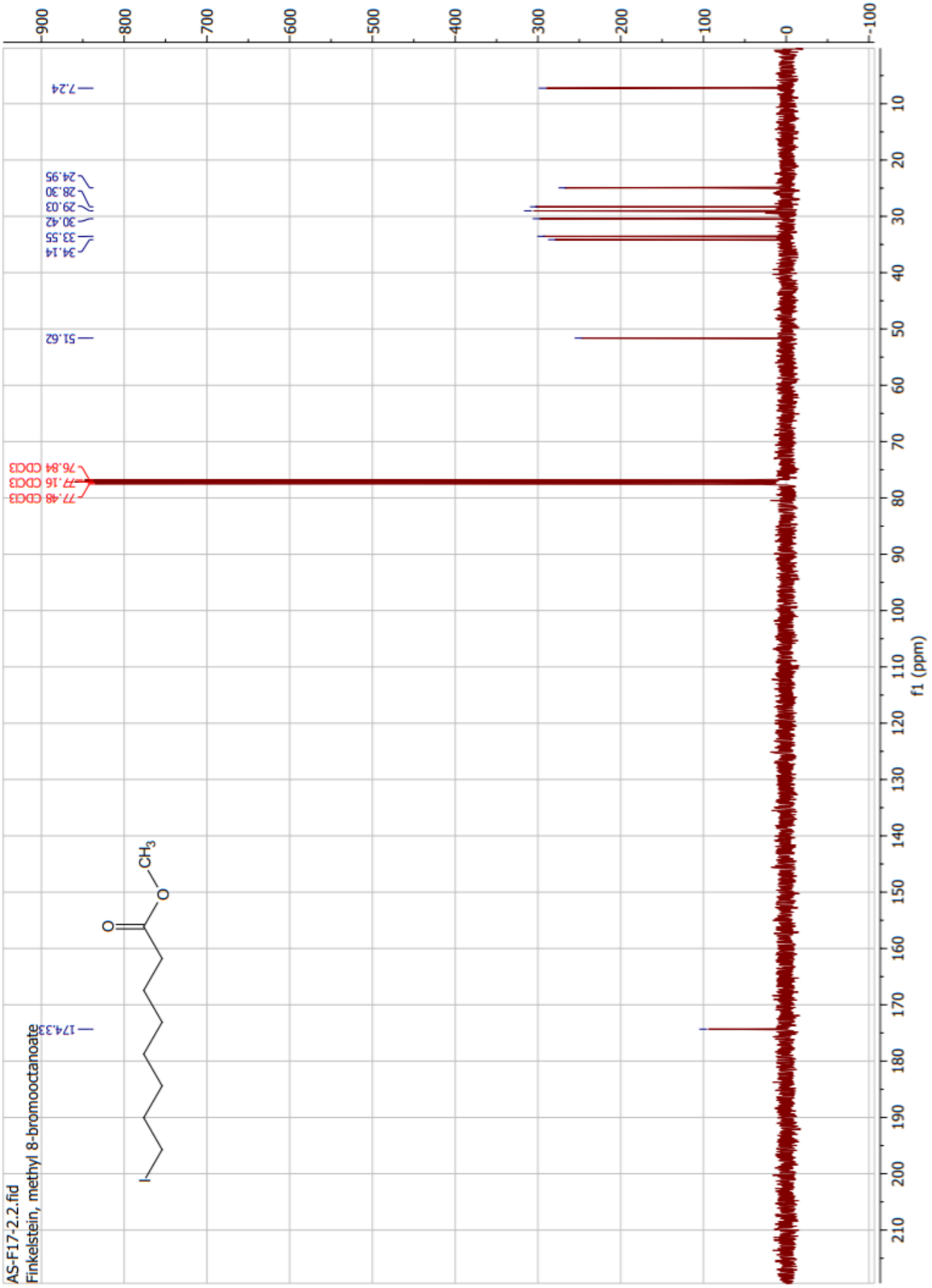

Figure A.21: *^{13}C NMR (100MHz, $CDCl_3$) spectrum of methyl 8-iodohexanoate (**101b**)*

A.9. ETHYL (*E*)-7-HYDROXYHEPT-2-ENOATE (**82**) SPECTRAL DATA

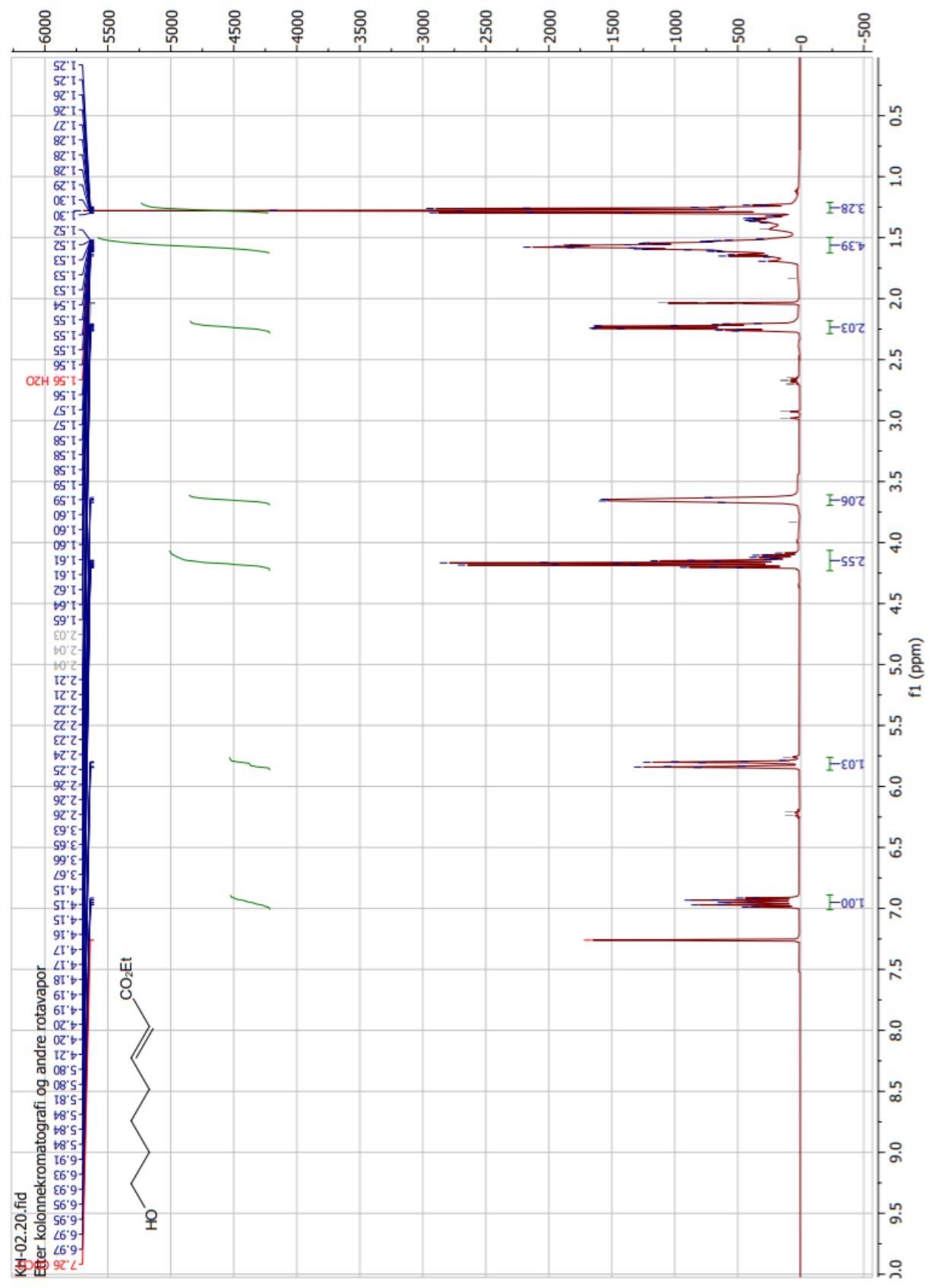

Figure A.22.: *^{1}H NMR (400MHz, $CDCl_3$) spectrum of ethyl (E)-7-hydroxyhept-2-enoate (**82**)*

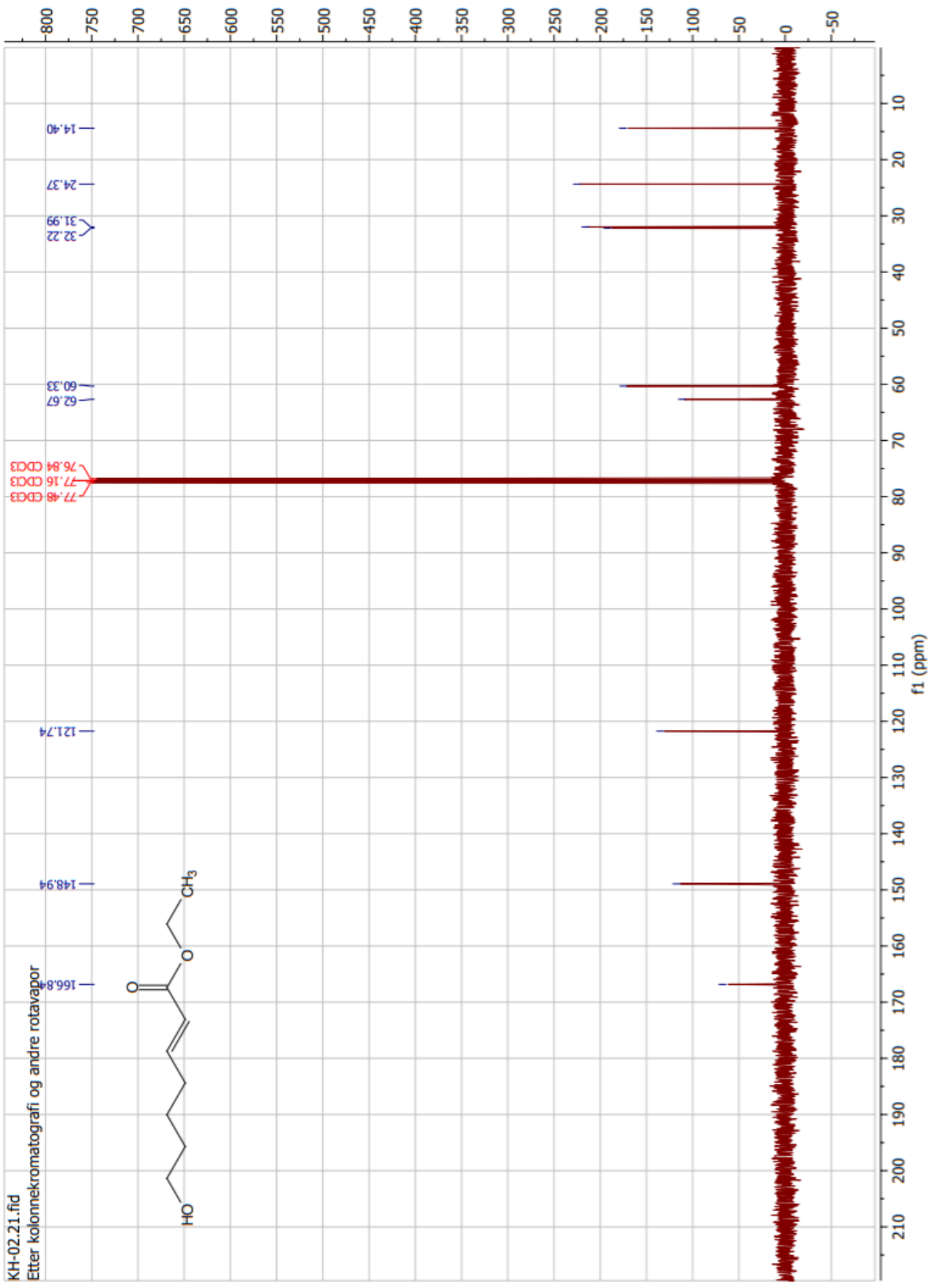

Figure A.23.: *^{13}C NMR (100MHz, $CDCl_3$) spectrum of ethyl (E)-7-hydroxyhept-2-enoate (**82**).*

A.10. ETHYL *(E)*-IODOHEPT-2-ENOATE (**107**) SPECTRAL DATA

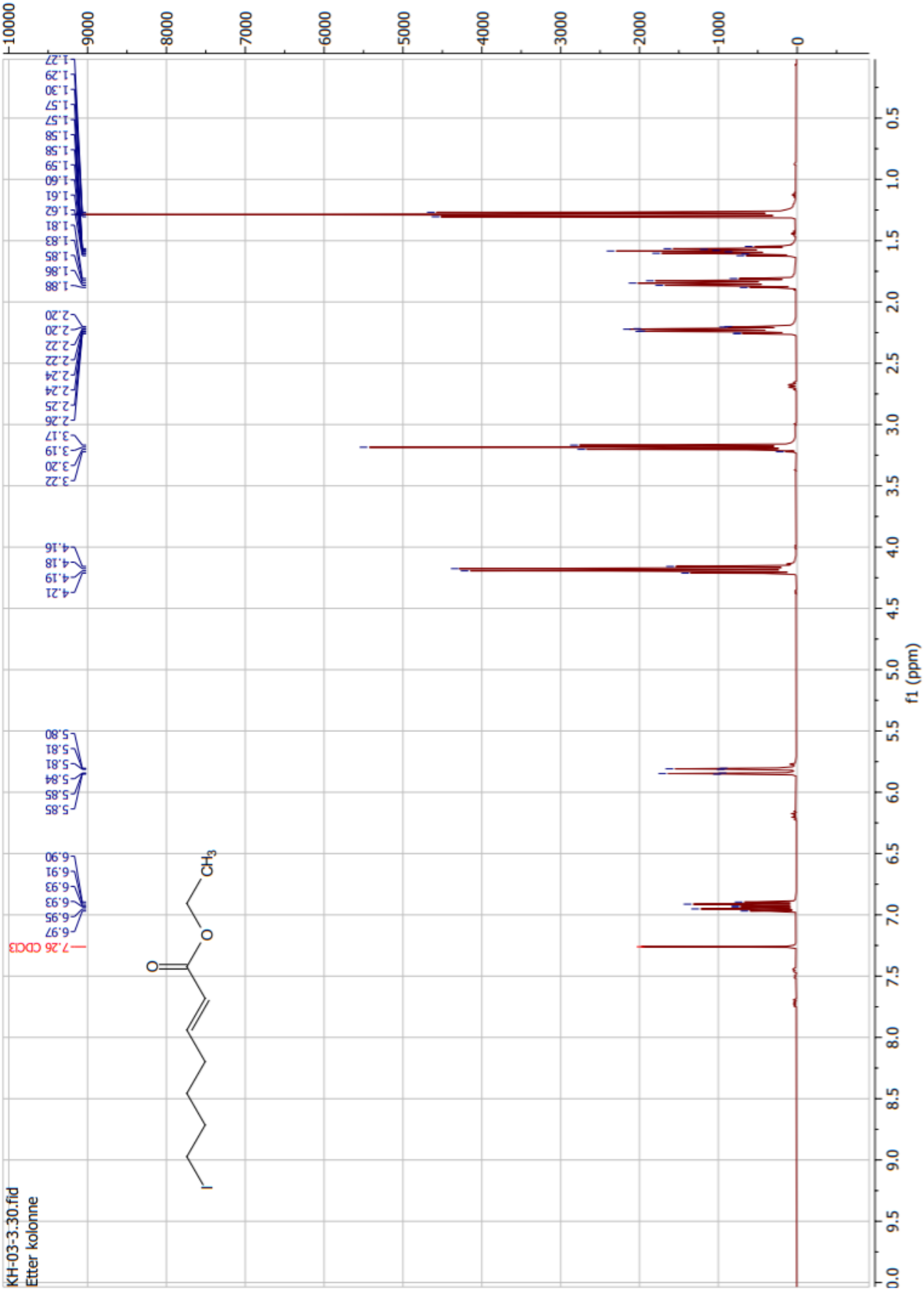

Figure A.24: *^{1}H NMR (400MHz, $CDCl_3$) spectrum of ethyl (E)-iodohept-2-enoate (**107**)*

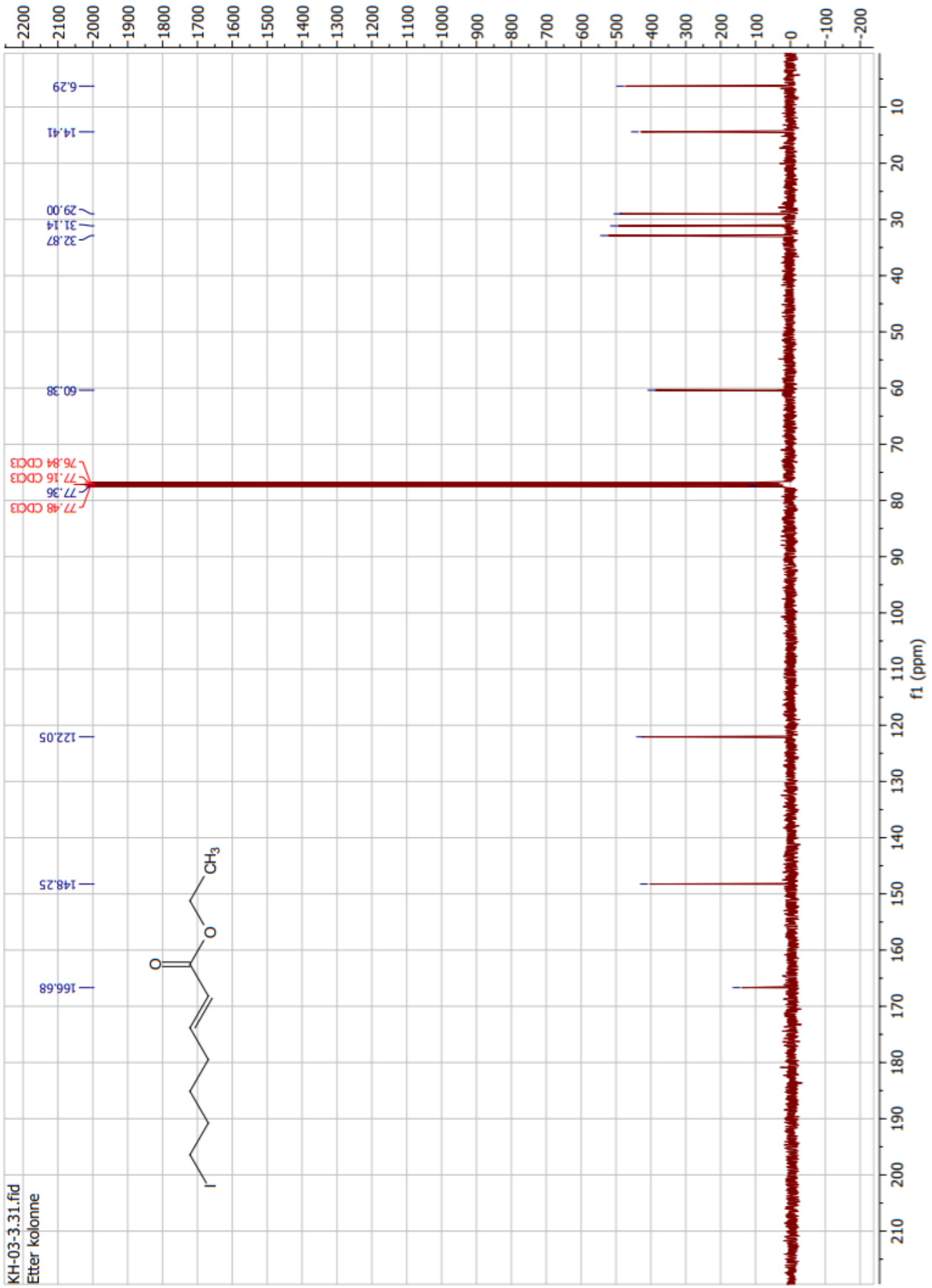

Figure A.25: *^{13}C NMR (100MHz, $CDCl_3$) spectrum of ethyl (E)-iodohept-2-enoate (**107**)*

A.11. Ethyl (E)-7-(triphenyl-5-phosphaneylidene)hept-2-enoate (**82**) Spectral Data

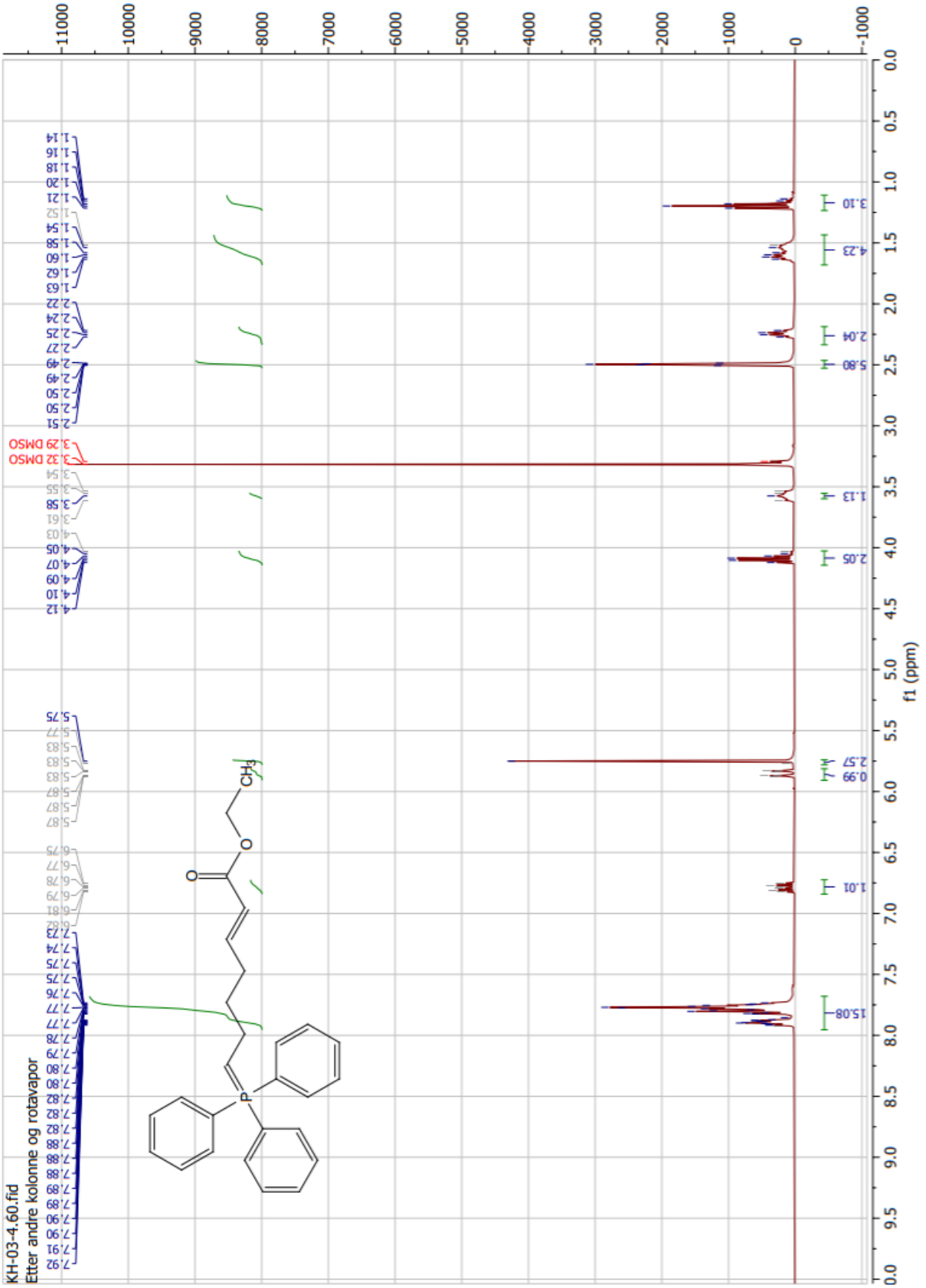

Figure A.26: *^{1}H NMR (400MHz, DMSO-d_5) spectrum of ethyl (E)-7-(triphenyl-λ5-phosphaneylidene)hept-2-enoate (**82**)*

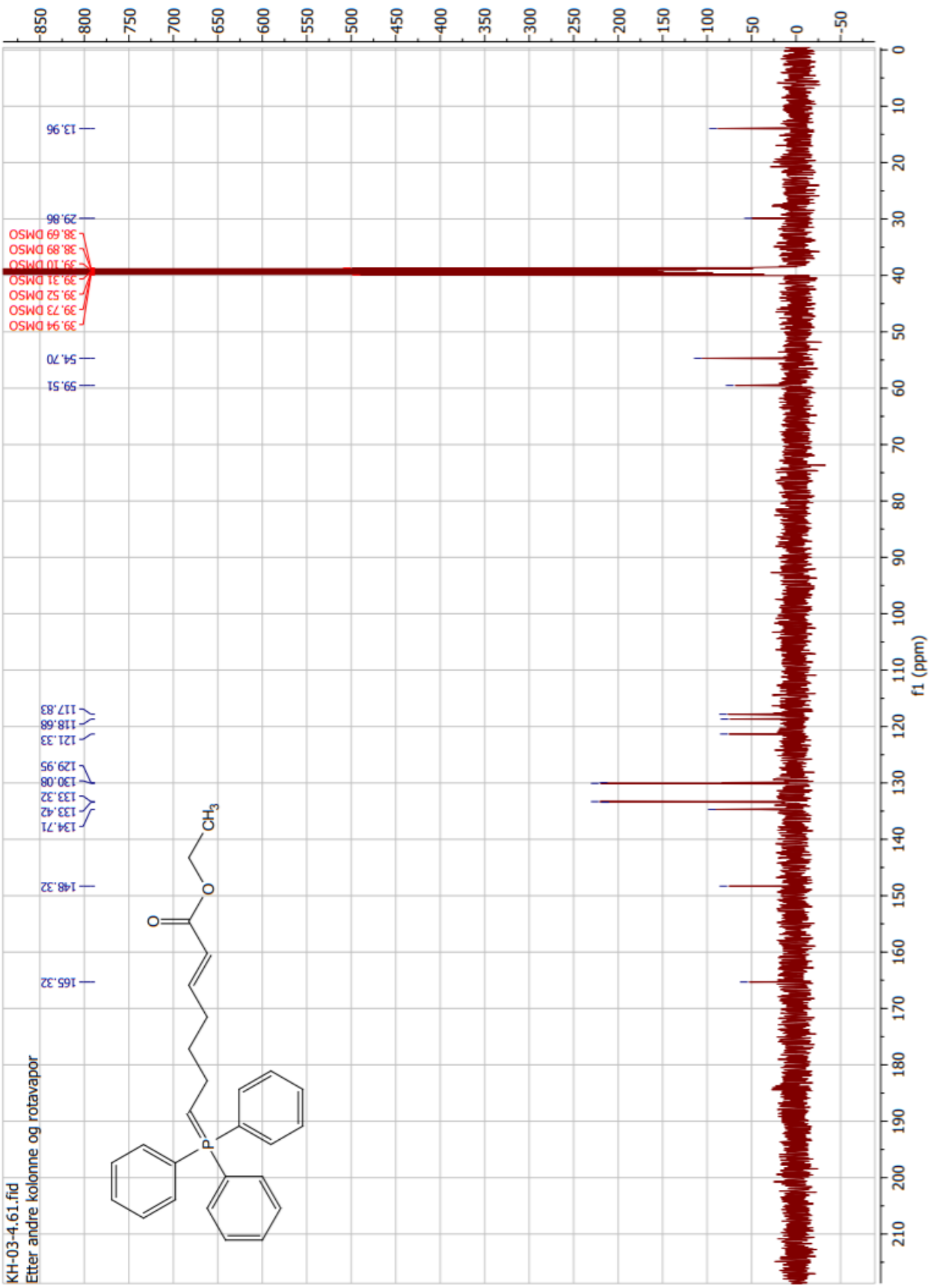

Figure A.27: *^{13}C NMR (100MHz, DMSO-d_5) spectrum of ethyl (E)-7-(triphenyl-λ5-phosphaneylidene)hept-2-enoate (**82**)*

A.12. 2-HEXYLTHIOPHENE (**70**) SPECTRAL DATA

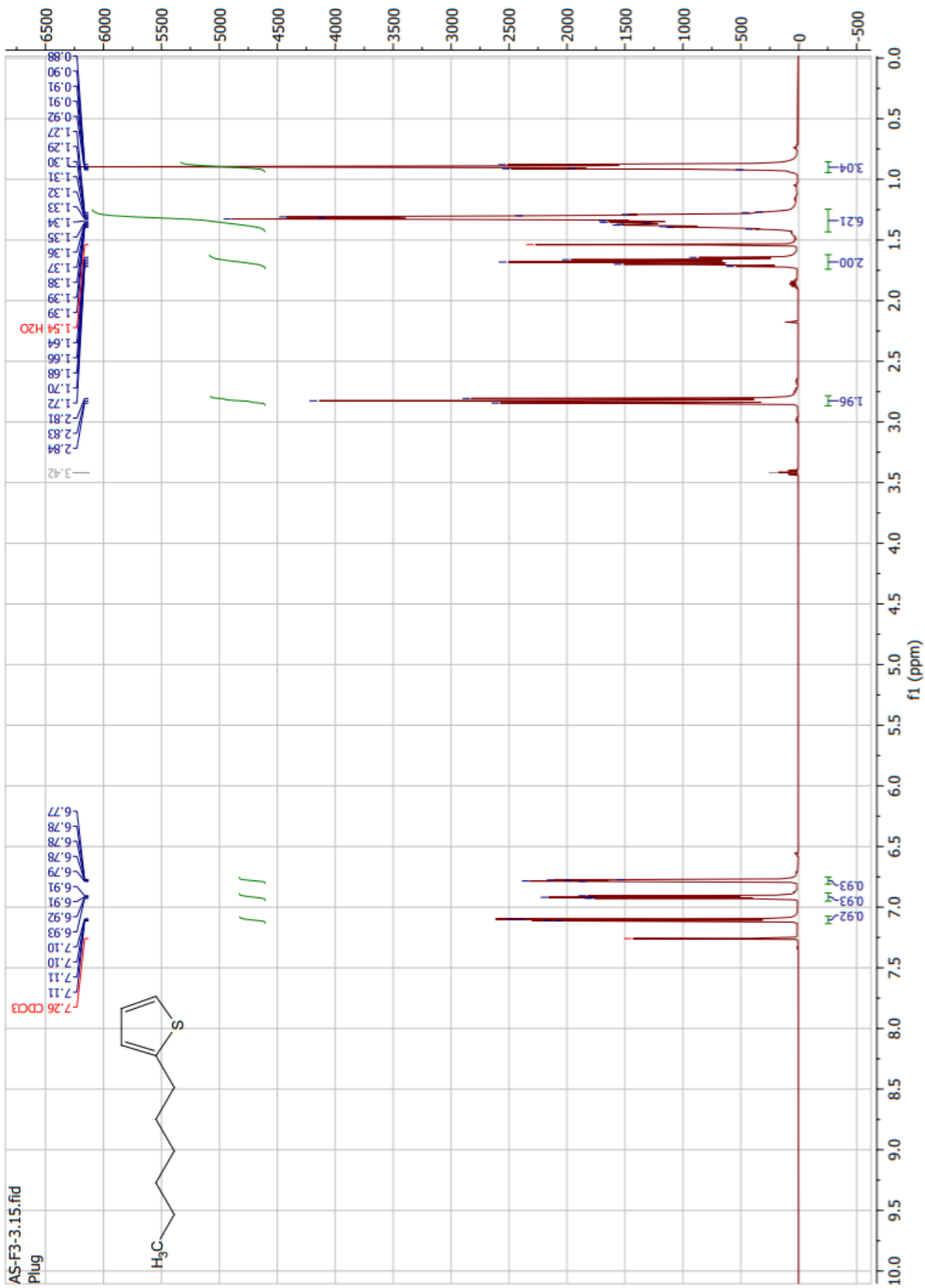

Figure A.28: *^{1}H NMR (400MHz, $CDCl_3$) spectrum of 2-hexylthiophene (**70**)*

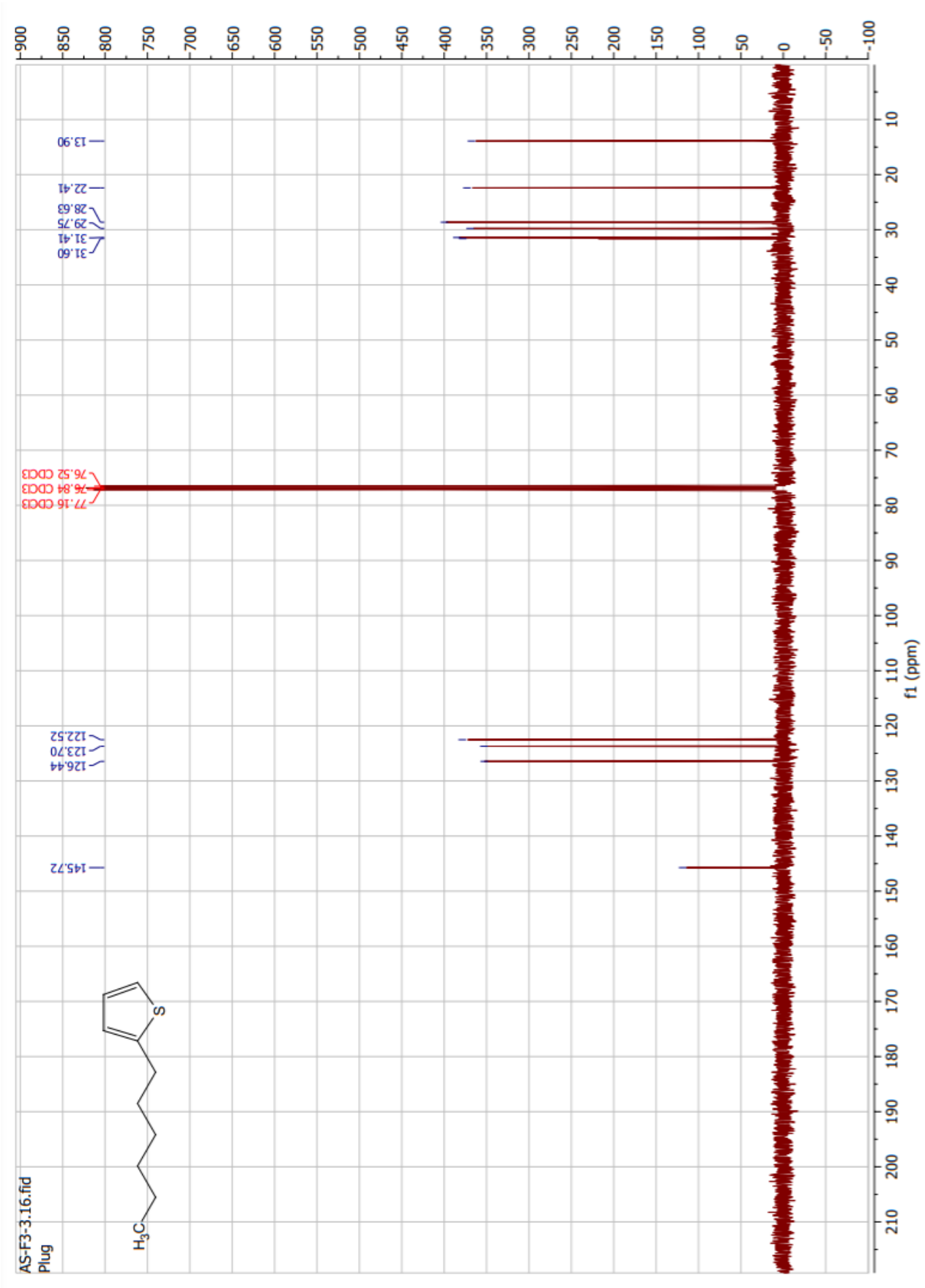

Figure A.29: *Shows the ^{13}C NMR (100MHz, $CDCl_3$) spectrum of 2-hexylthiophene (**70**)*

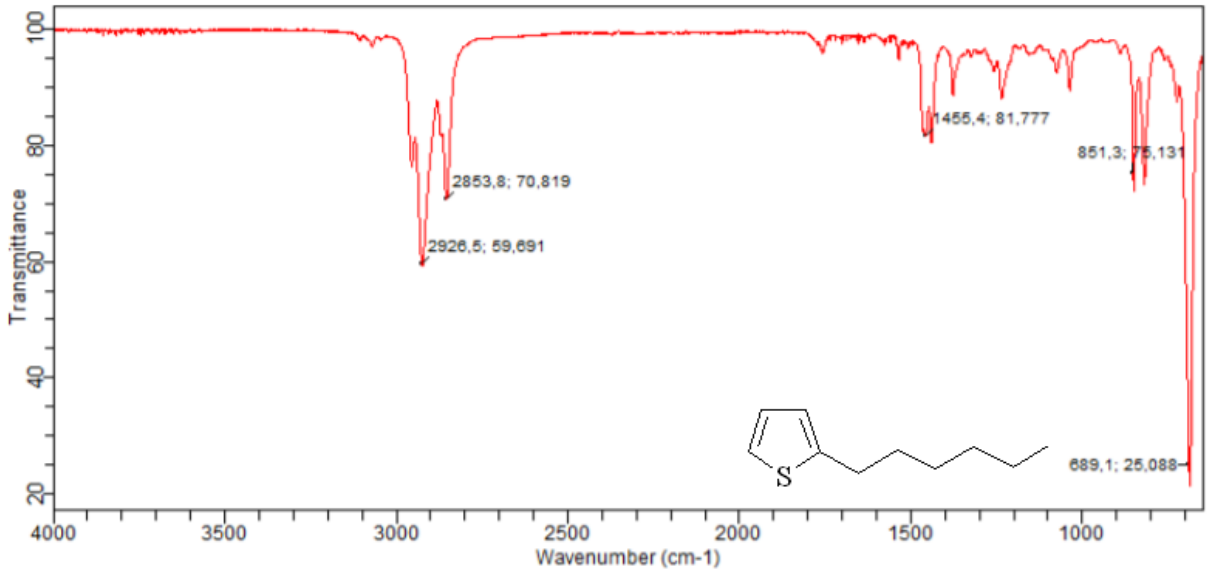

Figure A.30: *IR spectrum of 2-hexylthiophene (**70**)*

A.13. 2-BROMO-5-HEXYLTHIOPHENE (**68A**) SPECTRAL DATA

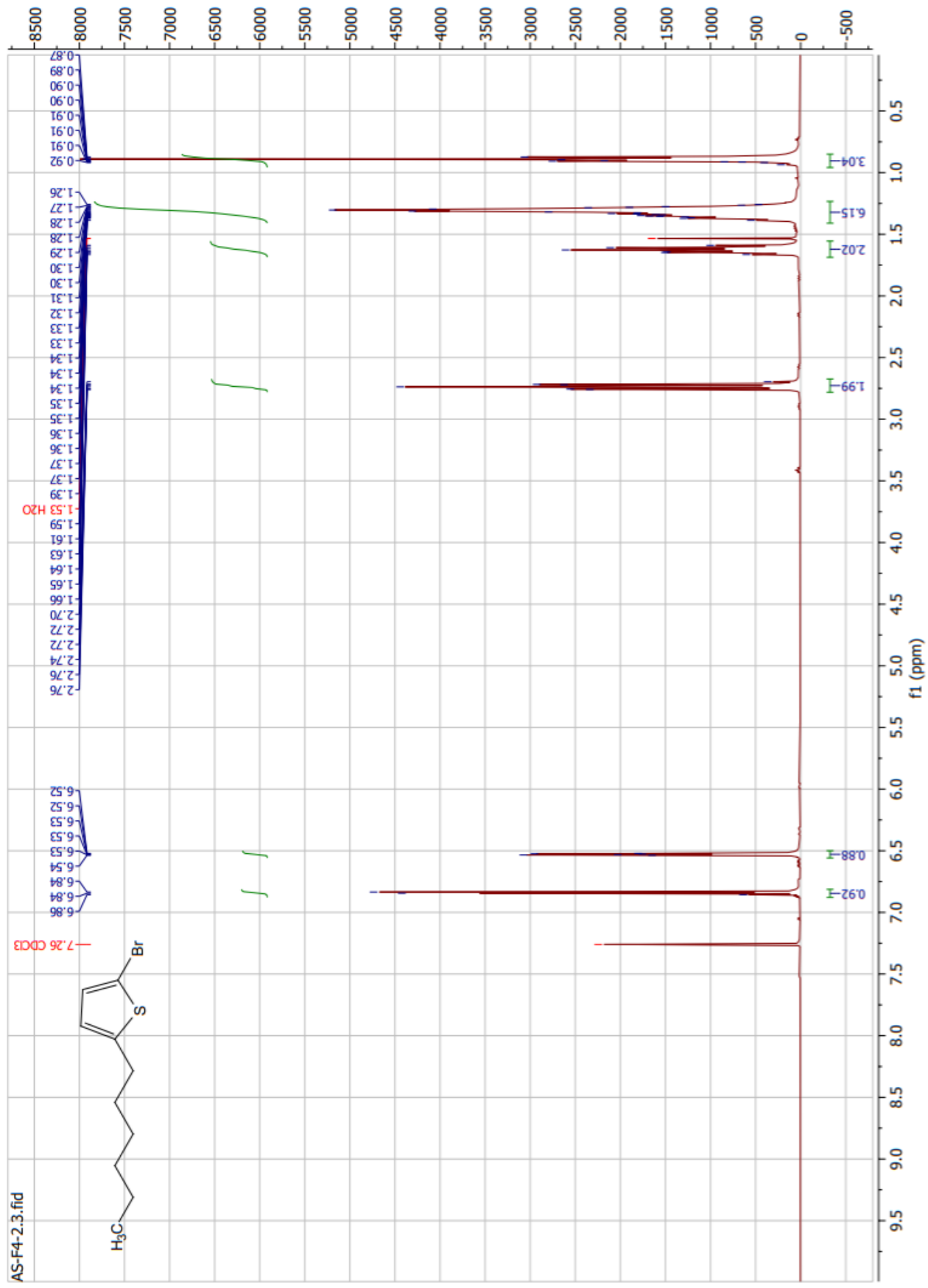

Figure A.31: *^{1}H NMR (400MHz, $CDCl_3$) spectrum of 2-bromo-5-hexylthiophene (**68a**)*

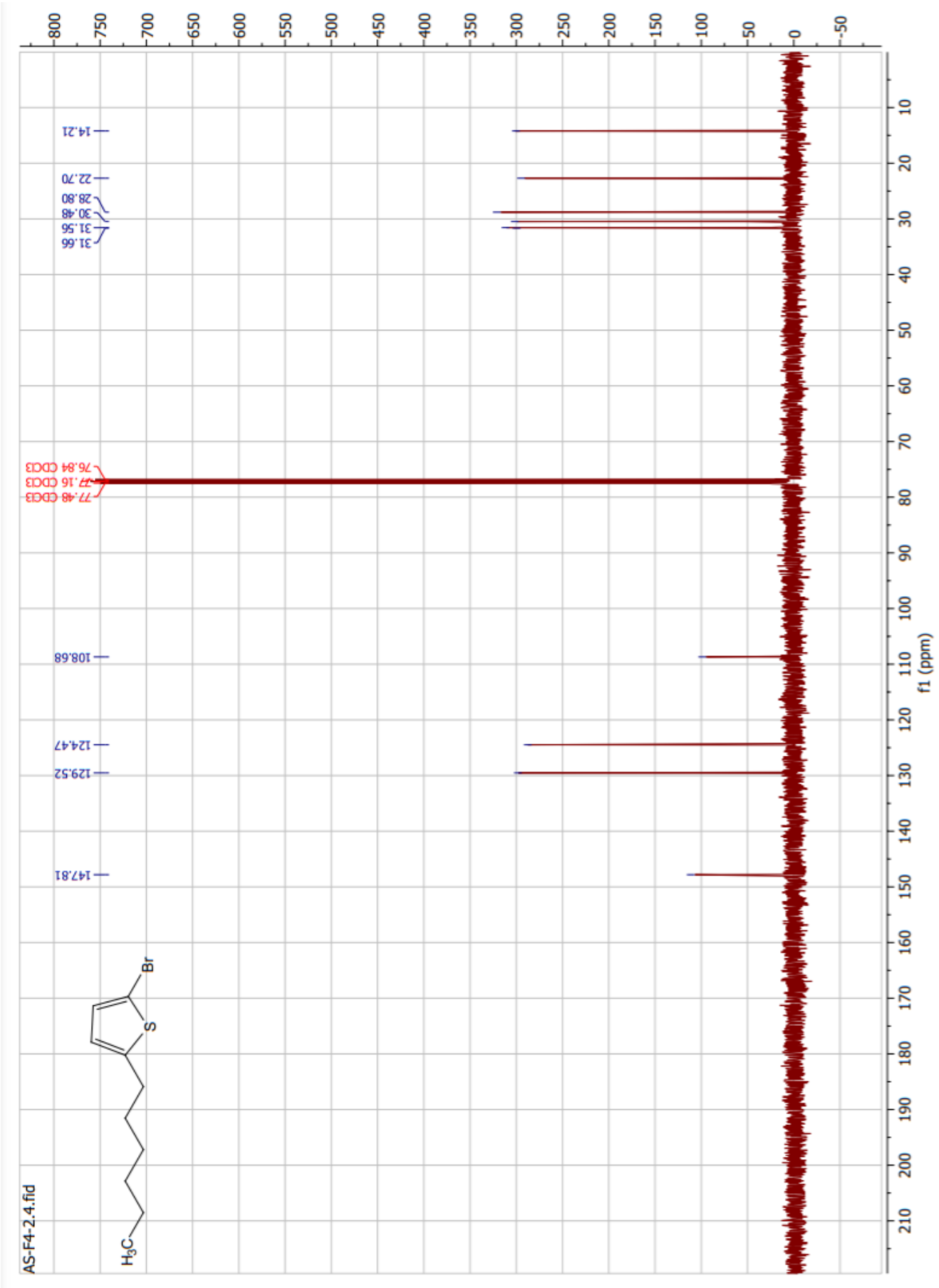

Figure A.32: *^{13}C NMR (100MHz, $CDCl_3$) spectrum of 2-bromo-5-hexylthiophene (**68a**)*

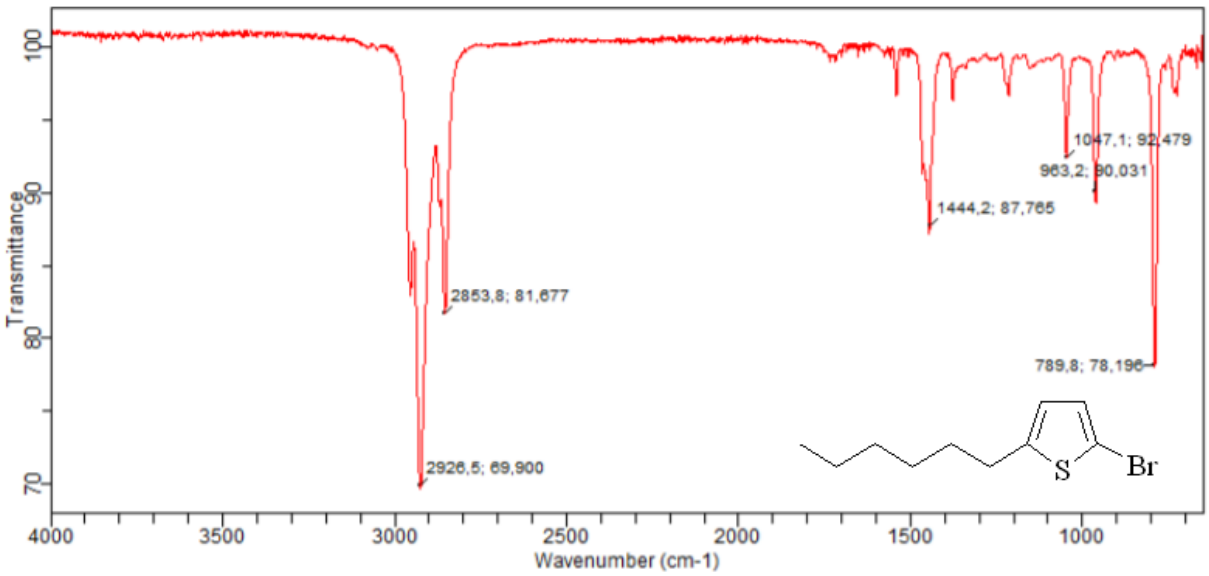

Figure A.33: *IR spectrum of 2-bromo-5-hexylthiophene (**68a**)*

A.14. 2-IODO-5-HEXYLTHIOPHENE (**68B**) SPECTRAL DATA

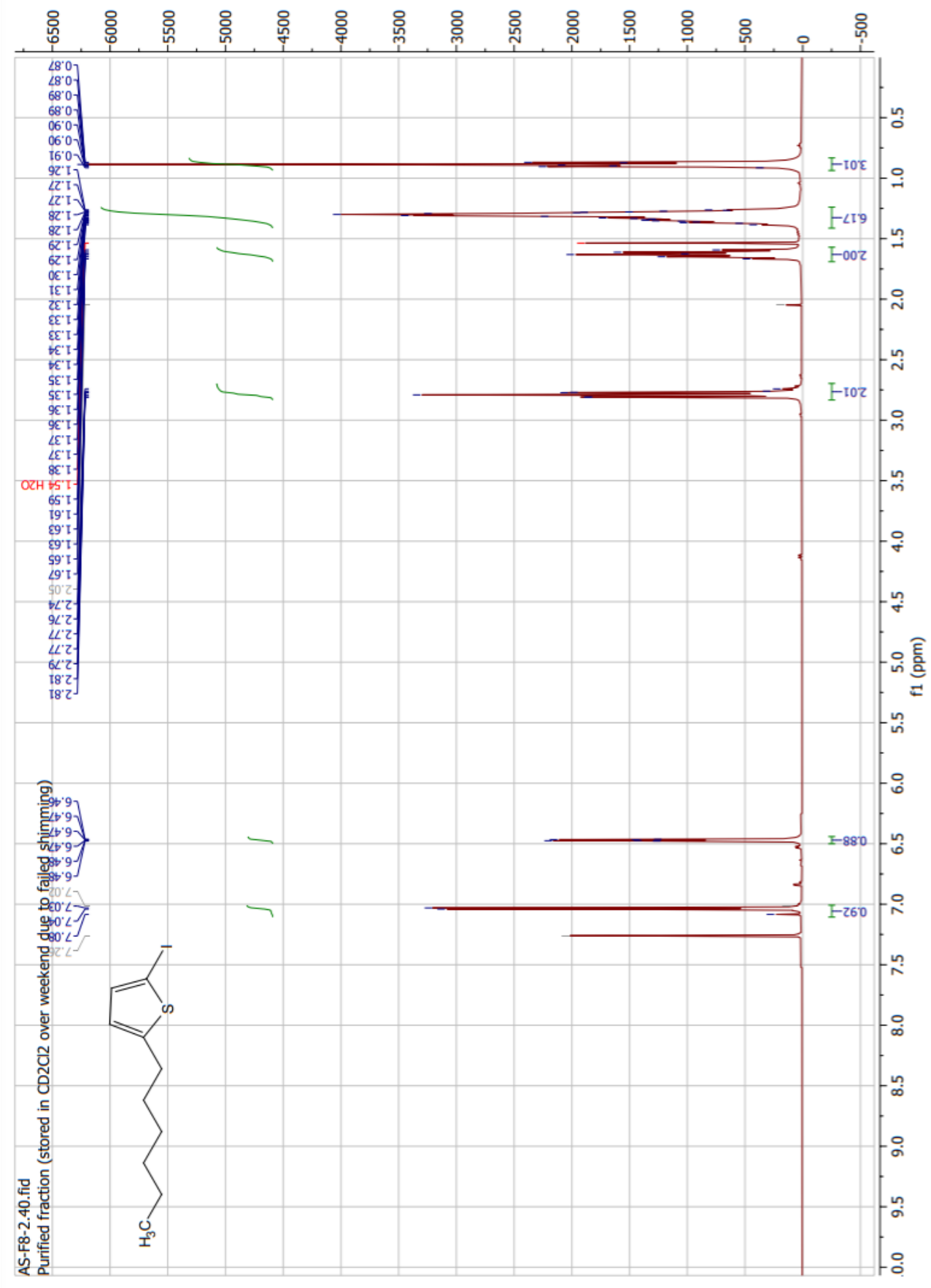

Figure A.34: *^{1}H NMR (400MHz, $CDCl_3$) of 2-iodo-5-hexylthiophene (**68b**)*

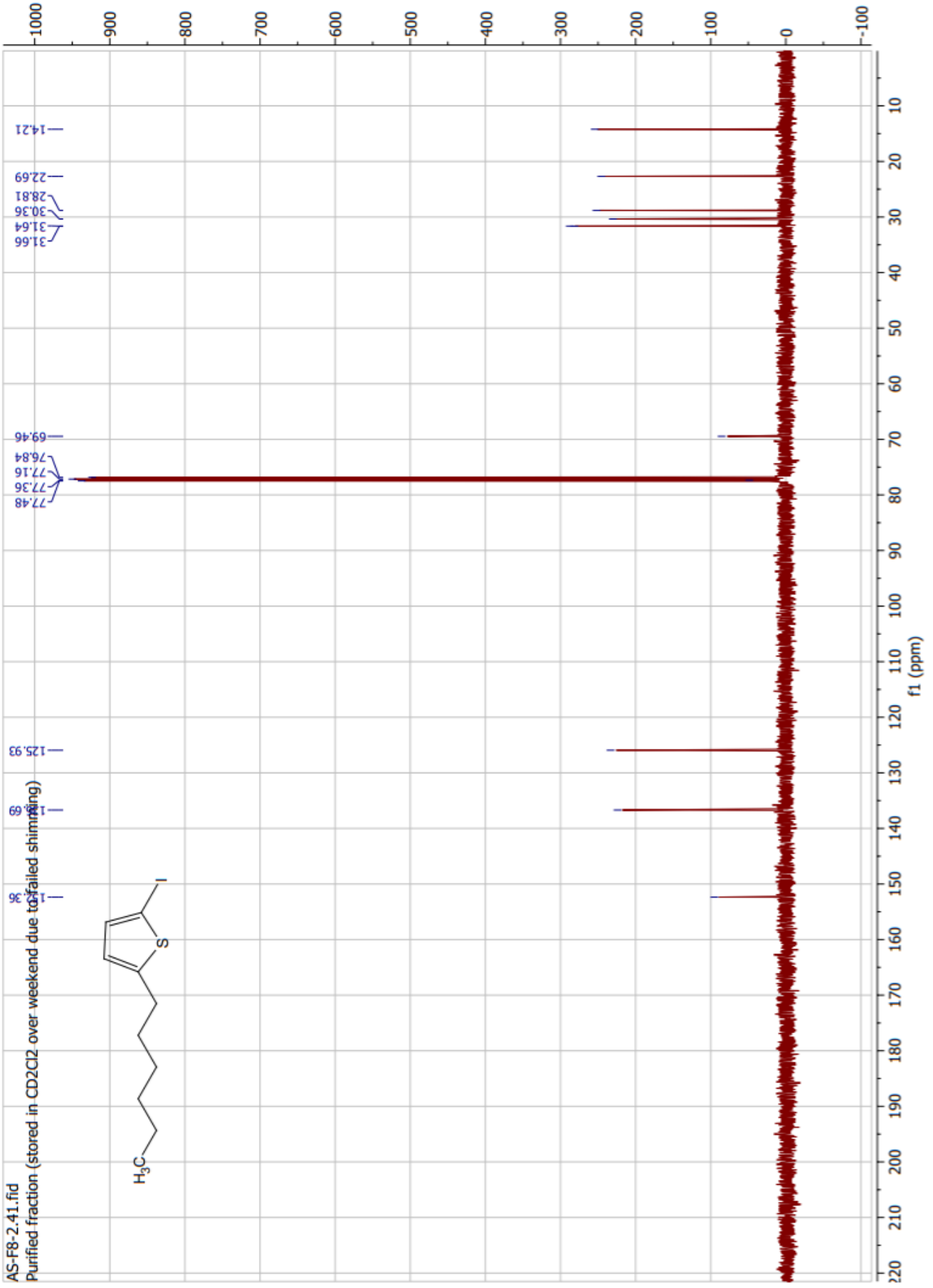

Figure A.35: *^{13}C NMR (100MHz, $CDCl_3$) spectrum of 2-iodo-5-hexylthiophene (**68b**)*

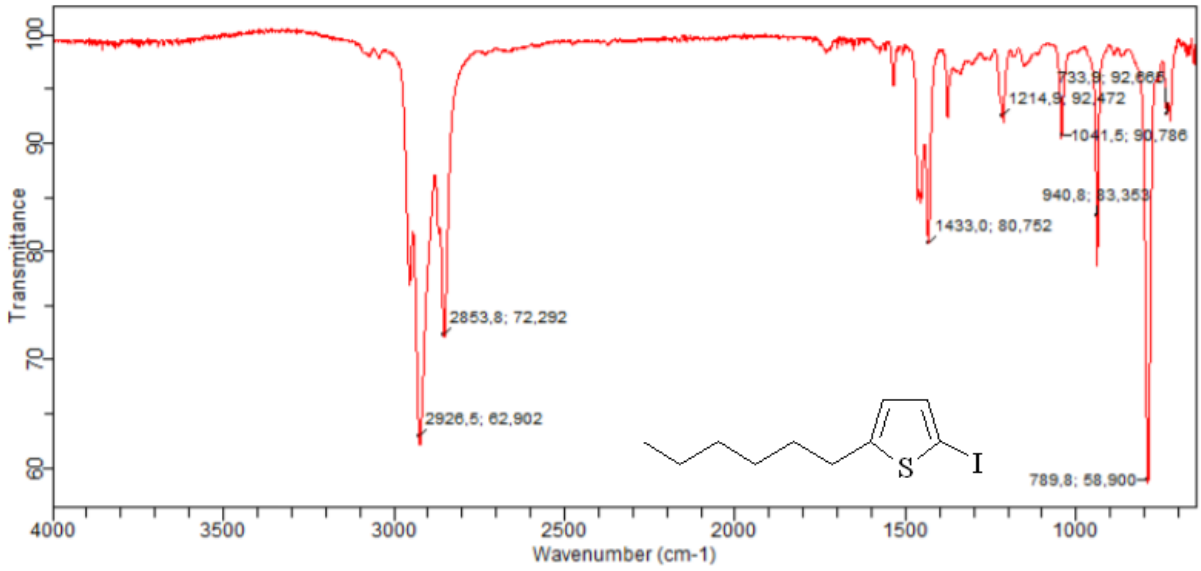

Figure A.36: *IR spectrum of 2-iodo-5-hexylthiophene (**68b**)*

A.15. 2-IODOTHIOPHENE (**103B**) SPECTRAL DATA

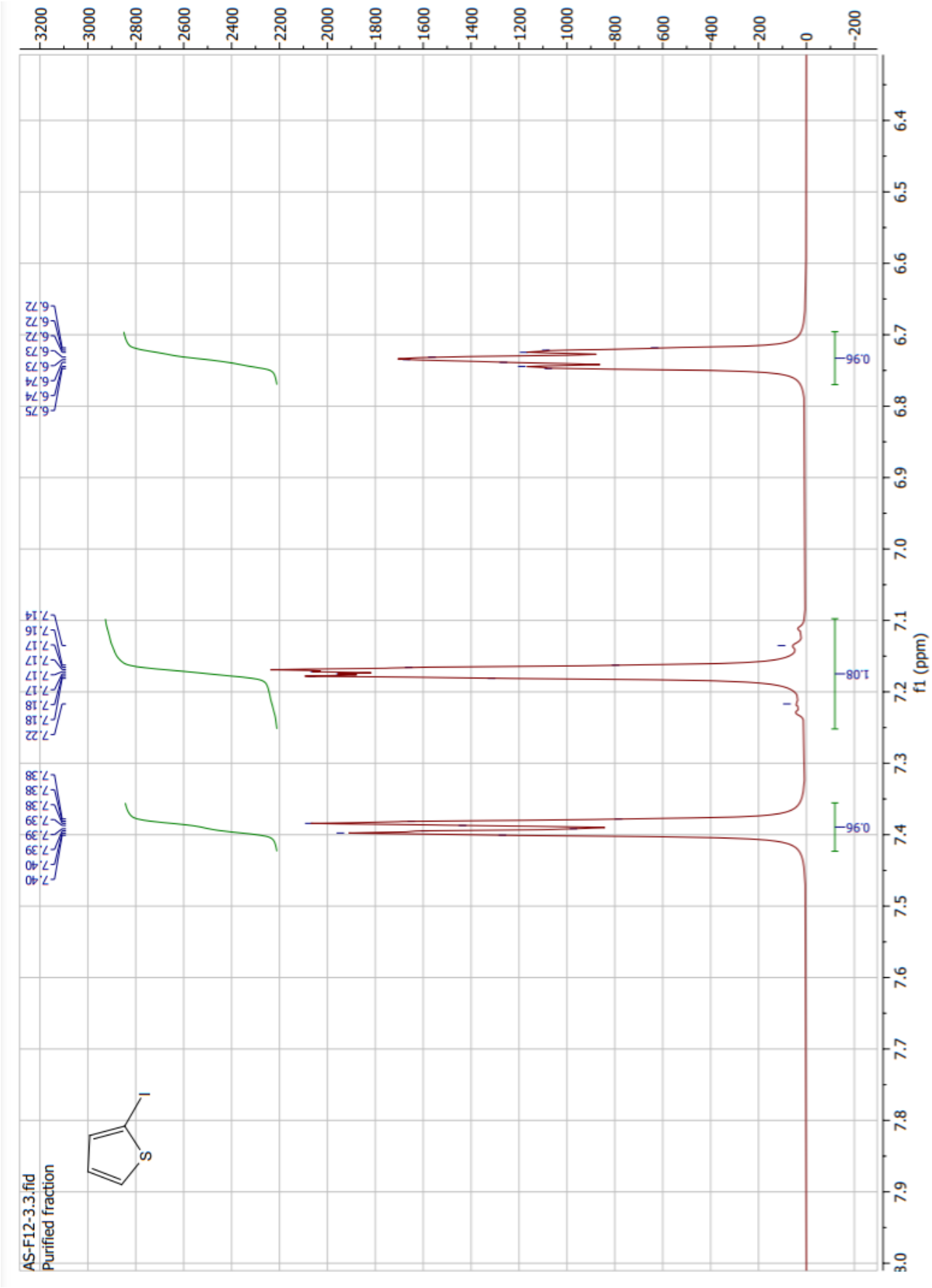

Figure A.37: *^{1}H NMR (400 MHz, MeOD-d_4) spectrum of 2-iodothiophene (**103b**)*

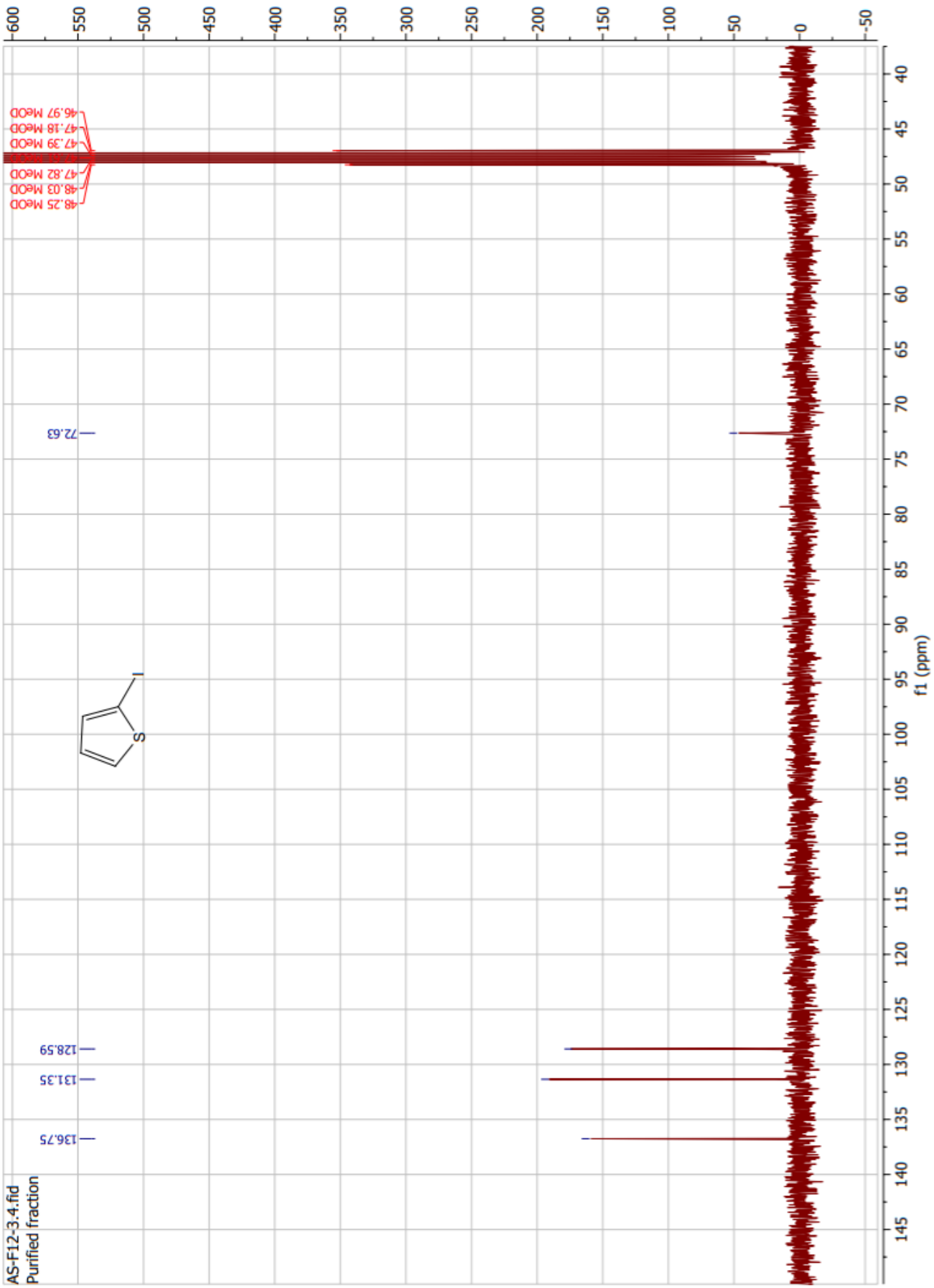

Figure A.38: *^{12}C NMR (100 MHz, MeOD-d_4) of 2-iodothiophene (**103b**)*

A.16. 2-BROMOTHIOPHENE (**103A**) SPECTRAL DATA

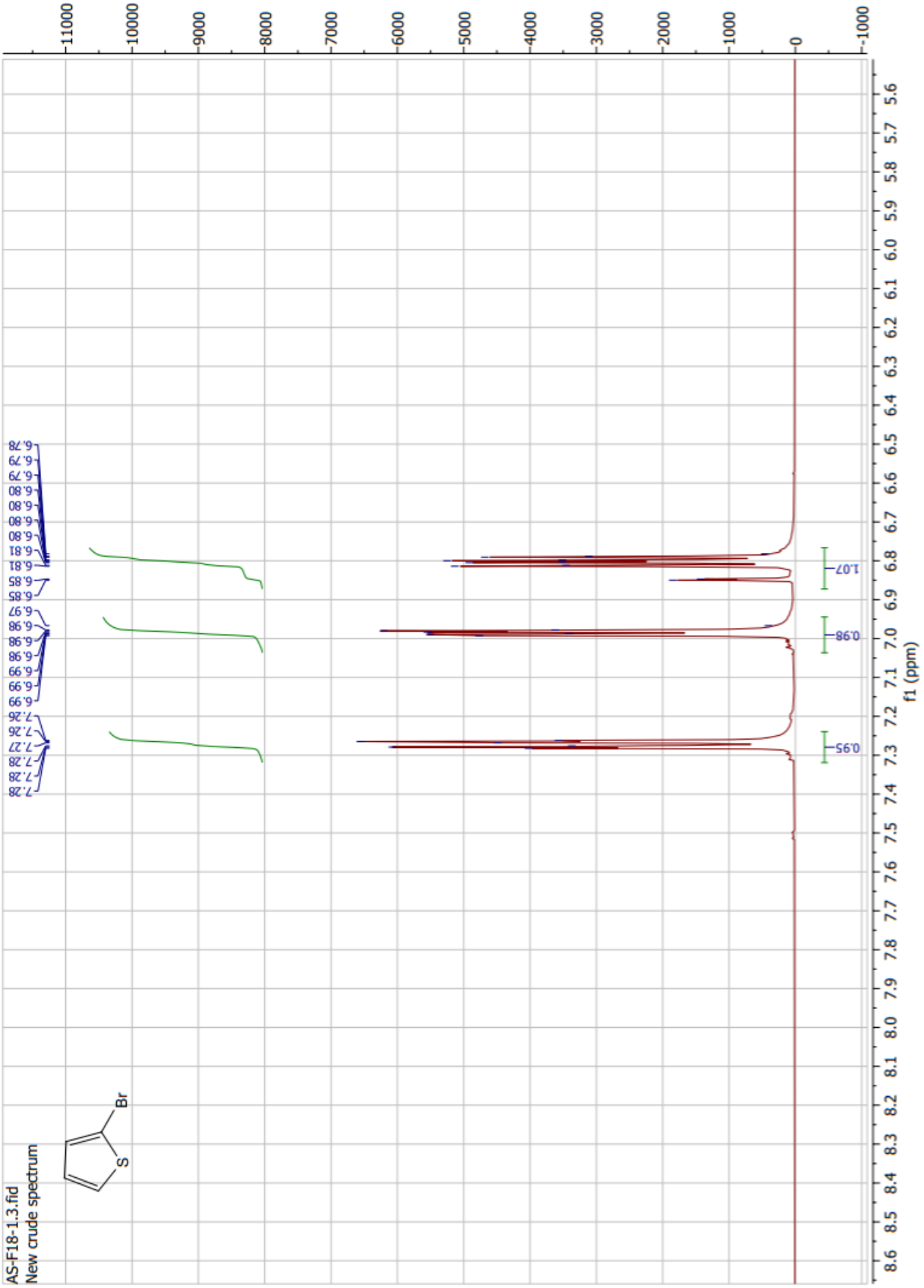

Figure A.39: *^{1}H NMR (400MHz, MeOD) spectrum of 2-bromothiophene (**103a**)*

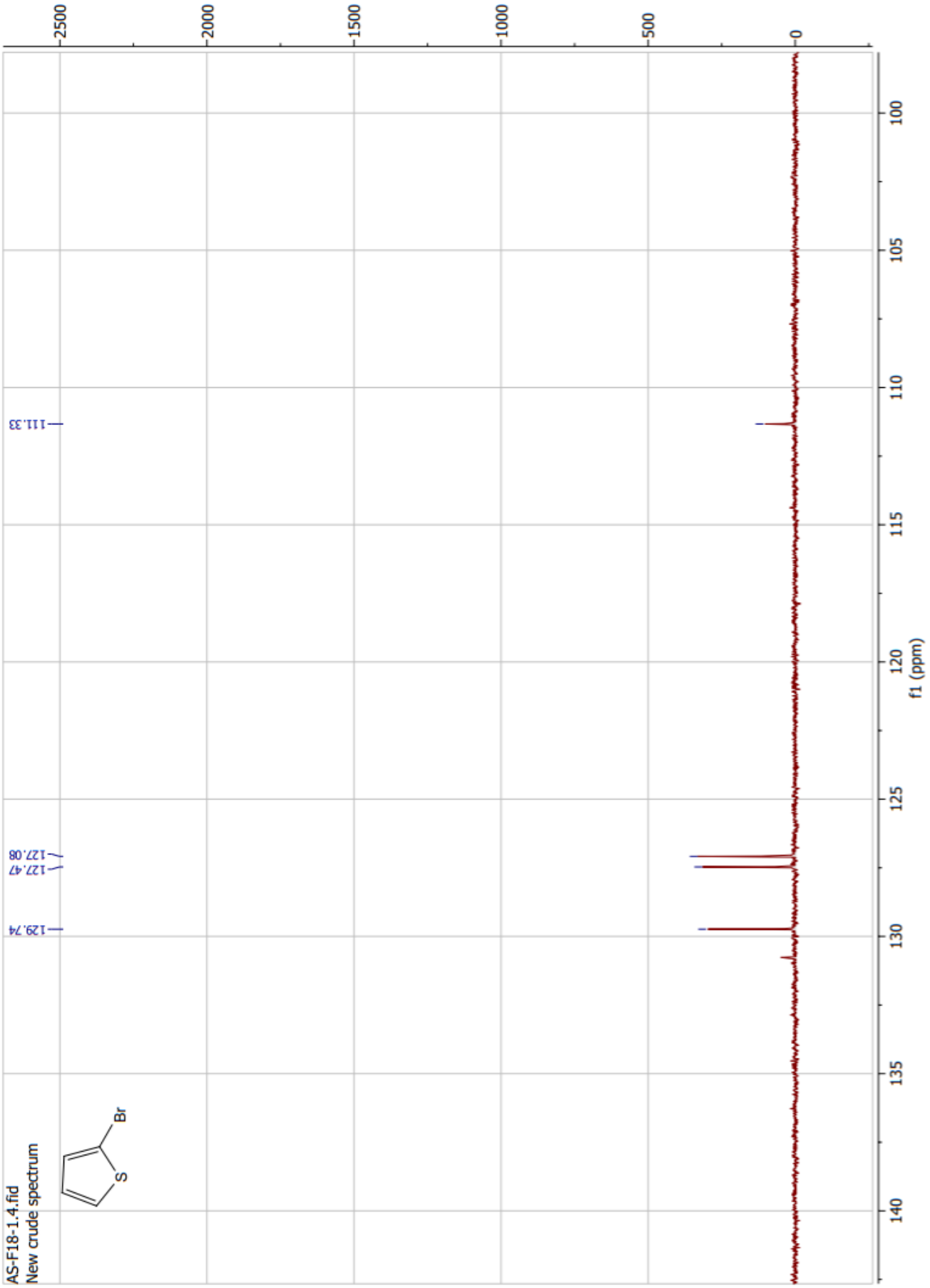

Figure A.40: *^{13}C NMR (100MHz, MeOD) spectrum of 2-bromothiophene (**103a**)*

A.17. 2-(5-HEXYLTHIOPHEN-2-YL)-ETHYNYL TRIMETHYLSILANE (**99**) SPECTRAL DATA

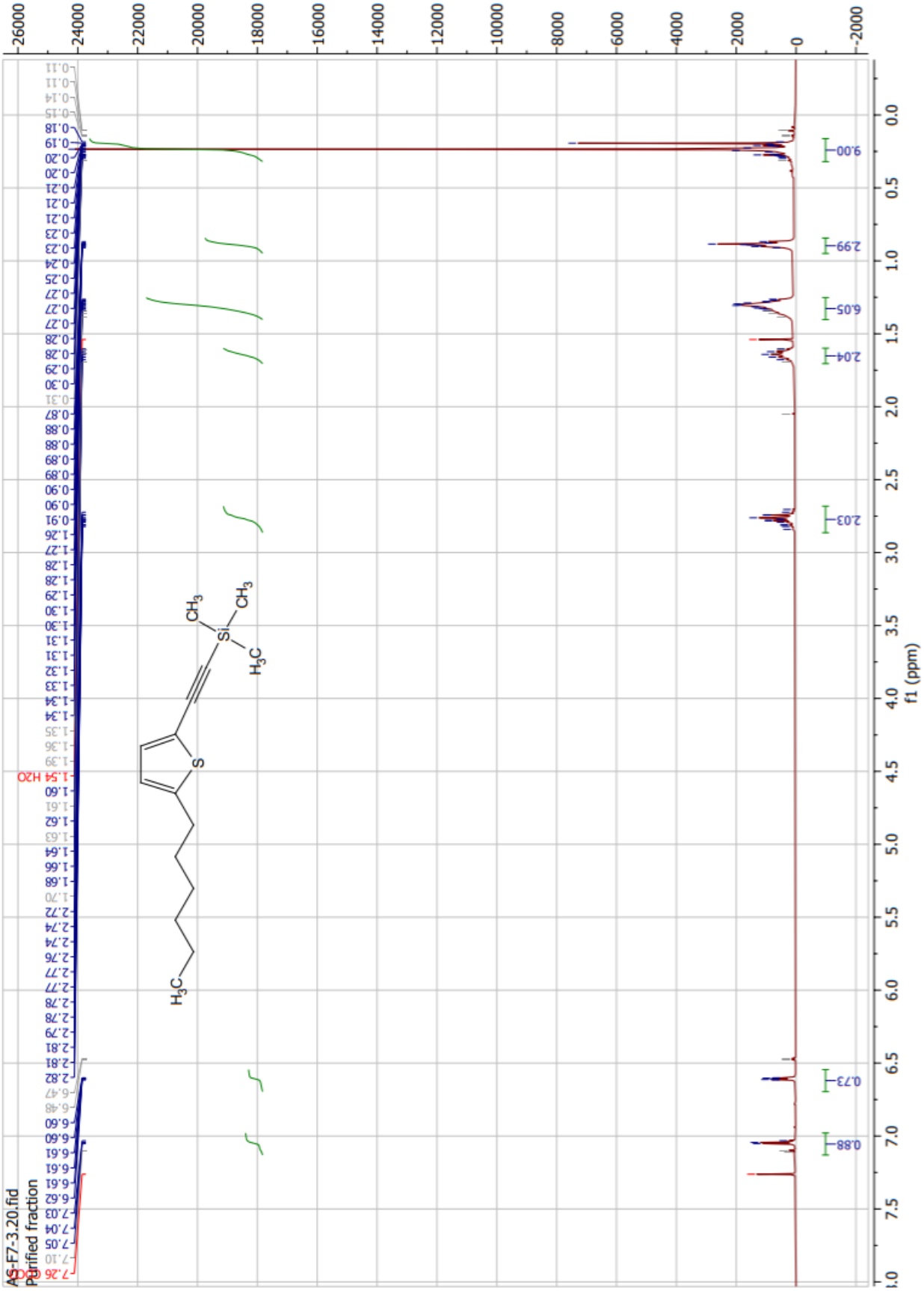

Figure A.41: *^{1}H NMR (400MHz, $CDCl_3$) spectrum of 2-(5-hexylthiophen-2-yl)ethynyl trimethylsilane (**99**)*

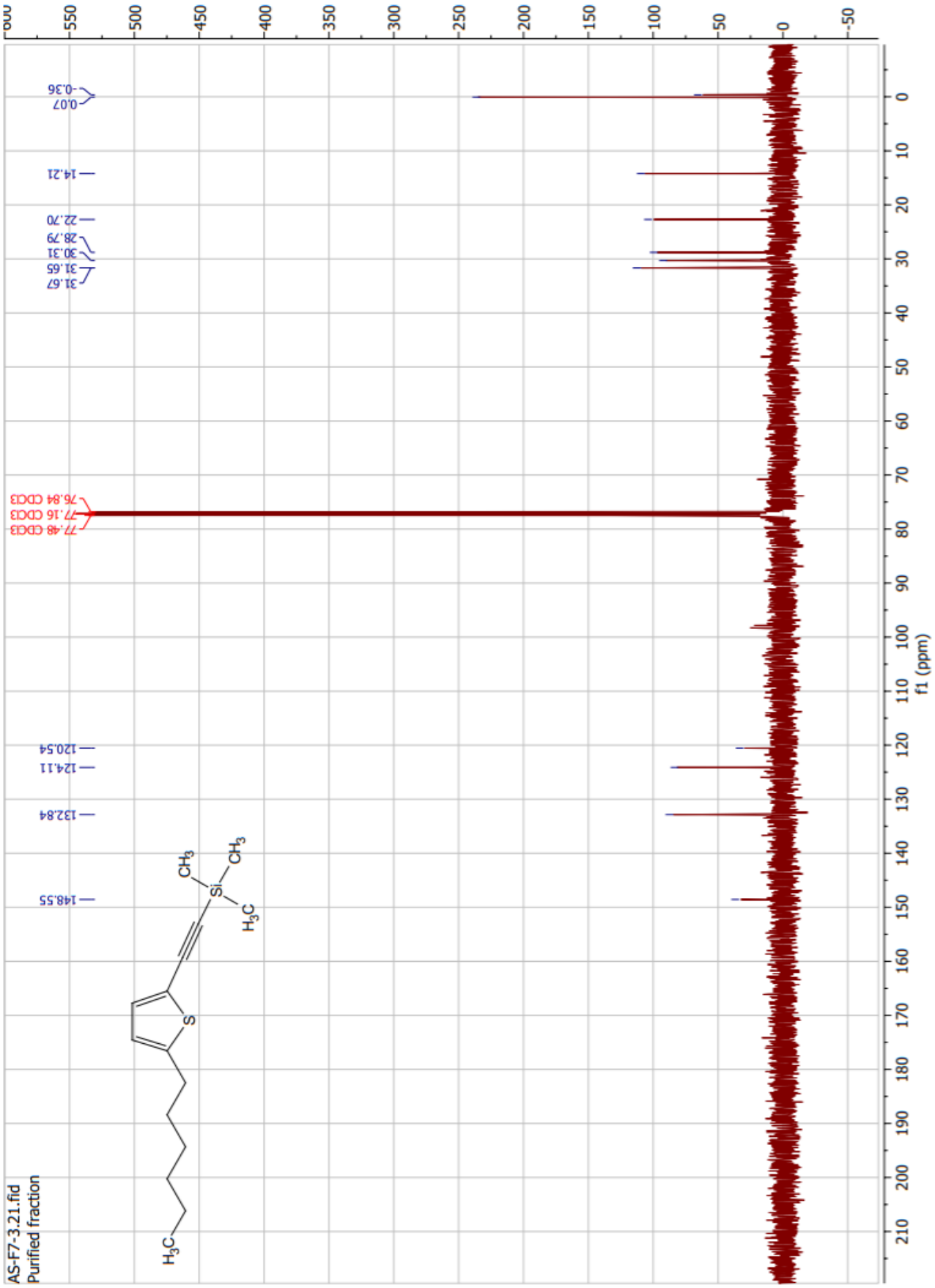

Figure A.42: *^{13}C NMR (100MHz, $CDCl_3$) spectrum of 2-(5-hexylthiophen-2-yl)ethynyl trimethylsillane (**99**)*

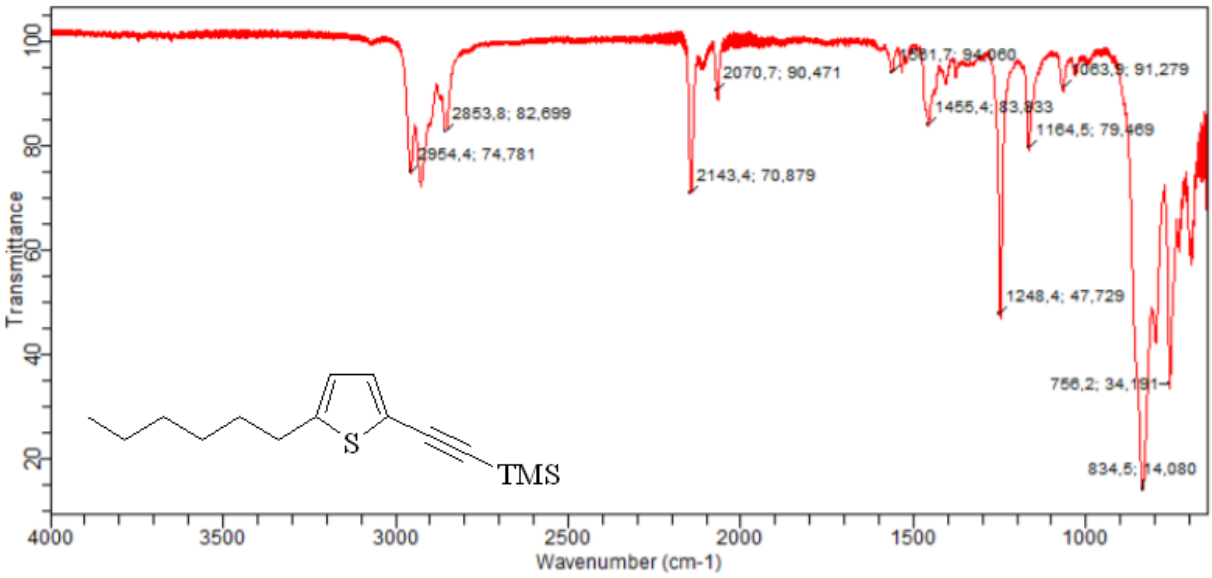

Figure A.43: *IR spectrum of 2-(5-hexylthiophen-2-yl)-ethynyl trimethylsilane* ***(99)***

A.18. 2-ETHYNYL-5-HEXYLTHIOPHENE (**76**) SPECTRAL DATA

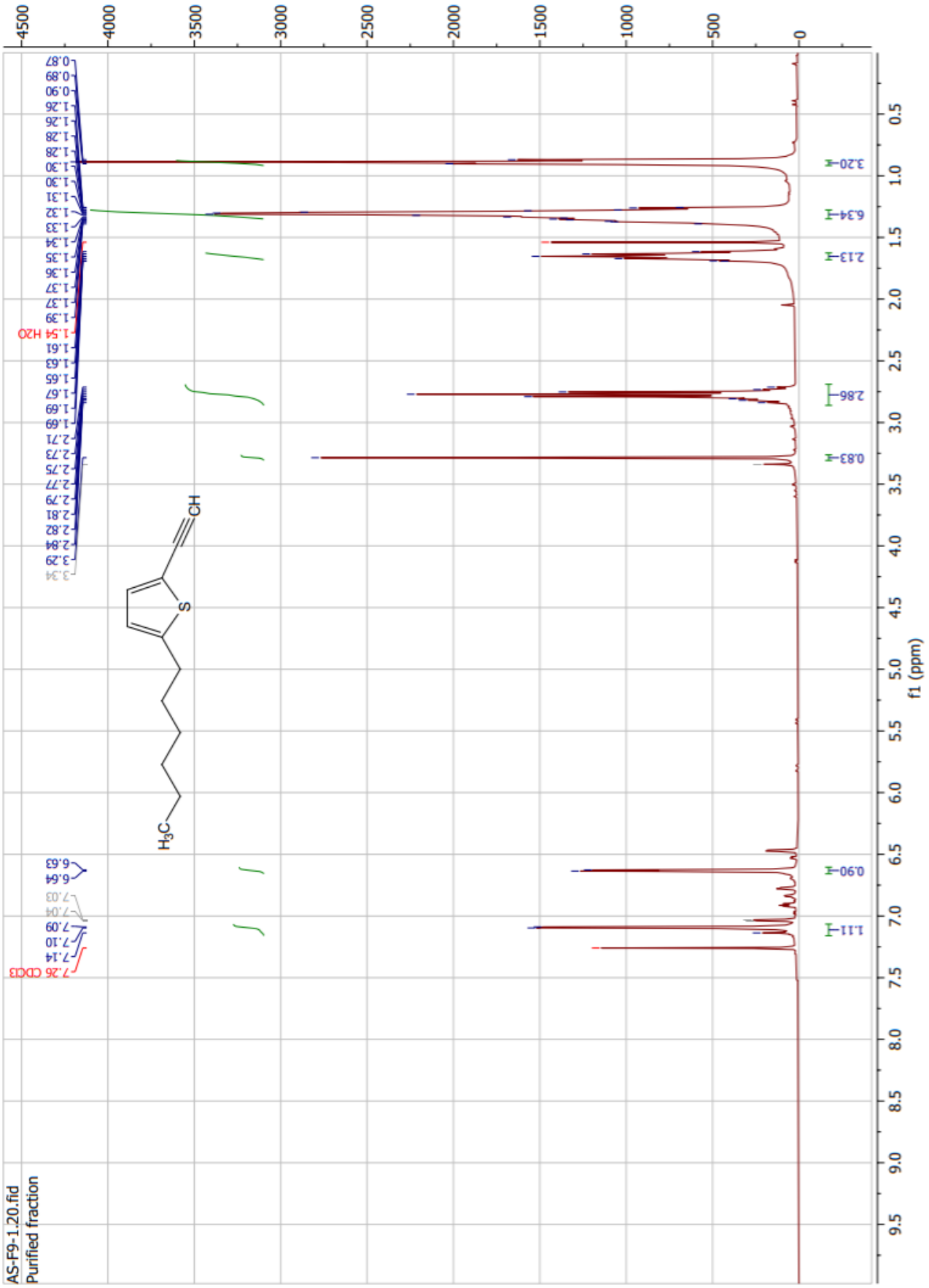

Figure A.44: *^{1}H NMR (400MHz, $CDCl_3$) spectrum of 2-ethynyl-5-hexylthiophene (**76**)*

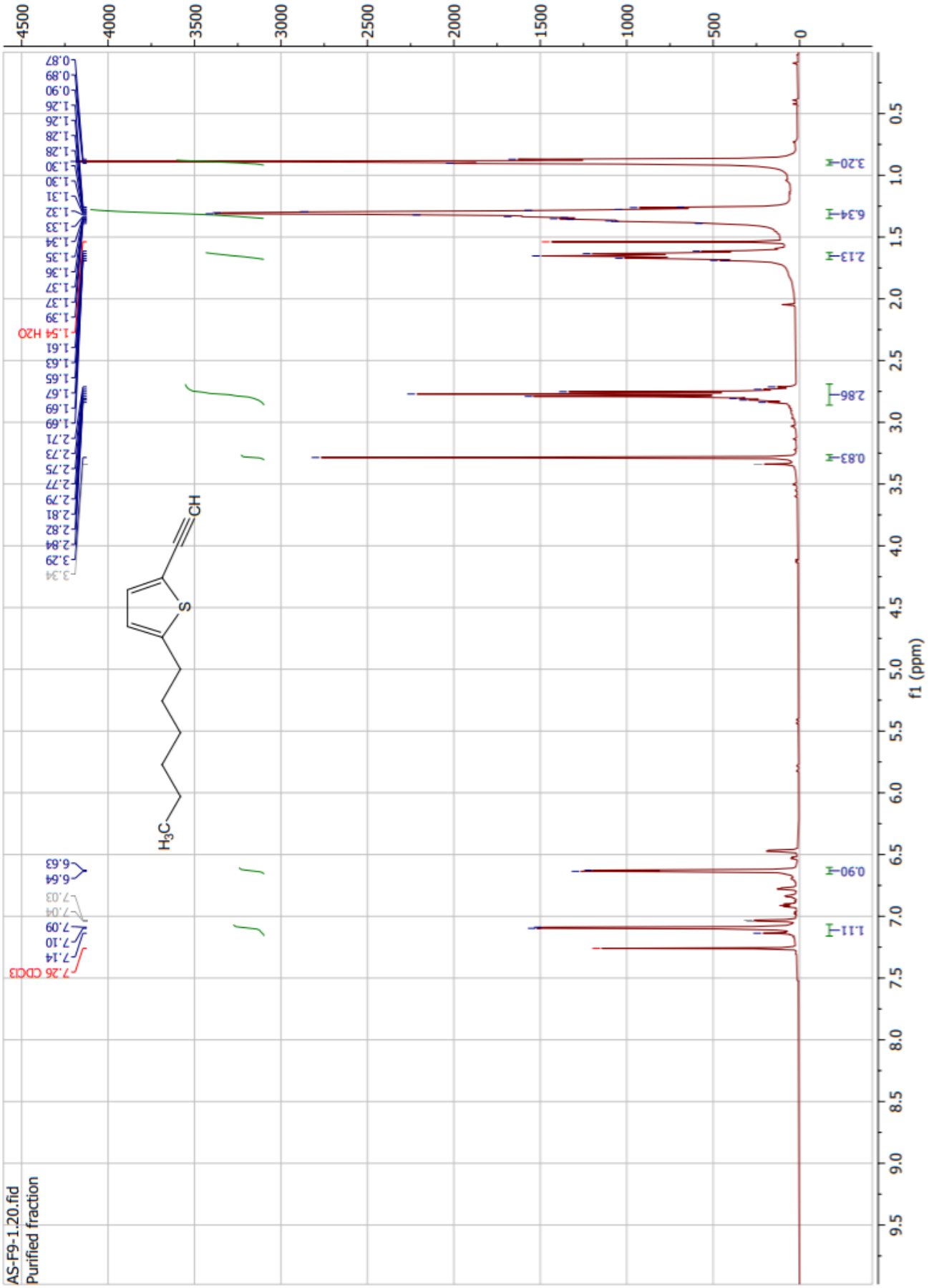

Figure A.45: *^{13}C NMR (100MHz, $CDCl_3$) spectrum of 2-ethynyl-5-hexylthiophene (**76**)*

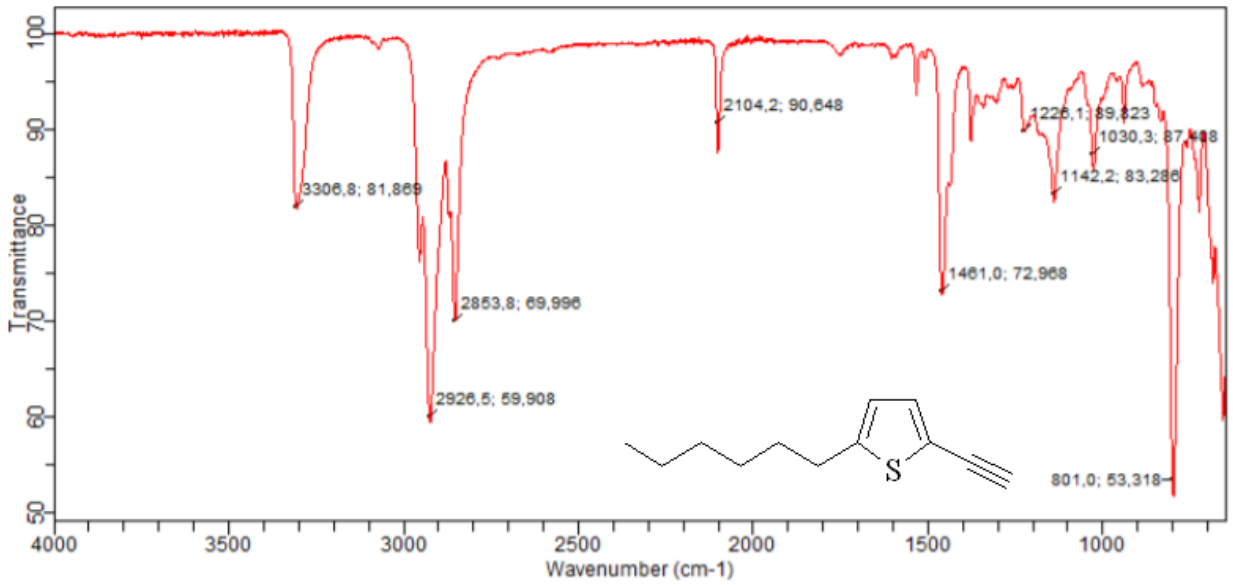

Figure A.46: *IR spectrum of 2-ethynyl-5-hexylthiophene (**76**)*

A.19. 5-HEXYLTHIOPHENE-2-CARBALDEHYDE (**80**) SPECTRAL DATA

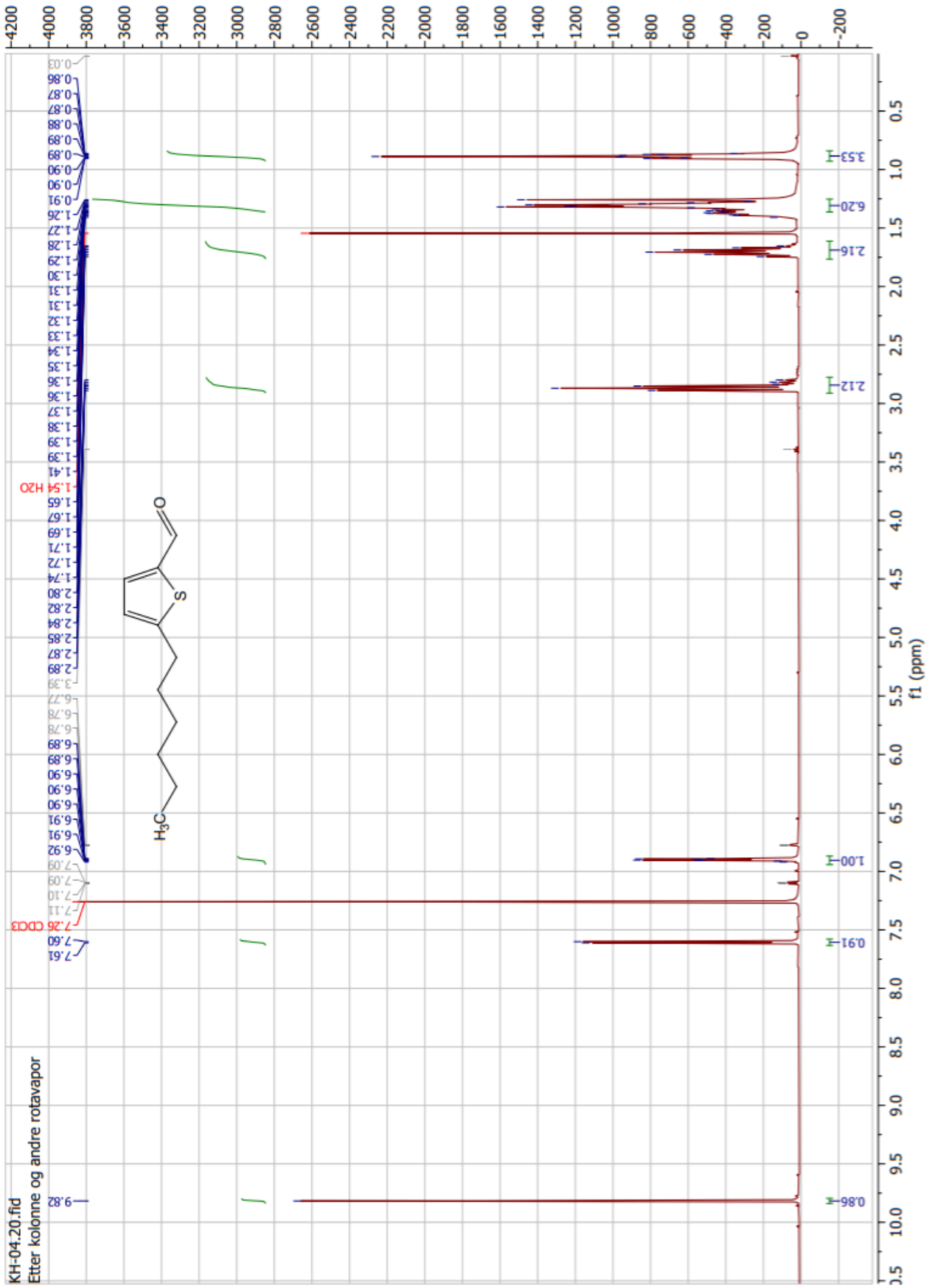

Figure A.47: *^{1}H NMR (400MHz, $CDCl_3$) spectrum of 5-hexylthiophene-2-carbaldehyde (**80**)*

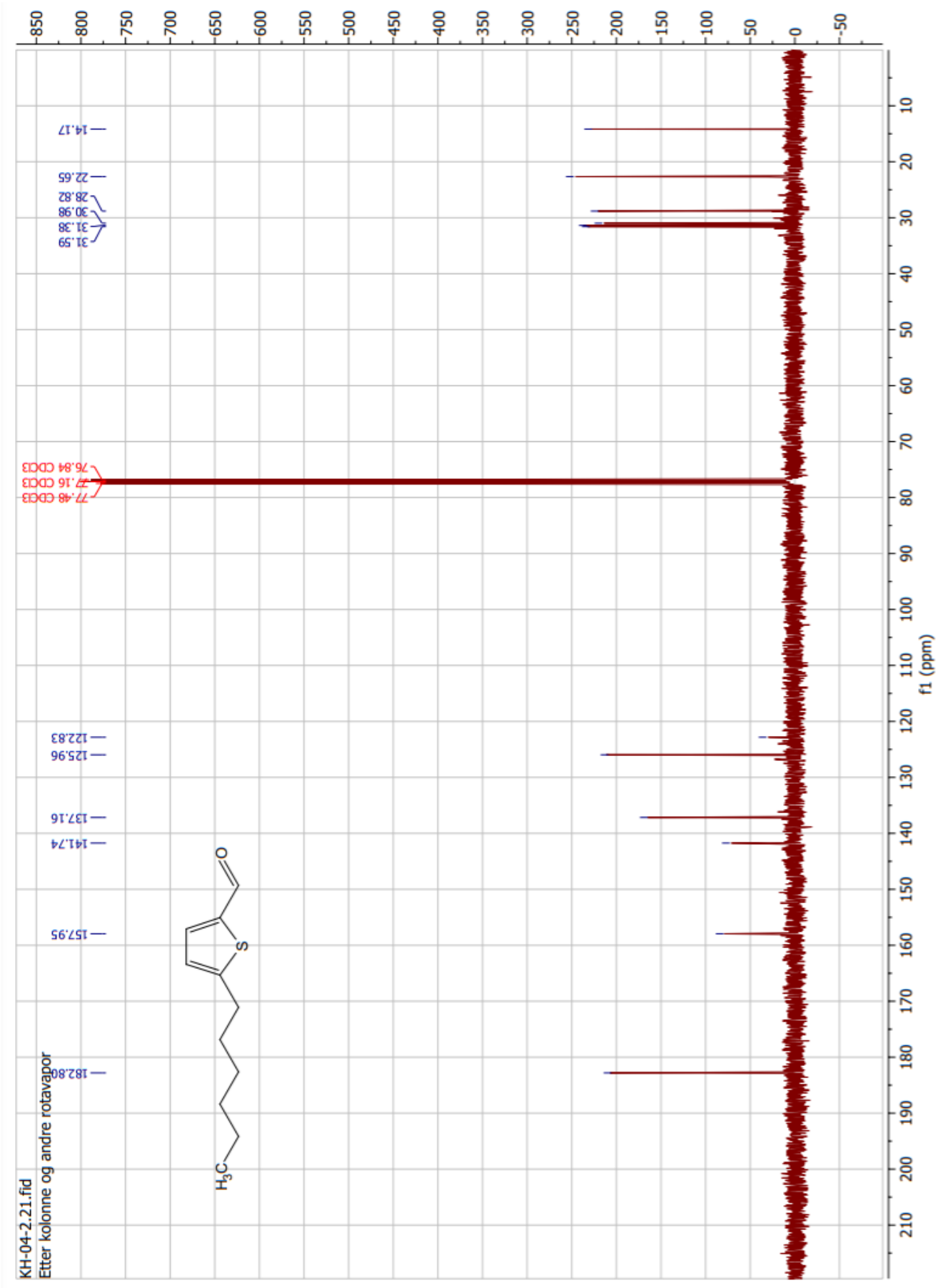

Figure A.48: *^{13}C NMR (100MHz, $CDCl_3$) spectrum of 5-hexylthiophene-2-carbaldehye (**80**)*

A.20. 3-(5-HEXYLTHIOPHEN-2-YL)-PROP-2-YN-1-OL (**108**) SPECTRAL DATA

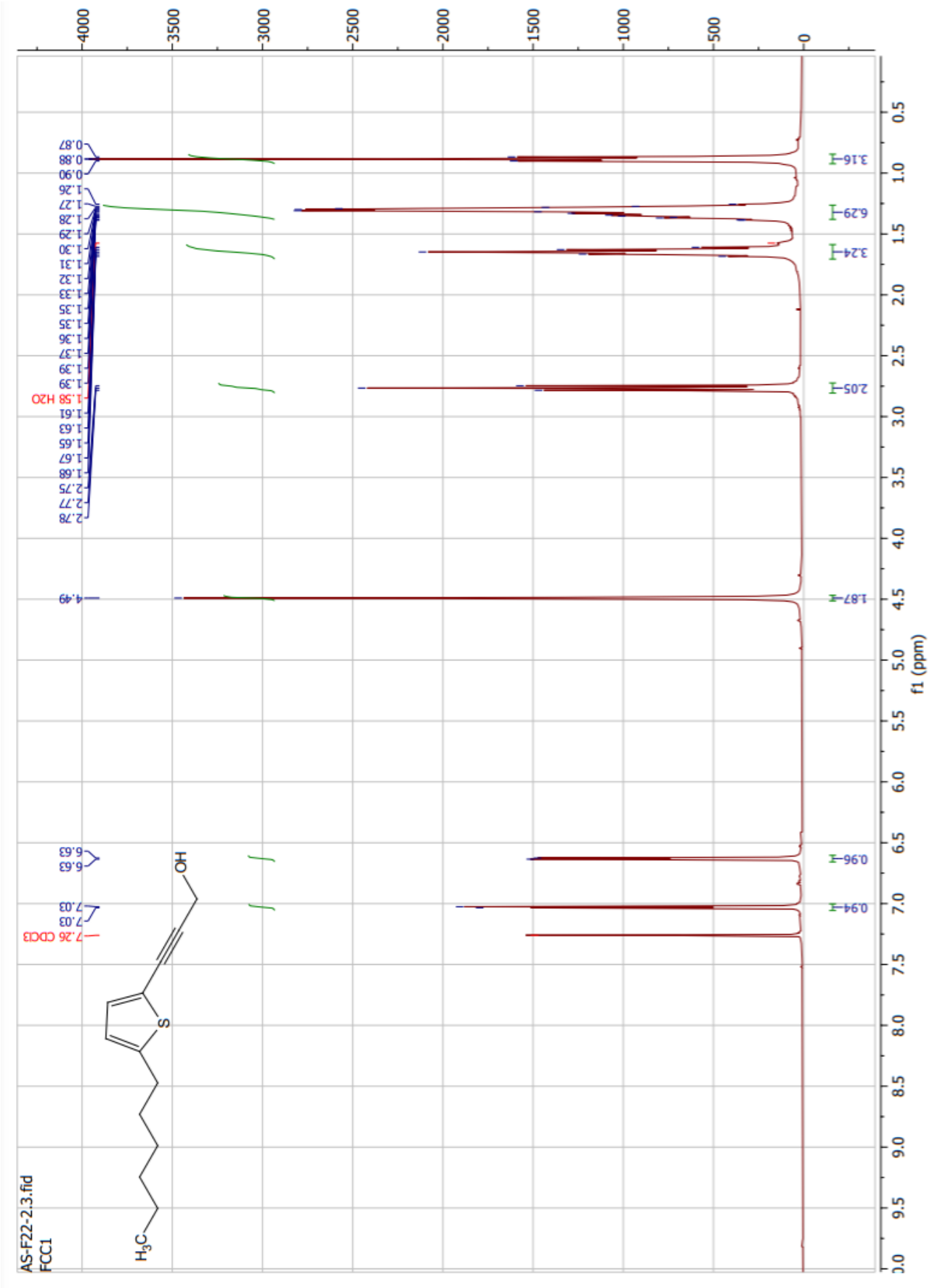

Figure A.49: *^{1}H NMR (400 MHz, $CDCl_3$), spectrum of 3-(5-hexylthiophen-2-yl)prop-2-yn-1-ol (**108**)*

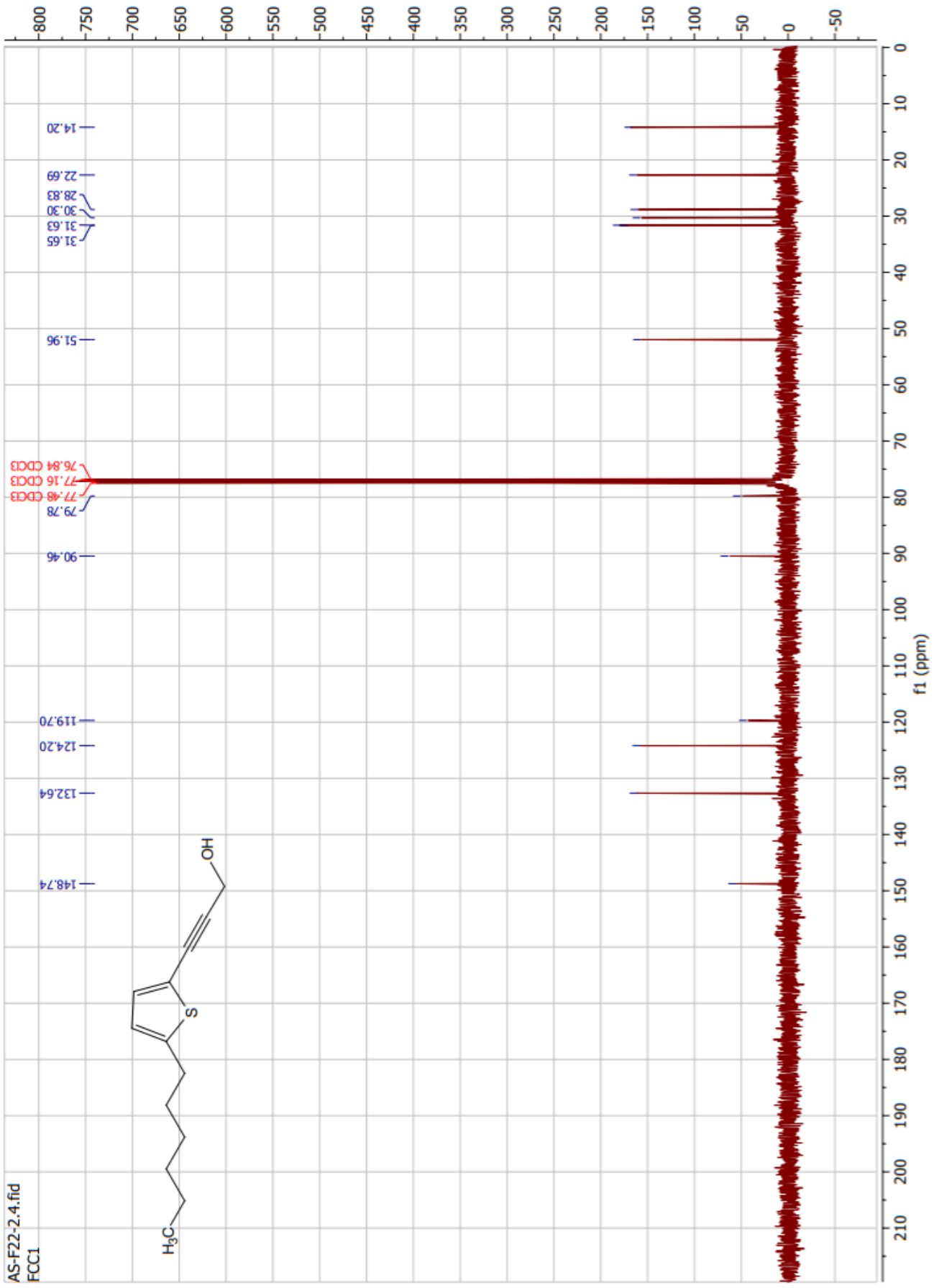

Figure A.50: *^{13}C NMR (100MHz, $CDCl_3$) spectrum of 3-(5-hexylthiophen-2-yl)prop-2-yn-1-ol (**108**)*

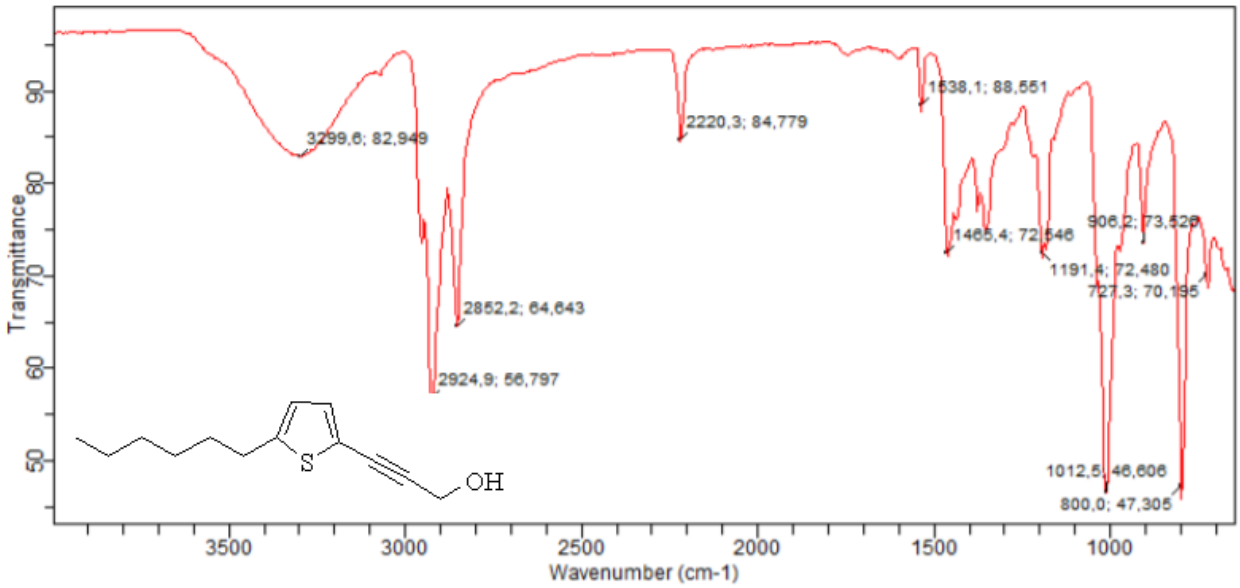

Figure A.51: *IR spectrum of 3-(5-hexylthiophen-2-yl)-prop-2-yn-1-ol (**108**)*

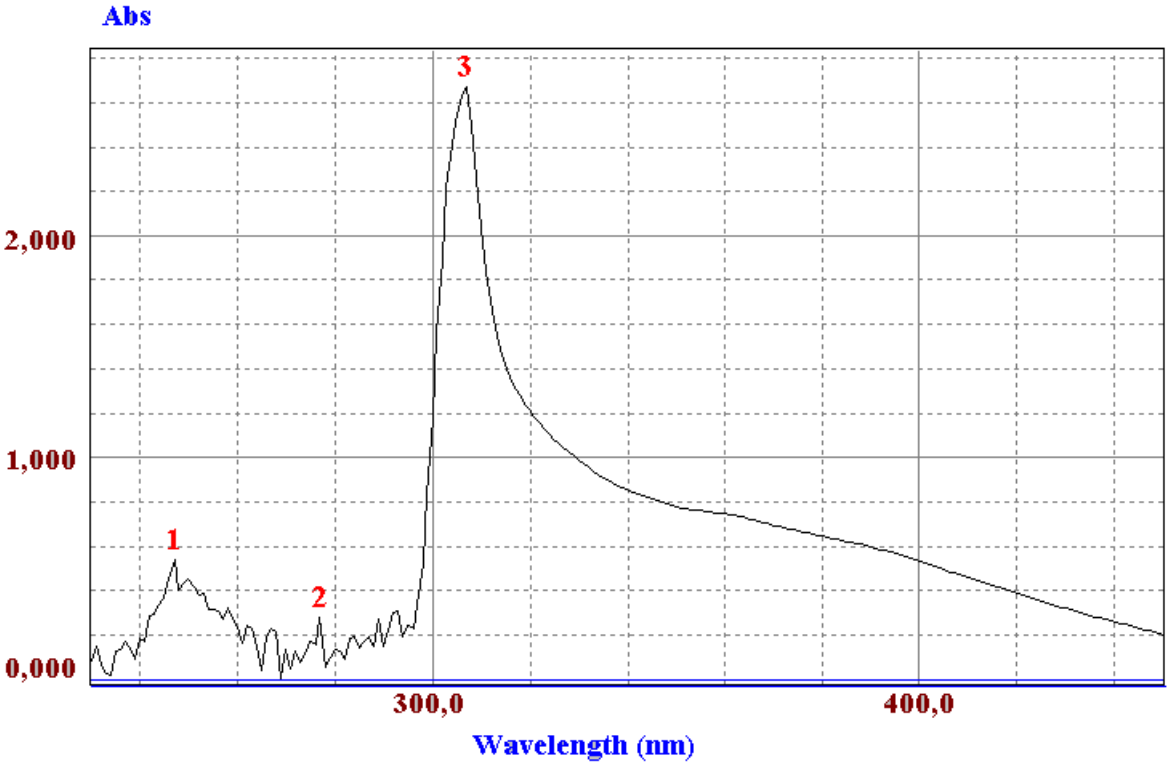

No.	Peak Type	Position	Height
1	Peak	246.8	0.540
2	Peak	276.8	0.282
3	Peak	306.6	2.764

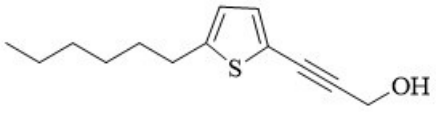

Figure A.52: *UV spectrum of 3-(5-hexylthiophen-2-yl)-prop-2-yn-1-ol (**108**)*

A.21. 2-(3-BROMOPROP-1-YN-1-YL)-5-HEXYLTHIOPHENE (**84**) SPECTRAL DATA

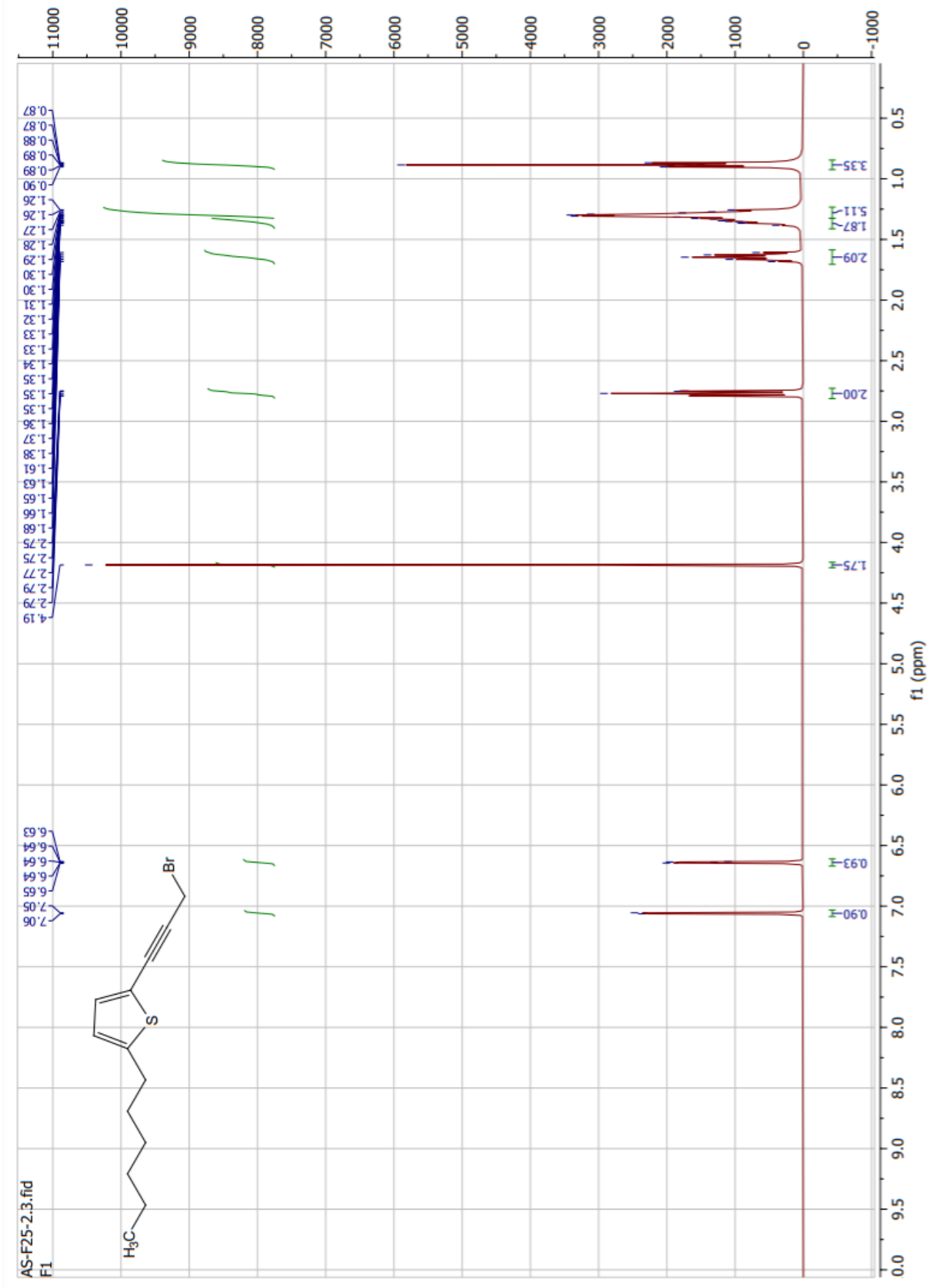

Figure A.53: *Shows the ^{1}H NMR (400MHz, $CDCl_3$) spectrum of 2-(3-bromoprop-1-yn-1-yl)-5-hexylthiophene (**84**)*

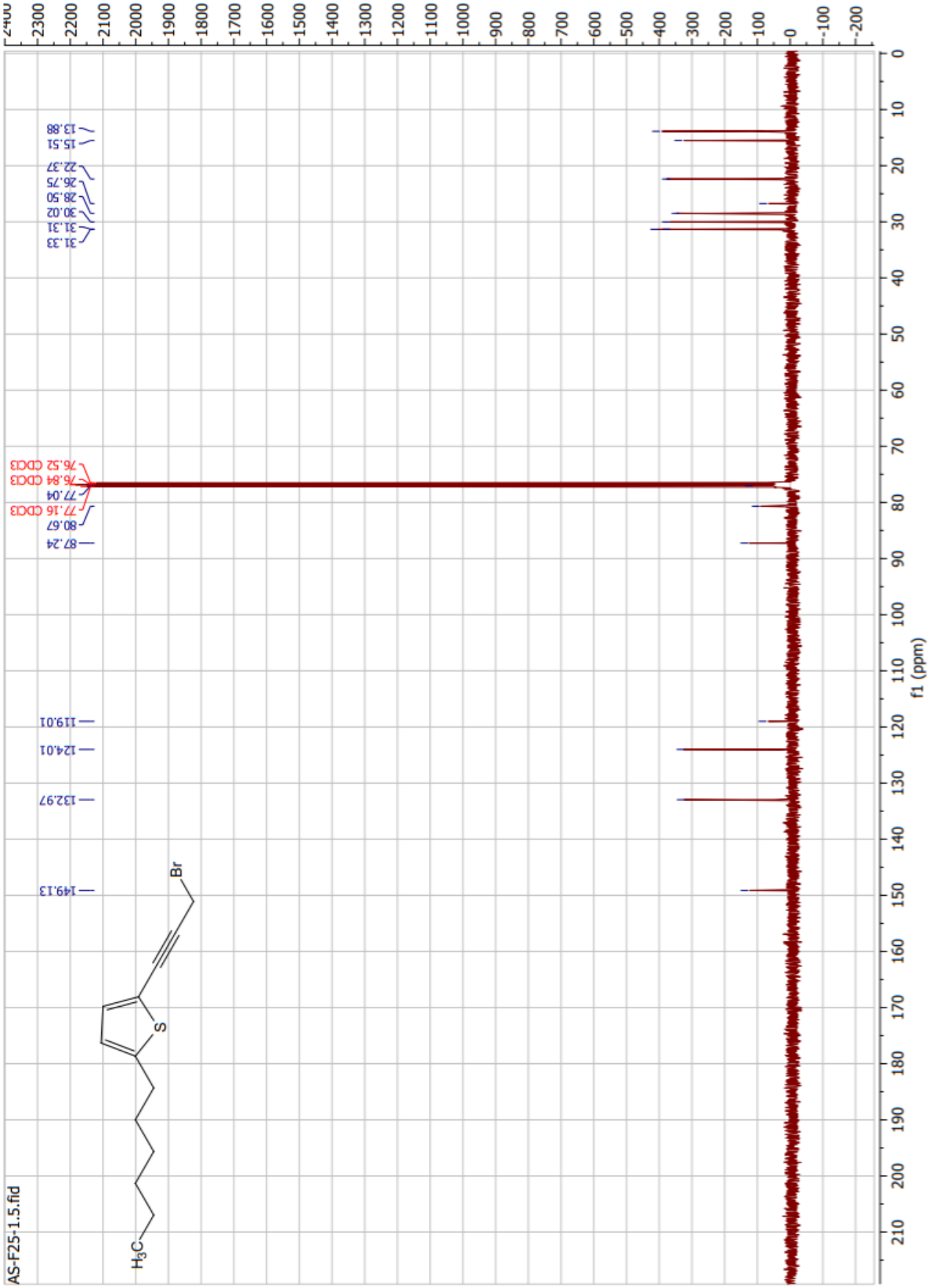

Figure A.54: *Shows the ^{13}C NMR (100MHz, $CDCl_3$) spectrum of 2-(3-bromoprop-1-yn-1-yl)-5-hexylthiophene (84)*

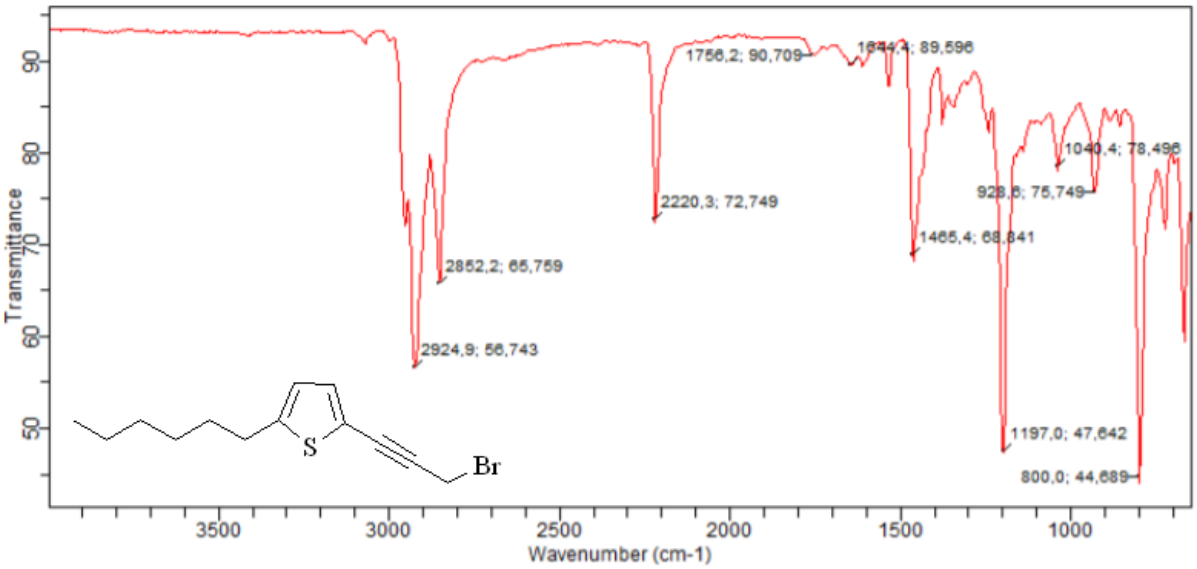

Figure A.55: *IR spectrum of 2-(3-bromoprop-1-yn-1-yl)-5-hexylthiophene (**84**)*

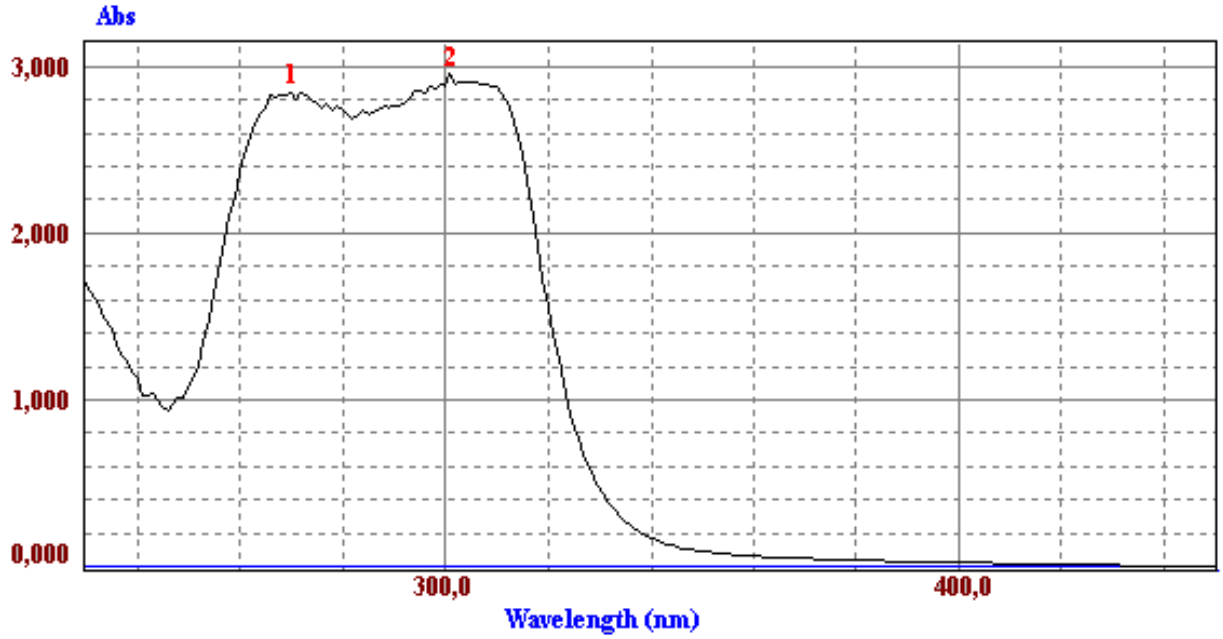

No.	Peak Type	Position	Height
1	Peak	269.7	2.844
2	Peak	301.1	2.958

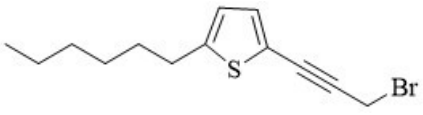

Figure A.56: *UV spectrum of 2-(3-bromoprop-1-yn-1-yl)-5-hexylthiophene (**84**)*

A.22. 6-(5-HEYXLTHIOPHEN-2-YL)HEXA-2,5-DYN-1-OL (**89**) SPECTRAL DATA

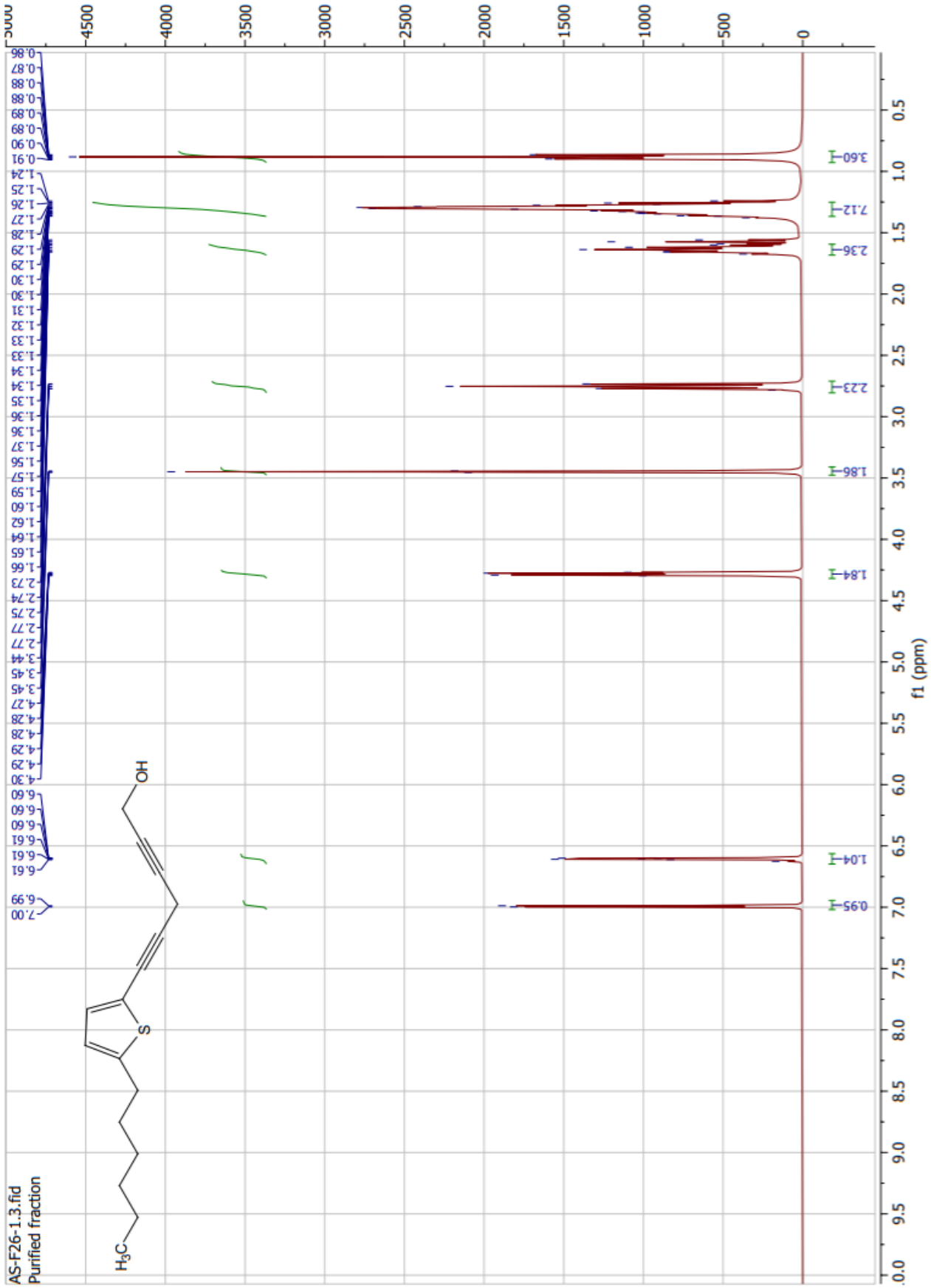

Figure A.57: *Shows the ^{1}H NMR (400MHz, $CDCl_3$) spectrum of 6-(5-hexylthiophen-2-yl)hexa-2,5-diyn-1-ol (**89**)*

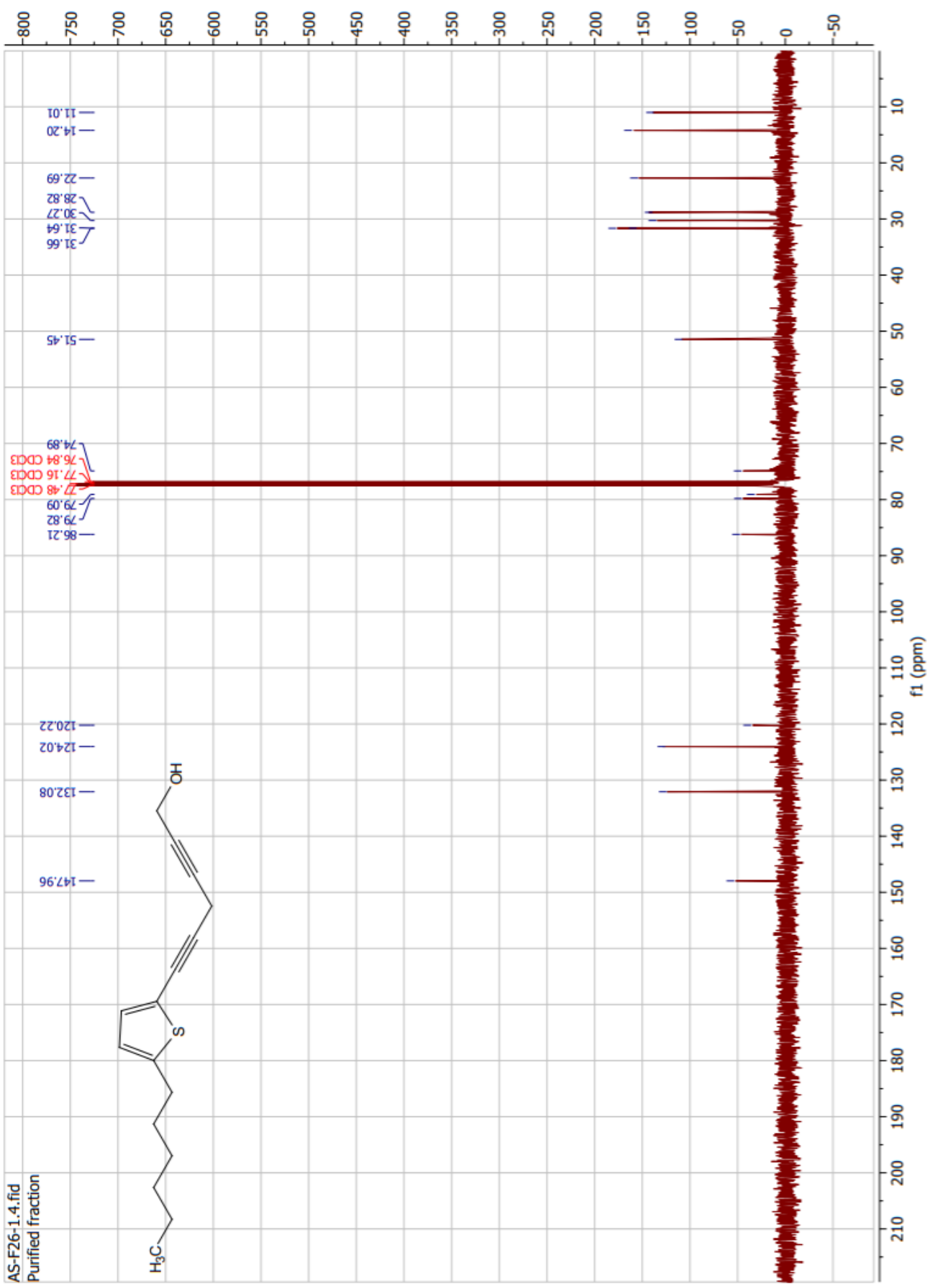

Figure A.58: *Shows the ^{13}C NMR (100MHz, $CDCl_3$) spectrum of 6-(5-hexylthiophen-2-yl)hexa-2,5-diyn-1-ol (**89**)*

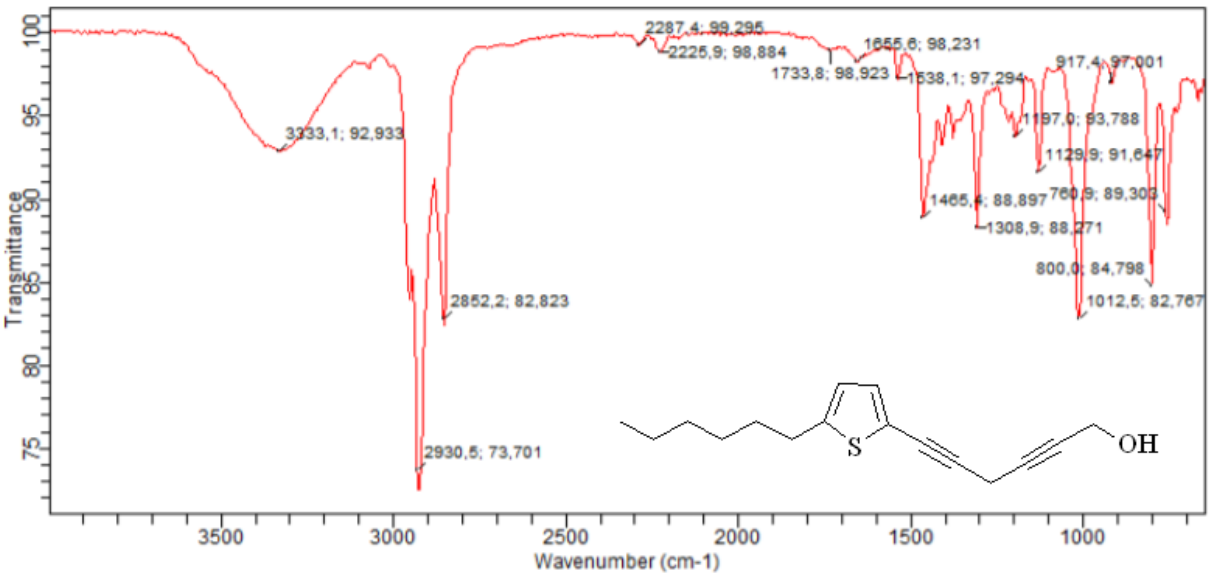

Figure A.59.: IR spectrum of 6-(5-hexylthiophen-2-yl)hexa-2,5-diyn-1-ol (89)

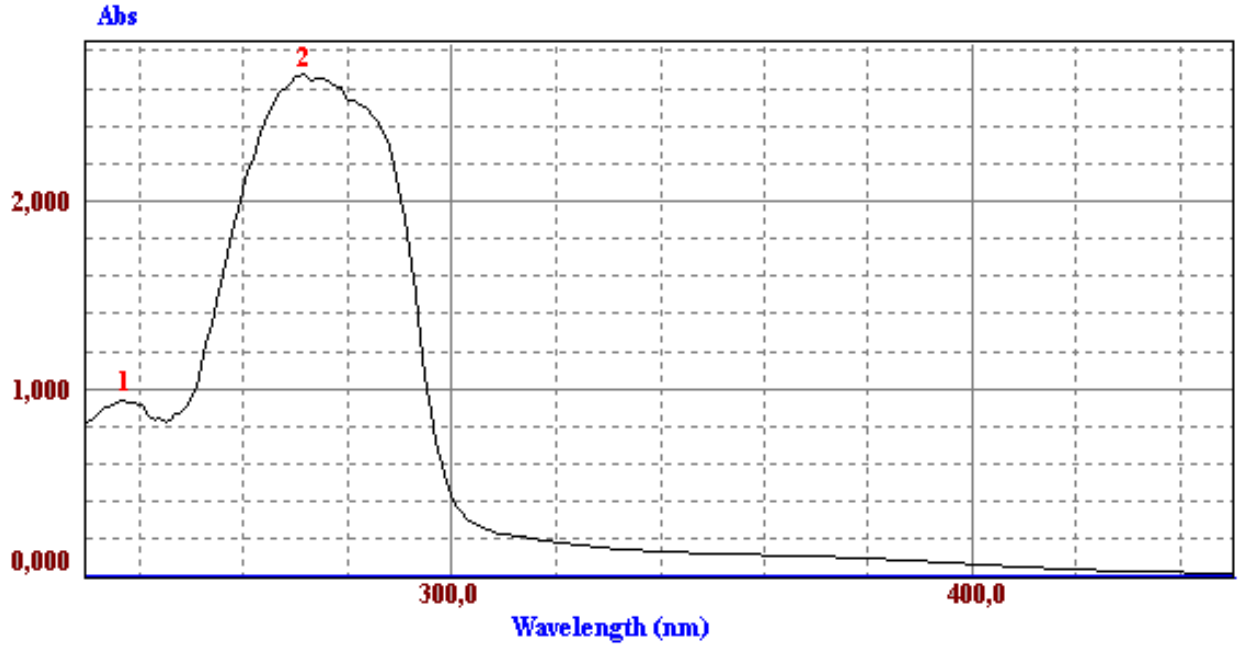

No.	Peak Type	Position	Height
1	Peak	236.9	0.940
2	Peak	271.6	2.678

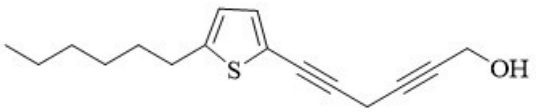

Figure A.60: UV spectrum of 6-(5.hexylthiophen-2-yl)hexa-2,5-diyn-1-ol (89)

A.23. 6-(5-HEXYLTHIOPHEN-2-YL)HEXAN-1-OL (**91**) SPECTRAL DATA

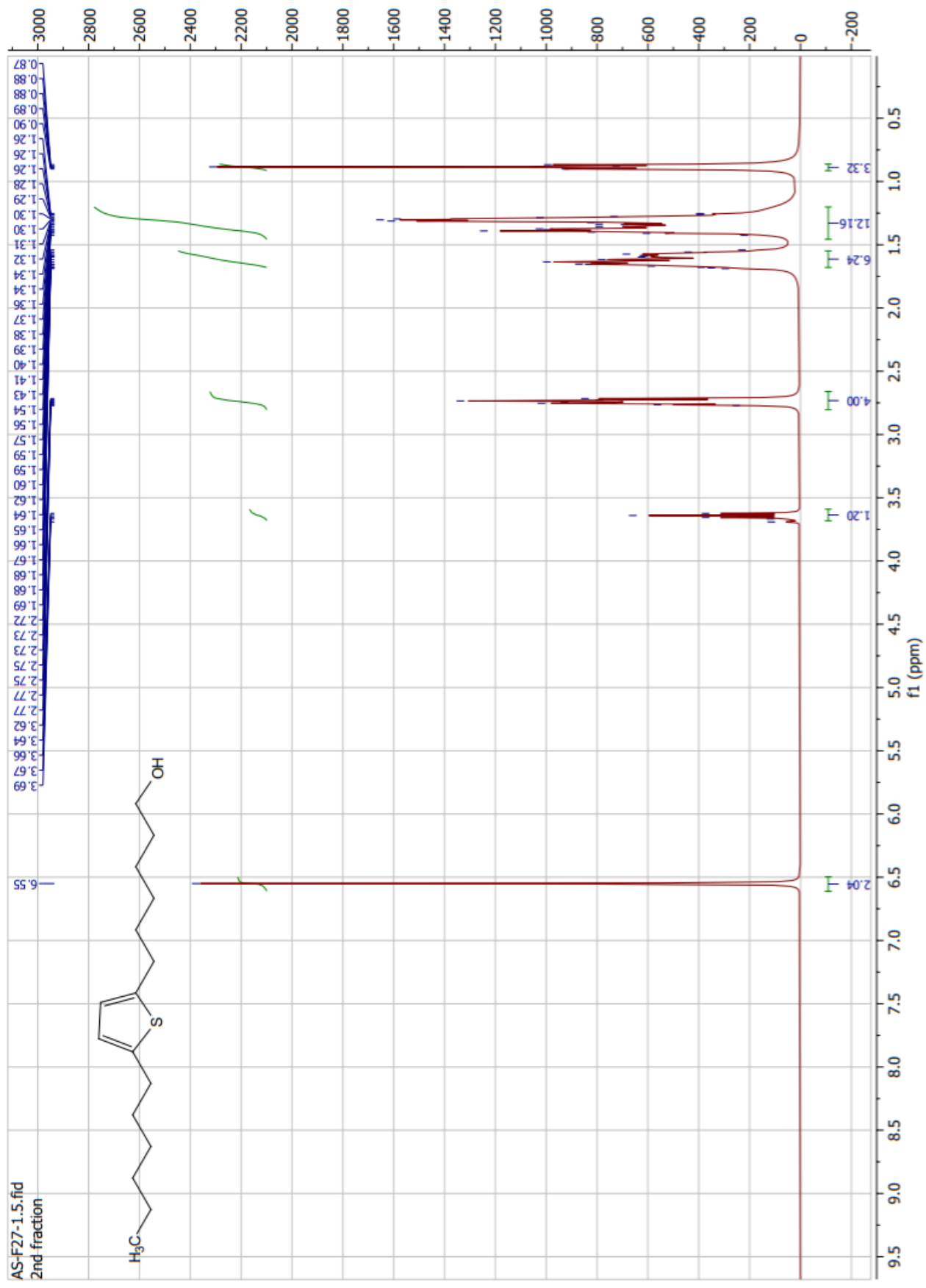

Figure A.61: *^{1}H NMR (400MHz, $CDCl_3$) spectrum of 6-(5-hexylthiophen-2-yl)hexan-1-ol (**91**)*

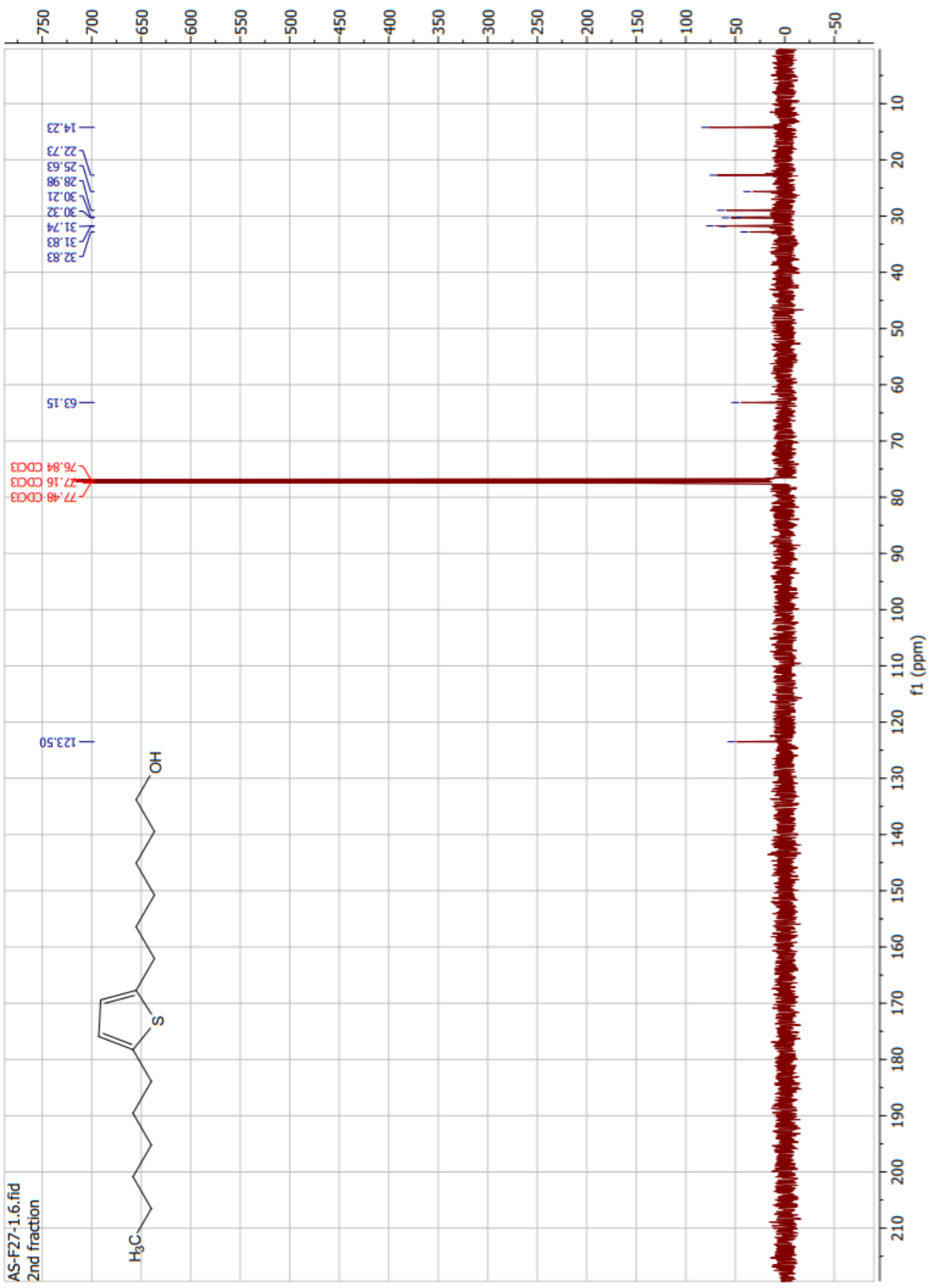

Figure A.62: *^{13}C NMR (100MHz, $CDCl_3$) spectrum of 6-(5-hexylthiophen-2-yl)hexan-1-ol (**91**)*

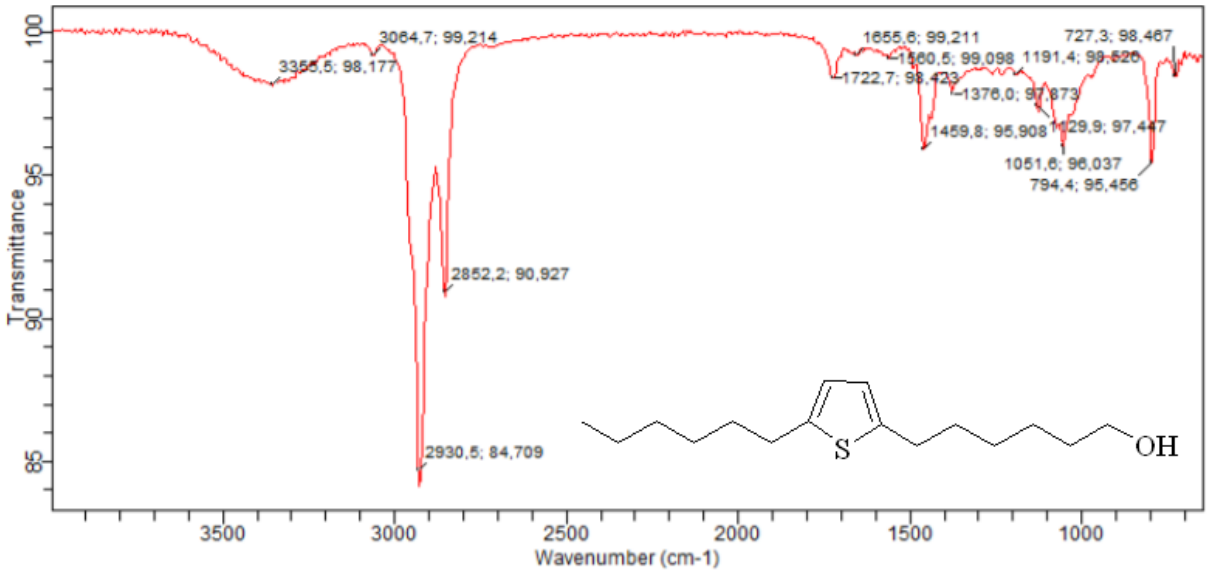

Figure A.63: *IR spectrum of 6-(5-hexylthiophen-2-yl)hexan-1-ol (**91**).*

A.24. 2,5-DIHEXYLTHIOPHENE (**111**) SPECTRAL DATA

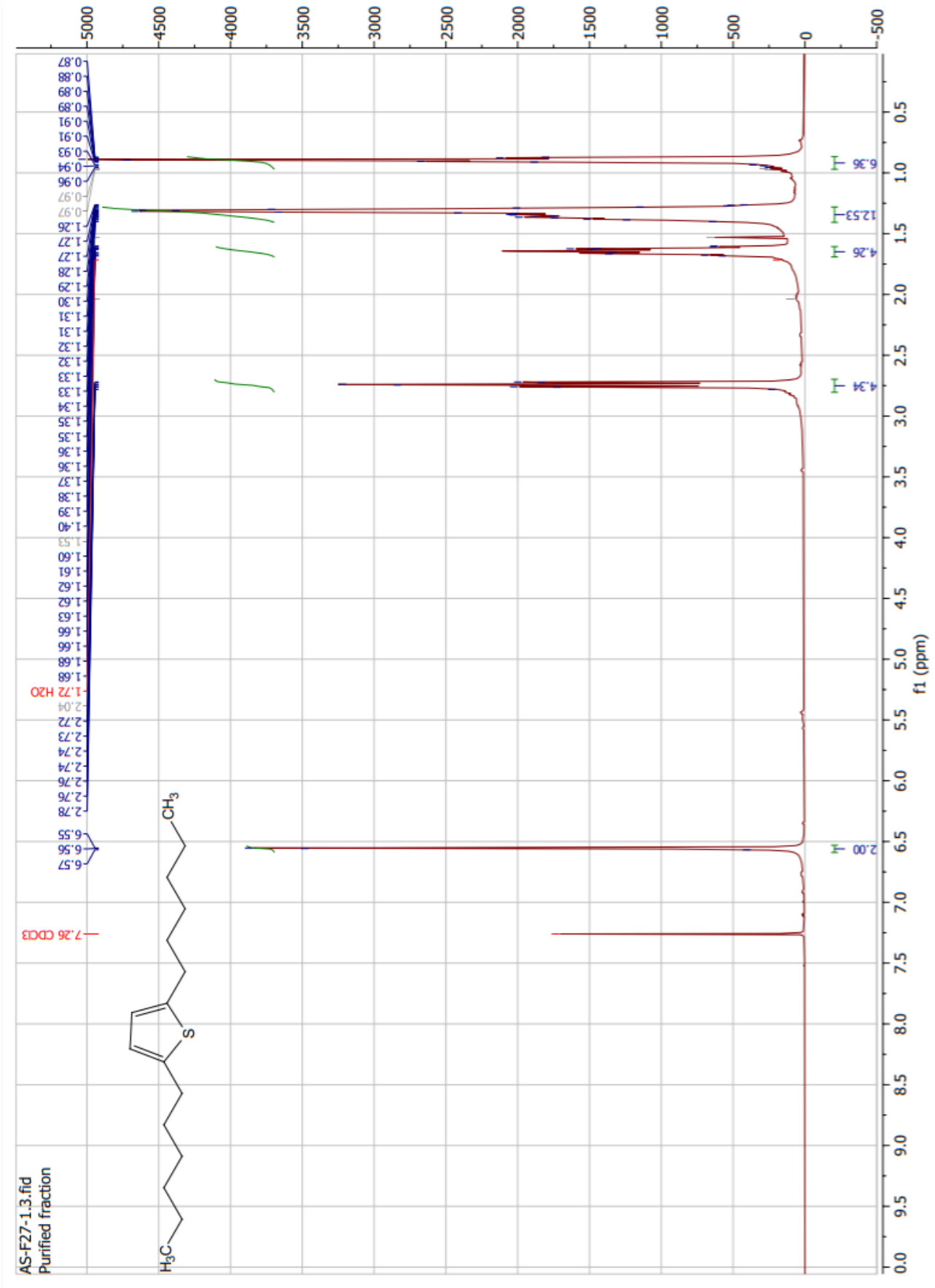

Figure A.64: *^{1}H NMR (400MHz, $CDCl_3$) spectrum of 2,5-dihexylthiophene (**111**)*

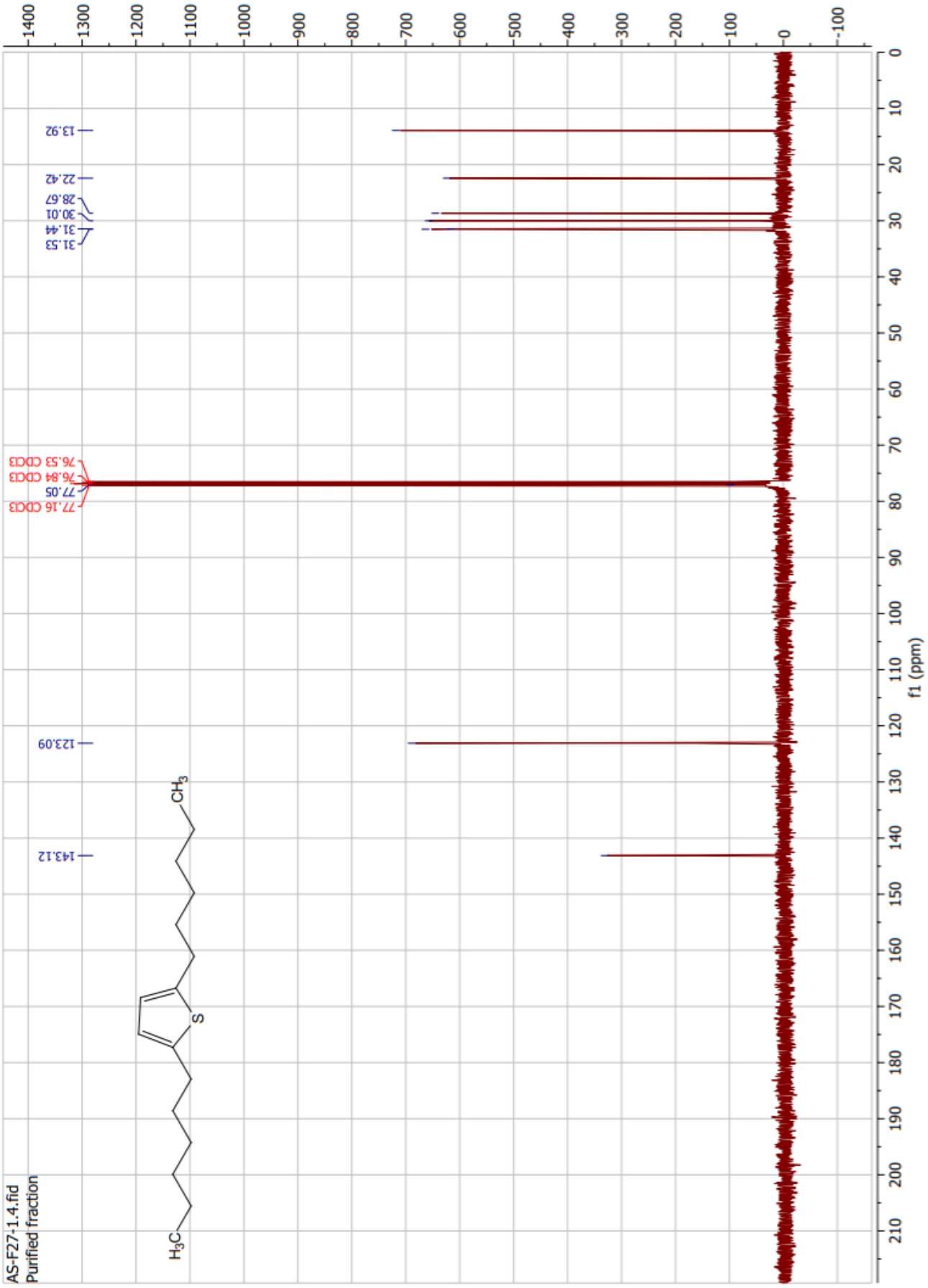

Figure A.65: *^{13}C NMR (100MHz, $CDCl_3$) spectrum of 2,5-dihexylthiophene (**111**)*

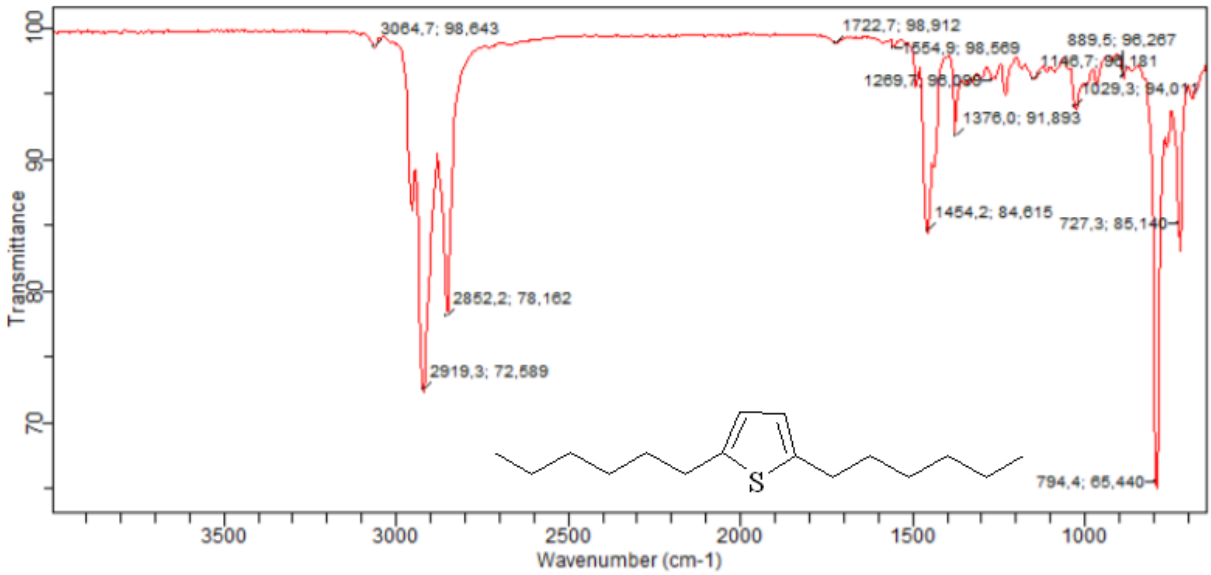

Figure A.66: *IR spectrum of 2,5-dihexylthiophene* ***(111)***

A.25. 6-(5-HEXYLTHIOPHEN-2-YL)HEXANAL (**87**) SPECTRAL DATA

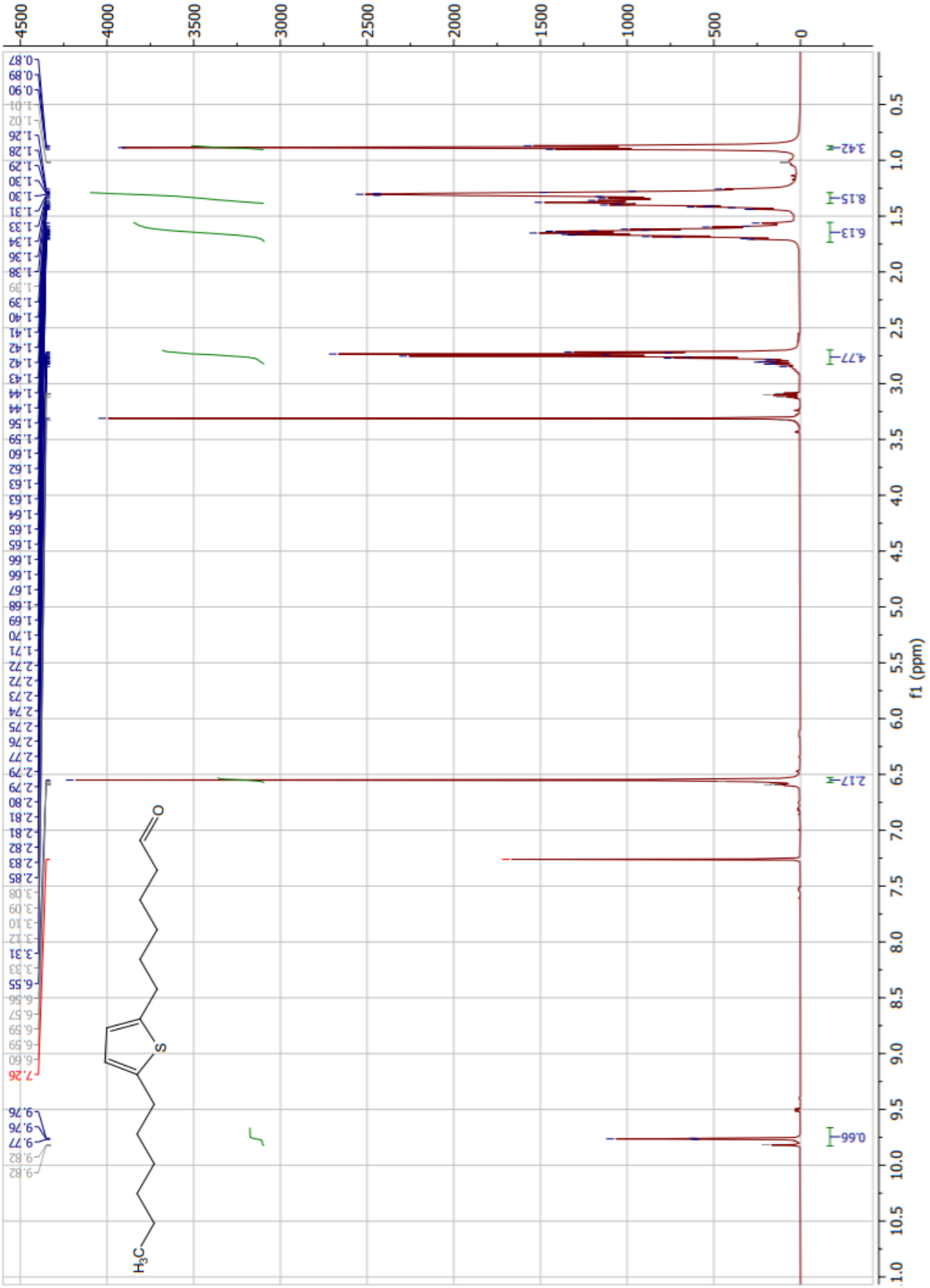

Figure A.67: *^{1}H NMR (400MHz, $CDCl_3$) spectrum of 6-(5-hexylthiophen-2-yl)hexanal (**87**)*

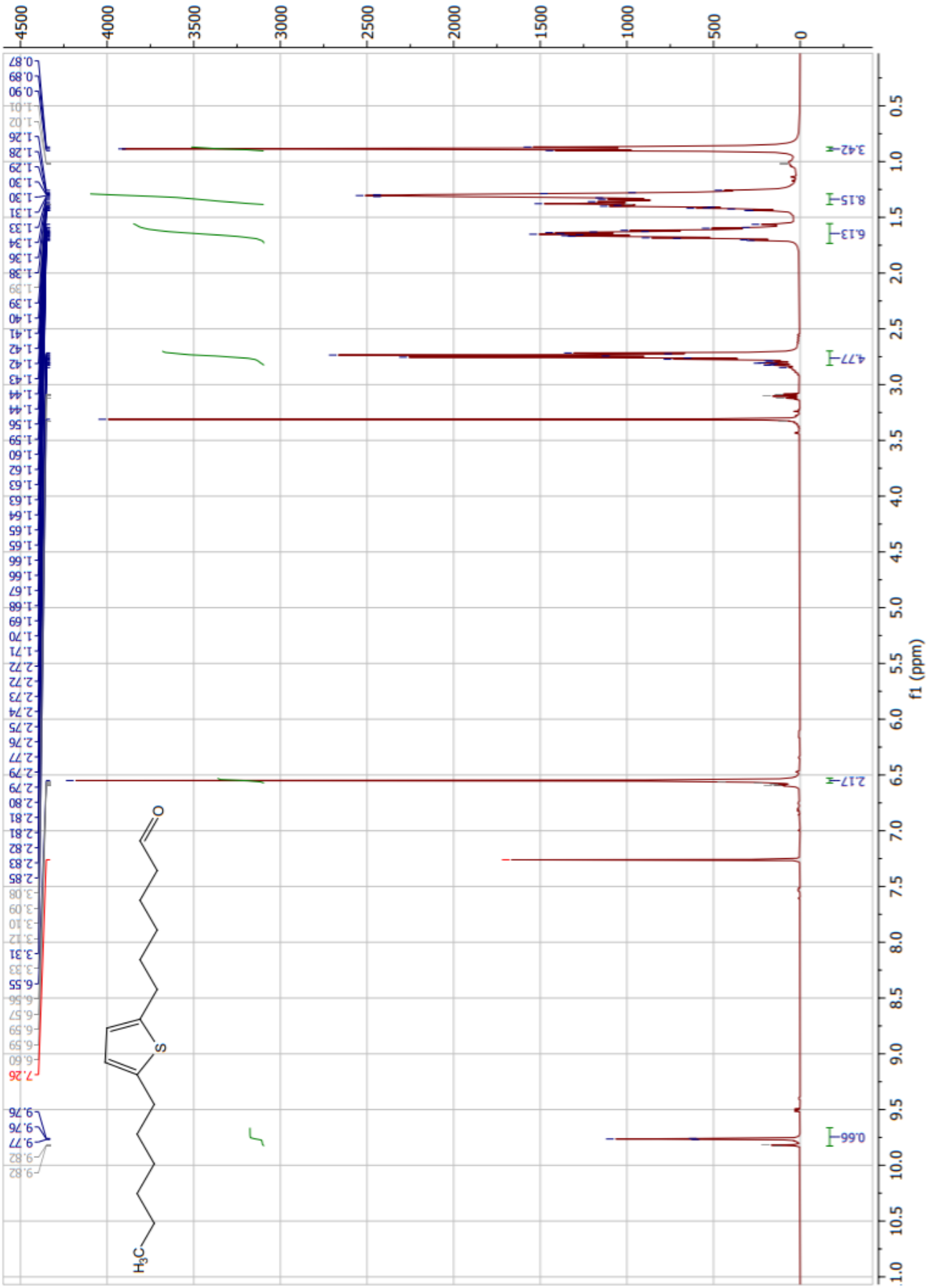

Figure A.68: *^{13}C NMR (100MHz, $CDCl_3$) spectrum of 6-(5-hexyøthiophen-2-yl)hexanal (**87**)*

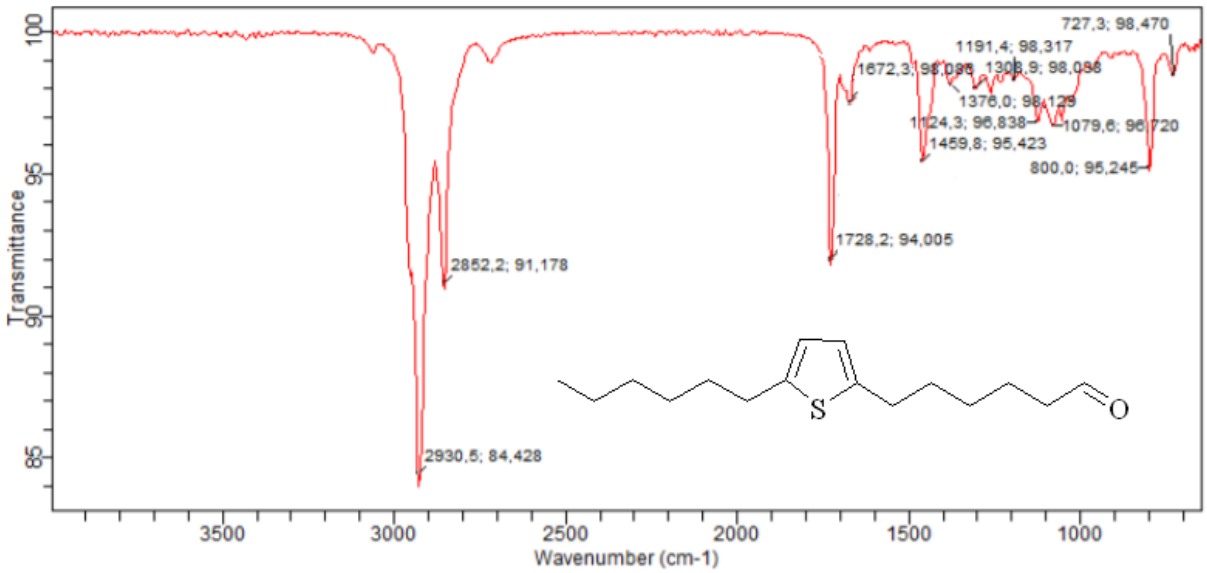

Figure A.69: *IR spectrum of 6-(5-hexylthiophen-2-yl)hexanal (**87**)*

A.26. ETHYL (*E*)-8-(5-HEXYLTHIOPHEN-2-YL)OCT-2-ENOATE (**86**) SPECTRAL DATA

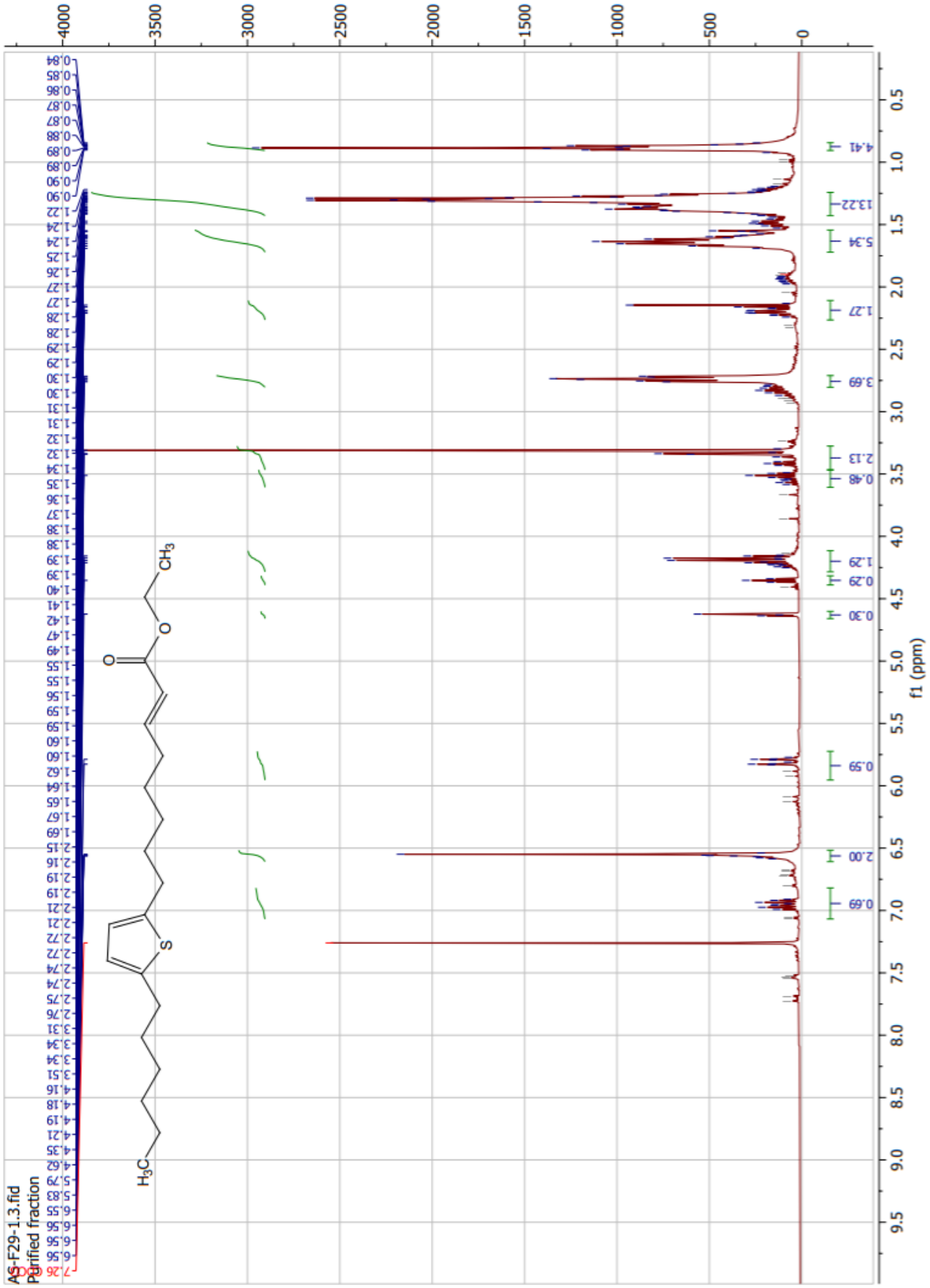

Figure A.70: *^{1}H NMR (400MHz, $CDCl_3$) spectrum of ethyl (E)-8-(5-hexylthiophen-2-yl)oct-2-enoate (**86**)*

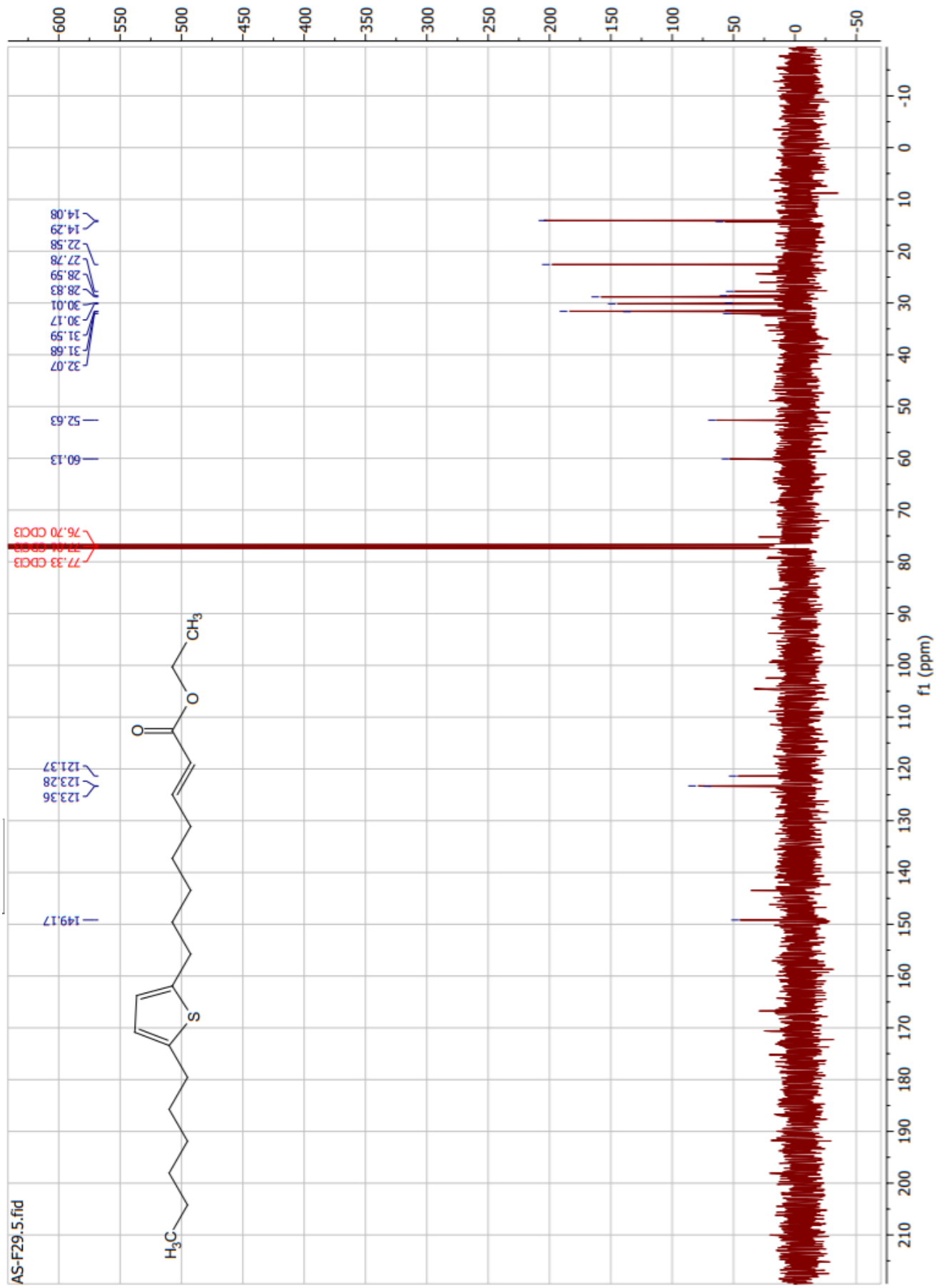

Figure A.71: *^{13}C NMR (100MHz, $CDCl_3$) spectrum of ethyl (E)-8-(5-hexylthiophen-2-yl)oct-2-enoate (**86**)*

Norges miljø- og biovitenskapelige universitet
Noregs miljø- og biovitskapelege universitet
Norwegian University of Life Sciences

Postboks 5003
NO-1432 Ås
Norway